

University of Nottingham
UK | CHINA | MALAYSIA

Targeting Thioredoxin Reductase in Pancreatic Cancer

Khaled Alhadyan, MSc

Thesis submitted to the University of Nottingham for the degree of Doctor of Philosophy

December 2018

Abstract

Pancreatic cancer (PC) is the fifth leading cause of cancer deaths in the United Kingdom, and responsible for 5% of all cancer deaths. Current treatment options, including surgery, chemotherapy and radiotherapy, have failed to improve five-year survival rates over the last 30 to 40 years, which remain very low, at ~5%. A number of resistance mechanisms may explain this lack of treatment success, one of these being inherent or acquired expression of redox proteins, i.e. proteins that can scavenge therapy-induced radicals, making treatment, such as radiation therapy, less efficient. Redox proteins are key members of cellular antioxidant systems, required to maintain redox homeostasis, with the thioredoxin (Trx) system being an important component. The Trx system consists of Trx, thioredoxin reductase (TrxR), and thioredoxin-interacting protein (TxNIP). Trx exists in mammalian cells in either a reduced (functional) form or an oxidised (non-functional) form. The reduced form of Trx regulates the redox state of different signalling molecules, and by regulating their redox state, can regulate cell growth, apoptosis, gene transcription, cell cycle progression and ROS levels. TrxR is the only known enzyme that can reduce (activate) Trx. Therefore, TrxR has been studied as a potential therapeutic target in different types of cancer. Indolequinone analogues (IQs) are novel bioreductive TrxR inhibitors produced at the University of Nottingham, and currently being developed as potential drugs against PC. The current thesis set out to examine the role of the Trx system, using novel TrxR inhibitors, in regulating PC cell proliferation and radiosensitivity.

The first component of the current thesis used two novel, putative TrxR inhibitors (IQ9 and IQ10) to investigate the effect that inhibiting TrxR had on cellular cytotoxicity (via proliferation and clonogenic survival assays), radiosensitivity, and cell cycle progression. This was done using three PC cell lines: PANC-1, MIA Paca-2 and BxPc-3. The study used gemcitabine (GM), an agent clinically used in the treatment of PC, and auranofin (AUR), a well-characterised TrxR inhibitor, as positive controls. Results indicate that IQs exhibited potent *in vitro* cytotoxicity at 24, 48 and 72 hours, with IC50 values in the low

nanomolar range. In the proliferation assay, PANC-1 cells showed low sensitivity to IQs (IC50=320-920 nM), while MIA Paca-2 (IC50=90-250 nM) and BxPc-3 cells (IC50=250-470 nM) showed high and intermediate sensitivity to IQs respectively. Results also indicate IQs as less toxic than GM (IC50=40-850 nM), but more toxic than AUR (IC50=400-2,550 nM) across all PC cell lines. In the clonogenic assay, GM (IC50=20-45 nM) appeared more potent than IQs (IC50=240-900 nM) across all PC cell lines. Increased radiosensitisation was observed for PANC-1 and BxPC-3 cells treated with IQs for 48 hours at 6 Gy, with no altered radiosensitisation in MIA Paca-2 cells. Although IQs appeared to sensitise PANC-1 and BxPc-3 cells to radiation at 6 Gy, the sensitiser enhancement ratio (SER) at 1% of survival for PANC-1 (SER=1.08-1.1) and BxPc-3 (SER=1.1-1.13) cells was low. Over a period of 48 hours, IC50 of IQ9 caused a significant cell cycle arrest in PANC-1 cells in the G0/G1 phase (P=0.024), with a significant decrease in S-phase (P=0.013); no effect was observed on the cell cycle progression of BxPc-3 cells.

The second component of the current study sought to investigate the potential mechanisms of action of IQs on the Trx system. This was done by examining the IQs effects on intracellular ROS levels (using flow cytometry) on the protein expression of Trx system family members, protein expression of reductase enzymes, TrxR activity (using insulin reduction assay), and radiation sensitivity. Since IQs are classified as bioreductive agents, the second component of the study also sought to observe the effect of hypoxia and drug treatment on proliferation, clonogenic survival, and on the protein expression of Trx system members and reductase enzymes. Results suggest that PC cells treated with IQs, in combination with H_2O_2, showed an increase in ROS levels compared to treatment with H_2O_2 only, with a maximum fold increase of 2. Western blots showed reduced expression of Trx only in BxPc-3 cells treated with the IC50's of IQs for 48 hours, with no notable changes in expression of TrxR and TxNIP. PANC-1 and MIA Paca-2 cell lines treated with IQs for 48 hours showed no changes in the expression of any of the Trx system proteins. PANC-1 and BxPc-3 cells treated with IQs showed a substantial decrease in TrxR activity, in a dose-dependent manner, with 4 hours' treatment yielding greater inhibition than 48 hours' treatment. Increased

radiosensitisation at 6 and 8 Gy was observed in PANC-1 cells treated with IQ9 or AUR for 4 hours, but may be of little biological relevance, as only a small increase in SER values (SER≤1.13) were observed. PANC-1 and BxPc-3 hypoxic cells were sensitive to IQ9, in terms of proliferation and clonogenic survival, compared to normoxic cells, but with a small increase in hypoxia cytotoxicity ratio (HCR) (HCR=1.2-2.4). IQ9 treatment did not alter the endogenous expression of reductase enzymes such as NQO1 and CPR in PANC-1 and BxPc-3 cells, neither in normoxic or hypoxic conditions.

The third component of the study studied Trx system protein expression in patient tumour specimens, determining prognostic significance and relationships with clinicopathological criteria. Two cancer patient cohorts were assessed, using immunohistochemistry (IHC) on tissue microarrays. The first cohort comprised 85 pancreatic adenocarcinomas (PAD), while the second cohort comprised 145 cancers of the bile duct and ampulla. In the first cohort, high expression of cytoplasmic (P=0.018) and nuclear (P=0.006) Trx were significantly associated with better overall survival, with nuclear Trx expression remaining significantly associated with survival in multivariate analysis (P<0.0001). In the second cohort, low cytoplasmic TxNIP expression was also associated with the presence of perineural invasion (P=0.025). High expression of cytoplasmic TxNIP was significantly associated with better overall survival (P=0.0002), which remains significant in multivariate Cox-regression analysis (P=0.013).

In conclusion, the current study suggests that targeting the TrxR system may be a useful potential strategy for treating PC. Current findings show that IQs are effective in PC cell lines as single agents, with IC50 values in the low nanomolar range. However, IQs were less potent than GM. IQs enhance radiotherapeutic efficacy in certain PC cell lines, but with low SER values, rendering the biological relevance of IQs as radiosensitisers somewhat questionable. IQs showed high efficacy in terms of inhibiting TrxR activity and increasing ROS levels in PC cells, with no notable alteration in endogenous protein expression of TrxR. Hypoxia increased the cytotoxic effect of IQs on PC cell lines but with low HCR values, making the biological significance of IQs as potential hypoxic cytotoxins doubtful. The Trx family protein expression can be used prognostically in patients with

pancreatic, bile duct and ampullary cancers, and may influence cancer cell susceptibility to anticancer agents.

Conference presentations

1- Poster presentation “Targeting thioredoxin reductase in pancreatic cancer”. The 17th International Conference on Oxidative Stress Reduction, Redox Homeostasis and Antioxidants”, Institute Pasteur, Paris, France, 13-15 June 2016.

2- Poster presentation “Targeting thioredoxin reductase in pancreatic cancer”. 2016 NCRI conference”, The BT Convention Centre, Liverpool, UK, 6 – 9 November 2016.

3- Poster presentation “Targeting Redox Proteins to Increase Radiotherapeutic Efficacy in Pancreatic Cancer”. The 5th International Conference on Radiation Medicine (ICRM), Alfaisal University, Riyadh, Saudi Arabia, 11 – 15 February 2018.

Awards

2016 BACR/CRUK Student Travel Award to attend 2016 NCRI conference.

Dedication

I dedicate my dissertation work to the memory of loved ones who have passed away during my study.

Dedicated to the memory of my father, Saleh Alhadyan, and my grandmother, Lolwah Alhadyan, who always believed in my ability to be successful in the research arena. You are gone but your belief in me has made this journey possible.

Dedicated to the memory of my colleague, Ms. Muneera Al-Buhairi, who was the first to teach me how to handle a pipette in a research laboratory. I am sure that she is now very proud of me.

Dedicated to the memory of my friend, Muteb Al-Osaimi, who always supported me and believed in my capability to achieve my goals.

Acknowledgement

First and above all, I praise God, the Almighty for providing me this opportunity and granting me the capability to proceed successfully.

At the very outset, I express my deepest sense of gratitude to Prof. Stewart Martin, my esteemed supervisor, for his teaching, warm encouragement, thoughtful guidance, critical comments and corrections of the thesis. Without his cooperation and kindness, this PhD. could not have been completed. My thanks extend to my second supervisor Prof. Ian Ellis, and to Prof. Chris Moody, Prof. Kaye Williams, Dr. Martyn Inman, Dr. Abed Zaitoun, Dr. Alan Mcintyre and Dr. Dileep Lobo for their collaboration and useful contributions.

I also want to acknowledge all former and current members of the Translational & Radiation Biology Research Group. I wish to express my sincere thanks to Dr. Sarah Storr, Dr. Yimin Zhang and Dr. Aula Ammar for their constructive suggestions and technical support. Many thanks to my lab mates and colleagues, Xuan Pu, Siwei Zhang, Bhudsaban Sukkarn, Nurul Abdullah, Chondrou Giota, Yao Anqi, Radhika Aiyappa, Richa Vasan and Sultan Sonbul, for the unique family-like environment that enabled me to survive the tough Ph.D. student life with comfort.

My deepest and heartfelt appreciation to my mother, Ms. Khadija Bahakeem, without your prayers and love I could not have gone so far in my studies; to my lovely wife, Dr. Deem Alakeel, my gorgeous daughter, Najla, for their selfless love, patience, support and understanding during the pursuit of my Ph.D degree that made the completion of my thesis possible; to my beautiful sisters, especially Ohoud, and my golden brother, my-father-in law, Akeel Alakeel, and my mother-in-law, Aisha Alakeel, for they were always beside me, supporting me, encouraging me during the happy and hard moments, pushing and motivating me, I consider myself the luckiest person in the world to have such a lovely and caring family standing beside me with their love and unconditional support.

I am thankful to King Faisal Specialist Hospital and Research Centre for sponsoring me to carry out this thesis. I would like to express my deep thanks to members of the Biomedical Physics Department; to my mentor Dr. Ghazi Alsbeih, who has enabled my capacity to conduct such a PhD. Thesis; to Dr. Belal Moftah, Ms. Najla Alharbi, Ms. Sara Al-Qahtani and Ms. Sara Elewaisi for their support and valuable prayers.

Last but not least, it is my fortune to gratefully acknowledge the support and love of my friends, for their love, care and support.

Abbreviations

3D	three-dimensional
5-FU	fluorouracil
ALDH	aldehyde dehydrogenase
AP-1	activator protein 1
AP-2	activator protein 2
ASK1	apoptosis signal-regulating kinase 1
ATCC	American Type Culture Collection
ATP	adenosine triphosphate
AUR	auranofin
BC	breast cancer
BCC	basal cell carcinoma
BED	biological effective dose
BER	base excision repair
BMI	body mass index
BSA	bovine serum albumin
BSO	buthionine sulfoximine
CA9	carbonic anhydrase 9
CEST	contrast-enhanced computerised tomography
CPR	NADPH cytochrome P450 reductase
CRC	colorectal cancer

CRLM	colorectal cancer liver metastasis
CRT	conventional radiation therapy
CSC	cancer stem cell
CT	computerised tomography
CTV	clinical tumour volume
DAB	diaminobenzidine
DC	detergent compatible
DCK	deoxycytidine kinase
DCTD	deoxycytidylate deaminase
DFdC	20,20-difluoro-20-deoxycytidine
DFdCDP	20,20-difluoro-20-deoxycytidine diphosphate
DFdCMP	20,20-difluoro-20-deoxycytidine monophosphate
DHFR	dihydrofolate reductase gene
DJ-1	protein deglycase
DM	dibetes mellitus
DMSO	dimethyl sulfoxide
DMEM	dulbecco's modified eagle's medium
DNTP	deoxy nucleotide triphosphate
DPC4	deleted in pancreatic cancer-4
DSB	double-strand break
ECL	enhanced chemiluminescence
ECM	extracellular matrix

EF24	diphenyl difluoroketone
EO9	33-hydroxy-5-aziridinyl-1-methyl-2-(1H-indole-4,7-indione)-propenol
FAMMM	familial multiple mole and melanoma
GI	gastrointestinal
GM	gemcitabine
GLS2	phosphate-activated mitochondrial glutaminase
GLUT1	glucose transporter 1
GPx	glutathione peroxidase
GR	glutathione reductase
GRX	glutaredoxins
GSH	glutathione
GSSG	oxidized glutathione
GSTP	glutathione S-transferase pi
GTV	gross tumour volume
HAP1	huntingtin-associated protein 1
HAPs	hypoxia-activated agents
HC	hepatoid carcinoma
HMEC	human microvascular endothelial cells
HNE	4-hydroxynonenal
HNSCC	head and neck squamous cell carcinoma
HR	hazard ratio

HCR	hypoxia cytotoxicity ratio
HIF-1	hypoxia-inducible factor 1
HR	homologous recombination
Hsps	heat-shock proteins
HU	hydroxyurea
IC50	half maximal inhibitory concentration
IHC	immunohistochemistry
IMRT	intensity-modulated radiotherapy
IMS	methylated spirit
IPMN	intraductal papillary mucinous neoplasm
IQ	indolequinone
IV	intravenously
IV-2	1-methyl-1-propyl-2 imidazolyl disulphide
JNK	p38/c-Jun NH2-terminal kinase
KRAS	Kirsten rat sarcoma viral oncogene homolog
LAPC	locally advanced pancriatic cancer
LET	linear energy transfer
LQ	linear quadratic model
MAPK	mitogen-activated protein kinase

MAPK	mitogen-activated protein kinase
MCN	mucinous cystic neoplasm
MDA	malondialdehyde
MEM	minimum essential medium eagle
MFI	fluorescence intensity
MGd	motexafin gadolinium
MMC	mitomycin C
mmHg	millimetre of mercury
MMR	mismatch repair
MOMP	mitochondrial outer membrane permeabilization
MTT	3-(4, 5-dimethylthiazolyl-2)-2, 5-diphenyltetrazolium bromide
MTS	3-(4,5-dimethylthiazol-2-yl)-5-(3-carboxymethoxyphenyl)-2-(4-sulfophenyl)-2H-tetrazolium
NAPDH	nicotinamide adenine dinucleotide phosphate oxidases
NF-κB	nuclear factor kappa-light-chain-enhancer of activated B cells
NHEJ	non-homologous end joining
NQO1	NAD(P)H:quinone oxidoreductase
Nrf-2	nuclear factor erythroid 2–related factor 2
NSCLC	non-small-cell lung cancer
NTCP	normal tissue complication probability
OAR	organs at risk
OER	oxygen enhancement ratio

PAD	pancreatic adenocarcinomas
PAHs	polycyclic aromatic hydrocarbons
PanIN	pancreatic intraepithelial neoplasia
PBS	phosphate buffered saline
PC	pancreatic cancer
PDH	pyruvate dehydrogenase
PDK1	pyruvate dehydrogenase kinase 1
PE	plating efficiency
PET/CT	positron emission tomography/computed tomography
PI	propidium iodide
pO_2	O_2 concentration
PPPD	pylorus-preserving pancreaticoduodenectomy
Prx	peroxiredoxin
PSC	pancreatic stellate cells
PSSG	protein S-glutathionylation
RNase	ribonuclease
RFS	relapse-free survival
ROS	reactive oxygen species
RR	relative risk
RRM1	ribonucleotide reductase catalytic subunit M1
SD	standard deviation

SER	sensitiser enhancement ratio
SF	surviving fraction
SF2	surviving fraction at 2 Gy
SMAD4	small mothers against decapentaplegic homolog 4
SOD	superoxide dismutase
SRB	Sulforhodamine B
SRBT	stereotactic body radiotherapy
SRB	sulforhodamine B
SRS	stereotactic radiosurgery
SSB	singlestrand break
STR	short tandem repeat
TBP2	thioredoxin binding protein 2
TBS	tris buffered saline
TCP	tumour control probability
TGF-β	transforming growth factor-β
TMA	tissue microarray
TNF α	tumour necrosis factor α
TP53	tumor protein P53
Trx	thioredoxin
TrxR	thioredoxin reductase
TxNIP	thioredoxin-interacting protein
UMP-CMP	pyrimidine nucleoside monophosphate kinase

VEGF	vascular endothelial growth factor
VDUP1	vitamin D3 up-regulated protein 1
χ^2	Pearson Chi Square
2-AAPA	2-acetylamino-3-[4-(2-acetylamino-2-carboxyethyl-sulfanylthiocarbonylamino)phenylthiocarbamoylsulfanyl]propionic acid

Table of Contents

Abstract i

Conference presentations v

Dedication vi

Acknowledgement vii

Abbreviations ix

Table of Contents xvii

List of Tables xxi

List of Figures xxi

Chapter 1: General introduction 1

1.1 General introduction to pancreatic cancer 2

1.1.1 Incidence and risk factors 2

1.1.2 Pancreatic cancer types 7

1.1.3 Symptoms 13

1.1.4 Diagnosis and staging 14

1.1.5 Mutations in pancreatic cancer 17

1.1.6 Treatments and Survival 22

1.2 Redox proteins 37

1.2.1 Redox homeostasis 37

1.2.2 *The cellular antioxidant system* 41

1.2.3 Redox proteins in cancer 49

1.3 Hypotheses and aims 57

1.3.1 Hypotheses 57

1.3.2 Aims and objectives 57

Chapter 2: Effect of indolequinones on cell proliferation, survival and radiosensitivity of pancreatic cancer cells 59

2.1 Abstract 60

2.2 Introduction hypothesis and aims 62
2.2.1 Redox protein regulation of radioresponse 62
2.2.2 Bioreductive agents 67
2.2.3 Hypotheses and aims 75
2.2.4 Aims 75
2.3 Materials and methods 76
2.3.1 General growth conditions..... 76
2.3.2 Cryopreservation 77
2.3.3 Cell recovery from cryopreservation 77
2.3.4 Pancreatic cancer cell lines..... 77
2.3.5 Cellular Characteristics of PC cell lines; growth curves and plating efficiency 79
2.3.6 Drugs and Drug preparation..... 80
2.3.7 Cytotoxicity experiments 81
2.3.8 Cell cycle analysis..... 85
2.3.9 Statistical analysis and graphs design..... 86
2.4 Results 87
2.4.1 Characteristic experiments; growth curves and PE 87
2.4.2 Cytotoxicity effect of GM, IQ9, IQ10 and AUR on PC cell lines 87
2.4.3 Radioresponse of PC cell lines. 95
2.4.4 Effect of IQs on cell cycle progression of PC cells. 97
2.5 Discussion 100

Chapter 3: Evaluation of mechanisms of action of IQs on the Trx/TrxR system in pancreatic cancer cell lines 108
3.1 Abstract 109
3.2 Introduction and aims 111
3.2.1 Hypoxia in tumour cells 111
3.2.2 Hypotheses..... 121
3.2.3 Aims 121
3.3 Materials and methods 122

3.3.1 Cell lines, culture conditions and drug preparation 122
3.3.2 Measurement of intracellular reactive oxygen species (ROS) levels 122
3.3.3 Western blot..... 123
3.3.4 Thioredoxin reductase activity 128
3.3.5 Drug-radiation combination clonogenic assay 130
3.3.6 Cytotoxicity experiments of PC cell lines in hypoxic conditions 130
3.3.7 Statistical analysis and graph design 133
3.4 Results 134
3.4.1 Effect of IQs on intracellular ROS levels..... 134
3.4.2 Effect of IQs on the expression of Trx system in PC cell lines 138
3.4.3 Effect of IQs on TrxR activity 144
3.4.4 Drug-radiation combination - clonogenic survival 146
3.4.5 Influence of hypoxia on IQs cytotoxicity..... 149
3.5 Discussion 156
Chapter 4: Thioredoxin system protein expression in carcinomas of the pancreas, bile duct and ampulla 167
4.1 Abstract 168
4.2 Introduction, hypothesis and aims 170
4.2.1 Role of expression of redox proteins in clinicopathological criteria and clinical outcome of cancer patients 170
4.2.2 Hypothesis..... 174
4.2.3 Aims 174
4.3 Materials and methods 175
4.3.1 Clinical samples 175
4.3.2 Optimization of antibodies for immunohistochemistry (IHC).... 177
4.3.3 IHC..... 177
4.3.4 Assessment of expression 179
4.3.5 Statistical analysis..... 182
4.4 Results 183

4.4.1 Optimizations of Trx, TrxR and TxNIP primary antibodies for IHC 183
4.4.2 Expression of Trx, TrxR and TxNIP in the PAD cohort and the bile duct and ampullary carcinoma cohort 184
4.4.3 Relationship of Trx, TrxR and TxNIP expression with clinicopathological variables in the PAD cohort and the bile duct and ampullary carcinoma cohort 186
4.4.4 Relationship of the Trx, TrxR and TxNIP protein expression with clinical outcome in the PAD cohort and the bile duct and ampullary carcinoma cohort 192
4.5 Discussion 198
Chapter 5: General discussion 204
5.1 General discussion 205
5.2 Limitations, future work and conclusions 214
5.2.1. Practical limitations for *in vitro* models 214
5.2.2. Theoretical limitation for *in vitro* models and future work 215
5.2.3. Conclusion 219
References 222
Appendix A: Supplementary information for Chapter 4 260
Appendix B: Copyright information 263

List of Tables

Table 1.1: TNM staging system of PC 15
Table 1.2: Summary of cellular antioxidants 41
Table 2.1: Tissue culture flasks and plates and the related reagents volume 76
Table 2.2: Donor patient's information, characteristics of PC cell lines and genetic status of four most common genes involved in PC development 78
Table 2.3: Cell culture medium. 79
Table 2.4: The proliferation IC50 values of GM, IQ10, IQ9 and AUR for PC cell lines and MDA-MB-231 BC cell line 92
Table 2.5: The clonogenic IC50 values of GM, IQ9 and IQ10 for PC cell lines. PANC-1, MIA Paca-2 and BxPc-3 PC cells were treated with GM or IQs for 48 hours, then, cells were plated for clonogenic survival 94
Table 2.6: PC cell line radiation sensitivity parameters 96

Table 3.1: Western blot buffers. 124
Table 3.2: Primary and secondary antibodies for Western blot. 126
Table 3.3: Clonogenic IC50 values of IQ9 for PANC-1 and BxPc-3 in normoxic and hypoxic conditions 164

Table 4.1: Clinicopathological variables of the PAD cohort of 85 patients and the bile duct and ampullary cohort of 145 patients 176
Table 4.2: The X-tile cut-point values of Trx, TrxR and TxNIP in the PAD cohort and bile duct and ampullary carcinoma cohorts 185
Table 4.3: Associations between Trx and TxNIP protein expression and various clinicopathological variables in the PAD cohort 187
Table 4.4: Associations between TrxR protein expression and various clinicopathological variables in the PAD cohort 188
Table 4.5: Associations between Trx and TxNIP protein expression and various clinicopathological variables in the bile duct and ampullary carcinoma cohort 190
Table 4.6: Associations between TrxR protein expression and various clinicopathological variables in the bile duct and ampullary carcinoma cohort 192
Table 4.7: Multivariate Cox Regression analysis of factors associated with overall survival in the carcinomas of the pancreas, bile duct and ampulla 194

Table 5.1: Summary of the main hypotheses, expected results and observed results of each cell line/marker applied to the current study 221

List of Figures

Figure 1.1: Structure of the pancreas…….. 8

Figure 1.2: Representative histological pictures of different types of PC…….. 12

Figure 1.3: Genetic progression model of pancreatic carcinogenesis…….. 21

Figure 1.4: GM mechanisms of action…… 26

Figure 1.5: Illustration of the concept of a therapeutic ratio in terms of dose-response relationships for tumour control and normal tissue damage…… 28

Figure 1.6: Comparison of the depth dose profiles of high energetic photons and protons…… 31

Figure 1.7: Formation of ROS…… 38

Figure 1.8: Redox proteins and ROS regulation…….. 44

Figure 1.9: Mechanisms and functions of Trx system in the living cells…… 48

Figure 1.10: Redox homeostasis and oxidative stress…….. 50

Figure 1.11: Scheme of the potential mechanism of PX-12…… 55

Figure 2.1: Involvement of redox proteins in the regulation of tumour cells radiosensitivity…….. 62

Figure 2.2: Chemical structures and molecular formulas of quinone, Indole, Indolequinone, mitomycin C, EO9, IQ9 and IQ10…… 69

Figure 2.3: Possible routes of bio-activation of E09 by one- and two-electron reducing enzymes…… 71

Figure 2.4: A proposed mechanism for the inhibition of TrxR by ES936…… 73

Figure 2.5: Growth curves for PC cell lines…… 87

Figure 2.6: Effect of GM on the proliferation of PC cell lines…… 88

Figure 2.7: Effect of IQ9 and IQ10 on the proliferation of PC cell lines…… 89

Figure 2.8: Effect of AUR on the proliferation of PC cell lines…… 90

Figure 2.9: Effect of AUR, IQ9 and IQ10 on the proliferation of MDA-MB-231 BC cell line…… 91

Figure 2.10: Clonogenic effect of GM on PC cell lines…….. 93

Figure 2.11: Clonogenic effect of IQs on PC cell lines…….. 93

Figure 2.12: Survival curves of PC cell lines after single dose irradiation…….. 95

Figure 2.13: Effect of IQs on radiosensitivity of PC cell lines…… 97

Figure 2.14: Optimization of the concentration of positive control hydroxyurea (HU) in cell cycle analysis…… 98

Figure 2.15: Effect of IQ9 on cell cycle of PC cells…….. 99

Figure 3.1: The vicious cycle of hypoxia and stroma in PC…… 118

Figure 3.2: Effect of H_2O_2 on proliferation of PC cell lines and MDA-MB 231 BC cell line …….. 134

Figure 3.3: Optimization of H_2DCF-DA and H_2O_2 concentration in ROS level assessment …….. 135

Figure 3.4: Effect of IQs on intracellular ROS level of PC cell lines…… 137

Figure 3.5: Effect of AUR on intracellular ROS level of PC cell lines and MDA-MB-231 BC cell line…… 138

Figure 3.6: Quantification of the endogenous expression of Trx and TrxR in PC and BC cell lines…… 139

Figure 3.7: Quantification of the endogenous expression of TxNIP in PC and BC cell lines…… 140

Figure 3.8: Effect of IQs on the expression of TrxR in PC cell lines…… 141

Figure 3.9: Effect of IQs on the expression of Trx and TxNIP proteins in BxPc-3 PC cell line …… 142

Figure 3.10: Effect of IQs on the expression of Trx system in PANC-1 PC cell line…... 143

Figure 3.11: Effect of IQs on the expression of Trx system proteins in MIA Paca-2 PC cell line…… 143

Figure 3.12: Effect of IQs on TrxR activity in PANC-1 PC cell line…… 145

Figure 3.13: Effect of IQs on the activity of TrxR in BxPC-3 PC cells…….. 146

Figure 3.14: Effect of IQs on radiosensitivity of MIA Paca-2 PC cell line following 1 hour treatment…… 147

Figure 3.15: Effect of AUR on radiosensitivity of PANC-1 PC cell line following 48 hours treatment…… 147

Figure 3.16: Effect of IQ9 and AUR on radiosensitivity of PANC-1 PC cell line following 4 hours treatment…….. 148

Figure 3.17: Effect of hypoxia on the proliferation of PC cell lines…….. 149

Figure 3.18: Effect of hypoxia on clonogenic survival of PC cell lines…… 150

Figure 3.19: Effect of IQ9 on the proliferation of PC cell lines under hypoxic and normoxic conditions…… 151

Figure 3.20: Effect of IQ9 treatment for 48 hours on clonogenic survival of PC cell lines under hypoxic conditions…… 152

Figure 3.21: Effect of IQ9 treatment for 4 hours on clonogenic survival of PC cell lines under hypoxic and normoxic conditions…….. 153

Figure 3.22: Effect of hypoxia on the expression of Trx and TrxR proteins in PC cell lines under hypoxic conditions…… 154

Figure 3.23: Effect of IQ9 on the expression of CPR and NQO1 proteins in PC cell lines under normoxic and hypoxic conditions…….. 155

Figure 4.1: Representative photomicrographs of protein expression…… 180

Figure 4.2: Representative photomicrographs of different staining patterns of Trx system protein expression from PAD TMAs……181

Figure 4.3: Assess the specificity of Trx, TrxR and TxNIP antibodies 188

Figure 4.4: Kaplan-Meier analysis of association between Trx and TrxR expression and overall survival in PAD cohort…… 192

Figure 4.5: Kaplan-Meier analysis of association between TxNIP expression and overall survival in the carcinomas of the pancreas, bile duct and ampulla……. 193

Figure 4.6: Kaplan-Meier analysis of association between Trx and TrxR expression and overall survival in bile duct and ampullary carcinoma cohort…… 195

Figure 4.7: Kaplan–Meier overall survival analysis between different subgroups of Trx expression in the bile duct and ampullary cohort…….. 196

Figure 5.1: Effect of IQ10 on growth delay of BxPc-3 and PANC-1 xenograft models ……..210

Chapter 1: General introduction

1.1 General introduction to pancreatic cancer

1.1.1 Incidence and risk factors

1.1.1.1 Incidence and mortality

A neoplasm is an abnormal mass of tissue, the growth of which exceeds and is uncoordinated with that of the normal tissue, and persists in the same excessive manner after the cessation of the stimuli which evoked the change (Willis, 1960). Cancer is a neoplasm that can invade nearby tissues and, in certain cases, spread to other parts of the body as a consequence of alterations in certain genes and physiological processes. In 2000, Hanahan and Weinberg identified six biological processes involved in the molecular and cellular mechanisms for cancer occurrence and growth (known as the hallmarks of cancer); these are: sustaining proliferative signalling, evading growth suppressors, resisting cell death, enabling replicative immortality, inducing angiogenesis and activating invasion and metastasis (Hanahan and Weinberg, 2000). Recently, the same group added four new biological processes; genome instability, tumour-promoting inflammation, reprogramming of cell bioenergetics and evading immune destruction (Hanahan and Weinberg, 2011). Cancer is a common disease, in 2012, 14.1 million new cancer cases were registered, and there were 8.2 million cancer-related deaths worldwide (Ferlay et al., 2014). In the United Kingdom, one new case of cancer is diagnosed every 2 minutes, and one cancer-related death occurs every 4 minutes - there were more than 356,860 new cancer patients and approximately 163,444 cancer patients died in 2014 (CanceRresearchUK, 2017a).

Worldwide, pancreatic cancer (PC) is the seventh leading cause of cancer deaths, with 331,000 deaths per year (Ferlay et al., 2014). In the United Kingdom, there were 9,618 new PC cases registered and 8,817 PC-related deaths in 2014, making it the fifth leading cause of cancer deaths, and responsible for 5% of all cancer deaths. PC five-year survival has not altered over the last 40 years and in the United Kingdom remains low, at ~5% (CancerResearchUK, 2017b). Similarly, in the United States, PC is the fifth cause of cancer

deaths, with the five-year survival increasing from 3.1% to 6.9% over the last 30 years (Sun et al., 2014). As there have been few new treatment modalities or prevention programs, PC is likely to become the second cause of cancer death in the United States by 2030 (Rahib et al., 2014).

Geographically, PC has shown variation between more developed regions and less developed regions in term of incidence and mortality. However, these variations may relate to the availability of diagnostic facilities or imperfect mortality data. The highest incidence rate was reported in North America (7.4 per 100.000) while the lowest rate was observed in Middle Africa (1.1 per 100.000) (Ferlay et al., 2014). Globally, men and women have almost similar rate of incidence (52.6% vs 48.4%) and mortality (52.5% vs 48.5%) of PC (Ferlay et al., 2014).

1.1.1.2 Risk Factors

The mechanisms of pancreatic carcinogenesis are not fully characterised. However, the variations in PC incidence across the world suggest that some factors, such as age, tobacco smoking, genetic, lifestyle and environment, play a role in PC risk. PC risk factors have been divided into modifiable risk factors, non-modifiable risk factors and unclear risk factors.

1.1.1.2.1 Modifiable Risk Factors

Modifiable risk factors are flexible factors that can be modified by intervention. Changing personal behavioural/lifestyles can lead to a reduction in the probability of developing the disease (Burt, 2001).

1.1.1.2.1.1 Tobacco smoking

Tobacco smoking is consistently reported as a major risk factor for PC. A recent meta-analysis reviewed 117 reports to investigate all potential PC risk factors. The study found that tobacco smoking was the major risk factor associated with PC, and responsible for 11–32% of all PC cases with a relative risk factor (RR) of 1.85 (Maisonneuve and

Lowenfels, 2015). Another meta-analysis, that included 42 studies, showed a significant association between smoking intensity and PC risk (P<0.0001). Compared with non-smokers, RRs of smokers were 1.5, 1.9, 2.0, and 2.1, for 10, 20, 30 and 40 cigarettes/day respectively (Zou et al., 2014). In the United Kingdom, 28.7% (26.2 % Men, 31.0% women) of all PC patients are tobacco smokers (Parkin et al., 2011). A recent study tracked the smoking behaviour of 6,507 of PC patients and 12,890 controls. The study found that current cigarette smokers are associated with a 2-fold increased risk of PC compared to the controls. The risk is significantly increased with smoking up to 40 years (2.4-fold) (Bosetti et al., 2012). Moreover, a genetic study, including 750 million-base-pair DNA from 23,219 transcripts in 24 patients with pancreatic adenocarcinoma (PAD), revealed a significant increase (P=0.04) in the number of gene mutations of smokers PC patients (53.1 mutations/tumour) compared to non-smokers PC patients (38.5 mutations/tumour) (Blackford et al., 2009).

1.1.1.2.1.2 Overweight and obesity

Overweight and obesity have been previously reported as PC risk factors, and they may decrease the survival rate of PC patients. In the United Kingdom, 12.2% (12.8% men, 11.5% women) of all PC patients are overweight (body mass index (BMI) ≥ 25) (Parkin et al., 2011). A pooled analysis study of 14 cohorts included 846,000 individuals (843,865 controls, 2,135 diagnosed with PC) found that PC risk was 47% higher among obese (BMI ≥ 30) compared to controls (BMI was between 21 and 22.9) (Genkinger et al., 2011).

1.1.1.2.2 Non-modifiable Risk Factors

Non-modifiable risk factors are fixed factors that cannot be modified through intervention or changing the individual's behavioural/lifestyle. The probability of the disease is stable over a lifetime (Burt, 2001).

1.1.1.2.2.1 Age

As with most other cancers advancing age is the most important risk factor for developing PC. In the United Kingdom, 96% of PC patients were aged above 50 at the time of diagnosis (CancerResearchUK, 2017b). In the United States, the median age at diagnosis is 62 years, with 13.7% of cases developing before age 50, and less than 2% before age 40 (Hassan et al., 2007).

1.1.1.2.2.2 Family history

A family history has been associated with PC incidence. A self-reported questionnaire study found that 20.1% of 149 PC patients had at least one first-degree relative diagnosed with PC (Lucas et al., 2017). A meta-analysis study reviewed the family history of 6,568 PC patients. A two-fold increase in PC risk was seen in those individuals that had an affected relative (Permuth-Wey and Egan, 2009). A registry-based study reviewed the family history of 5,179 PC patients from 838 families and found that the risk of developing PC was increased 4.5, 6.4 and 32-fold for those families who have one, two and three or more relatives diagnosed with PC respectively (Klein et al., 2004). All studies have recommended developing screening and surveillance programs for high-risk population of PC based on their family history.

1.1.1.2.2.3 Pancreatitis

Chronic pancreatitis is a wide range of progressive fibro-inflammatory diseases of the exocrine pancreas that eventually leads to gland damage (Majumder and Chari, 2016). A meta-analysis study reviewed 12 case-control studies and 10 cohort studies and found that individuals with chronic pancreatitis and tropical chronic pancreatitis, a juvenile form of chronic calcific non-alcoholic pancreatitis, had a 13.3-fold and 50-fold higher risk of developing PC respectively. A historical study followed up 246 patients that were diagnosed with pancreatitis from 10 different countries, the study estimated the cumulative risk of PC is 40% in patients with hereditary pancreatitis at age 70. This

cumulative risk is increased to 75% in patients with paternal inheritance pattern (Lowenfels et al., 1997).

1.1.1.2.3 Unclear risk factors

1.1.1.2.3.1 Diabetes mellitus (DM)

DM is classified as a potential risk factor for PC. A recent study compared the prevalence of DM in PC patients compared to common cancers (100 patients each cancer). The study found that patients with PC had a significantly higher prevalence of DM (68%) compared to age-matched patients with lung (19.6%), breast (19.4%), prostate (14.8%) and colorectal cancers (20.7%) (Aggarwal et al., 2013). Another meta-analysis study that included twenty case-control and cohort studies found that the RR of PC for DM patients to controls was 2.1 (Everhart and Wright, 1995). However, several studies have suggested that DM can be caused by the PC itself. A meta-analysis study, including 35 cohorts, found that DM was associated with an increase in RR of PC (RR= 1.94). However, authors observed that the RR reduced with duration of diabetes (RR=5.38 for <1 year-duration, RR=1.95 for 1–4 year-duration, RR=1.49 for 5–9 year-duration, RR=1.47 for ≥10 year-duration) (Ben et al., 2011). In conclusion, the relationship between DM and PC is not fully clear.

1.1.1.2.3.2 Alcohol consumption

As the association of alcohol with PC risk may be confounded by other major risk factors of PC (particularly pancreatitis and tobacco smoking), this association is still unclear. A meta-analysis study, including 21 case-control studies and 11 cohorts studies, observed that individuals with heavy alcohol consumption (>3 drinks per day), independent of pancreatitis or tobacco use, have a 22% higher risk to develop PC compared to controls. Furthermore, the study found a strong evidence that moderate alcohol consumption (<3 drinks/day) did not affect pancreatic carcinogenesis (Tramacere et al., 2010). Another recent case-control study, including 1,367 individuals (384 PC patients and 983 controls),

found no association between PC risk and alcohol consumption, either the amount of consumption or type of alcohol (Yellow et al., 2017).

1.1.1.2.3.3 *Exposure to certain chemicals*

Certain types of chemicals have been associated with increased risk of developing PC. A recent clinical case-control study, including 4,445 individuals (2,353 controls and 2,092 PC patients) matched for cases on age, race, sex and state/region of residence, found that certain chemicals were significantly associated with development of PC: pesticides (odd ratio (OR)=1.21), asbestos (OR=1.54), benzene (OR=1.70) and chlorinated hydrocarbons (OR=1.63) (Antwi et al., 2015). However, another study of 1,147 individuals (504 PC patients, 643 controls) working in a chemical exposure environment found no significant associations between pesticides (OR=0.90) or N-nitrosamines (OR=0.85) and development of PC (Fritschi et al., 2015).

Other minor risk factors that seem to be associated with PC include *helicobacter pylori* infection, dietary mutagen exposure, physical activity and diet (Stolzenberg-Solomon et al., 2001, Li et al., 2007, Jiao et al., 2009, Wu et al., 2016).

1.1.2 Pancreatic cancer types

The pancreas, located in the abdomen between the stomach and the spine, is one of the largest glands in the human body. Macroscopically, it is divided into three anatomical sections: head (78%), body (11%) and tail (11%) (Figure 1.1) (Sener et al., 1999). The pancreas consists of two major components: the exocrine (98% of pancreatic tissue) and endocrine glands. Ducts and small sacs, called acini on the end of the ducts, are the main components of the exocrine gland that secrete specific enzymes into the digestive system via the small intestine. The Islets of Langerhans are the main component of the endocrine gland that secret insulin to control the sugar level in the blood. Pancreatic enzymes are secreted via the main pancreatic duct (ductus pancreaticus) and other secondary ducts (Sener et al., 1999). The main pancreatic duct joins common bile ducts

to form the ampulla of Vater (hepatopancreatic ampulla) which is situated in the second part of the duodenum (Rela M, 2014). Approximately 60-70%, 10-20% and 5-10% of PCs occur in the pancreatic head, body and tail respectively, with exocrine tumours are the most common type of PCs (de la Santa et al., 2014). PC consists of a mixed microenvironment of cellular and non-cellular elements. It is composed of several distinct factors including PC cells, PC stem cells and tumour stroma (Hidalgo, 2012). In the current project, as will be shown in Chapter 4, three types of tumour tissues (carcinomas of the pancreas, bile duct and ampulla) were used to study the association between expression of certain redox proteins and the clinicopathological criteria and patients' survival outcome.

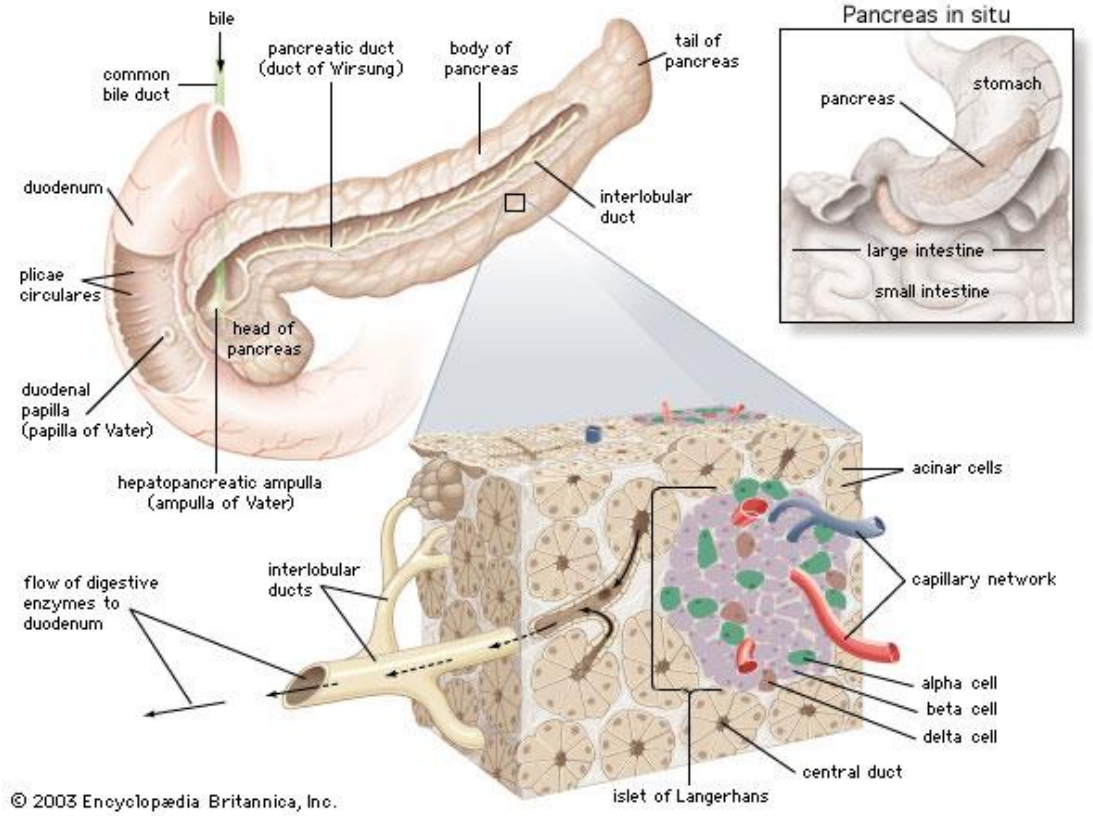


Figure 1.1: Structure of the pancreas. The main pancreatic ducts are: the principal duct (Wirsung's duct) that joins the pancreas to the common bile duct to supply pancreatic enzymes secreted from exocrine cells, the accessory duct (Santorini's duct) that can supply the second part of the duodenum with pancreatic enzymes and the distal common bile duct which joins with principal duct just prior to the ampulla of Vater. Source: Encyclopaedia Britannica, Inc., copyright 2003; used with permission.

1.1.2.1 Pancreatic ductal adenocarcinoma (PDAC)

Adenocarcinoma is a malignant tumour initiated in glandular epithelium: adeno means affecting a gland and carcinoma means cancer. Worldwide, PDAC is the most common type of adenocarcinoma representing 85% of all PCs, with a five-year survival of 6% (Siegel et al., 2014). PDAC is characterized by an early invasive mucin-producing, duct-forming epithelial neoplasm and lymph node metastases. The neoplastic glands usually invade nerves and vessels and can spread to the adjacent tissues. PDAC is typically a firm, white-yellow and poorly demarcated mass that changes the normal pancreatic structure. About 65% and 15% of PDAC arises in the proximal (head) and distal (body and tail) pancreas respectively (Lillemoe et al., 2000).

1.1.2.2 Other pancreatic cancer types

There are other types of PC representing 15% of all PCs: adenosquamous carcinoma, colloid carcinoma, hepatoid carcinoma, signet-ring cell carcinoma, medullary carcinoma, undifferentiated carcinoma and undifferentiated carcinoma with osteoclast-like giant cells. Figure 1.2 shows several representative histological pictures of different types of PC.

1.1.2.2.1 Adenosquamous carcinoma

Adenosquamous carcinoma represents 4% of all PCs (Madura et al., 1999). Histologically, adenosquamous carcinoma consists of two types of carcinoma cells: glandular adenocarcinoma and malignant squamous cell carcinoma making it a PC with a very poor prognosis. The median overall survival is 12 months, with aggressive behaviour, larger tumour size and more lymph node involvement (Katz et al., 2011).

1.1.2.2.2 Colloid carcinoma

Colloid carcinoma (mucinous noncystic carcinoma) is a rare pancreatic malignancy (1% of all PCs) occurring, frequently, in the head of the pancreas (Singhi et al., 2015). Colloid carcinoma was, historically, not well characterised pathologically. In the last decade, it

was often misdiagnosed as ductal adenocarcinoma. However, colloid carcinoma is associated with larger tumours, with lower stages and a relatively good prognosis (five-year survival is 57 months) (Adsay et al., 2001).

1.1.2.2.3 Hepatoid carcinoma (HC)

HC is a primary extrahepatic carcinoma with morphological and immunohistological evidence of hepatocellular differentiation. HC is extremely rare in the pancreas, and is more frequently reported in the stomach than other organs. The first pancreatic HC was seen in 1987, since then, few cases of pancreatic HCs were reported in the literature (Hruban et al., 1987). Due to lack of reported cases, the clinical behaviour, survival, and treatment are still unclear.

1.1.2.2.4 Signet-ring cell carcinoma

Signet ring cell carcinoma is an extremely rare PC type. To date, only seven cases have been reported (Radojkovic et al., 2017). However, signet ring cell carcinoma represents 15.7% and 0.45% of all gastric and colorectal cancers respectively (Maehara et al., 1992). Histopathologically, the nucleus moves to a side of the cancer cell due to pushing of the abundant intracytoplasmatic mucin. A tumour is diagnosed as a signet ring cell carcinoma when more than 50% of the cancer cells consist of this cell type (Shousha, 1982).

1.1.2.2.4 Undifferentiated carcinoma

Undifferentiated carcinoma was classified by the World Health Organisation (WHO) as a single category that includes osteoclast-like, osteoclastic or pleomorphic giant cell tumour, anaplastic carcinoma, sarcomatoid carcinoma and spindle cell carcinoma despite their histological differences. Occasionally, undifferentiated carcinomas may exist with osteoclast-like giant cells, this combination is classified by WHO as undifferentiated carcinoma with osteoclast-like giant (UCPOGC). This classification aims to distinguish UCPOGC from the plain undifferentiated carcinomas due to clinical and

histopathological distinctions between them (Bosman, 2010). UCPOGC cells are extremely rare, and occur in the pancreas more than in bile ducts and the ampullary regions with aggressive behaviour and poor prognosis (most patients died in 12 months) (Molberg et al., 1998, Paal et al., 2001).

1.1.2.2.5 Medullary carcinomas

Medullary carcinoma is rare in the pancreas. In the United States, medullary carcinoma represents 4% out of all PCs, with a two- and five-year survival rate of 29% and 13% respectively (Wilentz et al., 2000a). Histologically, medullary carcinoma has been described as a subset of adenocarcinoma that may have distinct pathogenesis (Goggins et al., 1998). Genetically, two studies showed, respectively, that 60% and 69% of pancreatic medullary carcinomas have wild-type K-Ras genes status with good prognosis and high overall survival (Goggins et al., 1998, Wilentz et al., 2000a). Therefore, medullary carcinoma may have a different carcinogenic pathway compared to most of the others pancreatic ductal carcinomas.

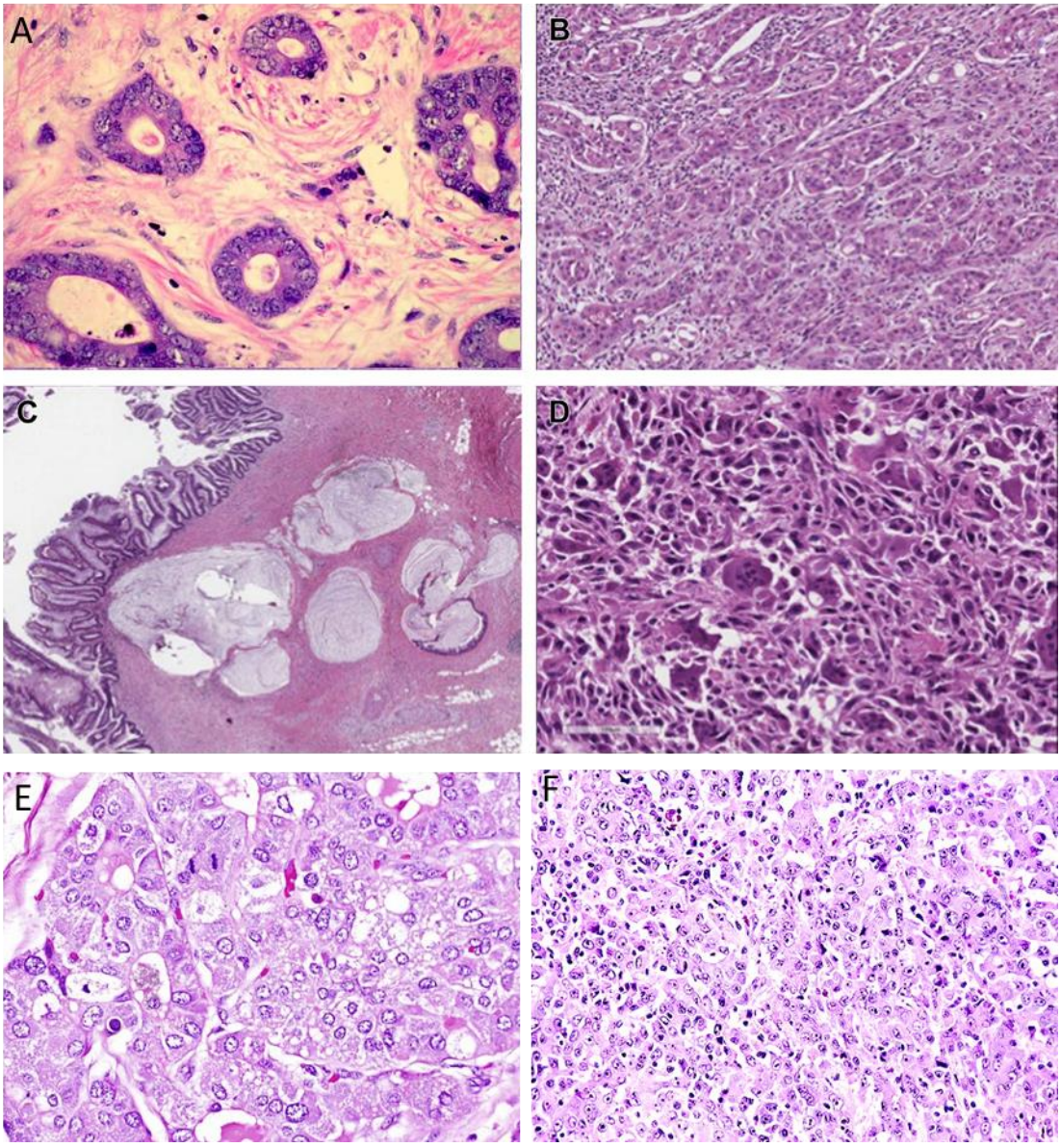


Figure 1.2: Representative histological pictures of different types of PC. PDAC (A), adenosquamous carcinoma (B), colloid carcinoma (C), UCPOGC (D), hepatoid carcinoma (E) and medullary Carcinoma (F). Adapted from: https://www.pathpedia.com (A), Luchini, C. et al. 2016. Pancreatic ductal adenocarcinoma and its variants. *Surgical pathology clinics*, 9(4), pp.547-560 (B, C and D), Chang, J. et al. 2016. Hepatoid carcinoma of the pancreas: case report, next-generation tumor profiling, and literature review. *Case reports in gastroenterology*, 10(3), pp.605-612 (E), Wilentz, R. et al. 2000. Genetic, immunohistochemical, and clinical features of medullary carcinoma of the pancreas: a newly described and characterized entity. *The American journal of pathology*, 156(5), pp.1641-1651 (F).

1.1.3 Symptoms

In general, early-stage PC is clinically silent. However, symptoms of PC become apparent after tumour invasion of adjacent tissues or metastasis and include abdominal pain, back pain, weight loss and maldigestion (Vincent et al., 2011). Weight loss and maldigestion can arise from anorexia and pancreatic ductal obstruction respectively (Alston et al., 2014). However, cancers arising in the head of the pancreas, considered as periampullary malignancies, such as ampulla, distal bile duct and duodenum cancers, can sometimes be diagnosed at earlier stages due to early symptoms (mainly obstructive jaundice). Conversely, cancers that arise in the body and tail of the pancreas are usually diagnosed at advanced stages due to the absence of earlier symptoms (Lillemoe et al., 2000).

Abdominal and back pain often present due to perineural and splanchnic neuronal compression of the adjacent tissues. In most cases, pain is a late symptom, and is associated with a lower chance of survival (Kelsen et al., 1997). In addition to abdominal pain, a recent study of 359 individuals (216 cases and 143 controls) found that weight loss and a rise in fasting glucose levels were significantly associated with PC 18 months before diagnosis (Sah et al., 2017). However, as mentioned earlier, the mechanism between DM and PC still unclear. In the United Kingdom, a recent study of 225 controls and 119 PC patients from 7 hospitals found a significant association between PC and several symptoms such as jaundice ($P<0.0001$), fatigue ($P=0.0001$), change in bowel habit ($P<0.0001$), weight loss ($P<0.0001$) and decreased appetite ($P=0{\cdot}0011$) (Walter et al., 2016). Occasionally, pancreatitis may present as a symptom due to the pancreatic-duct obstruction in PDAC patients (Vincent et al., 2011).

1.1.4 Diagnosis and staging

1.1.4.1 Diagnosis

Currently, a computerised tomography (CT) scan is the classical test to diagnose PC. Positron emission tomography/computed tomography (PET/CT) can provide more information for diagnosis, staging and prognostic evaluation of PC, but with no assessment of vascular invasion (Zhang et al., 2015). In contrast, contrast-enhanced CT (CECT) scanning is a recent and advanced diagnostic tool that can reveal the blood supply to the pancreatic mass, and provide clear images of the vascular invasion of tumours (Vargas et al., 2004). Furthermore, contrast-enhanced PET/CT is the most advanced examination that can provide better diagnostic information than classical PET/CT or CECT, and can provide details for presurgical assessment, evaluation of the resectability and diagnosis of postoperative recurrence (Buchs et al., 2011). Endoscopic ultrasound and CT-guided fine needle aspiration are cytological diagnostic tools that can be used to confirm radiology findings, with 80% sensitivity (Harewood and Wiersema, 2002). A recent study diagnosed 93 PC patients with CT and endoscopic ultrasound. The study found that both techniques agreed on mass detection (88%), mass size (67%), vascular invasion (74%) and lymph node involvement (82%) (Du et al., 2017). A biopsy specimen is not required when the radiological and cytological examinations confirm the occurrence of PC (Vincent et al., 2011).

Numerous studies have tried to identify molecular markers that could be used for PC diagnosis. A recent study found that the level of serum microRNA-192 (miR-192) was increased 5-fold in PC patients (n=10) compared to controls (n=40) with a sensitivity of 76% and a specificity of 55% (Zhao et al., 2013). Another study found a novel tumour-suppressive mRNA (miR-124) that was significantly highly methylated in PC tissues (n=10) compared to non-cancer tissues (n=10) (Wang et al., 2014).

1.1.4.2 Staging

The stage (describes the size of a tumour and how far it has spread from where it originated), grade (describes the appearance of the cancerous cells) and resection margin status of PC is defined by pathologic examination of the primary tumour. Pathologically, PC is classified according to TNM staging system: size of the primary pancreatic tumour (T), nearby lymph node involvement (N) and distant metastases (M) (Edge and Compton, 2010).

As Table 1.1 shows, a PC tumour is classified as T0 when confined to the top layers of pancreatic ductal cells and has not invaded deeper tissues or not spread outside of the pancreas. Small PC size (<2 cm) is classified as T1 representing 10% of all PCs and 4.5% of all metastatic PC. Nearly 90% of PCs are larger than 20 mm and classified as T2. Advanced stages have local extra pancreatic spread without (T3) or with (T4) involvement of adjuvant blood vessels. Stage I PC have lesions that are either small (stage 1A) or large (stage IB) and localised in the pancreas. Stage II lesions have spread-out of the pancreas without (stage IIA) or with (stage IIB) lymph node involvement. Stage III lesions involve adjacent major blood vessels, which decrease the probability of tumour surgical resection. Stage I, II and III show no sign of metastasis (M0), while stage IV cancers have distant metastases (M1), and are usually unresectable (Chari et al., 2015).

Stage	Primary tumour (T)	Regional lymph nodes (N)	Distant metastases (M)	Descripition
0	Tis	N0	M0	The tumour is confined to the top layers of pancreatic duct cells and has not invaded deeper
IA	T1	N0	M0	Limited to pancreas ≤ 2 cm.
IB	T2	N0	M0	Limited to pancreas > 2 cm.
IIA	T3	N0	M0	Extends beyond pancreas, but does not involve arteries.
IIB	T1-3	N1	M0	Any tumour with artery involvement with LN+.
III	T4	Any N	M0	Tumour involves arteries (may not resectable).
IV	Any T	Any N	M1	Any tumour with distant metastases.

Table 1.1: TNM staging system of PC. Data collected from: The American Joint Committee on Cancer (AJCC) TNM staging system. https://cancerstaging.org/references-tools/quickreferences/Documents/ PancreasSmall.pdf. Last update: 19 June2018.

Histologically, early disease manifests as distinctive precursor lesions. As most pancreatic malignancies are diagnosed in advanced stages, the identification of the precursor lesions can aid identification of the genomic features that cause progression to advanced stages, in addition to developing effective screening and targeted therapies for earlier stage malignancies (Eser et al., 2011).

1.1.4.2.1 PC precursor lesions

PC precursor lesions are divided into solid and cystic, mucinous and nonmucinous, benign or with a malignant potential of different degrees (Fric et al., 2017). The most common precursor lesions are the microscopic pancreatic intraepithelial neoplasia (PanIN), followed by macroscopic cysts; namely, the intraductal papillary mucinous neoplasm (IPMN) and the mucinous cystic neoplasm (MCN) (Matthaei et al., 2011).

PanINs are frequent lesions arising in small branch ducts (<5mm). Non-invasive PanIN lesions are classified into three grades according to the intensity of cytological and architectural alterations (Fric et al., 2017):

1- *PanIN1*: PanIN1 exists in 40% of normal pancreatic tissues with minimal alterations, and is classified into PanIN1a (flat lesion) and PanIN1b (micropapillary type) with minimal alterations.
2- *PanIN2*: PanIN2 has mild to moderate alterations including additional loss of polarity, nuclear crowding and cell enlargement.
3- *PanIN3*: PanIN3 is an advanced lesion with manifest epithelial cell budding into the lumen or luminal necrosis.

IPMN is a macroscopic lesion that has neoplastic papillary proliferation, secretion of mucin and duct dilation, and is located in the head of the pancreas in communication with the ducts. IPMN is slightly more in men than women (~3:2 ratio) and is classified into three stages: mild, moderate and high (Matthaei et al., 2011). IPMN stages can develop gradually and transform into invasive pancreatic ductal adenocarcinoma. IPMN has three types: main-duct IPMN (MD-IPMN), branch-duct IPMN (BD-IPMN) and the

mixed-type MD-IPMN. MD-IPMN is the most common type with poor prognosis, and is characterised by a dilation of the main duct (>5mm), while BD-IPMN is less common with a favourable prognosis, and is accompanied by symptoms of pancreatic irritation (Fric et al., 2017).

MCN is a mucin-secreting cystic epithelial neoplasm that has no contact to the ducts. MCN almost always occurs in the body and tail of the pancreas, and more frequent in women (98.1%), with a five-year survival of 96.6% (Yamao et al., 2011). Most MCNs are large (~10 cm) and contain thick mucin. About 33% of large resected MCN lesions are associated with invasive carcinoma (Wilentz et al., 1999). However, recent reports showed reduced frequency to 4-15% due to incidental diagnosis (Crippa et al., 2008, Yamao et al., 2011).

1.1.5 Mutations in pancreatic cancer

PC accumulates multiple genetic alterations. A genetic study analysed the sequences of 23,219 transcripts representing 20,661 protein-coding genes in 24 PCs. The study observed 63 genetic alterations in PC that involve in 12 cellular signalling pathways (Jones et al., 2008). Four genes were identified as driver genes in PC: KRAS (v-Ki-ras2 Kirsten rat sarcoma viral oncogene homolog), TP53 (Tumour Protein P53), CDKN2A (cyclin-dependent kinase Inhibitor 2A) and DPC4 (Deleted in Pancreatic Cancer-4) (Iacobuzio-Donahue, 2012).

A recent study found that 37% of PC patients have mutations in all four driver genes, and that a low number of altered driver genes was significantly associated with disease-free survival (P=0.008), overall survival (P=0.041) and absence of metastasis (P=0.002) (Yachida et al., 2012). Another study investigated the genetic mutations KRAS, CDKN2A, p53, and DPC4 in 42 pancreatic adenocarcinomas. It found that all pancreatic adenocarcinomas had a KRAS mutation. In addition, 38%, 38%, 15% and 8% of all PCs had four, three, two and one altered genes with a high concordance with DPC4 and CDKN2A mutations (P=0.007) (Rozenblum et al., 1997).

1.1.5.1 Genetic mutations

1.1.5.1.1 KRAS

Mutations of the KRAS oncogene are the most common genetic abnormality in PC that approaches about 90% of all PCs (Caldas and Kern, 1995). The RAS proteins (H-, K- and N-RAS) are guanine nucleotide binding proteins that can transmit signals from cell surface receptors and alter guanosine diphosphate-bound (GDP-bound) (inactive form) to guanosine triphosphate-bound (GTP-bound) (active form). Wild-type KRAS is in an inactivated state in non-dividing cells, and is temporarily activated during cell division. However, mutations in codons 12, 13 and 61 constitutively activate KRAS lead to accumulation of the GTP-bound (active form) resulting in induction of multiple signalling pathways involved in cell proliferation, survival, differentiation and gene expression (Malumbres and Barbacid, 2003, Zeitouni et al., 2016).

1.1.5.1.2 TP53

TP53 is a well-characterized tumour suppressor gene residing on chromosome 17p that is involved in regulation of the cell cycle (maintenance of the G2/M arrest), DNA repair (DNA binding protein) and apoptosis (inducer of cell death). Therefore, mutant TP53 in PC cells leads to uncontrolled cellular proliferation, genomic instability, impaired cell cycle regulation and inhibition of apoptosis (Lillemoe et al., 2000). Three genetic-based studies showed that TP53 mutations were present in 88%, 75% and 67% of all pancreatic adenocarcinomas respectively (Berrozpe et al., 1994, Moore et al., 2003, Kanda et al., 2013).

1.1.5.1.3 CDKN2A

CDKN2A (also known as p16 or p16INK4a) is another tumour suppressor gene, residing on chromosome 9, and encodes a protein, p16, that inhibits two cyclin D–dependent kinases (CDK4 and CDK6) leading to prevention of progression through the G1 cell cycle checkpoint. CDKN2A also encodes another protein, p14, that has negative regulatory

effects on growth as it serves to stabilize p53 (Bardeesy and DePinho, 2002). Approximately, 85% of all PAD have CDKN2A inactivation (Caldas et al., 1994). Furthermore, CDKN2A mutation can cause familial atypical mole-malignant melanoma (FAMMM) syndrome, which is identified as a risk factor of PC (Vasen et al., 2000).

1.1.5.1.4 DPC4

DPC4 is a tumour suppressor gene that encodes SMAD4 (small mothers against decapentaplegic homolog 4) protein. The SMAD4 protein plays an important role in signalling through the transforming growth factor-β (TGF-β) pathway, and controls cell growth, proliferation, differentiation and apoptosis. The DPC4 mutation in PC cells can abrogate the SMAD-dependent TGF-β signalling pathway leading to a selective growth advantage (Madura et al., 1999). SMAD4 and aldehyde dehydrogenase 1A1 (ALDH1A1) are inversely expressed in human pancreatic cells. TGF-β negatively regulates ALDH1A1 expression in a SMAD4-dependent manner, and in turn impairs the activity of pancreatic cancer-initiating cells (Hoshino et al., 2015). DPC4 inactivation occurs in 48% of all PC patients (Schutte et al., 1996). Garcia and colleagues showed that knocking out Smad4 in the exocrine compartment was responsible for enhanced PanIN formation (Garcia-Carracedo et al., 2015). A clinical phase II trial found a significant association between the pattern of disease progression of PC patients treated with chemotherapy and intact/loss of SMAD4 expression (P=0.016) (Crane et al., 2011).

1.1.5.1.5 Other mutations

In 2012, new additional genes were identified as driver genes in PC, including Acvr2a and Map2k4 (Mann et al., 2012). A recent study provided the most comprehensive molecular characterisation, to date, of the genomic alterations in PC by performing whole-genome sequencing and copy number variation analysis of 100 PDACs. The study found three new genes involved in PDAC, in low prevalence**:** KDM6A, PREX2 and RNF43 which were inactivated in 18%, 10% and 10% of all PDACs respectively (Waddell et al., 2015). Moreover, other mutated genes can be found in a small number of PCs (<20%)

including tumour-suppressor genes such as STK11, TGFBR1, TGFBR2, FBXW7 and EP300 and oncogenes such as GNAS, BRAF, MYB, AKT2 and EGFR (Jones et al., 2008).

1.1.5.2 Genetic instability in precursor lesions

As shown in Figure 1.3, gene mutations in PC are correlated with one or more precursor lesions of PC. Activating mutations in KRAS exist in more than 99% of low-grade PanIN lesions (Kanda et al., 2012). A meta-analysis study included 15 studies that examined 1,519 PC lesions and found that KRAS mutations were detected in 36%, 44% and 87% of PanIN-1A, PanIN-1B and high-grade PanIN lesions (PanIN-2 and PanIN-3) respectively (Löhr et al., 2005). Another study investigated KRAS mutations in 169 PanINs lesions (50 PanIN-1A, 52 PanIN-1B, 45 PanIN-2 and 22 PanIN-3 lesions) from 89 patients. The study found that KRAS mutation was detected in 92.0%, 92.3%, 93.3 and 95.4% of PanIN-1A, PanIN-1B, PanIN-2 and PanIN-3 lesions with no evidence of KRAS mutations detected in normal tissues (Kanda et al., 2012). Several genetic alterations identified in invasive PADs are also present in PanINs, with evidence of increasing prevalence of these alterations with PanIN-2. A recent study, of 180 PC patients, detected TP53 mutations in 9.1%, 17.8%, 38.1%, 47.6% and 75% of intermediate-grade IPMNs, PanIN-2 lesions, high-grade IPMNs, PanIN-3 lesions and invasive pancreatic adenocarcinomas respectively. However, no TP53 mutations were detected in PanIN-1 lesions or low-grade IPMNs (Kanda et al., 2013).

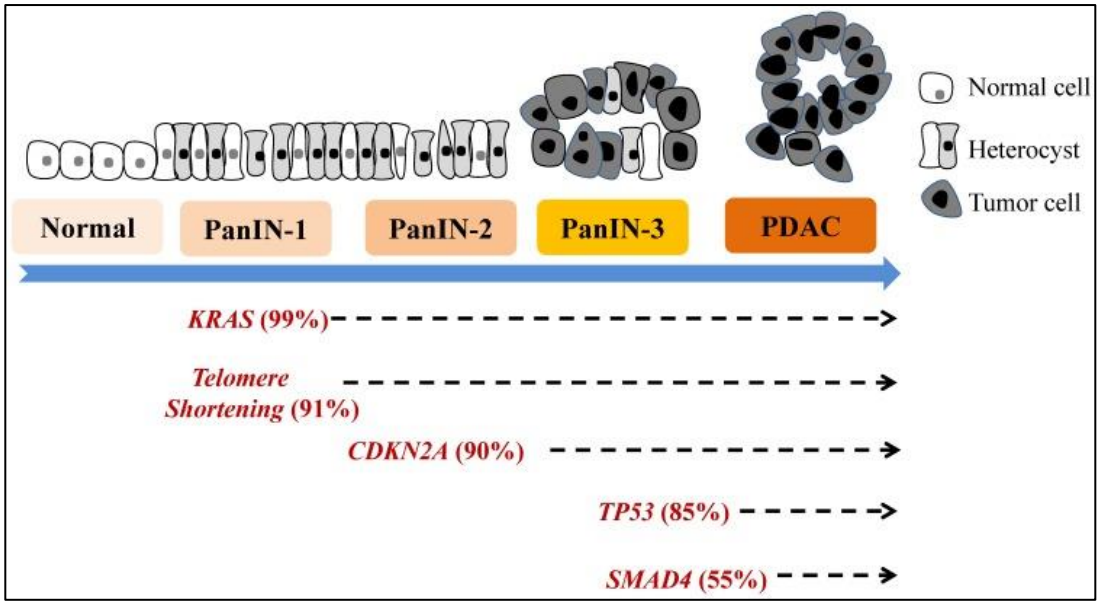


Figure 1.3: Genetic progression model of pancreatic carcinogenesis. The main molecular alterations that accumulate during pancreatic carcinogenesis can be classified as early (activating KRAS mutations), intermediate (inactivating mutations or epigenetic silencing of CDKN2A), and late (inactivating mutations of TP53 and SMAD4) genetic events. These genetic alterations are distributed heterogeneously in PanIN lesions. Source: Guo, J., Xie, K. and Zheng, S., 2016. Molecular biomarkers of pancreatic intraepithelial neoplasia and their implications in early diagnosis and therapeutic intervention of pancreatic cancer. *International journal of biological sciences*, 12(3), p.292; used with permission.

Similarly, a historical study analysed 33 PanINs and found that CDKN2A expression was absent in 30%, 27%, 55% and 71% of PanIN-1A, PanIN-1B, PanIN-2, and PanIN-3 lesions (Wilentz et al., 1998). Interestingly, another study found that CDKN2A and SMAD4 were inactivated in 100% and 38% of all IPMNs respectively (Biankin et al., 2002). An immunohistochemical study stained DPC4 marker in 188 PC duct lesions (82 PanIN-1A, 54 PanIN-1B, 23 PanIN-2 and 29 PanIN-3) from 40 PC patients. It found 100% of all lesions in PanIN-1A, PanIN-1B and PanIN-2 (low-grade) express DPC4. However, only 69% of PanIN-3 (high-grade) lesions expressed DPC4. The difference in DPC4 expression between low-grade and high-grade duct lesions was statistically significant ($P<0.0001$) (Wilentz et al., 2000b).

In contrast to PanIN and IPMN lesions, the genetic alterations in MCN lesions have not been well characterised. However, a recent study characterised the genomic alterations

of the neoplastic epithelium of 25 MCNs (16 MCNs with low-grade dysplasia and 9 high-grade with dysplasia or invasive carcinomas). The study found that KRAS mutations were present in 19% and 100% of low and high MCNs grades respectively. TP53 and CDKN2A mutations were present in 56%, for both, of high MCNs grades, with no mutations were detected in low MCNs grades (Conner et al., 2017).

1.1.6 Treatments and Survival

The main PC treatment types are surgery, chemotherapy and radiotherapy. However, treatment for PC differs between the United Kingdom and the United States (Tempero et al., 2011). Adjuvant radiotherapy is more commonly employed in the United States than in Europe and the United Kingdom, while combination chemotherapy is used more commonly in Europe and the United Kingdom than in the United States. Gemcitabine (GM) remains standard first-line chemotherapy in both continents as discussed later (Tempero et al., 2011).

Current treatment options for PC have failed to improve the five-year survival rate over the last 30 to 40 years. There is, therefore, an urgent need for new therapies. Several promising studies are ongoing to identify novel treatments for PC patients including novel chemotherapies/formulations, immunotherapies, cancer vaccines, targeting core pathways and novel combinations against the immunosuppressive tumour (Chiorean and Coveler, 2015).

1.1.6.1 Surgery

Surgical staging systems classify PC into resectable (resectable and borderline resectable) and unresectable (locally advanced pancreatic cancer (LAPC) and metastatic disease). LAPC is non-metastasized cancer but is also unresectable due to the involvement of the coeliac trunk or superior mesenteric artery (stage III disease) (Rombouts et al., 2015). Most of PCs at T1 to T3 stages are resectable, while T4 tumours that affect the celiac axis or superior mesenteric artery are unresectable. Generally,

operative mortality from pancreatic resection surgery is very low (1%) (Cameron et al., 2006).

Surgical resection is the best treatment for PC with a 5-survival rate of 23.4% (Sener et al., 1999). Unfortunately, only 10-20% of patients are eligible for resectable surgery while around 80% are unresectable due to metastasis (stage IV) (40%) or due to LAPC (40%) (Bilimoria et al., 2007, Gillen et al., 2010). Another study confirmed the previous data and showed that 20% of PCs were resectable at time of diagnosis, while the remaining 80% were unresectable, either due to metastasis (50%) or due to proximity to nearby vascular structures (30%) (Malik et al., 2012). However, a recent study followed up 10,595 PC patients, between 2009 and 2013, found that the proportion of case-eligible resectable surgery increased from 19.9% to 27.0% due to novel neoadjuvant treatments such as FOLFIRINOX, as discussed later (van der Geest et al., 2017). A recent review of diagnostic studies showed that diagnostic laparoscopy following CT may significantly reduce the number of patients undergoing surgical exploration without resection (Allen et al., 2016).

There are four different types of operations for PC patients: (1) Whipple's operation (pancreaticoduodenectomy) that includes removing the head of the pancreas, the lower end of stomach, the duodenum and part of bile duct, (2) Pylorus-preserving pancreaticoduodenectomy (PPPD) which is similar to a Whipple's operation but none of the stomach or duodenum is removed, (3) distal pancreatectomy that includes removing the body and tail of the pancreas and the spleen, and (4) total pancreatectomy that involves removing the whole pancreas, the duodenum, the gall bladder, part of the bile duct and part of the stomach (Bachmann et al., 2006). Several studies tried to develop different surgical techniques to decrease pancreaticoduodenectomy complications that include pancreatic anastomotic leaks and delayed gastric emptying. However, these trials have not shown any advantage of one technique over another (Vincent et al., 2011).

Furthermore, palliative surgery can enhance life quality of patients at advanced stages, with no curative intent. The palliative surgery removes the whole pancreas and other adjuvant tissues. Palliative surgery aims to relieve symptoms or to prevent certain complications such as obstructive jaundice, severe pain and gastric outlet obstruction (Scheufele and Friess, 2017).

1.1.6.2 Chemotherapy

Chemotherapy aims to target both primary lesions and micrometastatic disease at distant sites of a tumour. Chemotherapy in PC is utilised either as a single treatment (as preferred in Europe and the United Kingdom) or in combination with radiation as adjuvant/neoadjuvant treatment (as applied in the United States). Local disease progression can occur after 3 months of systemic chemotherapy in 29% of advanced PC patients (Huguet et al., 2007). Unfortunately, chemotherapy is associated with serious side effects which can affect overall health status and life quality of the patients. The main side effects of PC patients treated with chemotherapy are dry mouth, constipation, urinary retention, blurred vision, orthostatic hypertension, dizziness, peripheral oedema and somnolence (Koulouris et al., 2017).

1.6.2.1 Chemotherapy regimens

1.1.6.2.1.1 G*emcitabine (GM)*

GM is chemotherapeutic agent that has been used against cancer cells for more than 20 years (Plunkett et al., 1996). Currently, GM is a standard first-line chemotherapy treatment for locally advanced and metastatic PC (Vincent et al., 2011). In addition to PC, GM has been also used to treat different types of solid cancer, including ovarian, breast and non-small cell lung cancers, in combination with the platinum-based drugs such as cisplatin and carboplatin (Nagourney et al., 2008, Reck et al., 2009, Luchini et al., 2016).

Chemically, GM (20,20-difluoro-20-deoxycytidine; dFdC) is a deoxycytidine analogue, with multiple mechanisms of action in tumour cells (de Sousa Cavalcante and Monteiro, 2014). Briefly, GM (dFdC) is a prodrug, and is activated intracellularly by deoxycytidine kinase (dCK) to produce GM monophosphate (dFdCMP), then, it is phosphorylated again by pyrimidine nucleoside monophosphate kinase (UMP-CMP kinase) to produce GM diphosphate (dFdCDP, the main active form of GM) (Heinemann et al., 1988, Bouffard et al., 1993).

The main mechanism of action for GM is known as “masked chain-termination”; during DNA synthesis, DNA polymerase incorporates the dFdCDP into DNA. After the dFdCTP is incorporated, a single deoxynucleotide is also incorporated, occurs next to the dFdCDP incorporation, into the single DNA strand, making the DNA polymerases unable to proceed (Figure 4.1A) (Gandhi et al., 1996).

An additional mechanism of action for GM is known as “GM self-potentiation” (Figure 4.1B). This mechanism is based on the ability of GM to create covalent bonds with the active site of ribonucleotide reductase leading to inhibit deoxycytidylate deaminase (dCTD), one of the main enzymes in the deoxynucleotide metabolism and the cellular deoxynucleotide triphosphate (dNTP) pool balance. The inhibition of dCTD makes GM more likely to be activated by nucleotide metabolizing enzymes, and therefore incorporated into DNA (Heinemann et al., 1992).

GM treatment is not always effective. In certain cases, the fibrotic stroma, in particular hyaluronan (HA), surrounding the tumours seems to block GM penetration, and leads to tumour survival (Mahadevan and Von Hoff, 2007). Therefore, therapies that target the fibrotic stroma, such as hyaluronidase treatment, are being developed and entering clinical trials in combination with GM (Hingorani et al., 2016, Doherty et al., 2018).

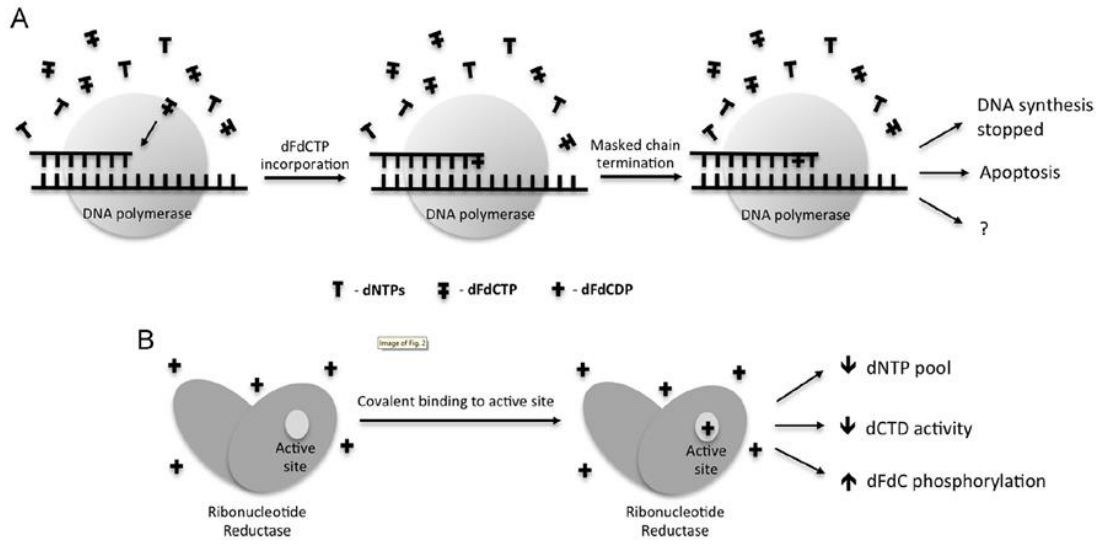


Figure 1.4: GM mechanisms of action. (A) Masked chain-termination mechanism; during DNA synthesis, DNA polymerase incorporates dFdCTP and, subsequently, single deoxynucleotide into DNA strand, making the DNA polymerase unable to proceed and then chain elongation is stopped. (B) GM self- potentiation; covalent binding of dFdCDP leads to inactivate ribonucleotide reductase. Inhibition of ribonucleotide reductase decreases dNTP pool and dCTD activity, making GM more likely to be activated by nucleotide metabolizing enzymes and therefore incorporated into DNA. Source: de Sousa Cavalcante, L. and Monteiro, G., 2014. Gemcitabine: metabolism and molecular mechanisms of action, sensitivity and chemoresistance in pancreatic cancer. *European journal of pharmacology*, 741, pp.8-16.; used with permission.

1.1.6.2.1.2 Other *chemotherapy regimens*

In addition to GM, various combinations of chemotherapy regimens such as oxaliplatin, irinotecan, fluorouracil and leucovorin are being tested in clinical trials (Smyth et al., 2015). A clinical study, that included 342 patients with metastatic PC, found that FOLFIRINOX (a chemotherapy mixture of oxaliplatin, irinotecan, leucovorin, and fluorouracil) was strongly associated with a survival advantage (median overall survival was 11.1 months) compared to GM (median overall survival was 6.8. months) or other single chemotherapy regimens (Conroy et al., 2011).

1.1.6.2.2 Adjuvant/neoadjuvant regimens

Adjuvant treatment is surgery followed by chemotherapy and/or radiotherapy to decrease the probability of recurrence. Adjuvant treatment is recommended 1–2

months after surgery with curative intent (O'Reilly, 2010). Two clinical studies found that the adjuvant treatment with a GM and capecitabine combination yielded a better response and increased overall survival rate compared with GM alone (Herrmann et al., 2007, Cunningham et al., 2009). Another recent study (n=730 resected PC patients, grade 3-4) confirmed previous studies and found that the median overall survival for PC patients treated with GM plus capecitabine or GM alone was 28.0 and 25.5 months respectively. The study recommended that the adjuvant combination of GM and capecitabine should replace treatment with GM alone, and become standard first-line chemotherapy following resection of PC (Neoptolemos et al., 2017). In contrast to adjuvant treatment, neoadjuvant/preoperative therapy can downstage 30% of unresectable locally advance PCs to be surgically resectable. In addition, neoadjuvant therapy can achieve similar median overall survival compared to patients who are initially resectable but without any preoperative treatment (Gillen et al., 2010).

1.1.6.3 Radiotherapy

1.1.6.3.1 Interaction of radiation with matter

Biologically, and assuming that the DNA is the 'target' molecule for radiation-induced damage, the effect of ionising radiation can be divided into direct and indirect effects. Ionizing radiation can directly damage the DNA by causing one or more of the following effects: base nucleotide damage, single-strand break (SSB), double-strand break (DSB) and clustered DNA damage. The indirect effect of radiation is characterised by the interaction of the radiation with other molecules, such as water that comprises 80% of a living cell. The indirect effect is responsible for two-thirds of total radiation effects (DNA damage) on the living cell (Lasnitzki, 1947), and mediated primarily via the radiolysis of water that can produce reactive oxygen species (ROS), toxic molecules such as the hydrated electron and hydroxyl radical, by a number of complex interactions including the following reactions (Samuel and Magee, 1953):

$$H_2O \rightarrow H_2O^+ + e^- \quad (1)$$

$$H_2O^+ + H_2O \rightarrow H_3O^+ + {}^{\bullet}OH \quad (2)$$

The hydroxyl radical is a highly reactive molecule that can attack molecules causing major damage to DNA, lipids and proteins. The types of ROS molecules and their effects on critical cellular targets are discussed in Section 1.2.1.

1.1.6.3.2 Basics of radiotherapy treatment

The main goal of radiotherapy is to enhance the radiation therapeutic ratio, which is defined by maximising radiation dose, and damage, to tumours in order to achieve highest tumour control probability (TCP), whilst minimising radiation dose to nearby healthy organs to achieve the lowest normal tissue complication probability (NTCP) (Eric J. Hall, 2012). The concept of the therapeutic ratio is illustrated in Figure 1.5, which shows theoretical dose-response curves for tumour control and normal tissue complication (Tannock, 2005, Khaled and Held, 2012).

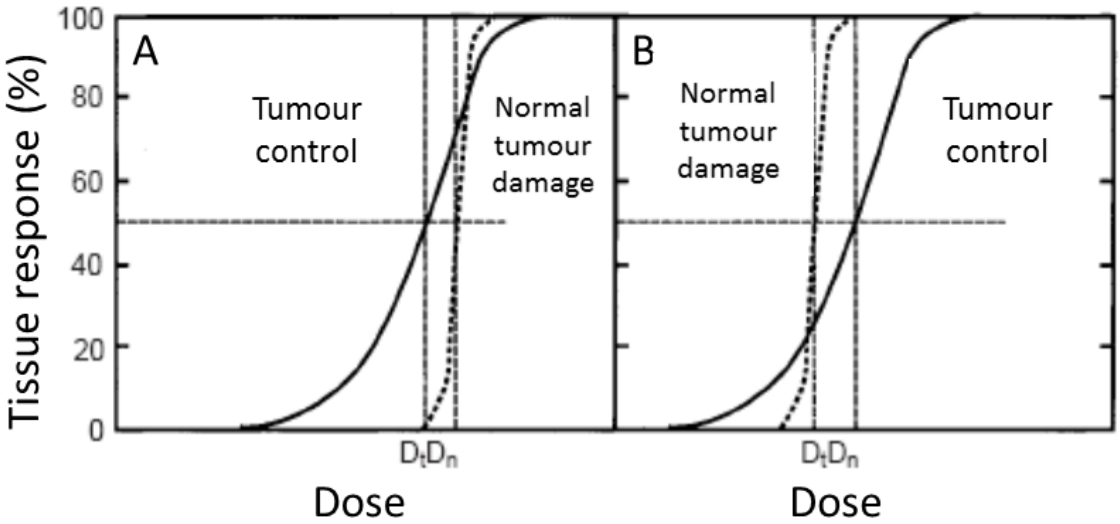


Figure 1.5: Illustration of the concept of a therapeutic ratio in terms of dose-response relationships for tumour control and normal tissue damage. Adapted from: TANNOCK, I. F. 2005. The basic science of oncology, McGraw-Hill.

Clinically, the therapeutic ratio is often defined as the percentage of tumour cures that are obtained at a given level of normal tissue complications, In vivo studies, the

therapeutic ratio is the ration of radiation doses D_{normal}/D_{tumour} required to produce a given percentage of complications and tumour control (usually 50%). As shown in Figure 1.5A, the curve describes a favourable therapeutic ratio as the tumour-control curve is displaced to the left of that for normal tissue damage. The greater this displacement, the more curable is the tumour. However, if the two curves are close together (As shown in Figure 1.5B) or the curve for tumour control is displaced to the right of that for complications, the therapeutic ratio is unfavourable because a high level of complications must be accepted to achieve even a minimal level of tumour control (Tannock, 2005, Khaled and Held, 2012).

Conventional radiation therapy uses low linear energy transfer (LET) radiation such as gamma rays and X-rays, produced by linear accelerators (LINAC's), and is known as external beam radiotherapy (EBRT). LET describes the amount of energy deposited by the radiation as it passes through an absorber, and has the units of keV/μm. Conventional RT is normally delivered in multiple small fractions (1.8-2 Gy), once a day (Monday-Friday), for a number of weeks, with the total dose delivered varying across different tumour types. Two-dimensional radiotherapy (2DRT) was historically the standard of care for conventional radiation therapy, however, advances in imaging and computer technology have enabled transition to 3-dimensional conformal radiotherapy (3-D CRT) that shapes the radiation beams to match the shape of the tumour (Purdy and Emami, 1995). Over the last couple of decades, technical improvements in radiation therapy delivery have been achieved such as intensity modulated radiotherapy (IMRT), image-guided radiotherapy (IGRT), 4-dimensional radiotherapy (4D-RT), stereotactic body radiotherapy (SBRT) and MRI linear accelerator (MRI-LINAC) based radiotherapy. IMRT is an advanced technique of high-precision radiotherapy that can modulate the intensity of the radiation dose within a given radiation field (Chui et al., 2001). IGRT uses CT-image scanning systems to verify tumour position prior or during radiotherapy (Kuriyama et al., 2003), and can integrate it with cone-beam computed tomography (CBCT) to give higher spatial resolution, sufficient soft-tissue contrast and repeated low dose images preceding, not during, a treatment course (Yan et al., 2013). 4D-RT avoids

the effect of the temporal changes in tumour position during the delivery of radiotherapy, and is mainly used to treat lung cancer (Keall, 2004). SBRT administers very high doses of radiation, using several beams of various intensities at different angels to precisely target the tumour (Timmerman et al., 2007). MR-LINAC RT uses a hybrid linear accelerator (linac) combined with a magnetic resonance imaging (MRI) scanner and allows for optimal imaging of tumours and organs-at-risk (OARs) during radiation delivery. It enables the LINAC to dynamically reconstruct each beam dose and calculate the corresponding anatomical changes over the beam delivery time (Lagendijk et al., 2008, Raaymakers et al., 2009). These advanced technologies of low LET radiotherapy increase TCP, by increasing the intensity of radiation delivery to tumours, and decrease the toxicity to healthy tissues (NTCP) by reducing margins for uncertainty and tumour motion.

High LET radiation, such as proton and heavy ion radiation, shows physical and biological advantages compared to conventional radiotherapy. It aims to increase tumour cell killing and minimize adverse effects of radiation to normal tissues using small number of radiation fractions. Briefly, due to large mass of high-LET particles, compared with electrons and photons, they travel in straight trajectories as they penetrate the human body (Bragg and Kleeman, 1905). When the high LET particles pass the entrance field, where normal tissues are usually exposed, they slow down due to collisions with electrons in matter (normal tissues) and release small amounts of energy along the track. This is referred to as the Bragg plateau (Figure 1.6A) (Bragg and Kleeman, 1905). However, when the high LET particles approach the end of their range, they begin to decelerate rapidly, depositing a large amount of energy in a very short distance, with little or no radiation dose received beyond this distance. This is referred to as the Bragg peak (Figure 1.6B), first described by Bragg and colleagues in 1905 (Bragg and Kleeman, 1905). However, low LET-radiation deposits energy in tissue in a highly dispersed manner (Figure 1.6C) (De Laney and Kooy, 2008).

Several reports showed that proton therapy may allow for the delivery of standard radiotherapy doses to PC while significantly reducing exposure to surrounding critical normal tissues. A comparison study between proton (n=2) and X-ray therapy (n=2) in PAD patients showed that proton therapy significantly reduced radiation dose received by the spinal cord (P=0.003), left kidney (P=0.025), right kidney (P=0.059), and liver (P=0.061) compared to X-ray therapy (Hsiung-Stripp et al., 2001). Another clinical study (phase I) showed that proton therapy offered a significant reduction of radiation dose to the liver, kidneys and small bowel compared to IMRT (Kozak et al., 2007). Furthermore, in solid tumours, including PC, it has been established that as the LET radiation increases, so the oxygen enhancement ratio (OER) decreases (OER is the enhancement of therapeutic or detrimental effect of ionizing radiation due to the presence of oxygen) (Barendsen, 1968). Hypoxia in PC will be discussed, in details, in Chapter 3 (Section 3.2.2.3).

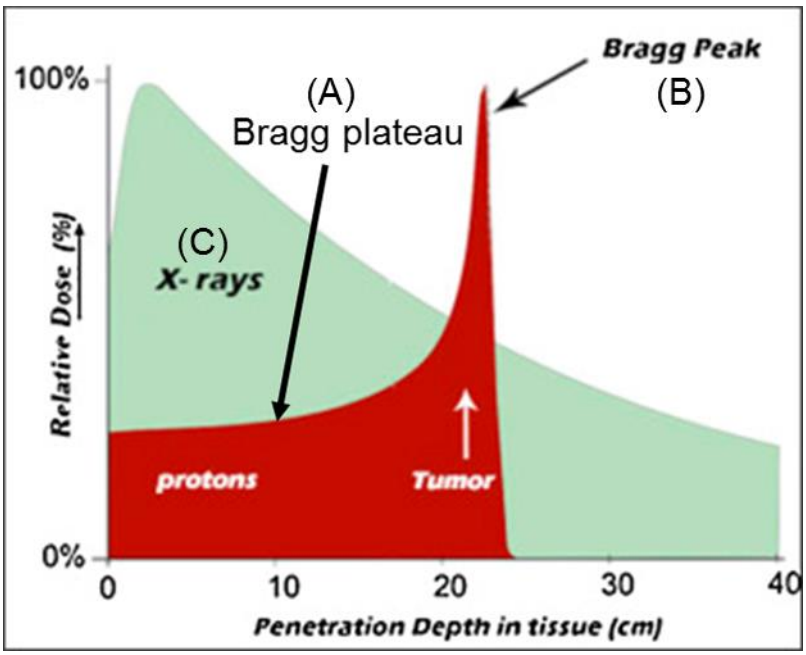


Figure 1.6: Comparison of the depth dose profiles of high energetic photons and protons. Protons show the characteristic inverse depth dose profile (Bragg peak). Adapted from: Desouky, O. and Zhou, G., 2016. Biophysical and radiobiological aspects of heavy charged particles. Journal of Taibah University for Science, 10(2), pp.187-194.

However, high-LET radiotherapy is expensive, with a limited number of particle therapy facilities worldwide (32 proton therapy facilities and 6 heavy ion therapy facilities) (Loeffler and Durante, 2013). However, several clinical trials showed that high-LET based radiation therapy showed no survival advantage over recent advanced techniques of low LET radiation (Zietman et al., 2005, Talcott et al., 2010, Zietman et al., 2010). Response to radiotherapy is not always successful due a variety of potential reasons, including radioresistance, that may be acquired (during treatment) or be inherent. The mechanisms of radioresistance are discussed, in detail, in Section 1.1.6.3.3. However, at a basic level, success or failure of conventional radiotherapy is associated with the four R's of radiotherapy; repair of DNA damage, redistribution of cells in cell cycle, repopulation, and reoxygenation of hypoxic tumour areas (Withers, 1975b).

1.1.6.3.3 The four R's of radiotherapy

In general, conventional radiation therapy is delivered in multifraction radiation doses. Four radiobiological phenomena influence the outcome of fractionated radiation therapy, which are: (1) *repair* of the sublethal or potentially lethal damage in normal cell and cancer cell, (2) *repopulation* of surviving normal and malignant cells between dose fractions and following treatment, (3) *redistribution* through cell cycle phases and (4) *reoxygenation* of hypoxic tumour cells. The four phenomena have been named the four R's of fractionated radiation therapy (Withers, 1975b):

Repair: each radiation fraction causes critical damages in both tumour and normal cells. However, normal cells have more efficient systems to repair damage in comparison to tumour cells. The time between the fractionated radiation doses allows the normal cells to repair the radiation damage more efficiently than tumour cells. There are three categories of radiation-induced cellular damage to mammalian cells; lethal damage, sublethal damage and potentially lethal damage. However, the mammalian cells can repair these damages by two mechanisms; potentially lethal damage repair (PLDR) and sublethal damage repair (SLDR) (Awwad, 2013). PLDR type can repair sublethal radiation damage within hours unless the cells receive an additional dose of radiation, whilst SLDR

type can alter the post-irradiation conditions, such as delayed mitosis, that allows the cells to repair themselves (Bedford, 1991). A number of DNA repair pathways, including homologous recombination (HR) and non-homologous end joining (NHEJ) for DSBs; and mismatch repair (MMR), nucleotide excision repair (NER) and base excision repair (BER) for SSBs, are responsible for the repair of DNA damage and preserve the genomic stability of the cell (Awwad, 2013).

Repopulation: repopulation is the increase in cell division for both normal and tumour cells at a certain time point during/after radiotherapy. In general, the acceleration of repopulation is different between tumour and normal cells. In tumour cells, the repopulation, of irradiation-survived cells, can start after 2-4 weeks after the initial radiation doses are delivered (early responding tissues); while normal cells start to repopulate after the entire conventional radiation course has been completed (late responding tissues). Therefore, the time gap between normal and tumour cells repopulation is a critical phenomenon that must be considered in radiotherapy especially if treatment time extends over five weeks (Withers et al., 1988).

Redistribution: each phase of the cell cycle shows different radiosensitivity: M phase is the most radiosensitive phase, late-S is the most radioresistant phase and both G1 and G2 phases show moderate radiosensitivity. The multi fractionation nature of radiotherapy gives increased probability of targeting cancer cells in a sensitive phase at some point during the radiotherapy course, especially to those cells which were in a resistance phase in a previous radiation fraction i.e. cells that were initially resistant (e.g. late-S phase cells) have time to redistribute into a more sensitive phase (e.g. M phase) and are killed by the next radiation fraction (Withers, 1975a).

Reoxygenation*:* generally, most of the solid tumours contain hypoxic regions either due to the limited diffusion distance of oxygen through the tumour mass (chronic hypoxia) or due to the temporary closing of blood vessels next to, or within, a tumour (acute hypoxia). Hypoxic cells are very resistant to radiation compared to the aerated cells. Hypoxia in PC and the mechanism of radioresistance of hypoxic cells will be discussed,

in details, in Chapter 3 (Section 3.2.2.3). Tumour reoxygenation, after every dose of radiation, can oxygenate hypoxic cells and increase their sensitivity to radiation over the course of the treatment; after each fraction of radiation, the outer malignant cells of the tumour mass are eliminated and, subsequently, oxygen flows to inner hypoxic cells, which were blocked previously by the outer malignant cells (Van Putten and Kallman, 1968).

Recently, ***radiosensitivity*** is a new member of the four R's family, i.e. the '5thR'. Each cell type has a different sensitivity to radiation, which may explain the variable susceptibility to cell death and the clinical heterogeneity between different cancer types. For example, lymphocytes, spermatogonia, erythroblasts, intestinal crypt cells are sensitive to radiation, while muscle and nerve cells are resistant (Steel et al., 1989).

1.1.6.3.4 Radiotherapy options in PC

As mention earlier, adjuvant radiotherapy is more commonly used in the United States than the United Kingdom and Europe. In the United States, The National Comprehensive Cancer Network (NCCN) recommends that use of radiotherapy for PC patients is based on five clinical scenarios; resectable/borderline resectable (neoadjuvant), resectable (adjuvant), LAPC (definitive), palliative (non-metastatic and metastatic) and recurrence (NCCN, 2018). In all previous scenarios, radiotherapy aims to prevent or delay the progression of local disease with minimizing the radiotherapy exposure to surrounding OARs (NCCN, 2018). The neoadjuvant treatment for patients with resectable/borderline resectable PC includes systemic chemotherapy with FOLFIRINOX or GM with/without subsequent chemoradiation (5-fluorouracil (5-FU) or GM and 36 Gy in 2.4 fractions or 45-54 Gy in 1.8-2 fractions) (Visser et al., 2012, Hoos et al., 2013, NCCN, 2018). Although clinical trials have shown encouraging outcomes for chemoradiation treatment (as shown later), there is no current chemotherapy regimen or radiotherapy dose accepted as standard for PC treatment. In resectable cases, resection of PC typically occurred within 4 weeks of radiotherapy. In borderline resectable cases, the PC is resected after 4-8 weeks of radiotherapy to allow for downstaging and downsizing of the tumour.

Surgical resection after 8 weeks of radiotherapy may potentially increase the difficulty of resection due to fibrosis induced by radiation (NCCN, 2018). In the adjuvant setting, chemotherapy is the standard treatment, with radiotherapy evaluated in several clinical trials (NCCN, 2018). However, if there is no prior neoadjuvant treatment with no evidence of recurrence or metastatic disease after PC resection, chemoradiation treatment (5-FU or GM and 45-46 Gy in 1.8-2 fractions) is an option after systemic chemotherapy (NCCN, 2018). For patients with LAPC, radiation therapy aims to prevent or delay local progression that may result in pain and/or local obstructive symptoms. Due to limited data, no standard radiation therapy is recommended for LAPC patients. However, the option of radiation therapy in LAPC patients includes; chemoradiation consisting of 45-54 Gy in 1.8-2 fractions or treatment with SRBT, with no recommended doses due to lack of data, but doses of 33 Gy (6.6 Gy × 5 fractions) and 25 Gy (5 Gy × 5 fractions) have been reported (Gurka et al., 2013, Herman et al., 2015, NCCN, 2018). Radiation therapy for palliative (non-metastatic and metastatic) patients aims to relieve pain, bleeding and/or ameliorate, with a recommended total dose of 30 Gy (30 Gy × 10 fractions) (NCCN, 2018).

To date clinical trials, as shown below, have yielded conflicting data and failed to resolve the debate regarding the efficacy of radiation therapy in treatment for PC. A recent large randomised clinical study (LAP07 trial) followed 269 PC patients for 36.7 months. The patients received chemotherapy alone (n=136, capecitabine) or chemo-radiotherapy (n=133, capecitabine combined with 54 Gy/30 days). The study found no significant difference in the rates of overall survival between the two groups (16.5 months and 15.2 months for chemotherapy alone and chemo-radiotherapy treatments respectively) (Hammel et al., 2016).

Clinical trials have also shown different efficacy of chemotherapeutic regimens such as GM, 5-FU and capecitabine in chemoradiation treatment; in the United Kingdom, a clinical phase II trial (SCALOP, Selective Chemoradiation in Advanced LOcalised Pancreatic cancer) included 74 patients with LAPC recruited from 28 local centres, and

aimed to assess the activity, safety and feasibility of GM-based (n=38) and capecitabine-based (n=36) chemoradiotherapy after chemotherapy induction. After 12 weeks of induction GM and capecitabine, patients received a further cycle of GM or capecitabine in combination with radiation (50.4 Gy in 28 fractions). The study found that median overall survival of capecitabine group (13.4 months) was significantly (P=0.012) lower than GM group (15.2 months), with no significant difference in 12-month overall survival (79.2% vs 64.2%) and median progression-free survival (12.0 months vs 10.4 months) respectively (Mukherjee et al., 2013). However, in the United States, a clinical study evaluated toxicity, efficacy and clinical outcomes of GM chemoradiation (n=53, GM (250–500 mg/m^2), 30 Gy in 10 fractions) and 5-FU chemoradiation (n=61, 5-FU (200–300 mg/m^2), 30 Gy in 10 fractions) in LAPC patients. No significant difference in 1-year survival was observed between GM chemoradiation (42%) and 5-FU chemoradiation (28%). However, patients receiving GM chemoradiation developed more severe acute toxicity than 5-FU chemoradiation (23% vs 2% (P< 0.0001) respectively) (Crane et al., 2002).

To increase the radiotherapeutic efficacy in PC treatment, recent clinical trials have focused on dose escalation as a strategy to improve local control. However, delivering high radiation doses to PC have been limited by the tolerance of nearby OARs such as duodenum, stomach and intestine, with gastrointestinal toxicity (GI) as the most important side effect. A recent clinical trial, that included 200 patients with LAPC, selected 47 (24%) patients with tumours located >1 cm from the luminal organs were for dose-escalated IMRT (biologically effective dose [BED] >70 Gy), while 153 (76%) LAPC patients having tumours located ≤1 cm from the luminal organs were treated with standard fractionation radiation therapy (BED ≤ 70 Gy). Results showed that patients receiving >70 Gy BED showed significantly higher overall survival (17.8 vs 15.0 months, P=0.03) and better local-regional recurrence-free survival (10.2 vs 6.2 months, P=0.05) than patients receiving ≤70 Gy BED (Krishnan et al., 2016). Another dose escalation trial (phase I) delivered high single radiation doses using SRBT to 15 LAPC patients (3,5 and 7 patients received 15, 20 and 25 Gy respectively, with no prior chemotherapy) with

acceptable acute GI (grade 2 or below) (Koong et al., 2004). The phase II of the previous trial included 19 PC patients that were treated with 45 Gy IMRT in combination with 5-FU followed by a single fraction of 25 Gy body stereotactic radiosurgery (SRS) boost to the primary tumour. Excellent local control in all patients was observed, but with no survival advantage along with severe acute GI toxicity (grade 3-4) (Koong et al., 2005). However, another recent clinical phase II trial increased the number of SRBT fractions from 1 to 5, with a total dose of 33 Gy delivered to 49 LAPC patients treated, previously, with systemic chemotherapy. The study showed an improvement in overall survival (median overall survival was 13.9 months), freedom from local disease progression (at 1 year was 78%), with low late GI toxicity (93.6 % of patients showed ≤ 2 grade of GI toxicity) (Herman et al., 2015). Another recent clinical phase II study used SRBT, after chemotherapy, to deliver 45 Gy in 6 fractions for 45 patients with LAPC. The median overall survival was 19 months with excellent local disease control (at 2 years was 90%) and low GI toxicity (95.6 % of patients showed ≤ 2 grade of late GI toxicity) (Comito et al., 2017). Results from clinical trials using SBRT in selected LAPC patients showed an improvement in overall survival, with low GI toxicity and short treatment time compared to classical fractionated radiotherapy. Therefore, SBRT is an attractive option for PC tumours located >1 cm from the luminal organs, such as lung or liver (Crane, 2016).

As discussed above, radiation therapy is not always effective; a number of resistance mechanisms may explain this lack of treatment success, one of these being inherent or acquired expression of redox proteins i.e. proteins that can scavenge radiation-induced radicals making the radiation therapy less efficient.

1.2 Redox proteins

1.2.1 Redox homeostasis

The term ‘redox’ is one of the major concepts in chemistry refers to a chemical reaction in which the oxidation number of a molecule, atom, or ion changes by gaining or losing an electron, and it describes two biological processes: reduction, which is a decrease in

oxidation state, and oxidation, which is an increase in oxidation state (Rinehart and Rinehart, 1973). In living systems, these two processes are carefully balanced by a series of proteins to maintain redox homeostasis. Levels of intracellular ROS are regulated by antioxidant systems, including non-enzymatic antioxidants and redox proteins (enzymatic antioxidant). ROS are produced either endogenously, through a series of mitochondrial reductions of oxygen (O_2) by electron-transfer reactions, or exogenously by, for example, the radiolysis of water as an indirect effect of ionising radiation (Figure 1.7). ROS reactions result in a number of products including three main molecules: superoxide anion (O_2^-), hydroxyl radical ($^{\bullet}OH$), and hydrogen peroxide (H_2O_2). Approximately 90% of ROS molecules are produced by mitochondrial oxidative metabolism as a result of three series reactions (Michaels and Hunt, 1978):

$O_2 + e^- \rightarrow O_2^-$ (Reaction 1)

$2O_2^- + 2H^+ \rightarrow H_2O_2 + O_2$ (Reaction 2)

$H_2O_2 + e^- \rightarrow {}^{\bullet}OH^- + OH^-$ (Reaction 3)

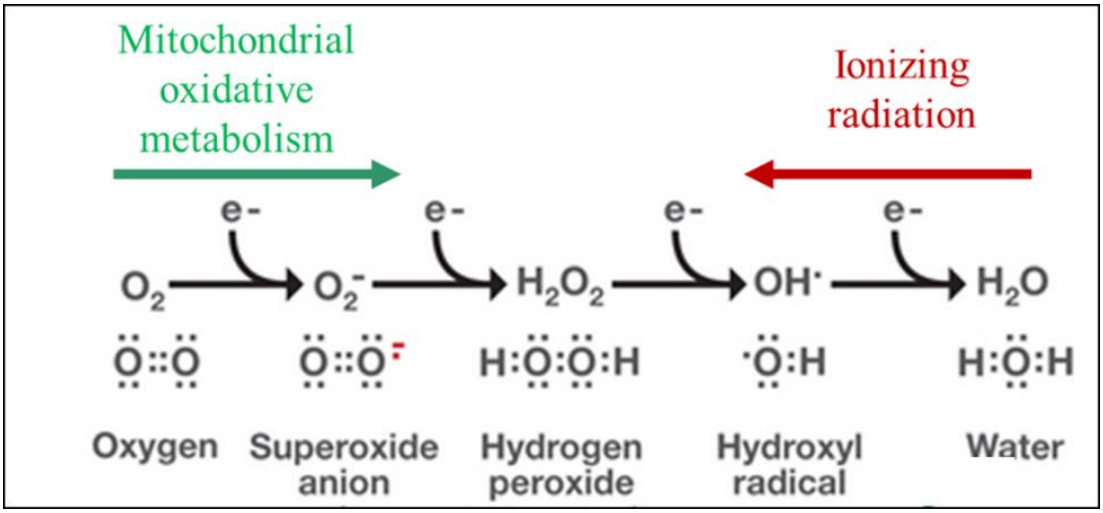


Figure 1.7: Formation of ROS. ROS produced either by reduction reactions of oxygen (O_2) through mitochondrial oxidative metabolism (green) or by radiolysis of H_2O as indirect effects of radiation (red). Adapted from: https://www.caymanchem.com/Article/2165; last update 15 June 2018.

ROS, as mentioned above, are induced exogenously by ionising radiation via the indirect effect and radiolysis of water but can also be induced by other exogenous factors such

as heat, trauma, ultrasound, ultraviolet light, ozone, tobacco, infection, excessive exercise and drugs (Demple and Harrison, 1994, Dahiya et al., 2013).

1.2.1.1 Effect of different ROS levels on cellular biomolecules

ROS play a major role, in several physiological processes in living systems, and can have both deleterious or beneficial effects, such as cell growth, necrosis, apoptosis, protease activities and gene expression, depending on cell type and context (Zuo et al., 2015).

Low levels of ROS are associated with beneficial cardioprotection, serve as signals mediatingphysiologic responses and induce mitogenic responses (Lu et al., 1998, Andreadou et al., 2009). A high concentration of ROS can induce 'oxidative' stress and have lethal effects on living cells. The main lethal pathways induced by ROS are: apoptosis, necrosis, autophagy, mitotic catastrophe with new pathways being identified such as paraptosis and anoikis (Ghosh et al., 2018). Two distinct apoptotic pathways have been identified when cells are exposed to high ROS levels: the extrinsic (Fas activation pathway) and intrinsic pathways (mitochondrial pathway) (Ozben, 2007). Both pathways initially activate an apical caspase (i.e. caspase-8 or caspases--9), which, subsequently, activates the downstream effector caspases-3 and caspases--7, leading to apoptotic cell death (Ozben, 2007). Briefly, in the extrinsic pathway, high ROS levels activate Fas receptor on the cell membrane, which in turn activates caspase 8 leading to cell apoptosis (Denning et al., 2002). The intrinsic pathway is activated by intracellular stressors i.e. high ROS concentrations causing mitochondrial damage. Briefly, in the stressed cells, proapoptotic BCL-2 family members promote mitochondrial outer membrane permeabilization (MOMP) and cytochrome c release into the cytoplasm, where they promote cell death (Sun et al., 2000).

Overproduction of ROS leads to DNA oxidative damage, oxidation of proteins and lipid peroxidation. High level of ROS causes oxidative damage to sugar and base moieties in DNA leading to deoxyribose oxidation, strand breakage, mutations and DNA protein crosslinks. Subsequently, DNA damage may lead to alterations in encoded proteins, resulting in inactivation of proteins. In general, sugar damage is caused by hydrogen

abstraction (removal of an atom or group from a molecule by a radical) from deoxyribose, while DNA bases oxidative damage is caused by the hydroxyl radical (•OH) (•OH attacks purine and pyrimidine bases, and the deoxyribose backbone with 8-Hydroxyguanine is the most commonly observed product), whereas H_2O_2 and O_2^- do not react with DNA bases at all (Dizdaroglu, 1993).

ROS molecules can also damage structural and enzymatic proteins by different pathways including protein modification (via protein unfolding and altered conformation), side-chain hydrophilicity, backbone fragmentation, protein aggregation (via covalent cross-linking or hydrophobic interactions) and altered interactions with biological partners (Davies, 2016).

At high ROS levels, lipid peroxidation in the cellular membrane can occur, leading to inactivation of receptors and enzymes, resulting in altered cellular function (Girotti, 1985). Among several products of lipid peroxidation, 4-hydroxynonenal (HNE), is the most characterised product due to its high electrophilic reactivity with low molecular proteins, such as glutathione, and, at higher concentration, with DNA (Esterbauer et al., 1991, Uchida, 2003, Pizzimenti et al., 2010). Malondialdehyde (MDA) is another major product of lipid peroxidation that is widely used as an indicator of lipid peroxidation in cancer patients, and has been reported to be mutagenic and carcinogenic (Basu and Marnett, 1983, Gönenç et al., 2001, Del Rio et al., 2005).

The level of damage to different biological targets (DNA, protein and lipids) depends on numerous factors; concentration of particular targets, rate constants for reactions of oxidant with target, the location of the target relative to that of the oxidant, occurrence of secondary damaging events, intra- and inter-molecular transfer reactions and the possibility and extent of repair and oxidant scavenging reactions (Davies, 2016).

1.2.2 *The cellular antioxidant system*

The cellular antioxidant system can be divided broadly into two groups: nonenzymatic antioxidants and antioxidant enzymes (Table 1.2).

Cellular antioxidants					
Nonenzymtic Antioxidant	Water-Soluble Antioxidant	Glutathione (GSH)	Antioxidant Enzymes (Redox Protein)	ROS-dependent enzymes	Superoxide dismutase (SOD)
					Catalase
		Flavonoids			Peroxiredoxin (Prx)
					Glutathione peroxidase (GPx)
		Uric Acid		Glutathione System	Glutathione reductase
		Ascorbic acid (vitamin C)		Thioredoxin system	Thioredoxin (Trx)
	Lipid-Soluble Antioxidant	Carotenoids and vitamin A			Thioredoxin reductase (TrxR)
		α-Tocopherol (Vitamin E)			Thioredoxin-interacting protein (TxNIP)
		α-Lipoic acid/ Dihydrolipic acid		Glutaredoxin System	Glutaredoxin (Grx)
		Ubiquinol/ Ubiquinone			

Table 1.2: Summary of cellular antioxidants.

1.2.2.1 The nonenzymatic antioxidants system

1.2.2.1.1 Water-soluble antioxidants

Water-soluble antioxidants include glutathione (GSH), flavonoids, uric acid, and ascorbic acid. Ascorbic acid and GSH perform their ROS scavenging activity primarily in the aqueous intracellular environment. Ascorbic acid is the most important water-soluble antioxidant in human plasma and mammalian cells, and has been an active area of research for decades as a therapeutic agent against different diseases including cancer. Ascorbic acid can scavenge ROS molecules such as the hydroxyl radical ($^{\bullet}OH$), alkoxyl ($RO^{\bullet}$) and peroxyl ($ROO^{\bullet}$) radicals. In addition, ascorbic acid is able to reduce the

tocopheroxyl radical to α-tocopherol (vitamin E) (Etsuo et al., 1982). However, ascorbate at pharmacologic concentrations can serve as an electron donor to generate ascorbate radical and hydrogen peroxide in a linear relationship, causing cell death (Chen et al., 2007). A recent study found that treating PC cell lines with ascorbate at pharmacologic concentrations significantly decreased cell viability and clonogenicity *in vitro* and inhibited tumour growth and prolonged survival *in vivo* (Du et al., 2010).

1.2.2.1.2 Lipid-soluble antioxidants

Lipid-soluble antioxidants located within the lipid bilayer of cellular membranes break the chain reactions of fatty acid peroxidation. α-tocopherol and ubiquinol are the most important lipid-soluble antioxidants (Frei et al., 1990).

Alpha-tocopherol and ubiquinol can scavenge reactive free radicals by becoming stable radicals themselves (i.e. tocopheroxyl radical and ubiquinone, respectively), which is a common mechanism in radical-scavenging antioxidants (Zhang and Martin, 2014). Ascorbic acid can regenerate α-tocopherol from tocopheroxyl free radicals in biological systems, which is a unique feature of α-tocopherol (Freisleben and Packer, 1993). Supplementation with α-tocopherol seems does not affect the rate of incidence or mortality of PC (Rautalahti et al., 1999).

1.2.2.2 Antioxidant enzymes/redox proteins

Antioxidant enzymes in cells have been classified into six categories: oxidoreductases, transferases, hydrolases, lyases, isomerases, and ligases (Foldes, 1978). Redox proteins represent the antioxidant enzyme group in the cellular antioxidant system. The majority of redox proteins can be allocated to one of four different systems: ROS-dependent enzymes, glutathione (GSH) system, thioredoxin (Trx) system and the glutaredoxin (Grx) system (Table 1.2). The ROS-dependent enzyme system is the only one that can affect ROS directly while the other three redox buffering systems need to donate electrons or reverse the formation of disulphides to regulate redox homeostasis (Giles, 2006).

1.2.2.2.1 ROS-dependent enzymes

ROS-dependent enzymes include superoxide dismutase (SOD), catalase, peroxiredoxin (Prx) and glutathione peroxidase (GPx). The reduction of O_2 to O_2^- can occur in mitochondria (during respiration), the cell membrane (by NADPH oxidase) and cytosol (by xanthine oxidase) (Figure 1.8, reaction 1) (Curtin et al., 2002). Both SOD and catalase do not require co-factors to transform O_2^- and H_2O_2 into H_2O_2 and H_2O respectively (Figure 1.8, reactions 2 and 3) (Paal et al., 2001, Siegel et al., 2014). However, GPx and Prx need a series of co-factors and proteins to fully function (Figure 1.8, reactions 4 and 5) (Weydert and Cullen, 2009).

SODs locate in different sites in the mammalian cell: CuZn-SOD (SOD1) is found in the nucleus and cytoplasm, Mn-SOD (SOD2) exists in mitochondria and extracellular SOD (EC-SOD) located in the extracellular matrix and fluids (Fattman et al., 2003). The primary function of catalase takes place in subcellular organelles such as peroxisomes (Weydert and Cullen, 2009). Catalase enzymes are divided into monofunctional and bifunctional classes. The monofunctional function acts as catalases, whereas the bifunctional catalases act as peroxidases (Chelikani et al., 2004). GPx has eight isoforms in the mammalian cell (GPx 1-8). GPx1 is the most common isoform in the cytoplasm as well as GPx2, while GPx3 is an extracellular isoform (Drevet, 2006).

In the mammalian cell, Prx has six different isoforms expressed within the cytosol (Prx I, II, VI), nucleus (Prx I), mitochondria (Prx III, VI), peroxisomes (Prx V) and endoplasmic reticulum (Prx IV) (Wood et al., 2003, Tavender et al., 2008). Each isoform contains a 'peroxidatic' cysteine residue as an active site that attacks peroxides and becoming oxidised to a cysteine sulfenic acid located in the N-terminal region. Prx I, II, III and IV are the best-characterized peroxiredoxins as they contain cysteine residue near the C-terminal as an additional active site (Ellis and Poole, 1997). Prxs scavenge intracellular ROS, with Trx systems act as its electron donors (Figure 1.8, reaction 5), while GPxs are activated through the GSH system (Figure 1.8, reaction 6) (Lillemoe et al., 2000).

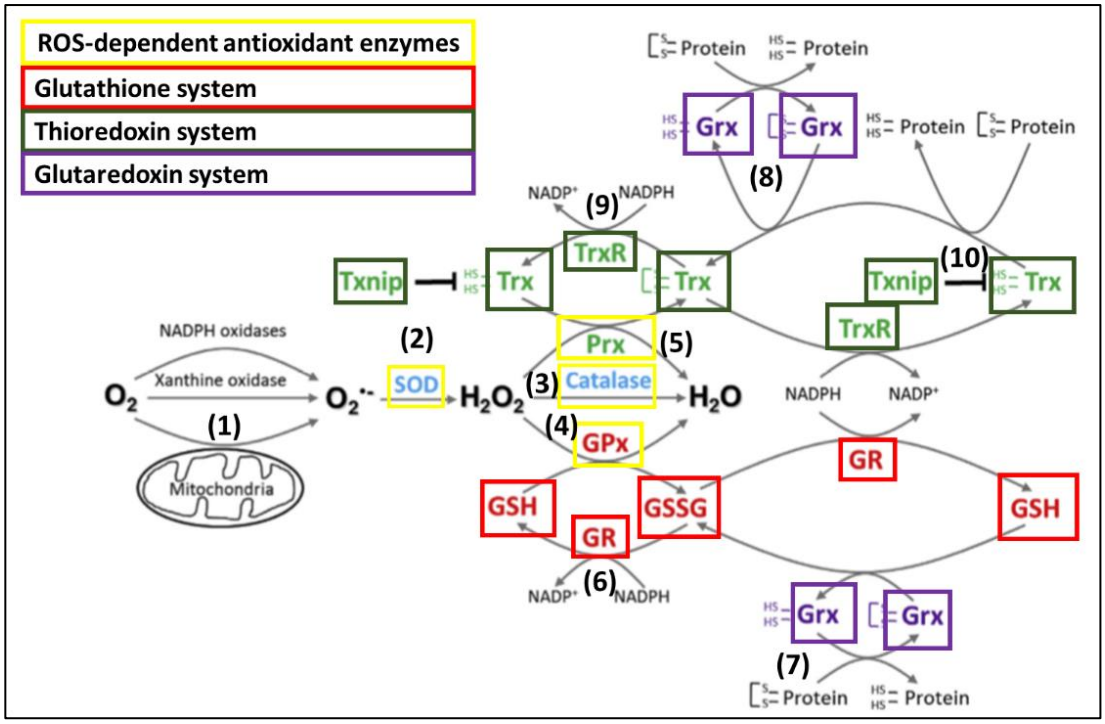


Figure 1.8: Redox proteins and ROS regulation. Abbreviations: peroxiredoxin (Prx); superoxide dismutase (SOD); glutathione peroxidase (GPx); reduced glutathione (GSH); oxidized glutathione (GSSG); glutathione reductase (GR); glutaredoxin (Grx); thioredoxin (Trx); thioredoxin reductase (TrxR); thioredoxin-interacting protein (TxNIP); nicotinamide adenine dinucleotide phosphate (NADPH), 'HS' represents the reduced form of the protein, and 'S' denotes the oxidized form. Adapted from: Zhang, Y. & Martin, S. G. 2014. Redox proteins and radiotherapy. *Clinical Oncology,* 26**,** 289-300.

1.2.2.2.2 The glutathione system

The GSH system is the most abundant antioxidant family within all cells (Meister, 1983), and its related transferases (glutathione s-transferases, GSTs) are one of the main systems involved in the maintenance of intracellular redox balance. The GSH system consists of three main components: reduced glutathione (GSH), oxidised glutathione (GSSG) and glutathione reductase (GR). GSH is a tripeptide, consisting of cysteine, glutamic acid and glycine, exists in two forms: reduced GSH (the activated form) and GSSG (oxidised GSH, the inactivated form) (Meister, 1983). GR is a dimeric flavoenzyme that can be stimulated by NAPDH to reduce GSSG to GSH (Figure 1.8, reaction 6) (Watson et al., 2003a). GSH conjugates with various endogenous and xenobiotic compounds, mediated by GSH-S-transferase (GST) to remove these compounds from the cell. As

shown in Figure 1.8, the GSH/GSSG system activates GSH peroxidase (GPx) which is a main arm used by the cell to scavenge H_2O_2 from the cell.

In extreme conditions of oxidative stress, cellular efficacy to reduce GSSG to GSH may be less, resulting in accumulation of GSSG within the cytosol. To maintain redox state, GSSG can be actively transported out of the cell or react with protein sulfhydryl groups (PSH) to form mixed disulphide (PSSG) (Traverso et al., 2013). In normal redox homeostasis, the GSH:GSSG ratio is usually 100:1. In contrast, under oxidative stress, the intracellular GSSG levels accumulate leading to a drop in GSH/GSSG ratio to 10:1 (Zitka et al., 2012).

1.2.2.2.3 The glutaredoxin system

Grxs are a group of versatile oxidoreductases belonging, structurally, to the thioredoxin (Trx) fold family of proteins since both Trx and Grx systems have the N-terminal Cys residue in their active site (Eklund et al., 1984). However, functionally, Grxs are more versatile with respect to the choice of substrate and reaction mechanisms than Trx system (Lillig et al., 2008). Human cells contain four Grx isoforms: the cytosolic dithiol Grx1, the mitochondrial Grx2 (Grx2a), the multidomain monothiol Grx3 and the mitochondrial single-domain monothiol Grx5 (Johansson et al., 2004). The main function of Grx system is to reduce S-glutathionylated proteins, making them one of the major deglutathionylases in living cells due to their high affinity and selectivity to glutathionylated proteins. Grxs use both GSH and Trx as electron donors to reduce S-glutathionylated proteins (Figure 1.8, reactions 7 and 8 respectively) (Johansson et al., 2004).

1.2.2.2.4 The thioredoxin system

The Trx system consists of thioredoxin (Trx), thioredoxin reductase (TrxR) and thioredoxin-interacting protein (TxNIP), which are a class of low molecular weight redox proteins characterised by conserved active site (-Cys-Gly-Pro-Cys) that are found in all Trx family proteins (Holmgren, 1989).

Trx proteins are 12 kDa proteins that include cytosolic thioredoxin-1 (Trx1), mitochondrial thioredoxin-2 (Trx2) and a larger thioredoxin-like protein (p32TrxL). The cytosolic Trx1 is the well-studied isoform and acts as the major disulphide reductase of proteins in the living cell. All Trx proteins share a similar three-dimensional (3D) structure that consists of five-stranded beta sheets that are surrounded by four alpha helices on the external surface of the proteins, with –Trp –Cys –Gly– Pro–Cys being an active site (Powis and Montfort, 2001). The most important amino acids in the active site are Cys32 and Cys35 that undergo reversible oxidation-reduction catalysed reaction by TrxR in an NADPH-$NAPD^+$ dependent manner (Figure 1.8, reaction 9). The biochemical reactions of the Trx system are covered, in detail, in Section 1.2.2.2.4.1.

TrxR is a member of the homodimeric pyridine nucleotide-disulphide oxidoreductase family and exists in two forms: cytosol (TrxR1) and mitochondria (TrxR2). TxNIP is also known as vitamin D3 up-regulated protein 1 (VDUP1) or Trx binding protein 2 (TBP2). TxNIP acts as an endogenous inhibitor of the Trx system, blocking the activity of Trx by interacting with the active catalytic centre of Trx (Figure 1.8, reaction 10) (Nishiyama et al., 1999). The Trx system is, as covered in Section 1.2.2.2.4.2, involved in various cellular pathways.

1.2.2.2.4.1 Biochemical reactions of the thioredoxin system

In general, the major function of Trx is to reduce two Cys residues in other proteins, including Prx proteins (reaction 3). Reduced thioredoxin acts as an electron donor to break (reduce) the disulphide bond of the cysteine residue in Prx that can then scavenge intracellular ROS. Therefore, the antioxidant activity of the Trx system is primarily exerted by Prx (Wood et al., 2003). In the cytoplasm, 95% of Trxs are in a reduced form with a very low redox potential (-280 millivolts (Mv), lower redox potential leads to higher reduction activity), making it one the of the most favourable and major dithiol reductants in the cell (Watson et al., 2003b). However, when Trx reduces a protein, it reverts to the oxidised form (inactive form), which is characterised by a disulphide bond between Cys32 and Cys35 (reaction 4). Therefore, oxidised Trx must be recycled to its

reduced form to regain its activity. TrxR is the only known enzyme that can reduce oxidised Trx by obtaining reducing equivalents from NADPH and pass them to the oxidised Trx (Arner and Holmgren, 2000).

The series of reactions is listed below:

$$Trx–(SH)_2 + X–S_2 \Leftrightarrow Trx – S_2 + X(SH)_2 \quad \text{(reaction 3)}$$

$$Trx – S_2 + NADPH \Leftrightarrow Trx – (SH)_2 + NADP^+ \quad \text{(reaction 4)}$$

As mentioned, TxNIP is a stress-responsive protein that inhibits Trx activity by preventing the recycling of oxidised Trx to the reduced form. TXNIP can inhibit the activity of Trx by two pathways. First, oxidised TxNIP 'Cys 247' binds reduced Trx 'Cys 32' and acts as a competitive inhibitor to remove Trx from proteins whose function is inhibited by separation from Trx, such as ASK1. Second, overexpression of TxNIP, by factors such as disturbed flow and high glucose, resulting in decreased activity of TrxR, leading to an increase in oxidative stress and apoptosis (Yamawaki et al., 2005).

1.2.2.2.4.2 Biological activities of the thioredoxin system

As indicated earlier, the Trx system regulates Prx but also affects the redox state of different signalling molecules, and by regulating their redox state, can regulate cell growth, apoptosis, gene transcription, cell cycle progression and ROS levels (Figure 1.9).

Reduced Trx1, the bioactive form, binds to apoptosis signal-regulating kinase 1 (ASK-1), a key apoptotic regulator whose activation is essential for tumour necrosis factor α (TNF α)-induced apoptosis, and transforms it to inactive form which protects cells against apoptosis (Baker et al., 1997). The growth and apoptosis effects of Trx may also be explained by the selective activation of a number of transcription factors such as NF-κB (nuclear factor kappa-light-chain-enhancer of activated B cells), glucocorticoid receptor, TP53, AP1 (activator protein 1) and AP-2 (activator protein 2) (Powis and Montfort, 2001).

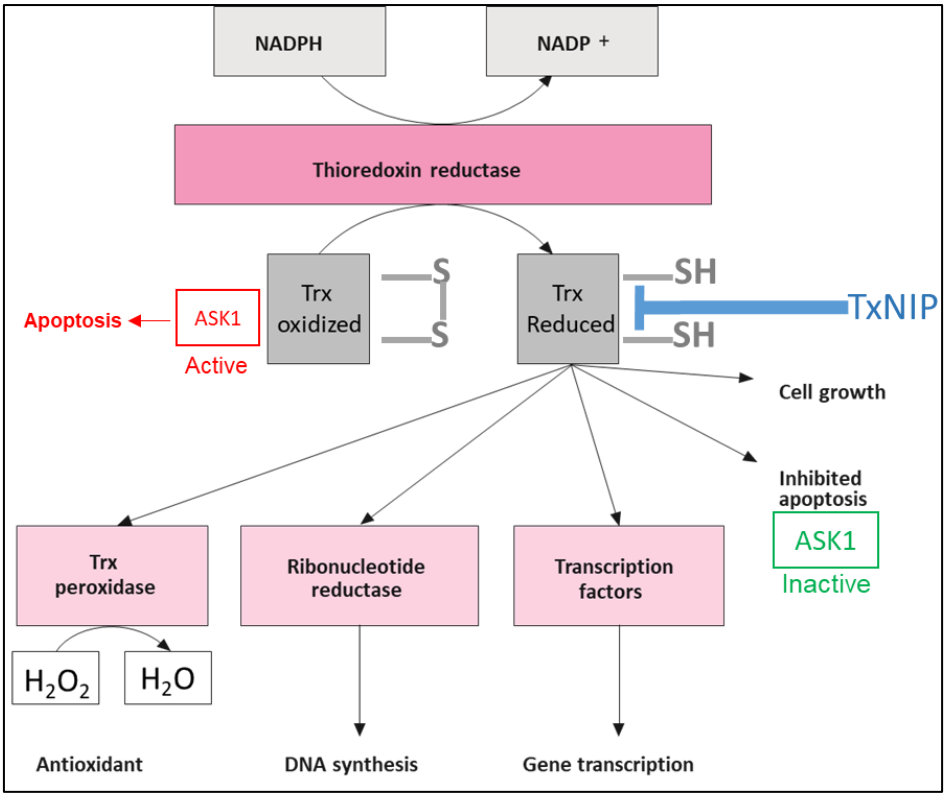


Figure 1.9: **Mechanisms and functions of Trx system in the living cells.** TrxR catalyses the conversion of oxidised Trx into reduced Trx in NADPH reaction manner. Reduced Trx: acts as an electron donor to Trx peroxidase to reduce H_2O_2 to water, reduce ribonucleotide reductase in DNA synthesis, increases the DNA binding of several transcription factors, increases cell growth and inhibits apoptosis. Adapted from: Mustacich, D. and Powis, G., 2000. Thioredoxin reductase. *Biochemical Journal*, 346(1), pp.1-8.

NF-κB plays a major role in cell response to oxidative stress, apoptosis and carcinogenesis (Gilmore et al., 1996). Trx1 increases the DNA binding activity of NF-κβ subunits, enhancing NF-κβ mediated gene expression leading to cell proliferation and survival (Hayashi et al., 1993). Schenk and colleagues observed that Trx1 was associated with DNA-binding of NF-κB transcription factor in cervical cancer cells in addition to enhancing DNA-binding of transcription factor AP-1, which is associated with gene-activating events that involved in growth, differentiation and cellular stress (Schenk et al., 1994). The glucocorticoid receptor is another transcriptional factor regulated by Trx. High levels of oxidative stress and oxidised Trx were associated with the decreasing of glucocorticoid receptor binding activity (Hutchison et al., 1991, Chakraborti et al., 1992). A significant increase in the expression of glucocorticoid receptor-mediated genes and

glucocorticoid receptor reporter activity were observed after transfection of Trx1 in breast cancer (BC) cells (Makino et al., 1999). The redox regulation of p53 DNA binding is maintained by cysteine residues in the DNA binding domain of p53, and enhanced by phosphorylation by specific kinases in response to DNA damage leading to regulate cell cycle-related genes (Banin et al., 1998). Therefore, Trx is involved in cell cycle regulation. Knockdown of Trx in cells showed a significant arrest in G1 phase, showing Trx is a positive cell cycle regulator by cyclin D1 transcription and the ERK/AP-1 signalling pathways (Mochizuki et al., 2009a). However, another study showed that 40% inhibition of Trx activity by a Trx inhibitor (PX-12) caused significant G2/M arrest in addition to an increase in ROS levels and apoptosis (You et al., 2014). Such differing results could be explained by the low inhibition of Trx (40%) and to unknown mechanisms of Px-12. Moreover, inhibition of TrxR may lead to G1/S phase arrest due to the involvement of the reduced Trx in DNA synthesis through reduction of s-ribonucleotide reductase, which is an enzyme that catalyses the formation of deoxyribonucleotides from ribonucleotides (Laurent et al., 1964). All cells that synthesis DNA require deoxyribonucleotide, which produced by reducing the hydroxyl group at the C20 of the ribose-moiety of ribonucleotide by ribonucleotide reductase (Gromer et al., 2004). A recent study showed that up-regulation of Trx1 and human ribonucleoside-diphosphate reductase large subunit (RRM1) can significantly enhance ribonucleotide reductase activity in colorectal cancer cells. Furthermore, dual inhibition of Trx1 and RRM1 produced a synergistic anticancer effect *in vivo* and *in vitro* (Lou et al., 2017b).

1.2.3 Redox proteins in cancer

Antioxidant supplementation has been implicated in cancer prevention and maintenance of general health (Klein et al., 2011). In addition, inhibition of antioxidant systems could be chemopreventive (Gorrini et al., 2013). In general, cancer cells are under continuous oxidative stress, due to high levels of ROS resulting from high metabolic activity, mitochondrial dysfunction, peroxisome activity, increased cellular receptor signalling, oncogene activity and high activity of oxidases, cyclooxygenases and

lipoxygenases (Figure 1.10) (Storz, 2005). Thus, redox proteins play a major role in cancer cell survival and proliferation by regulating the high oxidative stress, making it a potential target for cancer treatment. Therapies targeting redox proteins have been widely studied as either single modalities or in combination with chemotherapy or radiotherapy.

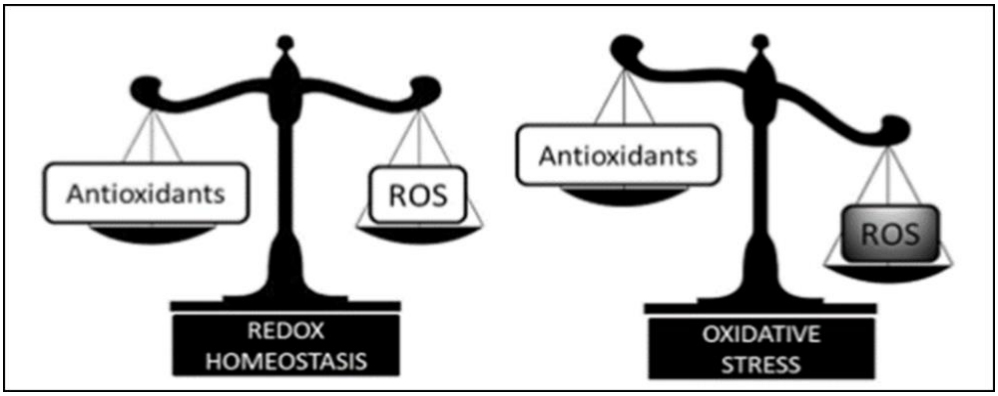


Figure 1.10: Redox homeostasis and oxidative stress. When the intracellular antioxidant systems are able to counterbalance the reactive oxygen species (ROS) level, redox homeostasis is maintained (left); but if the ROS levels constantly increase or/and the antioxidant systems are disrupted, ROS overbalance occurs and leads to oxidative stress (right). Source: Zhang, Y. & Martin, S. G., 2014. Redox proteins and radiotherapy. Clinical Oncology, 26, 289–300; used with permission.

1.2.3.1 Effect of redox proteins on cancer treatment: ROS-dependent enzymes, GSH and Grx systems

As indicated earlier, altering expression/activity of redox proteins in cancer cells has been studied in order to increase the efficacy of chemotherapy and radiotherapy. Redox protein regulation of the radioresponse of cancer cells will be discussed in the introduction of Chapter 2.

An *in vivo* study showed that knocking-down SOD2 together with a GPx inhibitor reduced oral cancer cell growth (4 to 20-fold) compared to control, with an increase in survival, and such tumour inhibition effects were enhanced by including a catalase inhibitor (Darby Weydert et al., 2003). Komatsu and colleagues observed that overexpression of SOD2 was associated with a significant decrease in plating efficiency (PE) of osteosarcoma cells due to accumulation of H_2O_2 (Komatsu et al., 2005). Another

study showed that different levels of SOD2 had different effects, *in vitro* and *in vivo*, on growth of oesophageal squamous carcinoma cells, apoptosis, PE and cell cycle distribution (Sun et al., 2013). The latter study showed that high levels of SOD2 promoted cell growth and PE rate, whereas moderate SOD2 levels suppressed tumour cell growth and PE, with an increase in apoptosis. Papa and colleagues observed a new mechanism between two isoforms of SOD in BC cells: SOD1 and SOD2. The loss of SOD2 expression was correlated with overexpression of SOD1. Furthermore, targeting SOD1 by a SOD1 inhibitor (LCS-1) could avoid an adaptation mechanism that maintains total ROS levels, leading to a drastic fragmentation and swelling of the mitochondrial matrix, with a significant increase in the level of mitochondrial O_2^- (Papa et al., 2014).

The GSH system is an important, and often the primary, redox buffering system in cells. High GSH levels have been observed in different types of tumours, and have been associated with clinical failure of chemotherapy (Calvert et al., 1998, Estrela et al., 2006). Therefore, several clinical trials have targeted the GSH system, either to sensitise tumours to chemotherapy agents such as melphalan (Bailey et al., 1997) or to reduce neurotoxicities in cancer patients treated with platinum-based chemotherapy (Block et al., 2008). The GSH:GSSG ratio has been used as a useful tool to assess the status of the cellular antioxidant system that controls redox homeostasis in different types of cancer cells (Meister, 1994). Furthermore, altering the GSH:GSSG ratio decreased the metabolic viability and clonogenicity of three different cancer cell lines (T98G glioblastoma, SNU80 thyroid carcinoma and KB oral carcinoma embryonic human cell lines) (Kaushik et al., 2014).

Reduced Grxs inhibit apoptosis either by binding to ASK1, in the same pathway as reduced Trx, or by reducing PSSG which acts as a critical regulator of apoptosis (Anathy et al., 2011). Silencing Grx-1 in bovine aortic endothelial cells caused disruption to the redox state of Akt protein, leading to a significant increase in apoptosis (Wang et al., 2007). A recent study showed that inhibition of the Grx system in hepatocellular carcinoma cells caused an increase in doxorubicin sensitivity and apoptosis, with a

significant decrease in expression of other antioxidants such as catalase, Trx and NAD(P)H:quinone oxidoreductase (NQO1) (C. Xavier, 2015).

1.2.3.2 Effect of redox proteins on cancer treatment: the Trx system

As mentioned earlier, the Trx system is an important redox system, and plays a major role in maintaining the intracellular ROS levels in cancer cells. Therefore, inhibiting the Trx system may alter the intracellular redox state and, subsequently, make cells more apoptotic and more sensitive to cancer treatments such as chemotherapy and radiotherapy. The role of the Trx system in regulation of the radioresponse of cancer cells will be discussed in Chapter 2, while the relationship of the Trx system's protein expression with the clinicopathological criteria and survival outcomes of cancer patients will be discussed in the introduction of Chapter 4.

1.2.3.2.1 Inhibition of the Trx system in pre-clinical studies

Among various Trx/TrxR inhibitors tested thus far, 1-methyl-1-propyl-2 imidazolyl disulphide (IV-2) has been the most widely studied in the literature (Li et al., 2016). IV-2, also known clinically as PX-12, is an irreversible inhibitor of the Trx/TrxR system and causes slow irreversible oxidation of the catalytic site Cys73 residue of Trx, and reversible oxidation of the catalytic site Cys32 and Cys35 residues of Trx (Kirkpatrick et al., 1998). IV-2 was classified as one of the most potent Trx/TrxR system inhibitors out of 700 disulphide analogues, with a mean GI_{50} (concentration that causes 50% growth inhibition) of 6.5 Amol/L against cancer cells in the NCI-60 cell line panel (Kirkpatrick et al., 1999). Therefore, IV-2 was extensively evaluated in several pre-clinical studies against different types of cancer.

MCF-7 BC cells treated with IV-2 caused an irreversible arrest in the G2/M phase of the cell cycle (Vogt et al., 2000). Another study showed that HeLa cervical cancer cells treated with IV-2 showed a significant inhibition of cellular proliferation and clonogenic survival, with an arrest in G1 phase of the cell cycle (Smart et al., 2004). IV-2 was known for a decade as a specific inhibitor of the Trx system. However, Huber and colleagues

showed that IV-2 could inhibit other proteins such as tubulin and cysteine proteases (papain and ficin) by interacting with their cysteine residues (Huber et al., 2008). An *in vivo* study showed that IV-2 treatment for 2 hours decreased microvascular permeability by 63% in HT29 xenograft tumours. However, the effect of IV-2 on microvascular permeability was decreased, to the pre-treatment values, after 48 hours' treatment (Jordan et al., 2005).

Auranofin (AUR) was the first oral gold (I) compound used for treating rheumatoid arthritis (Kean and Kean, 2008). It has shown high ability to inhibit TrxR, with anti-tumour activity across a panel of 36 cancer cell lines (Casini et al., 2009), and various cancer phenotypes including pancreatic, cervical, myeloma, lung and breast cancers, as will be discussed in detail in Chapter 2 (Yan et al., 2012, You et al., 2015, Bhatia et al., 2016, Raninga et al., 2016).

Motexafin gadolinium (MGd) is a novel anticancer agent based on a porphyrin-like structure that targets TrxR, in addition to GSH and ribonucleotide reductase (Magda and Miller, 2006). The mechanism of action of MGd is based on redox cycling that generates ROS molecules and catalyses the oxidation of intracellular reducing metabolites such as NADPH, GSH, ascorbic acid, and protein vicinal thiols (Magda et al., 2001, Magda and Miller, 2006). MGd was evaluated in clinical trials as a radiosensitiser, particularly in patients with brain metastases, as will be discussed in Chapter 2.

PMX290 (AJM290) and PMX464 (AW464) are quinol compounds, developed by the School of Pharmacy at the University of Nottingham (Wells et al., 2000). PMX290 was initially developed as a Trx inhibitor, but later studies found that it can also inhibit TrxR activity both in cell-free systems and in cell lysate (Chew et al., 2008a). Microarray and mass spectrometry analysis showed that PMX464 reacts with cysteine residues 32 and 35 of Trx (Biaglow and Miller, 2005). Both inhibitors showed high selectivity and potency against colon (HCT116 and HT29), renal (CAKI-1 and ACHN) and breast (MCF-7 and MDA-MB-435) cancer cell lines (Wells et al., 2000, Biaglow and Miller, 2005, Jones et al., 2006),

with initial results suggesting that PMX464 could sensitise MCF-7 BC cells to radiation (Zhang, 2008).

A recent study showed that a natural product named Diphenyl difluoroketone (EF24) exhibits high inhibition efficiency of TrxR and displays synergistic lethality with 5-FU in gastric cancer cells (Zou et al., 2016).

Limited studies have investigated the mechanism, function and effect of Trx2 in cancer treatment. However, Trx2 has been well studied in maintaining cardiac function by ROS elimination, preserving the mitochondrial integrity and suppressing apoptosis (Conrad et al., 2004, Huang et al., 2015).

Overexpression of TxNIP has been associated with decreased Trx activity, increased ROS levels, inhibited cell growth, cell cycle arrest and increased apoptosis in prostate cancer cells (Wei et al., 2017). Furthermore, transfecting TxNIP into tumour cells caused a significant reduction in cell growth due to arrest at the G0/G1 phase (Han et al., 2003). In contrast, inhibition of TxNIP expression was associated with tumour growth and metastasis in melanoma cells (Goldberg et al., 2003).

Recently, a novel generation of indolequinone analogues (IQs), produced at the University of Nottingham as novel bioreductive agents, have been shown to have actions in regulating the Trx system in PC cells (Yan et al., 2009, Yan et al., 2012). The current project sought to evaluate the mechanism of action of IQs on PC cell lines as single agents and in combination with ionising radiation, as will be discussed in Chapters 2 and 3.

1.2.3.2.2 Inhibition of the Trx system in clinical trials

Since IV-2 showed both significant *in vitro* cytotoxicity and encouraging *in vivo* antitumor activity, it was identified, at that time, as the first specific irreversible inhibitor of the Trx system to undergo clinical evaluation (under the name of PX-12) in cancer patients. PX-12 was evaluated in a total of five clinical trials; four phase I and one Phase II clinical trial. The first phase I study evaluated the effect of PX-12 in 38 patients with advanced

solid tumours (sarcoma, colorectal, appendiceal and renal cancers) (Ramanathan et al., 2007). Patients were treated with 9–226 mg/m^2 of PX-12, given intravenously (IV) for 1 or 3 hours on a daily X5 schedule repeated every 21 days (patients had not received chemotherapy or radiotherapy for at least four weeks prior to PX-12 treatment). After minutes of infusion, PX-12 was rapidly metabolised to 2-mercaptoimidazole and 2-butanethiol (Figure 1.11). The 2-butanethiol caused "garlic like" odour on the breath, which was a major logistical challenge for the administration of PX-12. PX-12 was well tolerated up to a dose of 226 mg/m^2 by a three-hour infusion, with a disease stabilisation observed at lower doses (9-36 mg/m^2). However, the tolerance dose seemed impractical due to the need for negative pressure area during infusion to prevent the odour of 2-butanethiol (Ramanathan et al., 2007). The second phase I study (phase IB) included 32 patients with advanced solid tumours treated with 300-450 mg/m^2/day of PX-12. The study used a portable delivery pump for 24 or 72 hours' infusion every 7-14 days or 21 days respectively. The study found that 400 mg/m^2/day of PX-12, either at 24 or 72 hours, was safe, tolerable and decreased the intensity of a cough and odour compared to the previous clinical trial. Also, the study found that patients with higher plasma Trx levels showed the best probability of having stable disease (Ramanathan et al., 2009).

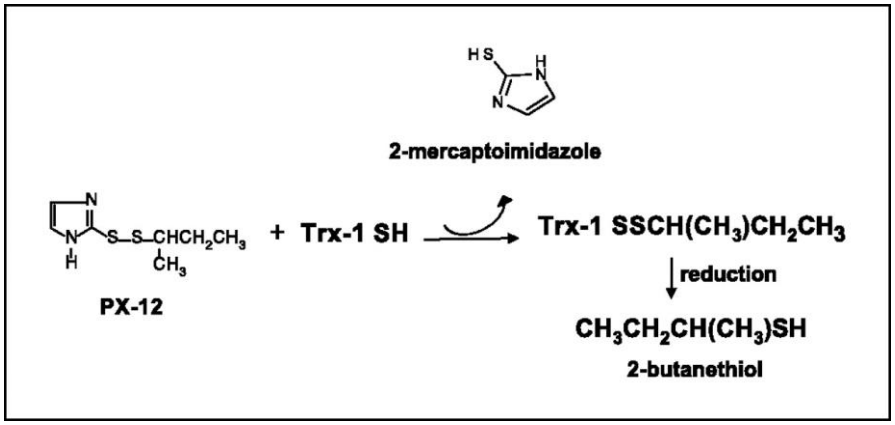


Figure 1.11: **Scheme of the potential mechanism of PX-12.** PX-12 interaction with reduced thiols (SH) of Cys73 on the active site of Trx results in thio-alkylated Trx and release of 2-mercaptoimidazole. The irreversible oxidation of Cys73 prevents the reduction of Trx by TrxR. Further reduction of the thio-alkylated Trx can release the volatile 2-butanethiol that caused "garlic like" odour on the breath and may be expelled through the lungs. Source: Ramanathan, R. K. et al. 2007. A Phase I pharmacokinetic and pharmacodynamic study of PX-12, a novel inhibitor of thioredoxin-1, in patients with advanced solid tumours. *Clinical Cancer Research,* 13, 2109-2114; used with permission.

The third phase I study included 14 patients with advanced refractory cancers treated with a 72-hour infusion of PX-12 on days 1, 2 and 3 of a 21-day cycle at a starting dose level of 300 mg/m^2/day. The PX-12 dose was escalated until the dose-limiting toxicity (DLT) was identified. In a total of 14 patients; 1, 10 and 3 patients were enrolled in the following dose cohorts: 300, 400 and 500 mg/m^2 respectively. The study concluded that 400 mg/m^2/day of PX-12 as a 72-hour infusion appeared to be safe and tolerable, with stable disease was observed in 7 patients (18%) (Ramanathan et al., 2012). The fourth Phase I study included 18 patients with advanced gastrointestinal cancers treated with PX-12 for a 24-hour infusion once a week at a starting dose level of 300 mg/m^2/day. The PX-12 dose was escalated until DLT was identified. The study found that the starting dose was the maximum tolerated dose with no evidence of any clinical activities. Furthermore, the pharmacokinetic analysis showed no significant trends in changes in the levels of plasma Trx pre or post PX-12 treatment (Baker et al., 2013).

The Phase II study should have included 28 advanced PC patients treated with chemotherapy. However, only 17 patients passed the entry criteria for the study, which included a certain level of cancer antigen 19-9 (CA 19-9) and standardised uptake value (SUV). The patients were treated with PX-12 (54 or 128 mg/m^2) for a 3-hour IV infusion daily X5 days every 21 days. The study aimed to achieve ≥40% of progression-free survival (PFS) in patients after four months of PX12 treatment. However, the results showed that no patient exceeded a PFS of 4 months, with a median PFS value of 0.9 months, with only two patients showed stable disease. The study was not completed and was terminated early (Ramanathan et al., 2011).

Aggregate clinical trials showed a lack of antitumor activity of PX-12, with an atypical toxicity profile such as strong pungent odour, respiratory irritation and pneumonitis. Also, recent evidence suggests that PX-12 can interact with other targets such as tubulin and cysteine proteases, which may explain the rapid metabolism of PX-12 in plasma proteins. Therefore, the results of clinical results suggest that further clinical development of PX-12 is not feasible. Although inhibiting the Trx system is still a target

of interest for developing novel anti-cancer agents, PX-12 was the only known drug that was clinically evaluated, at that time, as a specific inhibitor of the Trx/TrxR system.

Several other inhibitors of the Trx system were evaluated or have been investigated in clinical trials of cancer treatment either as bioreductive agents (as will be discussed in Chapter 2) such as apaziquone (EO9) and mitomycin C (MMC) or as other agents with different biological mechanisms such as ethaselen, arsenic trioxide, and dimesna (Mehta et al., 2009, Paz et al., 2012, Wang et al., 2011, Zhang et al., 2017a). However, these inhibitors are known as multi-target drugs and are not specific to the Trx system.

In conclusion, from the above, it can be seen that current treatment options for PC have failed to improve survival rates, with TrxR being a potential novel therapeutic target in PC. The current thesis set out to examine the role of the Trx system, using novel TrxR inhibitors, in regulating PC cell proliferation and radiosensitivity. The current thesis set out to examine the role of the Trx system, using novel TrxR inhibitors, in regulating PC cell proliferation and radiosensitivity by addressing the hypotheses mentioned below.

1.3 Hypotheses and aims

1.3.1 Hypotheses

1. Radiosensitivity and cell cycle progression of PC cells are altered by treatment with IQs.
2. IQ treatment impairs the function of the Trx system in PC cell lines.
3. Hypoxia increases the cytotoxic efficacy of IQs on PC cell lines.
4. Elevated protein expression of Trx and TrxR is an adverse prognostic factor for overall survival in patients with pancreatic, bile duct and ampullary cancers. .

1.3.2 Aims and objectives

1. Assess the effect of IQs on cellular cytotoxicity and radiosensitivity of PC cell lines by proliferation and clonogenic survival assays.

2. Investigate the role of IQs in Trx system function by examining a variety of *in vitro* assays including oxidative stress, cell cycle status, activity of TrxR and protein expression of Trx system family members in PC cell lines pre and post IQs treatment.
3. Observe the effect of hypoxia (1% O_2) on proliferation, clonogenic survival, protein expression of Trx system family members and expression of reductases enzymes in PC cell lines pre and post IQs treatment.
4. Investigate the association between the expression of Trx system proteins and the clinicopathological criteria and patient survival outcome, using conventional immunohistochemistry (IHC), in 230 tumours from pancreatic, bile duct and ampullary cancer patients.

Chapter 2: Effect of indolequinones on cell proliferation, survival and radiosensitivity of pancreatic cancer cells

2.1 Abstract

Background: Redox proteins are key members of cellular antioxidant systems, required to maintain redox homeostasis, with the Trx system being an important component. New analogues of indolequinones (IQs) were produced at The University of Nottingham as TrxR inhibitors. TrxR plays an important role in regulating cell growth, proliferation, gene transcription, redox homeostasis and apoptosis. The current chapter sought to determine the action of IQs on PC cell lines as single agents and in combination with ionising radiation. Furthermore, the current chapter investigates the cytotoxic effect of GM, an agent clinically used in the treatment for PC, and AUR, a well characterised TrxR inhibitor, on PC cell lines as positive controls.

Methods: In vitro cytotoxicity assays (proliferation and clonogenic survival), GM, IQs (IQ9 and IQ10) and AUR were assessed in PANC-1, MIA Paca-2 and BxPc-3 human PC cell lines. In the proliferation assay, subconfluent cells were treated with 50, 100, 250, 500 and 1000 nM of GM or with 0, 100, 250, 500 and 1000 nM of IQs or with 0, 500, 1000, 2000 and 4000 nM of AUR, with 0 nM as a control. Cells were counted, analysed and plotted over a 72-hour time course. In the clonogenic assays, cells were plated in T25 flasks and treated, 24 hours later, with 10, 25, 50, 100 and 250 nM of GM or with 100, 250, 500 and 1000 nM of IQs, with 0 nM as a control, for 48 hours before being plated for colony formation. In the drug-radiation combinations - clonogenic survival assay, cells were treated with the clonogenic IC50 of IQ9 and IQ10 for 48 hours, then irradiated with a single dose of 1, 2, 4, 6 or 8 Gy. Following irradiation, cells were trypsinised and plated for clonogenic survival. Effects of IQ9 and AUR on cell cycle progression of PANC-1 and BxPc-3 cells were assessed using flow cytometric analysis.

Results: IQs exhibit potent *in vitro* cytotoxicity at 24, 48 and 72 hours with IC50 values in the low nanomolar range. In the proliferation assay, PANC-1 cells showed low sensitivity to IQs (IC50=320-920 nM), while MIA Paca-2 (IC50=90-250 nM) and BxPc-3 cells (IC50=250-470 nM) showed high and intermediate sensitivity to IQs respectively. Results showed that IQ9 and IQ10 are less toxic than GM (IC50=40-850 nM), but more

toxic than AUR (IC50=400-2,550 nM) across all PC cell lines. PANC-1 cells seem less sensitive to GM than MIA Paca-2 and BxPc-3 cells. In the clonogenic assay, GM (IC50=20-45 nM) seems more potent than IQs (IC50=240-900 nM) across all PC cell lines. Clonogenic survival showed that MIA Paca-2 cells (IC50=240-260 nM) were more sensitive to IQs than PANC-1 (IC50=730-900 nM) and BxPc-3 cells (IC50>1000 nM). Increased radiosensitisation was observed for PANC-1 cells treated with IQs (51% increase for IQ9 ($P<0.0001$) and 48% increase for IQ10 ($P<0.0001$) at 6 Gy compared to control). A marginally increased radiosensitisation was observed for BxPc-3 cells treated with IQs (25% for IQ9 ($P<0.05$) and 23% for IQ10 ($P=0.192$) compared to control), with no altered radiosensitisation in MIA Paca-2 cells. Although IQs seem to sensitise PANC-1 and BxPc-3 cells to radiation at 6 Gy, the sensitiser enhancement ratio (SER) at 1% of survival for PANC-1 (SER=1.08-1.1) and BxPc-3 (SER=1.1-1.13) cells was low. The IC50 of IQ9 for 48 hours caused a significant cell cycle arrest of PANC-1 cells in the G0/G1 phase ($P=0.024$) with a significant decrease in S-phase ($P=0.013$), while no effect was observed on cell cycle progression of BxPc-3 cells.

Conclusion: IQs are highly effective on PC cell lines as single agents, with IC50 values in the low nanomolar range. However, IQs was less potent than GM and more potent than AUR. IQs treatment can cause cell cycle arrest and enhance radiotherapeutic efficacy in certain PC cell lines, but with low SER values.

2.2 Introduction hypothesis and aims

2.2.1 Redox protein regulation of radioresponse

As introduced in Chapter 1, redox proteins play a major role in cancer cell survival and proliferation by regulating the high levels of oxidative stress often found in cancer cells, making them potential targets for cancer treatment either as single modalities or in combination with conventional therapies. Redox buffering systems have been studied widely in terms of the role they play in regulating radioresponse of tumour cells, with the intent to inhibit these systems to modulate intracellular ROS levels that can induce lethal effects (Zhang and Martin, 2014). The involvement of redox proteins in radioresponse is summarised in Figure 2.1, and discussed below.

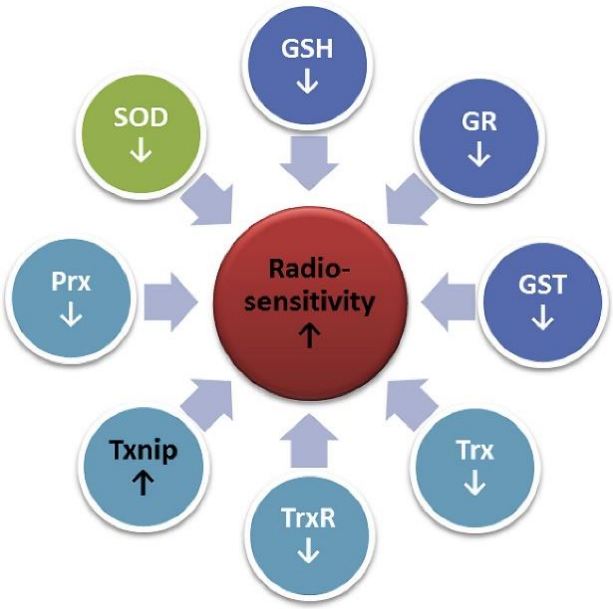


Figure 2.1: Involvement of redox proteins in the regulation of tumour cells radiosensitivity. GSH, reduced glutathione; GR, glutathione reductase; GST, glutathione S-transferase; Trx, thioredoxin; TrxR, thioredoxin reductase; TxNIP, thioredoxin-interacting protein; Prx, peroxiredoxin; SOD, superoxide dismutase. Source: Zhang, Y. & Martin, S. G. 2014. Redox proteins and radiotherapy. *Clinical Oncology*, 26, 289-300; used with permission.

2.1.1.1 SODs in regulating radioresponse

SODs play a major role in regulating the effects of irradiation in cancer therapy. The effect of modulating SOD expression has been studied to either alter radiosensitivity of tumour cells or to protect normal tissues against radiation. A recent study found that SOD2 overexpression was associated with radioresistance in myeloma cells, while knock-down caused significantly enhanced radiosensitivity and chemosensitivity (Brown et al., 2012). Another study investigated the expression of SOD1 in U118-9 human glioma cells (wild-type, neo vector control and stably overexpressing SOD1) irradiated with 10 Gy. It showed that SOD1-overexpressing cells were radioresistant compared to wild-type and neo vector control cells (Gao et al., 2008). Another, *in vivo* study showed that treating human microvascular endothelial cells (HMEC) and SA-NH mouse sarcoma cells with thiol-containing drugs lead to increase in expression and activity of SOD resulting in radiation resistance of both normal and tumour cells (Murley et al., 2008).

Overexpression of SOD seems to have a protective effect on normal tissues against radiation. An *in vivo* study showed that overexpression of SOD2 in oral cavity mucosa was associated with the absence of radiation-induced mucositis, a major toxicity of radiotherapy for head and neck cancer (Guo et al., 2003). Another study investigated, *in vitro* and *in vivo*, the radiosensitive effect of stable transfection of SOD2 in HT-29 colorectal cancer cells and CCD 841 CoN normal colorectal cells. The study showed that overexpression of SOD2 increased the radiosensitivity of HT-29 cells ($P<0.01$) and concurrently protected CCD 841 cells from radiation damage ($P=0.02$) compared to control cells (Zhang et al., 2017b).

2.1.1.2 GSH system in regulating radioresponse

Alteration of radiosensitivity through modulating intracellular GSH levels has been well studied over the last 3-4 decades. Historical studies showed that inhibition of GSH system by buthionine sulfoximine (BSO), a specific GSH synthesis inhibitor, can increase radiosensitivity in A549, V79 and A549 lung carcinoma cell lines in both normoxic and hypoxic conditions (Biaglow et al., 1983, Mitchell et al., 1983). A later study found that

head and neck squamous cell carcinoma (HNSCC) cells treated with BSO and dimethyl fumarate (DMF, a GSH-depleting agent) for 4 hours before 10 Gy irradiation led to 10% decrease in the endogenous level of GSH and increase radiation apoptotic cell death over control (Boivin et al., 2011). A novel study has shown knocking out phosphate-activated mitochondrial glutaminase (GLS2, a key enzyme in the conversion of glutamine to glutamate) in cervical cancer cells can cause a significant decrease in cellular GSH levels and an increase in ROS levels leading to a significant improvement in radiation response (Xiang et al., 2013). GR inhibition by 2-AAPA, an irreversible GR inhibitor, showed a significant increase in ROS levels and radiosensitivity of skin, breast, lung and ovarian human cancer cell lines over control (Zhao et al., 2009). A recent study used the GSH:GSSR ratio to monitor different redox homeostatic levels to examine variation in radiation sensitivity between two prostate cancer cell lines (PC3 and DU145) (Jayakumar et al., 2014).

2.1.1.2 Prxs in regulating radioresponse

Prxs are an important system to scavenge ROS in living cells, with a number of studies have investigated the effects of different levels of endogenous Prxs expression on radioresponse, and studying the alteration of endogenous expression of Prxs following radiation. Overexpression of Prxs following radiation was observed, and was associated with an increase in radioresistance, in a dose- and time-dependent manner, in cancer cell lines such as HT29 colon cancer cells, rat C6 glioma cells and MCF-7 BC cells (Chen et al., 2002, Wang et al., 2005), and in normal cell lines such as mouse intestinal epithelial IEC-6 cells (Bo et al., 2005). Another study showed that inhibiting Prx I in SW480 colon cancer cells, using a recombinant siRNA vector targeting Prx-I, was significantly associated with an increase in radiosensitivity and apoptosis (Zhang et al., 2005).

A proteomic study investigated the expressions of 20 different proteins following 4 Gy radiation in 10 head and neck cancer cell lines. Authors observed that high expression of Prx II and glutathione S-transferase pi (GSTP) was significantly correlated with the

radioresistance in head and neck cancer cell lines (Se Lee et al., 2008). A recent study found that silencing Prx2, using shRNA, can significantly increase ROS level and radiosensitivity in HCT116, Caco-2 and T84 colorectal cancer cell lines compared to control (Cerda et al., 2017). Furthermore, a novel study observed an increase in radiosensitivity, *in vivo* and *in vitro*, and apoptosis in oesophagal cancer cell lines after silencing two highly expressed isoforms of Prxs (Prx1 and Prx5) (Gao et al., 2011).

2.1.1.3 Trx system in regulating radioresponse

Trx system is one of the most widely studied redox buffering systems in regulating radioresponse of tumour cells. Inhibition of Trx system, mainly by targeting TrxR, sensitise tumour cells to irradiation by altering their ability to detoxify ROS. In last decades, numerous TrxR inhibitors were pre-clinically evaluated to increase the radiosensitivity of cancer cells, with a limited number of these inhibitors were investigated in clinical trials. As shown in Section 1.2.3.2, IV-2 is one of the most potent Trx-system inhibitors. *In vitro* study showed that Hela cervical cancer cell line treated with a IV-2, following irradiation, showed a significant decrease in clonogenic survival over control (Smart et al., 2004). A combination of a novel TrxR-inhibitor, phosphine gold(I) compound [Au(SCN)(PEt(3))], and ionizing radiation reduced the surviving fraction by 50% in U1810 human lung cancer cell line (Selenius et al., 2012). Recently, four novels Platinum (Pt) complex drugs were developed as novel inhibitors of TrxR, and showed a significant increase in ROS levels, growth inhibition and radiosensitivity in A375 melanoma cancer cell line, with a significant arrest in cell cycle progression (Xie et al., 2014). The same cell line treated with novel TrxR inhibitors, selenadiazole derivatives, showed a significant increase in cytotoxicity, ROS levels, apoptosis and radiosensitivity (Liang et al., 2014). A recent study at The University of Nottingham showed that inhibiting Trx system by metformin can cause a significant radiosensitising effect on BC cell lines in a phenotype specific fashion (Zhang et al., 2014). A recent study found that AUR, a well-characterised TrxR inhibitor, treatment increases the radiosensitivity of EMT-6 and 4T1 murine mammary carcinoma cells in both aerobic and hypoxic conditions. The radiosensitisation of these cells was accompanied by ROS

overproduction, mitochondrial dysfunction, DNA damage and apoptosis (Wang et al., 2017). Furthermore, the latter study showed an additional *in vivo* radiosensitisation after dual inhibition of Trx and GSH systems by AUR and BSO respectively.

D-allose, one of the rare sugars, can induce specific up-regulation of TxNIP and subsequent G1 cell cycle arrest in hepatocellular carcinoma cells (Yamaguchi et al., 2008). The up-regulation of TxNIP, by D-allose treatment, caused a significant increase in radiosensitivity, ROS level and apoptosis in human head and neck cancer cells (Hoshikawa et al., 2011). As indicated in Section 1.2.3.2, MGd is a well-characterised inhibitor of Trx system. Several pre-clinical and clinical studies have shown the value of MGd as a radiation sensitizer particularly in patients with brain metastases (Thomas and Khuntia, 2011). A clinical Phase III trial evaluated the radiosensitivity effect of MGd in 554 patients with brain metastases from non–small-cell lung cancer (279 patients were treated with radiotherapy plus MGd, while 275 patients were treated with radiotherapy alone). The MGd-radiotherapy patients showed favourable neurologic outcomes compared to radiotherapy alone patients, with a significant prolongation of the interval to neurologic progression (24.4 months vs 8.8 months, P=0.004) (Mehta et al., 2009).

In vivo studies and clinical trials that targeting redox buffering systems, such as Trx system, in tumour cells showed limited success either as single agents or in combination with conventional cancer treatments. A major challenge of these inhibitors, in terms of drug delivery or drug activation, is the aggressive behaviour of the tumour microenvironment which is characterised by hypoxia. The oxygenation status of tumour cells in solid tumours has long been believed to be a major factor that can decrease tumour response to cancer treatments, in particular radiotherapy. Over the last decades, a number of tumour-specific targeting strategies have been investigated against hypoxia such as bioreductive agents (also known as hypoxia-activated agents (HAPs)), hypoxia-selective gene therapy, targeting the hypoxia-inducible factor 1 (HIF-1) transcription factor and the use of recombinant obligate anaerobic bacteria (Brown and Wilson, 2004). The current study investigates the effect of novel HAPs, IQ-based agents, against PC cells as single agents and in combination with radiation.

2.2.2 Bioreductive agents

In 1972, the term 'bioreductive' was introduced to describe certain agents that have a mechanism of selective reduction/activation at low O_2 levels (hypoxic conditions) and become more potent than the parent compound (Lin et al., 1972). The mechanism of selectivity of a class of bioreductive agents (indolequinone-based agents) toward hypoxic cells is specifically covered in Section 2.2.2.2. In 1990, Workman and Walton established 'enzyme directed bioreductive drug development' program. This program aims to analyse cancer patients' biopsies and then select specific patients for bioreductive treatment based on the relative activities of certain reductases and O_2 levels in tumours versus normal tissues (Workman and Walton, 1990). Furthermore, other factors may contribute to the selectivity of these patients such as the redox potential, radical pKa, the nature of radical/radical decay kinetics, level of O_2 during drug activation, the ability of O_2 to reverse the bioactivation process, substrate specificity and the distribution of enzyme activity between tumour and normal tissues (Wardman et al., 1995, Phillips, 1998).

Several well-characterised bioreductive agents were investigated in cancer clinical trials, as single agents or in combination with chemo-radiotherapy. These agents either showed no antitumour activity, such as pimonidazole (Dische et al., 1993), etanidazole (Eschwège et al., 1997), tirapazamine (Rischin et al., 2008), PR-104 (McKeage et al., 2012) and TH-302 (evofosafamide) (Van Cutsem et al., 2016), or showed antitumour activity, such as nimorazole (Overgaard et al., 1998, Overgaard et al., 2005) or being under clinical evaluation such as AQ4N (novacea) and TH-4000 (tarloxotinib) (Mistry et al., 2017). The current chapter investigates the effect of IQ-based agents against PC cells, as single agents or in combination with radiation. The clinical outcomes of another well-characterised bioreductive agents such as mitomycin C (quinone-based agent) and EO9 (IQ-based agents) are discussed in details in Sections 2.2.2.1 and 2.2.2.2 respectively. Bioreductive agents have a range of chemical structures such as nitro compounds, aromatic noxides, aliphatic N-oxides, quinones, indolequinones (analogues of quinones)

and transition metal complexes (Mistry et al., 2017). The current chapter investigates the effect of IQ-based agents on PC cells.

2.2.2.1 Quinones

Quinone compounds exist in plants, bacteria and fungus at high concentration compared to mammalian tissues (Thomson, 2012). They also occur as a result of air pollution (such as diesel exhaust, tobacco and wood smoking) by photochemical reactions of polycyclic aromatic hydrocarbons (PAHs) with NO_3, ozone, and OH^- (Schmeltz et al., 1977, Lane et al., 1996). Chemically, quinones (Figure 2.2A) are regarded as cyclic unsaturated diketones resulting from the oxidation of aromatic compounds such as benzene and naphthalene. Biologically, quinones are cytotoxic molecules that can produce ROS and cause oxidative cycling.

Mitomycin C (MMC, Figure 2.2D), also known as mutamycin, was discovered in the 1950's, and was approved for clinical use as an antibiotic in 1974 (Verweij and Pinedo, 1990). In 1980, MMC was first recognised as a quinone-based bioreductive agent with preferential activity against hypoxic cancer cells (Kennedy et al., 1980). Subsequent *in vitro* and *in vivo* studies showed that MMC, alone or combined with radiation, was more effective against hypoxic cells than normoxic cells in different types of cancer (Rockwell and Kennedy, 1979, Rockwell et al., 1982, Keyes et al., 1985). Due to the encouraging results of preclinical studies, MMC was involved in several clinical trials of a variety of solid tumours including bladder, breast, cervical, colon, gastric, non-small cell lung and pancreatic cancers. Clinical trials showed that MMC, either alone or in combination with chemoradiation, had no significant benefit on patients' clinical outcome (Verweij and Pinedo, 1990). However, MMC showed significant improvement only in anal cancer treatment in combination with radiation and 5-FU, making it a standard therapy of anal cancers in the United Kingdom (James et al., 2013).

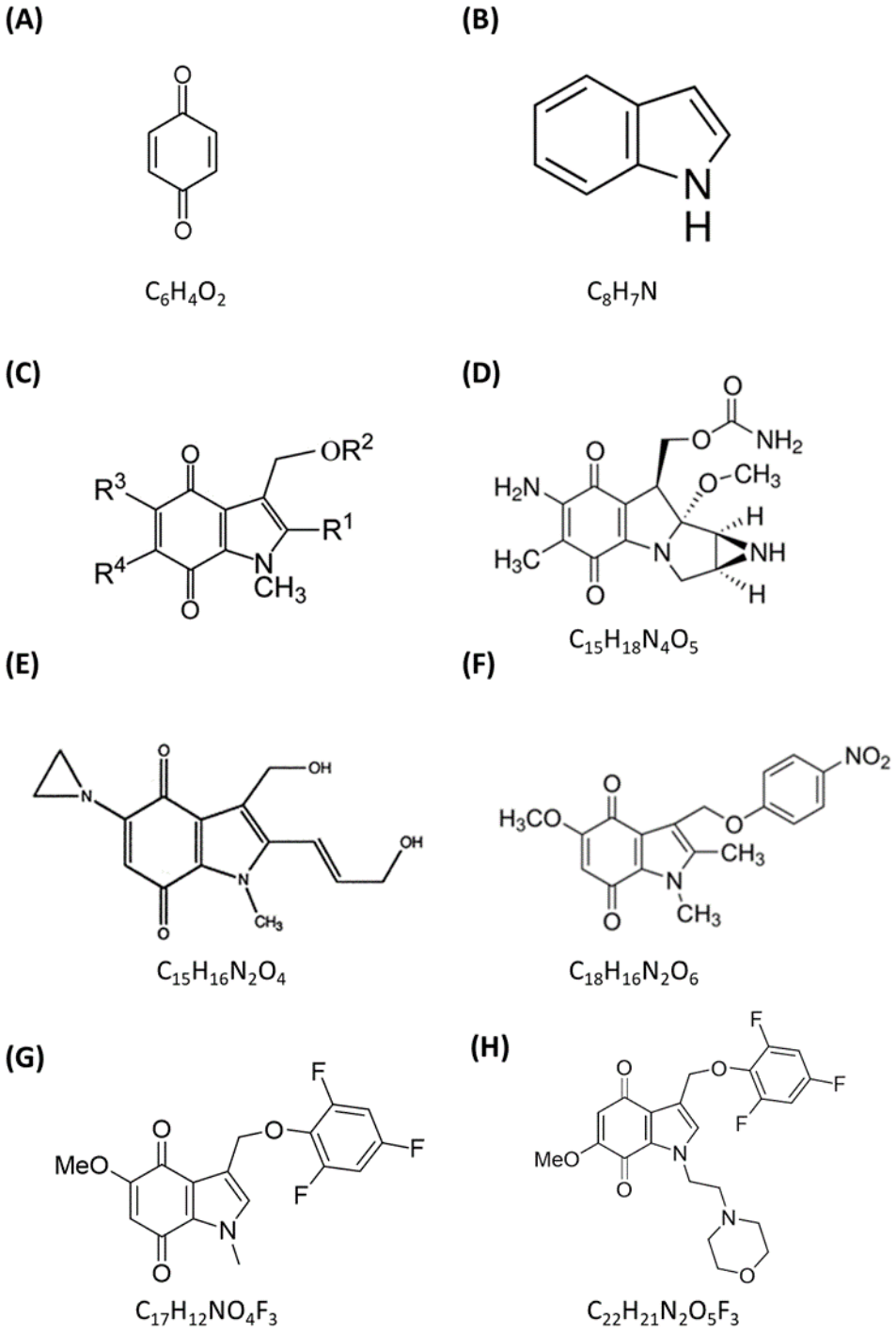


Figure 2.2: Chemical structures and molecular formulas of quinone (A), Indole (B), Indolequinone (C), mitomycin C (D) EO9 (E), IQ9 (G) and IQ10 (H). Abbreviation; MeO=methoxy group (O–CH_3), R=organic groups.

2.2.2.2 Indolequinones (IQs)

IQ (Figure 2.2C) molecule is based on an indole (Figure 2.2B) with two additional ketone groups (quinone) attached to the ring structure (Hanson, 2001). IQs are electron deficient conjugated molecules that can accept two electrons in one- or two-electron reduction processes, and subsequently inhibit a cellular target by reacting with its active site (e.g. NQO1 or TrxR), with greatest selectivity towards hypoxic cells by a mechanism discussed below.

As shown in Figure 2.3, IQs-based agents (for example EO9) can undergo one-electron reduction, by NADPH cytochrome P450 reductase (CPR), to produce semiquinone radicals (Figure 2.3, reaction 1), followed by another one-electron reduction, by CPR, to produce hydroquinones (Figure 2.3, reaction 2). However, in the presence of O_2, semiquinone is oxidised, by reducing O_2 to O_2^-, to IQs (the parent compounds) (Figure 2.3, reaction 3). Also, in the presence of O_2, hydroquinone is oxidised, by reducing O_2 to O_2^-, to semiquinone (Figure 2.3, reaction 4) (Wardman et al., 1995, Phillips, 1998). Although oxygen radicals, resulting from oxidation of semiquinones and hydroquinone, are scavenged by cellular detoxifying enzymes, rapid redox cycling itself can be toxic to the cells due to depletion of the reduced co-factors (Workman et al., 1992).

Also, IQs-based agents can undergo two-electron reduction, in one step, to produce hydroquinone (Figure 2.3, reaction 5) by NAD(P)H:quinone oxidoreductase (NQO1, also known as DT-diaphorase) flavoenzyme in an oxygen-independent process (Wardman et al., 1995, Phillips, 1998). NQO1 plays a detoxification role since it prevents the one-electron reduction of IQs-based agents and, subsequently, blocks oxidative cycling and ROS production (O_2^- radicals), making it a potential target in cancer treatment (Iyanagi and Yamazaki, 1970).

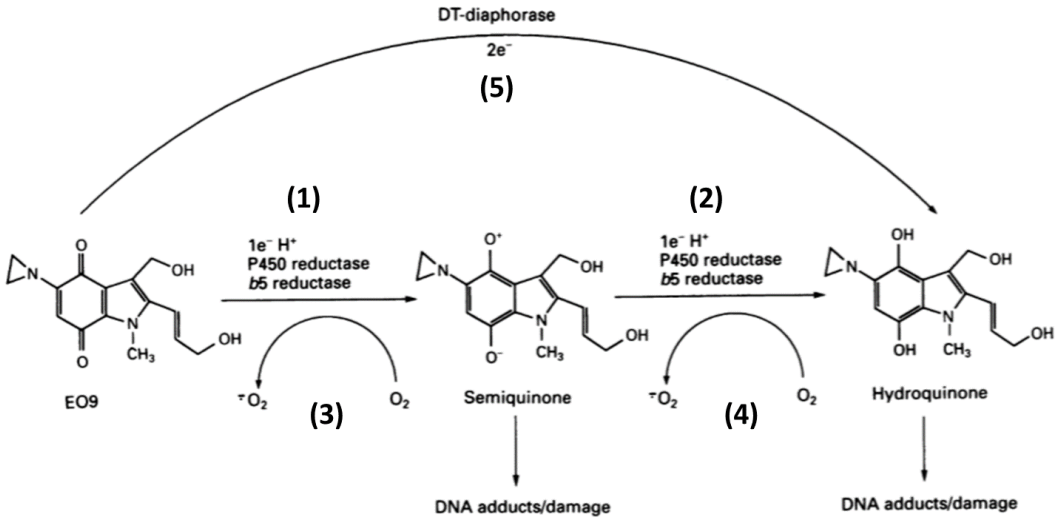


Figure 2.3: Possible routes of bio-activation of E09 by one- and two-electron reducing enzymes. The one-electron reduction of EO9 by P450 reductase (CPR) generates semiquinones (reaction 1) followed by another reduction by P450 reductase (CPR) to produce hydroquinone (reaction 2). In the presence of O_2, semiquinones and hydroquinones are oxidised to EO9 and semiquinones respectively, by reducing O_2 to O_2^- radicals (reaction 3 and 4). Also, EO9 can undergo two-electron reduction by NQO1 (reaction 5) to produce stable hydroquinone in an oxygen-independent process. Adapted from: Plumb, J. A., M. Gerritsen, and P. Workman. "DT-diaphorase protects cells from the hypoxic cytotoxicity of indolequinone EO9." *British journal of cancer*, 70.6 (1994): 1136-1143; used with permission.

2.2.2.2.1 EO9 (Apaziquone)

EO9 (33-hydroxy-5-aziridinyl-1-methyl-2-(1H-indole-4,7-indione)-propenol), clinically known as apaziquone, (Figure 2.2E) is an IQs-based bioreductive agent produced at the University of Amsterdam in the mid-1980s as an analogue of MMC (Oostveen and Speckamp, 1987). EO9 is reduced either by CPR and xanthine oxidase in one-electron reduction process or by NQO1 in a two-electron reduction process (Maliepaard et al., 1995, Bailey et al., 2001).

In contrast to MMC and most of the other bioreductive agents, preclinical studies showed that EO9 was highly cytotoxic, in both normoxic and hypoxic conditions, against different types of cancer (Roed et al., 1989, Phillips, 1996, Bailey et al., 2001). Under normoxic conditions, several studies showed that EO9 exhibited cytotoxic effects against different cancer cell lines, with good correlations between high NQO1 activity and high EO9 chemosensitivity ~~were~~ reported (Robertson et al., 1992, Plumb et al.,

1994a, Plumb et al., 1994b, Collard et al., 1995). However, under hypoxic conditions, EO9 was effective only against cancer cell lines with low NQO1 activity, suggesting that other reductases such as CPR and xanthine oxidase play a critical role in the hypoxic selectivity of EO9 (Plumb et al., 1994a, Plumb et al., 1994b, Robertson et al., 1994). In conclusion, cell lines with high NQO1 activity tend to be the most sensitive to E09, while cell lines with low NQO1 activity tend to be the most resistant cell lines to EO9, due to their low NQO1 activity, this resistance can be overcome in hypoxia. The low cytotoxic effect of EO9 on NQO1-rich cell lines under hypoxic conditions showed that the reduction of EO9 by NQO1 is an oxygen-independent process, while the reduction of EO9 by CPR is an oxygen-dependent process. Therefore, theoretically, EO9 can target the hypoxic regions of NQO1-deficient tumours and both aerobic and hypoxic regions of NQO1-rich tumours (Workman, 1994).

In animal models, an hourly dose of EO9 was active against different human cancer cell lines established as xenografts in nude mice. However, all xenografts failed to respond to E09, as a single dose or daily dose, with no correlation ~~was~~ observed between EO9 cytotoxicity and NQO1 activity (Phillips et al., 1992b, Collard et al., 1995).

Due to the encouraging results of pre-clinical studies, EO9 was evaluated in several clinical trials. The first phase II clinical study included 92 patients with breast (n=22), colorectal (n=26), gastric (n=20) and pancreatic (n=24) cancers treated with a 5 minutes intravenous (i.v.) infusion of EO9 at a weekly dose of 12 $mg.m^{-2}$. Unfortunately, EO9 showed no anti-tumour activity, with reversible proteinuria, nausea and vomiting have occurred in 45%, 26% and 13% of patients during the treatment course respectively (Dirix et al., 1996). The second phase II clinical study included 38 chemotherapy naïve patients with advanced NSCLC treated with two different EO9 doses schedules by a single bolus i.v. injection in arm A 12 mg/m^2 weekly or a single bolus i.v arm B 22 mg/m^2 every three weeks. No anti-tumour activity of EO9 was observed, with reversible proteinuria, asthenia, nausea and vomiting were reported during treatment cycles (Pavlidis et al., 1996). The major expected reason for the failure of EO9 in the clinical

trials is the rapid clearance of EO9. The half-life of EO9 in mice and human were 3 and 0.9-19 minutes at the maximum tolerated doses of 3 and 27 $mg.m^{-2}$ administered i.v. respectively (Workman et al., 1992, Schellens et al., 1994). Furthermore, the level of NQO1 activity and hypoxia status were not assessed in patients' tumour samples, which was a main deficiency in the design of EO9's clinical trials (Phillips et al., 2013). Following the disappointing failure of EO9 in clinical trials, new generations of IQs were developed.

2.2.2.2.2 ES936

ES936 (5-methoxy-1,2-dimethyl-3-[(4-nitrophenoxy)methyl]indole-4,7-dione) (Figure 2.2F) is an IQ-based molecule was developed as a specific inhibitor of NQO1 (Winski et al., 2000). As shown in Figure 2.4, the mechanism of action of ES936 was based on the ability of NQO1 to reduce ES936 to unstable hydroquinone that binds to the active site of NQO1 (Winski et al., 2001).

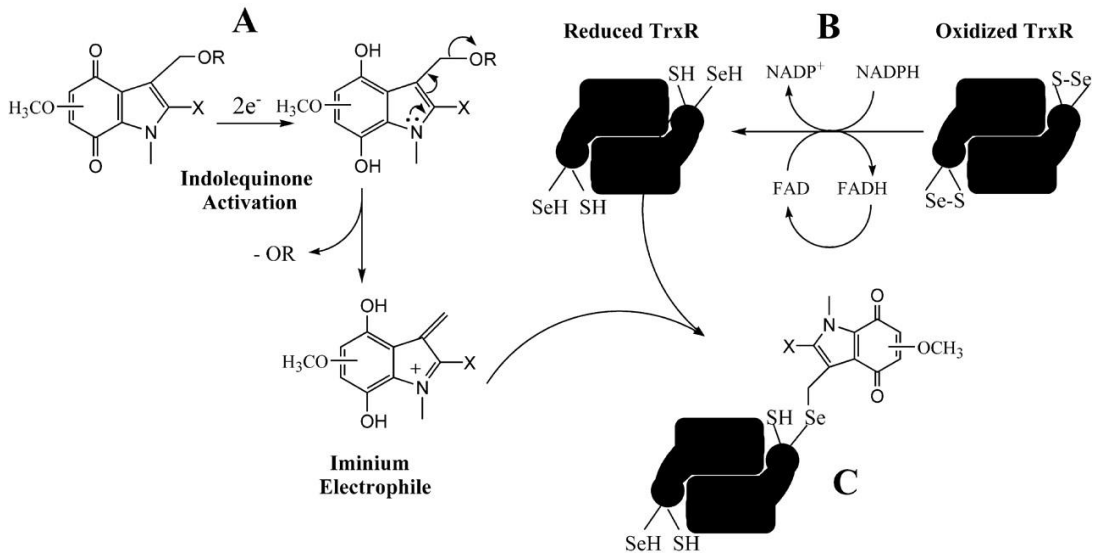


Figure 2.4: A proposed mechanism for the inhibition of TrxR by ES936. (A) ES936 is activated/reduced by reductases such as NQO1 and CPR to generate hydroquinone form of ES936 (reactive iminium electrophile). (B), reduction of oxidised TrxR by NADPH to generate the reduced C-terminal selenocysteine. (C), inhibition of TrxR via alkylation of the reduced C-terminal selenocysteine by the reactive iminium electrophile. Iminium electrophile, resulted from ES936 activation, acts as a substrate for TrxR and subsequently preventing it from reacting with oxidised Trx. Source: Yan, C., et al. 2009. Potent activity of indolequinones against human PC: identification of TrxR as a potential target. *Molecular Pharmacology*, 76, 163-72; used with permission.

ES936 showed high cytotoxic effect on different cancer cell lines, with half maximal inhibitory concentration (IC50) value in the nanomolar range (Winski et al., 2001, Dehn et al., 2003, Dehn et al., 2006). However, a subsequent study showed that NQO1 inhibition by ES936 does not correlate with growth inhibitory activity against PC cell lines, suggesting that other molecular targets may be relevant to explain the potent activity of ES936 (Reigan et al., 2007). In 2008, TrxR was identified as a potential target of ES936 (Chew et al., 2008b). As shown in Figure 2.4, ES936 is reduced to a hydroquinone either by NQO1 (one step, two-electron reduction) or CPR (two steps, one-electron reduction). Then, reduced ES936 (hydroquinone) inhibits TrxR by reacting with C-terminal selenocysteine residues in its active site, and subsequently preventing it from reacting with the oxidised Trx. The study showed a correlation between the inhibition of TrxR activity, by ES936, and the growth inhibitory activity of HCT-16 human colon carcinoma cells (Chew et al., 2008b).

2.2.2.2.3 ES936 analogues

In 2009, a series of ES936 analogues (8 analogues) was developed by Prof. Christopher Moody at the University of Nottingham, with a similar mechanism of action of ES936, as potential anti-cancer agents against PC (Yan et al., 2009). Only two studies have evaluated the efficacy of these analogues, as single agents, in PC cell lines (Yan et al., 2009, Yan et al., 2012). The first study (Yan et al., 2009) included nine IQs (ES936 and eight analogues of ES936); the ninth IQ (IQ9) (Figure 2.2G) is the analogue that is evaluated in the current project, in addition to a new analogue (IQ10) (Figure 2.2H). IQs showed higher potency than ES936 against three PC cell lines (PANC-1, MIA Paca-2 and BxPc-3 cell lines), with IC50 values in the nanomolar range. In the same study, two ES936 analogues (IQ3 and IQ6) were selected to screen against the NCI-60 cell line panel and were found to be cytotoxic against renal, colon and melanoma cancer cell lines, with IC50 values in the nanomolar range. The study also showed that MIA Paca-2 cells treated with IQ3 and IQ9 for 4 hours showed 90% inhibition in TrxR activity, with significant

antitumor activity against pancreatic MIA Paca-2 xenograft tumours implanted into female athymic nude (Yan et al., 2009).

In the second study, the same group applied IQ3 and IQ9 analogues to investigate a potential apoptosis mechanism that is induced by IQs in PC cell lines (Yan et al., 2012). The study found that inhibition of TrxR in MIA Paca-2 cells caused a shift of cellular redox state due to the accumulation of oxidised Trx. Authors observed that oxidized Trx can activate apoptosis signal-regulating kinase 1 (ASK1), an upstream activator of p38/c-Jun NH2-terminal kinase (JNK) in the mitogen-activated protein kinase (MAPK) apoptotic signalling cascade. By using liquid chromatography-tandem mass spectrometry analysis, the study confirmed that C-terminal selenocysteine of TrxR was the main adduction site of the IQ-derived iminium electrophile. Also, the study showed that IQ3 and IQ9 were highly cytotoxic against PC cells, with IC50 values in the nanomolar range. Moreover, both analogues showed an 11-fold greater inhibition potency of TrxR activity than AUR (Yan et al., 2012). Although these two studies have shown that ES936 analogues were highly cytotoxic and effective as single agents towards PC cells, the radiosensitising effect of these analogues has never been studied. Therefore, the current chapter aims to investigate the effect of IQs on radiations sensitivity and cell cycle progression of PC cells by addressing the hypotheses mentioned below.

2.2.3 Hypotheses and aims

Radiosensitivity and cell cycle progression of PC cells are altered by treatment with IQs.

2.2.4 Aims

1. Asses the cytotoxic effect of IQs on PC cell lines.
2. Observe the radioresponse of PC cell lines treated with IQs for 48 hours.
3. Investigate the effect of IQs on cell cycle progression of PC cell lines.

2.3 Materials and methods

2.3.1 General growth conditions

Tissue culture was performed in class II biological safety hood, which was wiped with 70% ethanol before and after tissue culture. All cell lines were cultured at 37˚C in a humidified incubator with 5% CO_2, with three different types of routine culture media, as will be described in Section 2.3.4, supplemented with 10% Iron-Supplemented Donor Calf serum (PAA Laboratories, Austria). Serum was heat inactivated (56˚C water bath for 45 minutes) before use. T75 cm^2 tissue culture flasks were used for routine cell culture, and another size of tissue culture flasks (T25 and T175 cm^2) and plates (6-well plate) were used according to the requirement of specific experiments. All tissue culture related reagents were pre-warmed to 37˚C in a water bath. The types of tissue culture flasks and plates, and the medium volume applied for each of them are listed in Table 2.1.

Flask/plate size	Volume of medium (ml)	Volume of 1× trypsin-EDTA (ml)
T175 cm^2	25	7
T75 cm^2	15	5
T25 cm^2	5	2
6-well plate	2	0.5

Table 2.1*:* Tissue culture flasks and plates and the related reagents volume.

All cell lines are subcultured when reaching 80-90% confluence, with a maximum passage window of 15. To subculture, the original medium was removed and cells washed with phosphate buffered saline (PBS) (without Ca^{2+} and Mg^{2+}) (Sigma). Cells were detached from the flask by adding a very low volume of trypsin-EDTA (0.5mg/ml, Sigma). The flask was incubated at 37˚C for 3-5 minutes. Flasks were observed using a microscope to ensure cell detachment. Complete medium was added at an appropriate ratio to deactivate trypsin-EDTA, and then the solution of the cell was transferred into a new tissue culture flask and placed into the incubator. Cell line authentication via Short

Tandem Repeat (STR) profiling test (every six months) and Mycoplasma test (every 1-2 months) are conducted routinely for all cell lines in this project.

2.3.2 Cryopreservation

Cells were frozen and preserved in liquid nitrogen to keep them at low passage number. For cryopreservation, cells were brought into suspension using trypsin-EDTA and counted using a haemocytometer. Cells were centrifuged at 1000 rpm (revolutions per minute) for 5 minutes and $1x10^6$ resuspended in 1 ml of freezing media (10% dimethyl sulfoxide (DMSO)) (Sigma) in a labelled cryovial. Cells were placed at -80˚C overnight in Mr Frosty freezing container before transferring to liquid nitrogen until further use.

2.3.3 Cell recovery from cryopreservation

After disinfecting the vial with 70% ethanol, the cell suspension was transferred into 9 ml of complete medium. The suspension was then centrifuged at 1000 rpm for 5 minutes. Then, the supernatant was discarded, and the cell pellet resuspended in complete medium. Then, cells were transferred into a $T25cm^2$ tissue culture flask, and placed into the incubator. Culture medium was changed the following day, and cells cultured following routine procedures.

2.3.4 Pancreatic cancer cell lines

Three human adenocarcinoma PC cell lines (PANC-1, MIA Paca-2 and BxPc-3) were selected for this project based on their previous responses to IQs as single agents (Yan et al., 2009, Yan et al., 2012). Also, these PC cell lines, as shown in Table 2.2, represent different molecular characteristics in those genes involved in PC development. Donor patient's information and characteristics for each PC cell line are shown in Table 2.2 (Deer et al., 2010). The relationship of genotype to phenotype of PC cell lines is still unclear as there are few studies available that investigate the impact of these mutations on PC cells behaviour (Deer et al., 2010). Two studies found no association between the

mutational status of PC driver genes (KRAS, TP53, CDKN2A and DPC4) and the grade of differentiation or the biological behaviour of PC cell lines (Sipos et al., 2009, Monti et al., 2004). However, a single study indicated a potential association between in vivo metastatic behaviour and P53 status (Loukopoulos et al., 2004).

Cell line	Age/ Gender	Derivation	Doubling time	Metastasis	KRAS	P53	P16	DPC4
MIA Paca-2	65, Male	Primary tumour	40 hours	ND	12 Cys	248 Trp	HD	Wild type
PANC-1	56, Female	Primary tumour	52 hours	Yes	12 Asp	273 His	HD	Wild type
BxPc-3	61, Female	Primary tumour	48-60 hours	No	Wild type	220 Cys	Wild type	HD
MDA-MB-231	51, Female	Primary tumour	16 hours	Yes	12 Asp	280 Arg	67 Leu	AAD 223-301
MCF-7	69, Female	Primary tumour	33 hours	Yes	12 Asp	Wild type	67 Leu	Wild type

Table 2.2: Donor patient's information, characteristics of PC cell lines and genetic status of four most common genes involved in PC development. Data were collected from: Eckert, L.B. et Al. 2004. Involvement of Ras activation in human breast cancer cell signaling, invasion, and anoikis. Cancer research, 64(13), pp.4585-4592. Berns, E. et al. 1995. Infrequent CDKN2 (MTS1/p16) gene alterations in human primary breast cancer. British journal of cancer, 72(4), p.964. Schutte, M. et al. 1996. DPC4 gene in various tumor types. Cancer research, 56(11), pp.2527-2530. De Winter, J.et al. 1997. DPC4 (SMAD4) mediates transforming growth factor-b1 (TGF-b1) induced growth inibition and transcriptional response in breast tumor cells. Oncogene, 14, pp.189l-1899. Kao, J., Salari. et al. 2009. Molecular profiling of breast cancer cell lines defines relevant tumor models and provides a resource for cancer gene discovery. PloS one, 4(7), p.e6146. Deer, E. L. et al. 2010. Phenotype and genotype of PC cell lines. *Pancreas*, 39, 425-35. Abbreviation: ND=not described, HD=homozygous deletion, AAD=amino acid deletions.

In the current project, for specific experiments, two human BC cell lines (MCF-7 and MDA-MB-231) were used as positive control cell lines, as both cell lines have been well-characterised in published literature, in terms of studying the Trx system in different types of cancer (Berggren and Powis, 2001, Farina et al., 2011, Sun et al., 2012, Zhang, 2014, Bhatia et al., 2016). All cell lines were originally obtained from the American Type Culture Collection (ATCC). BxPc-3, MIA Paca-2 and MCF-7 cell lines were cultured in RPMI-1640 medium, PANC-1 cell line was cultured in Dulbecco's Modified Eagle's

Medium (DMEM) and MDA-MB-231 cell line was cultured in Minimum Essential Medium Eagle (MEM). Table 2.3 describes the specific medium for each cell line with all additional reagents.

Cell line	Reagent	Source	Volume
MIA Paca-2, BxPc-3 and MCF-7	RPMI-1640 medium	R8758, Sigma	500 ml
	Heat Inactivated Iron Supplemented Donor Calf Serum	PAA laboratories	56 ml
	Penicillin/Streptomycin (with 10,000 units penicillin and 10 mg streptomycin/mL)	P4333, Sigma	5.6 ml
PANC-1	Dulbecco's Modified Eagle's Medium	D5546, Sigma	500 ml
	Heat Inactivated Iron Supplemented Donor Calf Serum	PAA laboratories	5.6 ml
	Penicillin/Streptomycin (with 10,000 units penicillin and 10 mg streptomycin/mL)	P4333, Sigma	5.6 ml
MDA-MB-231	Minimum essential medium eagle (MEM)	M5650, Sigma	500 ml
	Heat Inactivated Iron Supplemented Donor Calf Serum	PAA laboratories	56 ml
	L-Glutamine (200 mM)	G7513, Sigma	5.6 ml
	MEM Non-essential amino acids solution (100x)	M7145, Sigma	5.6 ml
	Penicillin/Streptomycin (with 10,000 units penicillin and 10 mg streptomycin/mL)	P4333, Sigma	5.6 ml

Table 2.3: Cell culture medium.

2.3.5 Cellular Characteristics of PC cell lines; growth curves and plating efficiency

Growth curves and plating efficiency (PE) experiments were used to evaluate the cellular characteristics of PC cell lines. For growth curves, subconfluent PANC-1, MIA Paca-2 and BxPc-3 cells were trypsinised and resuspended as single cells in complete cell culture medium. 1×10^5 cells of each cell line (2×10^5 for MIA Paca-2) were plated in each well of a 6-well plate (3 wells/time point) and incubated overnight to allow cells attachment. At 24, 48, 72 and 96 hours after seeding, cells were trypsinised, and the number of cells

was counted using a haemocytometer (Gizmo). The cell number was assessed by mixing 20 ul of cell solution with 20 of trypan blue (to exclude dead cells stained with trypan blue if needed), then, 8 ul of the mixture was loaded into the haemocytometer chamber (including nine squares). The total number of cells in five squares (the upper left and upper right, the lower left and lower right and the one directly in the centre) was multiplied by 4000 to give the total number of cells per ml. Cell counts were recorded, analysed and plotted over a 96-hour time course. Experiments were repeated independently three times. The doubling time was estimated from the growth curve of each cell line.

PE, an inherent characteristic of cell lines, was assessed using the clonogenic survival assay. Generally, subconfluent cells, without any treatment, were initially plated for clonogenic assay, to assess optimal cell numbers, in a series of densities (i.e. 100, 200, 400, 800 and 1000 cells per flask) and incubated without disturbance for two weeks (MIA Paca-2) or three weeks (PANC-1 and BxPc-3). The incubation time that gave the highest PE and appropriate colony size (colonies containing more than 50 cells were scored as survivors) was applied in future studies. PE for each cell line was assessed from controls and was defined as:

$$\boldsymbol{PE = \left(\frac{number\ of\ colonies}{number\ of\ cells\ plated}\right)}$$

2.3.6 Drugs and Drug preparation

IQ9 and IQ10 are novel analogues of ES936 synthesised and developed by Professor Chris Moody at the School of Chemistry in The University of Nottingham. IQs agents were initially diluted in DMSO as 10 mM, aliquoted and stored as a stock solution (stored at -20˚C). Each batch of IQs was tested against PC cells, in terms of proliferation and clonogenic assay, prior to actual experiments. GM was used as a positive cytotoxic control for PC cell lines. GM (Hospira, 2 grams) was kindly gifted from Professor Srinivasan Madhusudan at Division of Cancer and Stem Cells, City Hospital Campus,

Nottingham City Hospital. 300 mg of GM was dissolved in 10 ml of NaCl solution to obtain a 100 mM stock solution (stored at RT, for up to 21 days). AUR was used as a TrxR inhibition positive control for PC cell lines. AUR was purchased from Sigma, 10 mg were dissolved in 1473.8 µL of DMSO to obtain 10 mM, aliquoted and stored as a stock solution (stored at -20˚C).

In the current project, all experiments that investigated the response of cancer cells to a certain drug, untreated cells (0 nM) were treated with corresponding concentration of NaCl solution (for GM treatments) or DMSO (for IQs and AUR treatments) in the highest concentration of IQs, AUR and GM to confirm that any antitumour activity was a direct effect of the drug and not the diluter.

2.3.7 Cytotoxicity experiments

2.3.7.1 Proliferation assay

Subconfluent cells were trypsinised and resuspended as single cells in complete cell culture medium. 1×10^5 (2×10^5 for MIA Paca-2) cells were plated in each well of a 6-well plate and incubated overnight to allow cells to attach. On the following day, cells were treated with 50, 100, 250, 500 or 1000 nM of GM or with 100, 250, 500 or 1000 nM of IQs or with 500, 1000, 2000 or 4000 nM of AUR, with 0 nM as a control. At 0, 24, 48 and 72 hours after cells were treated, cells in each well (3 wells for each dose) were trypsinised and counted using a haemocytometer. Cell counts were recorded, analysed and plotted over a 72-hour time course. In the current project, all IC50 values, either in the proliferation or clonogenic assays, were estimated from the dose-response curves of each experiment. Data represent the average cell number ± standard deviation (SD) of three wells of one experiment. Experiments were repeated independently three times for GM, IQ9 and IQ10 treatments, and two times for AUR treatment.

2.3.7.2 Clonogenic assay

2.3.7.2.1 Drug alone clonogenic assay

Subconfluent cells were trypsinised and resuspended as single cells in complete cell culture medium. 5×10^5 cells were plated in each T25 flask and incubated overnight to allow cells to attach. On the following day, cells were treated for 48 hours with 10, 25, 50, 100 or 250 nM of GM or with 0, 100, 250, 500 or 1000 nM of IQs, with 0 nM as a control. Then, cells in each flask were trypsinised, counted and diluted at appropriate concentrations and plated into T25 cm^2 tissue culture flasks at low densities (3 flasks/dose/experiment). Cells were incubated for three weeks (two weeks for MIA Paca-2) at 37°C and 5% CO_2 to allow colony formation (30-100 colonies per flask were required). To maximise the plating efficiency of BxPc-3 cells, 5% gelatine (Sigma) coated flasks were used at the time of incubation of colony formation. Flasks for the clonogenic assay were incubated in an exclusive incubator separated from the routine tissue culture. Following incubation colonies were gently washed once with PBS, fixed with 50% methanol in 0.9% saline solution for 15 minutes, fixed with methanol for another 15 minutes, and then stained with 0.5% crystal violet for 30 minutes.

Cell survival was assessed for each drug concentration as follows:

$$Surviving\ Fraction\ (SF) = \left(\frac{number\ of\ colonies\ from\ each\ drug\ concetration}{number\ of\ cells\ seeded\ \times PE}\right)$$

Data represent the average SF ± standard deviation (SD) of two experiments, with each experiment containing three parallel flasks.

2.3.7.2.2 Radiation alone clonogenic assay

Cells were subconfluent at irradiation. X-ray-irradiation was conducted using an RS225 Xstrahl X-ray cabinet irradiation system (Xstrahl Limited, UK) with a single dose of 1, 2, 4, 6 or 8 Gy. X-rays were delivered at 195 kV, 10 mA, with a dose rate of 0.87 Gy/min. The cabinet was fitted with a 0.5 mm copper filter and used a 48.4 cm focus-to skin

distance. Dosimetry was routinely assessed by Radiotherapy Physics staff in the Department of Oncology, Nottingham University Hospitals NHS Trust, City Hospital campus. Sham-irradiated cells were used as controls. Cells were immediately trypsinised counted, diluted at appropriate concentrations and plated for clonogenic survival assay following irradiation. Colonies were stained and SF was calculated for each radiation dose as follows:

$$Surviving\ Fraction\ (SF) = \left(\frac{number\ of\ colonies\ from\ each\ radiation\ dose}{number\ of\ cells\ seeded\ \times PE}\right)$$

Radiation cell survival data were plotted as the logarithm of the surviving fraction versus radiation dose. Therefore, data can be presented mathematically based on hypothetical models for the mechanisms behind cell lethality. Linear Quadratic model (LQ) is the current golden standard mathematical model to fit the cell survival curve resulted from radiation toxicity, assuming that there are two mechanisms to cell death by radiation: single lethal event (α) and accumulation of sublethal events (β) based on the following formula:

$$Surviving\ Fraction\ (SF) = \ e^{-\alpha D-\beta D^2}$$

Where: SF is surviving fraction, D is radiation dose, α is proportional to dose and β is proportional to the squared dose.

A clonogenic survival calculator software, designed by *Deutsches Krebsforschungszentrum (DFKZ)* (Germany) (http://angiogenesis.dkfz.de/oncoexpress/software/cscal/index.htm), was used the above formula to fit the survival curves into LQ model, and to calculate α, β and α/β values.

The α/β ratio describes the curvature of the radiation cell survival curve. The alpha/beta ratio is the dose where cell killing due to the linear and quadratic components are equal. Higher α/β ratio indicates the increase in the linearity of cell survival curve; whereas lower α/β ratio indicates the increase in the curvature of the cell survival curve (Eric J. Hall, 2012). In radiotherapy, the low α/β values (1.5 to 5 Gy) are observed in late responding normal tissues, which indicate that radiation toxicity to the normal tissues is

high and should be using smaller radiation fractions than the 2 Gy, a standard fraction in conventional radiotherapy. By contrast, the high α/β values (6-14 Gy) are observed in acutely responding normal tissues, which indicate that the acute responses of normal tissues are relatively linear over the radiation doses (Williams et al., 1985).

2.3.7.2.3 Drug-radiation combination clonogenic assay

In the drug-radiation combination clonogenic assay, for each experiment, cells were irradiated with and without a subsequent treatment with IQs. Cells were plated and treated with/without a clonogenic IC50 value of IQ9 and IQ10 for 48 hours. A treatment of 48 hours with IQs was allowed before irradiation to keep consistent with other assays and give cells enough time to respond to IQs treatment. Following IQs treatment cells were irradiated with a single dose of 0, 1, 2, 4, 6 or 8 Gy. Then cells were trypsinised, counted, plated for clonogenic survival assays (cell number and flask size were adjusted according to irradiation dose) and stained as described in Section 2.3.7.2.1.

The SF of cells treated with IQs at 0 Gy was assessed as follow:

$$SF\ of\ cells\ treated\ with\ IQs\ at\ 0\ gy = \left(\frac{number\ of\ colonies\ from\ IC50\ treatment}{number\ of\ cells\ seeded\ \times PE}\right)$$

The SF of cells treated with IC50's of IQs was assessed for each radiation dose (except 0 Gy) as follows:

$$SF = \left(\frac{number\ of\ colonies\ from\ each\ radiation\ dose}{number\ of\ cells\ seeded\ \times PE\ \times SF\ of\ IQ\ treated\ cells\ at\ 0\ Gy}\right)$$

The sensitizer enhancement ratio (SER) was used to evaluate the radiosensitisation efficacy of IQs. SER is defined as a ratio of radiation doses in the absence and in the presence of the drug which produces the same biological effect. SER at 1% of survival can be calculated as follow:

$$SER = \left(\frac{Radiation\ dose\ of\ control\ at\ 1\%\ of\ survival}{Radiation\ dose\ of\ treated\ cells\ at\ 1\%\ of\ survival}\right)$$

2.3.8 Cell cycle analysis

PANC-1 and BxPc-3 cells were selected to investigate the effect of IQs on cell cycle, as both cell lines showed an increase in radiosensitivity after IQs treatment. Propidium iodide (PI) (Sigma) is able to bind DNA and is applied as a fluorescent stain for DNA in fixed cells. Cell cycle analysis is based on flow cytometry analysis of cellular DNA content by PI staining and deconvolution of the cellular DNA content frequency histograms, which reveals the distribution of cells in three major phases of the cycle (G0/G1 vs S vs G2/M) (Crissman and Hirons, 1994). To mimic the experimental conditions were used in irradiation experiments, subconfluent cells were treated with IC50's of IQ9 or 1000 nM of AUR for 48 hours at 37˚C in a humidified incubator with 5% CO_2. Untreated cells (0 nM) were set as negative control, while cells treated with 5 mM of hydroxyurea (HU) (Sigma) for 24 hours were set as a positive control; HU was diluted in H_2O as 500 mM, aliquoted and stored as a stock solution (stored at 4-8˚C). HU is a well-characterised DNA replication inhibitor that blocked the cell cycle of mammalian cells, and the majority of the cell population was arrested in G0/G1 phase (Pfeiffer and Tolmach, 1967).

After drug treatment, cells were trypsinised, and at least 1×10^6 cells centrifuged at 1000 rpm for 5 minutes, and then washed once with PBS and centrifuged again. After removing the supernatant, the cell pellet was resuspended and fixed in 5 ml of cold 70% ethanol in PBS and immediately stored at 4°C for at least 24 hours. Samples may be stored in this way for up to 7 days if required. When samples were to be analysed, cells were pelleted by centrifuging at 1000 rpm for 5 minutes. The ethanol was removed each pellet resuspended in a mixture of 400 µl of PBS and 100 µl of 1 mg/ml Ribonuclease (RNase) (Sigma) dissolved in dH_2O. RNase A prevents PI from staining RNA in the samples (Burrell, 1993). Finally, 5 µl of the PI solution at 0.25 mg/ml in dH_2O was added, and samples incubated in the dark at 37˚C for 30 minutes. After incubation, samples were analysed using MACSQuant flow cytometer (Miltenyi Biotec) by reading with fluorescence channel B3 at 488 nm. The proper gate was set to include the single cells in the flow cytometer analysis only and gate out the doublets. Analyse B3 histograms

with WEASEL Flow Cytometry Software (v.3.0.2) and the percentage of cells in each phase of cell cycle (i.e. G0/G1, S and G2/M) was plotted. Data represent the average percentage ± standard deviation of three independent experiments, with each experiment performed in a single data set.

2.3.9 Statistical analysis and graphs design

In the current project, a minimum of three experiments was required to apply statistical analysis, and error bars in all figures represent the standard deviation (SD) of a minimum of two independent experiments (Cumming et al., 2007). For combining SDs from individual experiments when pooling data, the following formula was used:

$$SDs = \sqrt{\left((n_1 - 1) \times SD_1^2 + (n_2 - 1) \times SD_2^2 + (n_3 - 1) \times SD_3^2\right) / (n_1 + n_2 + n_3 - y))}$$

Where SDs is the combined standard deviation, y is a number of experiments (here 3), SD_1 and SD_2 are the standard deviations in individual experiments and n_1 n_2 and n_3 are number of replicates in each experiment (Krishnaiah, 1980).

A Student's t-test was applied for statistical analysis of results using SPSS 23.0 software. A P-value of <0.05 considered being statistically significant.

All graphs in Chapter 2 and 3 were designed using Sigma Plot 12.5 software, while graphs in Chapter 4 were designed using SPSS 23.0 software. The combination of multiple graphs in a single figure was designed using Microsoft PowerPoint 2013.

2.4 Results

2.4.1 Characteristic experiments; growth curves and PE

The doubling times of PANC-1, MIA Paca-2 and BxPc-3 were, as shown in Figure 2.5, estimated as 41, 32 and 35 hours respectively, while PEs, retrieved from three independent experiments, were 0.29 (SD=0.017), 0.47 (SD=0.032) and 0.14 (SD=0.011)respectively. Results of characteristic experiments, growth curves and PEs, are comparable with published studies as discussed in Section 2.5.

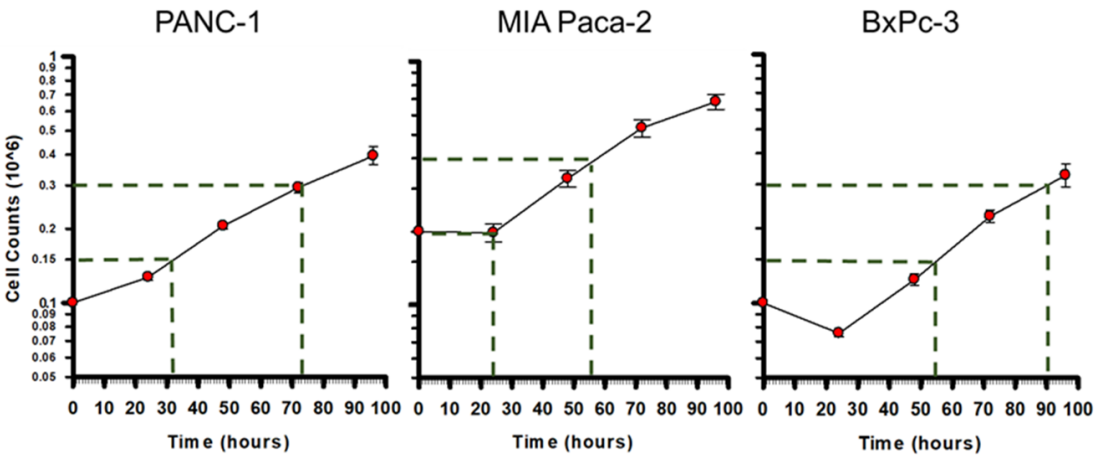


Figure 2.5: Growth curves for PC cell lines. The doubling times of PANC-1, MIA Paca-2 and BxPc-3 PC cells were calculated as 41, 32 and 35 respectively. The doubling time was estimated from the growth curves of each cell line. Data represent the mean ± standard deviation of three independent experiments, with each experiment performed in triplicate.

2.4.2 Cytotoxicity effect of GM, IQ9, IQ10 and AUR on PC cell lines

2.4.2.1 Effect of GM, IQ9, IQ10 and AUR on proliferation of PC cell lines

Effect of GM on the proliferation of PC cell lines was performed as this would be used in future experiments as a comparator. Figure 2.6 shows the effect of GM on each PC cell line, for each time point. PANC-1 is less sensitive than BxPc-3 and MIA Paca-2 cells after 24 and 48 hours' treatments. However, after 72 hours' treatment, all PC cell lines are extremely sensitive to all GM doses. Table 2.4 shows the IC50 values of GM for each PC cell line at 24, 48, 72 hours. MIA Paca-2 and BxPc-3 cells showed a similar sensitivity to

GM (IC50=40-75 nM) at all time points. However, PANC-1 cells showed low sensitivity to GM after 24 and 48 hours' treatment, with IC50 values of 850 and 260 nM respectively. However, after 72 hours' treatments, the IC50 value of GM for all PC cell lines was 40 nM. The current results of GM effect on proliferation of PC cell lines are comparable with published studies as discussed in Section 2.5.

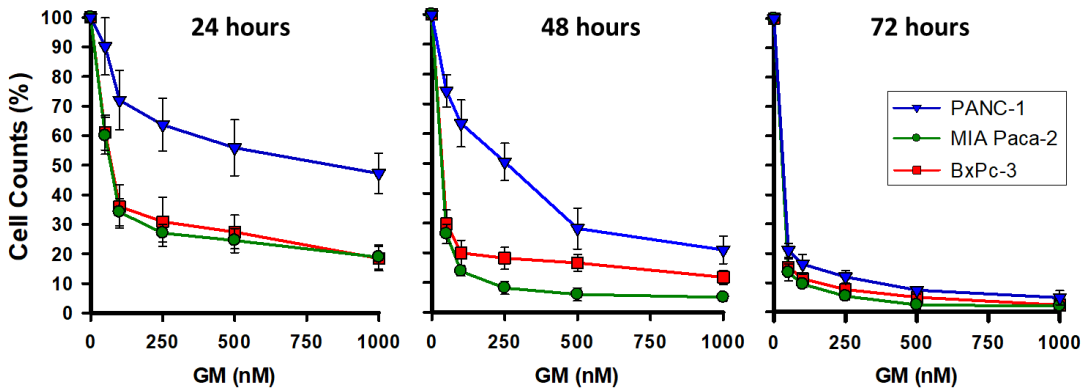


Figure 2.6: Effect of GM on the proliferation of PC cell lines. Cell counting of PANC-1, MIA Paca-2 and BxPc-3 treated with GM was plotted as a percentage of control (0 nM) for each time point. Data represent the mean ± standard deviation of pooled data of three independent experiments, with each experiment performed in triplicate.

Figure 2.7 shows the effect of IQ9 and IQ10 on the proliferation of each PC cell line, for each time point; while Table 2.4 shows the estimated IC50 values of IQ9 and IQ10 for each PC cell line. As shown in Figure 2.7 and Table 2.4, PANC-1 cells showed low sensitivity to IQs (IC50=320-920 nM), while MIA Paca-2 (IC50=90-250 nM) and BxPc-3 cells (IC50=250-470 nM) showed high and intermediate sensitivity to IQs respectively. Current results show that proliferation IC50 value of IQ9 for PC cell lines was found to be much higher than published studies (Yan et al., 2009, Yan et al., 2012), as discussed in Section 2.5, while IQ10 has never been evaluated against PC cells. In addition, PC cell lines were treated with GM at 250 nM for each time point as a positive control drug. As shown in Figure 2.7, effect of GM at 250 nm (single black point in each figure) was comparable with its previous findings (Figure 2.6). Current results show that GM seems to be more potent, at most concentrations and time points, than IQs against PC cell lines.

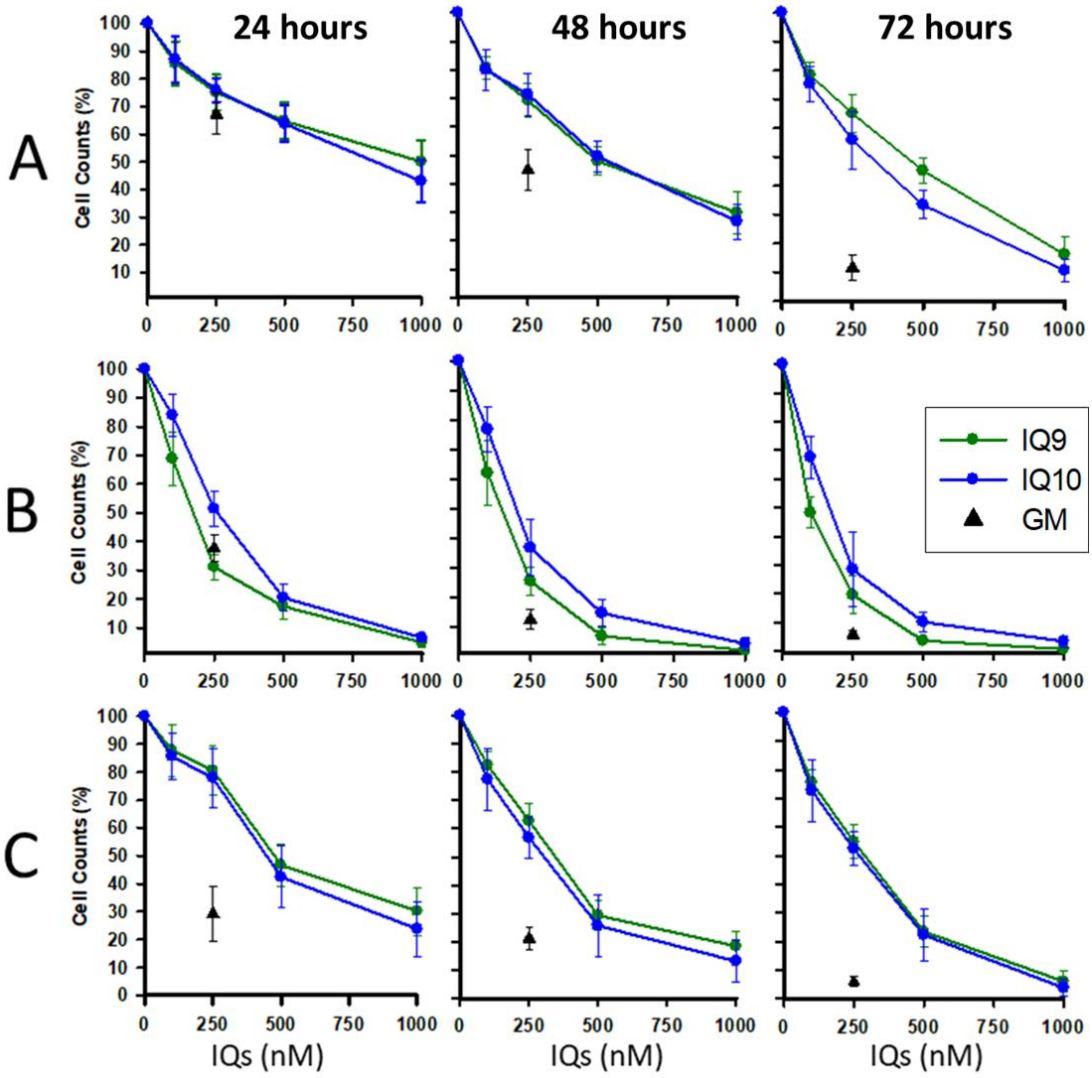


Figure 2.7: Effect of IQ9 and IQ10 on the proliferation of PC cell lines. Cell counting of PANC-1 (A), MIA Paca-2 (B) and BxPc-3 (3) treated with IQs was plotted as a percentage of control (0 nM) for each time point. The single black points in each graph represent the effect of GM at 250 nM on PC cells as positive controls. Data represent the mean ± standard deviation of pooled data of three independent experiments, with each experiment performed in triplicate.

Figure 2.8 shows the effect of AUR on the proliferation of each PC cell line, for each time point; while Table 2.4 shows the estimated IC50 values of AUR for each PC cell line.

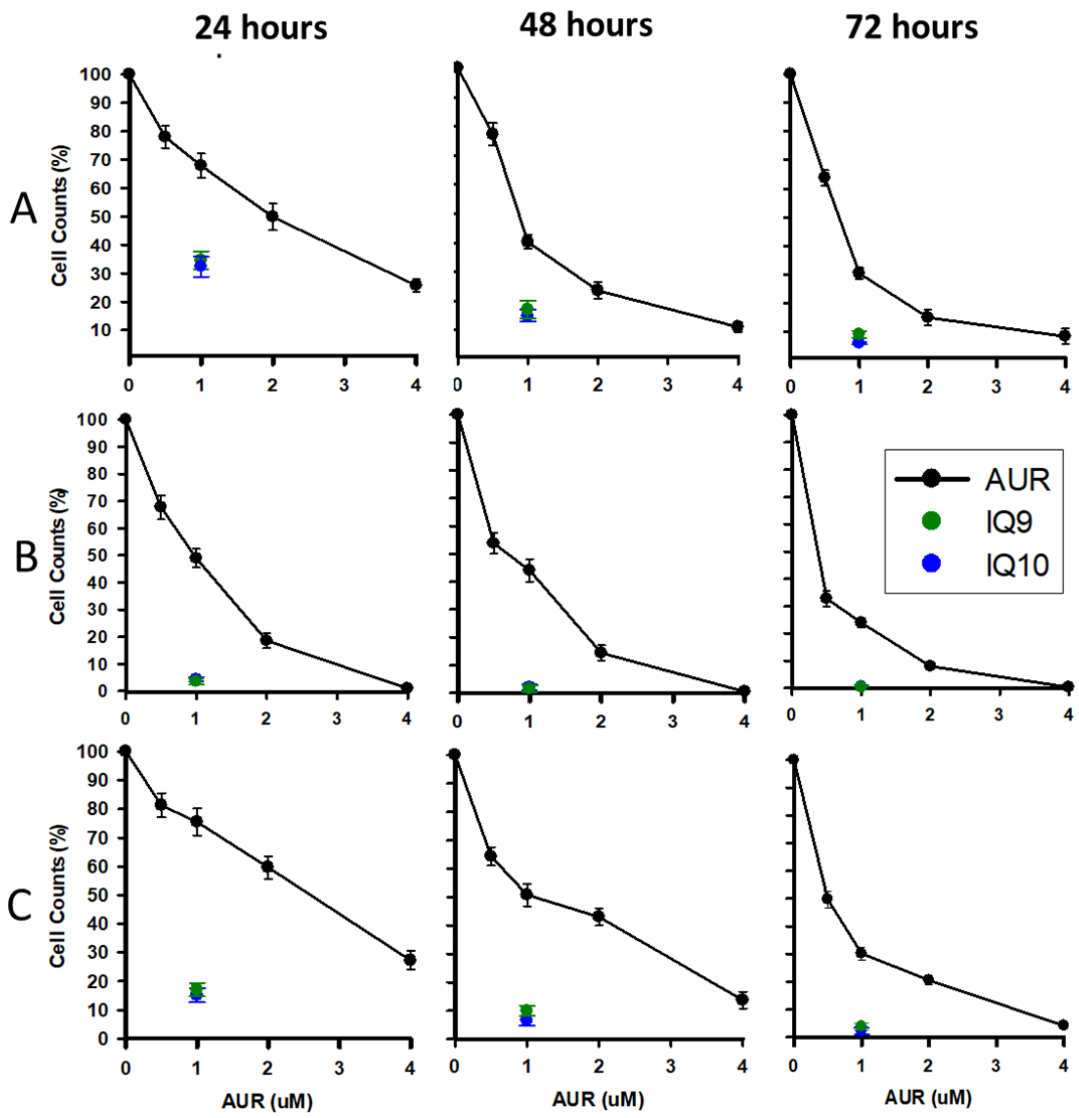


Figure 2.8: Effect of AUR on the proliferation of PC cell lines. Cell counting of PANC-1 (A), MIA Paca-2 (B) and BxPc-3 (C) PC cell lines treated with AUR was plotted as a percentage of control (0 nM) for each time point. The green and blue points in each graph represent the effects of IQ9 and IQ10 at 1000 nM on PC cells as positive controls respectively. Data represent the mean ± standard deviation of pooled data of two independent experiments, with each experiment performed in triplicate.

As shown in Figure 2.8 and Table 2.4, MIA Paca-2 was the most sensitive PC cell line to AUR with IC50 values between 400 and 1050 nM. While PANC-1 and BxPc-3 cells showed almost similar sensitivity to AUR, with IC50 values between 500 and 2550 nM. The current results of AUR effect on proliferation of PC cell lines are comparable with published studies as discussed in Section 2.5. In addition, PC cell lines were treated with

IQ9 and IQ10 at 1000 nM for each time point as positive controls. As shown in Figure 2.8, the effect of IQ9 (green points) and IQ10 (blue points) on PC cell lines was comparable with their previous findings (Figure 2.7).

Since the effect of AUR on the proliferation of PC cell lines was low compared to IQ9 and IQ10, AUR was used against MDA-MB-231 BC cell line as it has been well-characterised previously in published literature. Figure 2.9 shows the effect of AUR and IQs on proliferation of MDA-MB-231 BC cell line, while Table 2.4 shows the estimated IC50 values of AUR and IQs for MDA-MB-231 cells.

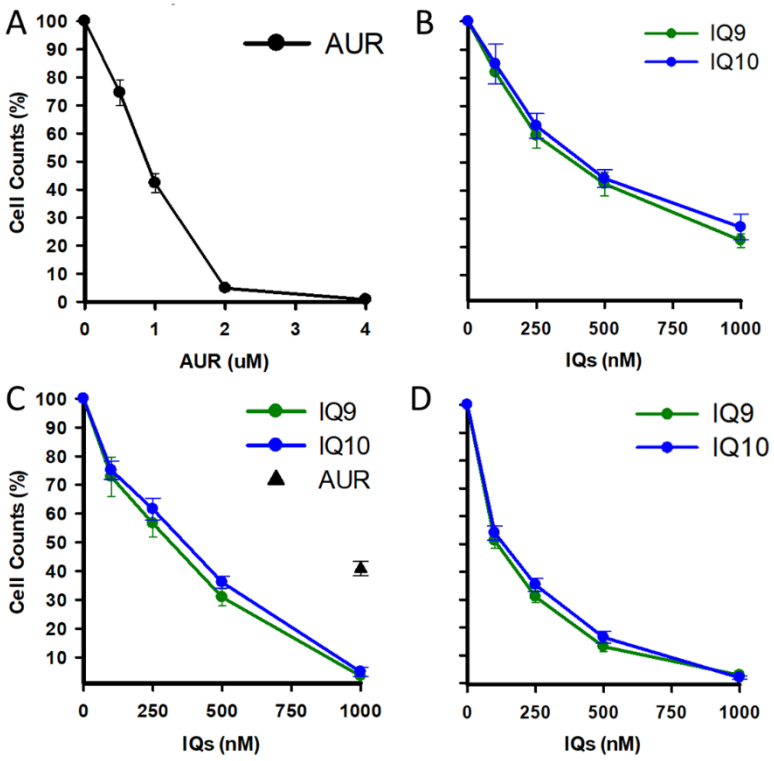


Figure 2.9: Effect of AUR, IQ9 and IQ10 on the proliferation of MDA-MB-231 BC cell line. MDA-MB-231 cells treated for 48 hours (A) or with IQ9 and IQ10 for 24 (B), 48 (C) and 72 (D) hours. Cell counting was plotted as a percentage of control (0 nM) for each time point. The black point on the graph (C) represents the effect of AUR at 1000 nM on MDA-MB-231 cells as a positive control. Data represent the mean ± standard deviation of pooled data of two independent experiments, with each experiment performed in triplicate.

As shown in Figure 2.9 and Table 2.4, MDA-MB-231 cells are more sensitive to IQ9 and IQ10 than AUR at 48 hours' treatments, with IC50 values of 900, 320, 380 and 900 nM

respectively. Generally, the IC50 values of AUR, IQ9 and IQ10 for MDA-MB-231 cells were in the same rang of IC50 values for PC cell lines. The current results of AUR effect on the proliferation of MDA-MB-231 BC cells are comparable with published studies as discussed in Section 2.5, while IQ9 and IQ10 have never been tested against MDA-MB-231 BC cells.

Cell line	Drug	IC50 nM (24 hours)	IC50 nM (48 hours)	IC50 nM (72 hours)
PANC-1	GM	850	260	40
	IQ9	920	470	440
	IQ10	800	490	320
	AUR	2000	900	700
MIA Paca-2	GM	70	40	40
	IQ9	180	160	90
	IQ10	250	200	170
	AUR	1050	750	400
BxPc-3	GM	75	40	40
	IQ9	470	350	270
	IQ10	430	290	250
	AUR	2550	1100	500
MDA-MB-231	GM	N/A	N/A	N/A
	IQ9	400	320	120
	IQ10	430	380	150
	AUR	N/A	900	N/A

Table 2.4: The proliferation IC50 values of GM, IQ10, IQ9 and AUR for PC cell lines and MDA-MB-231 BC cell line. IC50 values retrieved from three (GM and IQs) or two (AUR) independent experiments, with each experiment performed in triplicate. Abbreviations: N/A, not applied/performed.

2.4.2.2 Clonogenic effect of GM, IQ9 and IQ10 on PC cell lines

Initial experiments showed that PC cell lines were very sensitive to GM treatment in the clonogenic survival assay compared to the proliferation assay; no colonies were observed after 250, 500 and 1000 nM of GM treatment for all PC cell lines. Therefore, the dose range of GM was decreased to 0, 10, 25, 50, 100 and 250 nM instead of the initial dose range used in the proliferation assay (0-1000 nM). Figure 2.10 shows the clonogenic effect of GM on PC cell lines; while Table 2.5 shows the estimated clonogenic IC50 value of GM for PC cell lines.

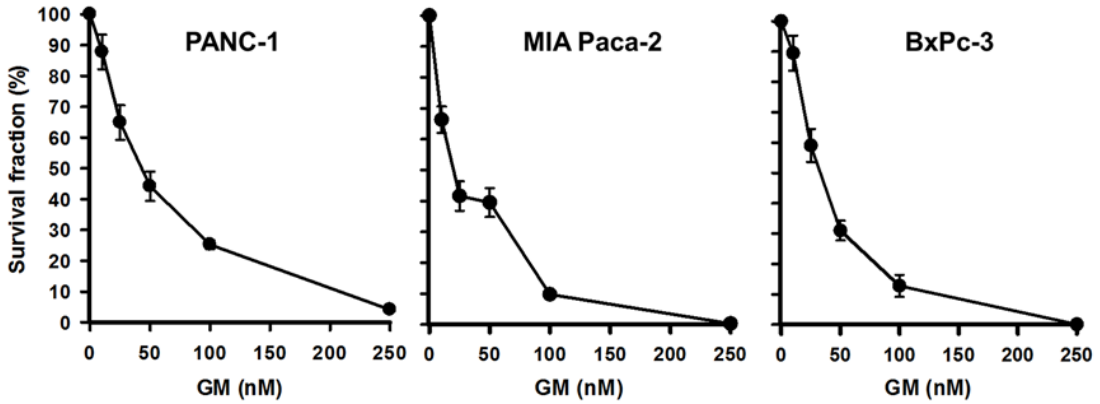


Figure 2.10: Clonogenic effect of GM on PC cell lines. Survival fraction of PANC-1, MIA Paca-2 and BxPc-3 PC cell lines treated with GM was plotted as a percentage of control (0 nM). Average PEs: PANC-1=0.37, MIA Paca-2=0.43 and BxPc-3=0.12. Data represent the mean ± standard deviation of pooled data of two independent experiments, with each experiment performed in triplicate.

As shown in Figure 2.10, all PC cell lines were sensitive of GM with IC50 values of 45, 20 and 34 for PANC-1, MIA Paca-2 and BxPc-3 cells respectively. No colonies were observed in MIA Paca-2 and BxPc-3 cells after treatment with 250 nM of GM. The current results of GM effect on clonogenicity of PC cell lines are comparable with published studies as discussed in Section 2.5. Figure 2.11 shows the clonogenic effect of IQs on PC cell lines; while Table 2.5 shows the clonogenic IC50 values of IQs for PC cell lines.

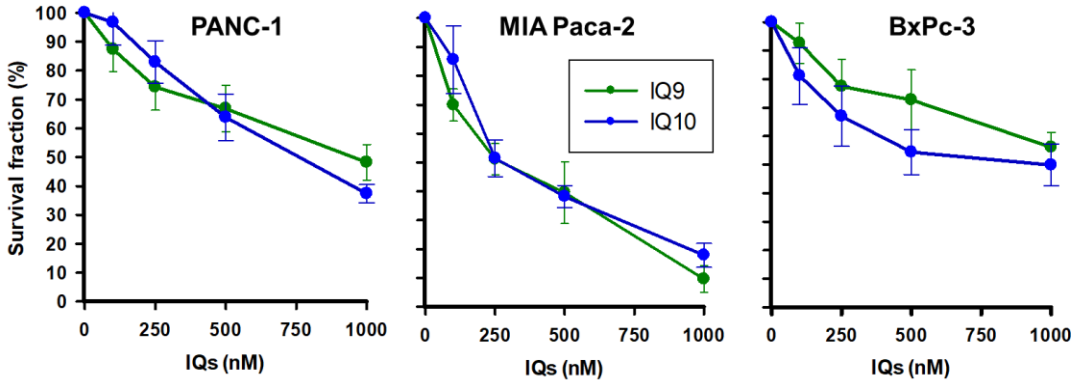


Figure 2.11: Clonogenic effect of IQs on PC cell lines. Survival fraction of PANC-1, MIA Paca-2 and BxPc-3 PC cell lines treated with IQs was plotted as a percentage of control (0 nM). Average PEs: PANC-1=0.21, MIA Paca-2=0.37 and BxPc-3=0.12. Data represent the mean ± standard deviation of pooled data of two independent experiments, with each experiment containing three parallel data sets.

As shown in Figure 2.11, MIA Paca-2 cells were more sensitive to IQs than PANC-1 cells. The IC50's of IQ9 at 48 hours treatment against PANC-1 and MIA Paca-2 cells were 900 and 250 nM respectively, and for IQ10 against PANC-1 and MIA Paca-2 cells were 730 and 240 nM respectively (Table 2.5). BxPc-3 cells were highly resistant to IQs, with no IC50 values were observed in the dose-response curves as current dose range of IQ9 and IQ10 was insufficient to inhibit the SF of BxPc-3 cells to 50%. Therefore, the IC50's of IQs for BxPc-3 are expected to be >1000 nM. Current data show that clonogenic IC50's of IQ9 for BxPc-3 cells were found to be much higher than previous studies (Yan et al., 2009, Yan et al., 2012), whilst current IC50's of IQ9 for MIA Paca-2 cells were comparable with the latter study – discussed later. IQ10 has never been evaluated against PC cells, and IQs have never been evaluated against PANC-1 cells.

Cell line	Drug	IC50 nM (48 hours)
PANC-1	GM	45
	IQ9	900
	IQ10	730
MIA Paca-2	GM	20
	IQ9	260
	IQ10	240
BxPc-3	GM	34
	IQ9	>1000
	IQ10	>1000

Table 2.5: The clonogenic IC50 values of GM, IQ9 and IQ10 for PC cell lines. PANC-1, MIA Paca-2 and BxPc-3 PC cells were treated with GM or IQs for 48 hours, then, cells were plated for clonogenic survival. IC50 values were estimated from the dose-response curves of each treatment. IC50 values retrieved from two independent experiments, with each experiment containing three parallel data sets.

2.4.3 Radioresponse of PC cell lines.

2.4.3.1 Radiation survival curves – clonogenic survival

Figure 2.12 shows the clonogenic survival characteristics of PC cell lines treated with radiation alone; while Table 2.6 shows linear quadratic model parameters (α, β and α/β) and SF2 values (SF2 is a widely used parameter to report cellular radiosensitivity and is the surviving fraction of exponentially growing cells that were irradiated using a clinically relevant dose of 2 Gy). As shown in Figure 2.12 and Table 2.6, PANC-1 (SF2=0.41) cells were less sensitive to radiation than MIA Paca-2 (SF2=0.33) and BxPc-3 (SF2=0.29) cells. Although published studies have shown wide variation in SF2 values of PC cell lines, SF2 values of the current results are comparable to those values in the literature as shown in Section 2.5.

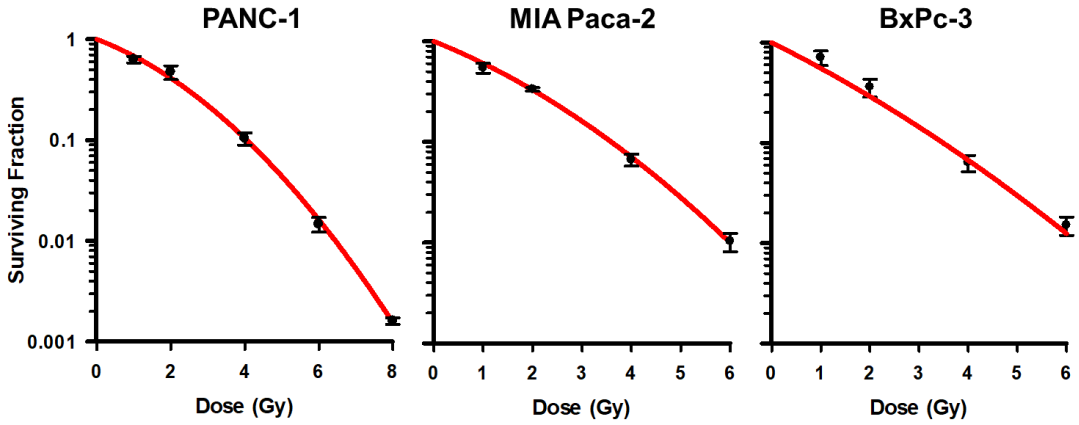


Figure 2.12: Survival curves of PC cell lines after single dose irradiation. Irradiation survival curves were fitted to the linear quadratic model. Average PEs: PANC-1=0.28, MIA Paca-2=0.45 and BxPc-3=0.15. Data represent the mean ± standard deviation of pooled data of eight (PANC-1) or five (MIA Paca-2) or six (BxPc-3) independent experiments with each containing three parallel data sets.

Cell line	SF2	Alpha (α)	Beta (β)	Alpha/Beta (α/β)
PANC-1	0.41	0.61	0.07	5.26
MIA Paca-2	0.33	0.48	0.048	9.88
BxPc-3	0.29	0.56	0.02	20.3

Table 2.6: PC cell line radiation sensitivity parameters. Values were derived from the linear-quadratic model of eight (PANC-1) or five (MIA Paca-2) or six (BxPc-3) independent experiments. Abbreviation; SF2=Surviving fraction at 2 Gy, α=single lethal event (proportional to dose), β=sublethal events (proportional to the squared dose), α/β=the dose where cell killing due to the α and β components are equal.

2.4.3.2 Drug-radiation combinations - clonogenic survival

The effects of IQs on the radiosensitivity of PC cell lines were assessed by clonogenic survival. PANC-1 and MIA Paca-2 PC cells were treated with clonogenic IC50's doses of IQs for 48 hours before irradiation. As indicated above in Section 2.4.2.2, the clonogenic IC50's of IQ9 for PANC-1 and MIA Paca-2 cells were 900 and 260 respectively; whilst IC50's of IQ10 for PANC-1 and MIA Paca-2 cells were 730 and 240 respectively. A concentration of 500 nM IQ9 and IQ10 was selected to treat BxPc-3 cells before irradiation although IC50's of IQs is expected to be >1000 nM. The concentration of 500 nM of IQs was the only available option as any concentration above 500 nM of IQs causes an insufficient number of BxPC-3 cells to perform the drug-radiation clonogenic assay (e.g. treatment with 1000 nM of IQ9 and IQ10 for 48 hours causes 87% and 96% growth inhibition in BxPc-3 cells respectively, Figure 2.7C).

As mentioned in Section 2.3.7.2.3, cells were then irradiated with a single dose of 1, 2, 4, 6 or 8 Gy, trypsinised and plated for clonogenic survival. As shown in Figure 2.13, a significant increase in radiosensitisation was observed for PANC-1 cells at 6 Gy compared to control (51% increase for IQ9 ($P<0.0001$) and 48% increase for IQ10 ($P<0.0001$)). No statistical analysis and SD analysis were performed for results of PANC-1 cells treated with IQs at 8 Gy since these results, at this dose, came from only a single experiment (Section 2.3.9). Also, as shown in Figure 2.13, a marginally increased radiosensitisation was observed for BxPc3 cells at 6 Gy (25% for IQ9 ($P<0.05$) and 23%

for IQ10 (P=0.192) compared to control, with no altered radiosensitisation was observed in MIA Paca-2 cells. Although IQs seem to sensitise PANC-1 and BxPc-3 cells at 6 Gy, SER values were low. The SER values of PANC-1, MIA Paca-2 and BxPc-3 treated with IQ9 were 1.08, 1.07 and 1.13 respectively; while the SER values of PANC-1, MIA Paca-2 and BxPc-3 treated with IQ10 were 1.1, 1.03 and 1.1 respectively.

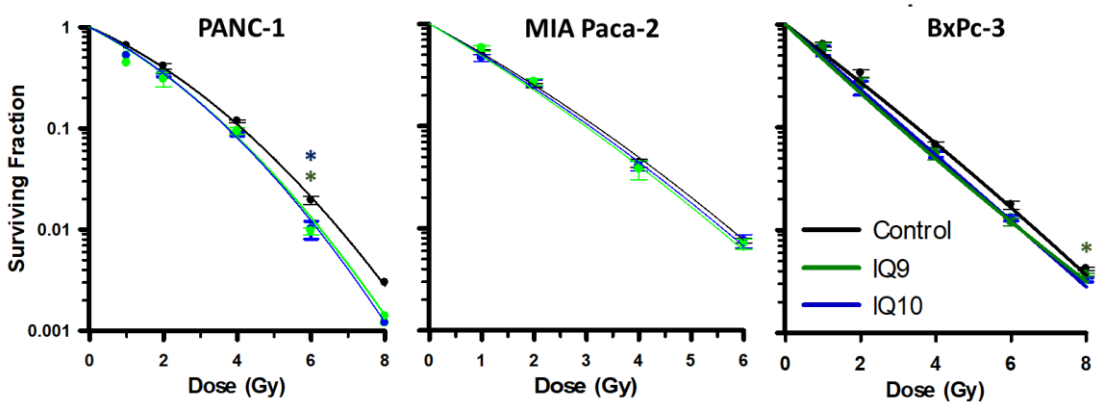


Figure 2.13: Effect of IQs on radiosensitivity of PC cell lines. Irradiation survival curves of PANC-1, MIA Paca-2 and BxPc-3 cells were fitted to the linear quadratic model. Average PEs: PANC-1=0.28, MIA Paca-2=0.41 and BxPc-3=0.16. Data represent the average of pooled data of two independent experiments for MIA Paca-2 cells, three experiments for BxPc-3 cells. For PANC-1 cells, data represent three experiments at 2, 4 and 6 Gy, two experiments at 1 Gy and one experiment at 8 Gy. Each experiment contains three parallel data sets. Average of three independent experiments ± standard deviation were analysed using the Student t-test. * P<0.05 vs control.

2.4.4 Effect of IQs on cell cycle progression of PC cells.

In order to investigate the potential mechanisms of action of IQs in PC cell lines, IQs effects on cell cycle progression of PANC-1 and BxPc-3 were assessed using flow cytometry as described in Section 2.3.8. PANC-1 and BxPc-3 cells were selected to investigate the effect of IQs on their cell cycle progression as both cell lines showed radiation sensitivity after IQs treatment. IQ9 was selected for the cell cycle assay to represent IQs agents, while AUR was selected as a comparator to evaluate the effect of TrxR inhibition on cell cycle progression of PC cells.

HU is a well characterised positive control for cell cycle analysis as it arrests cells at G0/G1 phase after 24 hours' treatment (Pfeiffer and Tolmach, 1967). A single

optimisation experiment was conducted to select the appropriate concentration of HU against PC cells for subsequent cell cycle analysis with IQ9 and AUR. As shown in Figure 2.14, 5 mM of HU could arrest the cell cycle of PANC-1 and BxPc-3 at G0/G1 phase more than 1 and 2.5 mM of HU (cells without drug treatment were set as control). Therefore, cells treated with 5 mM of HU for 24 hours were set as the concentration of HU, as positive control, for subsequent cell cycle analysis. No statistical analysis and SD analysis were performed for results of HU optimisation since these results came from only a single experiment (Section 2.3.9).

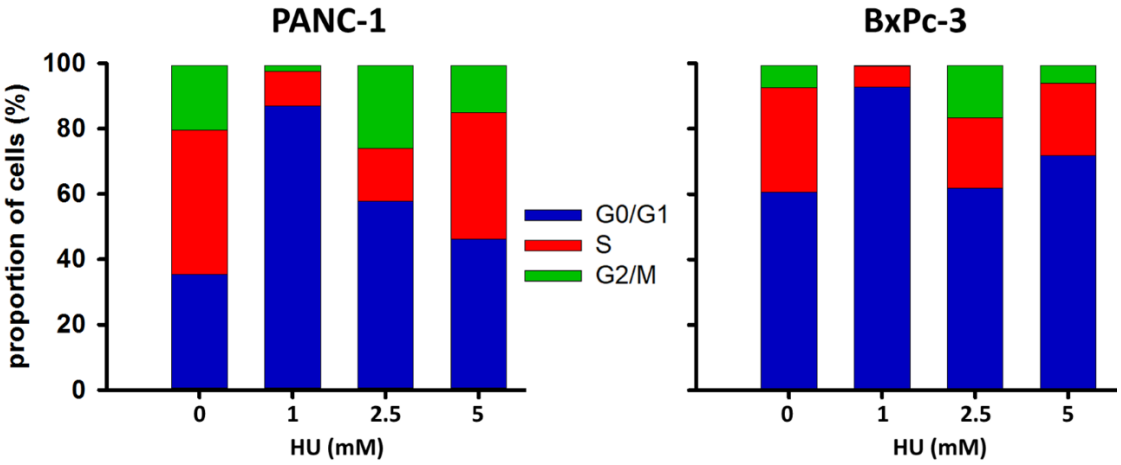


Figure 2.14: Optimization of the concentration of positive control hydroxyurea (HU) in cell cycle analysis. Cells treated with 1, 2.5 or 5 mM of HU for 24 hours (cells without HU treatment were set as control) were collected, and cell cycle was analysed. The percentage of PANC-1 (left) and BxPc-3 (right) in each phase of the cell cycle were plotted. Data derived from one experiment performed in a single data set.

Under control conditions, PANC-1 cells displayed a typical distribution of 35% in the G0-G1 phase, 44% in the S-phase and 21% in the G2-M phase, whilst BxPc-3 cells displayed a typical distribution of 61% in the G0-G1 phase, 32% in the S-phase and 7% in the G2-M phase. The typical distributions of both cell lines are comparable to published studies as shown in Section 2.5. PANC-1 and BxPc-3 cells were treated with IQ9 for 48 hours at concentration of 900 nM (the clonogenic IC50 value of IQ9 at 48 hours' treatment) and 500 nM (concentration selected for BxPc-3 in radiation sensitivity experiment) respectively. In addition, both cell lines were treated with 1000 nM of AUR for 48 hours

as a comparator. As shown in Figure 2.15, PANC-1 cells treated with IC50 of IQ9 (900 nM) for 48 hours were significantly arrested at G0/G1 phase (P=0.024) with a significant decrease in the S-phase (P=0.013); while 1000 nM of AUR for 48 hours did not significantly alter the cell cycle progression. BxPc-3 treated with 500 nM of IQ9 or 1000 nM of AUR showed no significant alteration in cell cycle progression.

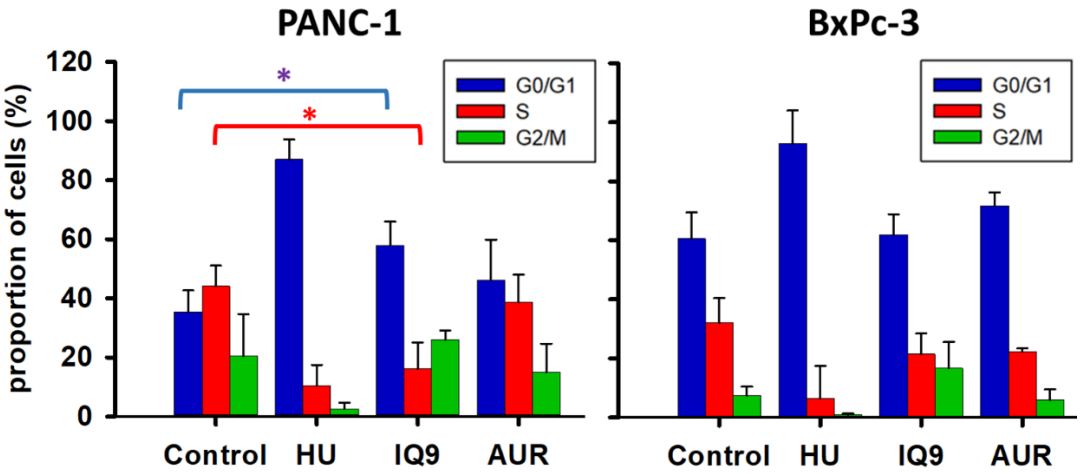


Figure 2.15: Effect of IQ9 on cell cycle of PC cells. PANC-1 (left) and BxPc-3 (right) cells treated with 900 and 500 nm of IQ9 for 48 hours respectively, or with 1000 nM AUR for 48 hours or with 5 mM of hydroxyurea (HU) for 24 hours (cells without drug treatment were set as control) were collected and cell cycle was analysed. The percentages of cells in each phase of the cell cycle were plotted. Data represent the mean ± standard deviation of three independent experiments, with each experiment performed in a single data set, which are analysed using the Student T-test. * P<0.05 vs control.

In general, IQs exhibit potent cytotoxicity against PC cell lines, with IC50 values in the low nanomolar range. However, IQs was less potent than GM and more potent than AUR. IQs cause cell cycle arrest and enhance radiotherapeutic efficacy in certain PC cell lines, but with low SER values.

2.5 Discussion

Current treatment options for PC have failed to improve five-year survival rates which remain very low, at ~5%; there is an urgent need to identify new treatment modalities. Redox proteins are key members of cellular antioxidant systems, required to maintain redox homeostasis, with the Trx system being an important component. The Trx system regulates the redox state of different signalling molecules, and by regulating their redox state, can regulate cell growth, apoptosis, gene transcription, cell cycle progression and ROS levels. Furthermore, the Trx system is one of the cellular antioxidants systems that has been targeted in an attempt to enhance the quality of radiotherapy by inhibiting TrxR. PANC-1, MIA Paca-2 and BxPc-3 PC cell lines were used to investigate the influence of the Trx system, using novel TrxR inhibitor (IQs), GM and AUR in cellular cytotoxicity and radiosensitivity.

Growth curves and survival characteristics (Section 2.4.1) were conducted for each cell line in order to determine the best time range for evaluating the effects of anti-cancer drugs. Current data shows that doubling times of PANC-1 (41 hours) and MIA Paca-2 cells (32 hours) are comparable to the published literature that showed PANC-1 and MIA Paca-2 cells have a doubling time of 52 and 40 hours respectively (Yunis et al., 1977, Deer et al., 2010). However, the doubling time of BxPc-3 cells (35 hours) was slightly faster than a previous study (48-60 hours) (Deer et al., 2010). In another study, BxPc-3 cells exhibited a doubling time of 24 hours, even faster than current findings (Cullen et al., 2003b). In terms of PE, current data show that PEs of PANC-1 (0.29), MIA Paca-2 (0.47) and BxPc-3 (0.14) PC cell lines are comparable to published studies; a study has investigated the role of K-Ras inhibition in radiosensitivity of PC cell line showed that the PEs of MIA Paca-2 and BxPc-3 were 0.51 and 0.17 respectively (Brunner et al., 2005). In another study, PANC-1 and MIA Paca-2 cells exhibited PEs of 0.49 and 0.22 respectively (Morak et al., 2011), while another study showed that PE value of PANC-1 cells was 0.37 (Mantoni et al., 2011). The results from such cell line characterisations, doubling time

and PE, give confidence that cells, and culture techniques, are appropriate to what is expected from the literature and that novel data is, therefore reliable.

Current data (Section 2.4.2.1) show that PANC-1 cells are less sensitive to GM than MIA Paca-2 and BxPc-3 cells. As mentioned in Section 2.3.4, the relationship of genotype to PC cells behaviour is still unclear (Deer et al., 2010). Therefore, there is no clear evidence to justify the variation in GM sensitivity among PC cell lines.

The proliferation IC50 values of GM for PANC-1, MIA Paca-2 and BxPc-3 PC cell lines were 850, 70 and 75 nM at 24 hours' treatment, 260, 40 and 40 nM at 48 hours' treatment and 40, 40 and 40 nM at 72 hours' treatment respectively. Current findings are comparable to those from recent studies that showed PANC-1 cells seem to be less sensitive to GM compared to MIA Paca-2 and BxPc-3 cells (Giroux et al., 2006, Lo et al., 2008, Pan et al., 2008). However, published studies showed high variations in terms of proliferation IC50 values of GM for PC cell lines, and that may be due to the different methods used to assess the proliferation. Current study used a 'cell counting' assay as a method to assess proliferation, while others used different methods such as the 3-(4, 5-dimethylthiazolyl-2)-2, 5-diphenyltetrazolium bromide (MTT) assay, the 3-(4,5-dimethylthiazol-2-yl)-5-(3-carboxymethoxyphenyl)-2-(4-sulfophenyl)-2H-tetrazolium (MTS) assay, the sulforhodamine B (SRB) assay and the propidium iodide (PI) assay which may account for the variable results. Current results are confirmed by a study that showed PANC-1 cells were less sensitive to GM amongst PC cell lines with an estimated IC50 value of 40 uM, while BxPc-3 (IC50=50 nM) and MIA Paca-2 (IC50=10 nM) cells were sensitive to GM (Giroux et al., 2006). However, two studies showed that PANC-1 and MIA Paca-2 cells showed a similar sensitivity to GM over 72 hours' treatment using the SRB and MTT Assays respectively (Xu et al., 2001, Chen et al., 2012). Interestingly, another study showed that PANC-1 cells were extremely resistant to GM (10% decrease in growth inhibition at 100 uM of GM for 72 hours' treatment) using the MTS assay, while MIA Paca-2 and BxPc-3 showed intermediate and high sensitivity to GM respectively (Pan et al., 2008). In contrast to current findings, Cao and colleagues observed that PANC-1 and MIA Paca-2 cells were responding equally to GM, using the

MTS assay for 48 hours' treatment, with estimated IC50 values of 7uM and 10uM respectively (Cao et al., 2015). Rathos and colleagues also observed that MIA-Paca-2 cells (IC50=733 nM) were less sensitive to GM, after 48 hours' treatment, than PANC-1 (IC50=225 nM) and BxPc-3 (IC50=80 nM) cells using the PI assay (Rathos et al., 2012). In general, current findings were consistent to most of published studies that showed PANC-1 cells were less sensitive to GM than MIA Paca-2 and BxPc-3 cells.

From clonogenic data (Section 2.4.2.2), current findings show that clonogenic IC50 values of GM after 48 hours' treatment for PANC-1, MIA Paca-2 and BxPc-3 cells were 45, 20 and 34 nM respectively. A recent study showed that PANC-1 cells were less sensitive to GM, after 24 hours' treatment, than MIA Paca-2 and BxPc-3 cells with clonogenic IC50 values of 480, 160 and 50 nM respectively (Parsels et al., 2009). Another recent study showed that PANC-1 and BxPc-3 cells treated with GM for 4 hours showed similar sensitivity to GM, with clonogenic IC50 values of ~150 and ~100 nM respectively (El Shafie et al., 2013). The differences in clonogenic IC50 values in the literature may be due to differing GM exposure times before plating for survival. From both the proliferation and clonogenic assays, PANC-1 cells seem less sensitive to GM than MIA Paca-2 and BxPc-3 cells which is in general agreement with the literature. GM was, therefore, used as positive control drug to ensure cells were responding appropriately in each experiment and to compare against the cytotoxicity of IQs novel drugs on the PC cell lines.

Current findings show that PANC-1 cells were less sensitive to IQs compared to MIA Paca-2 and BxPc-3 cells. The proliferation IC50 values of IQs for PANC-1 were between 320 and 920 nM while the proliferation IC50 values of IQs for MIA PaCa-1 and BxPc-3 were between 90 and 470 nM. Since the analogues of ES936 are novels, only two studies examined the effects of these analogues on PC cells. The first study (Yan et al., 2009) used the MTT assay to estimate the proliferation IC50 values of 8 analogues of ES936 (the eighth analogues was IQ9) for PANC-1, MIA PaCa-2 and BxPc-3 cells after 4 and 72 hours' treatments. The proliferation IC50 values of IQ9 for MIA Paca-2 and BxPc-3 cells after 72 hours' treatment were 18 and 48 nM respectively; while current findings show

that the IC50 values of IQ9 for MIA Paca-2 and BxPc-3 cells after 72 hours' treatment were 90 and 270 nM respectively. IQ9 was not tested against PANC-1 cells at that time, however, other analogues of ES936 showed that PANC-1 cells were less sensitive to IQs compared to MIA Paca-2 and BxPc-3 cells for 72 hours' treatment, with proliferation IC50 values between 24 and 149 nM (Yan et al., 2009). The second study showed that proliferation IC50 values of IQ3 and IQ9 for MIA Paca-2 cells after 72 hours' treatment were 74 and 18 nM respectively (Yan et al., 2012). Current data are comparable to these two studies in terms of PANC-1 cells being the least sensitive to IQs, MIA Paca-2 cells being the most sensitive to IQs and BxPc-3 cells showing intermediate sensitivity. However, the two previous studies showed lower IC50 values of IQs for PC cell lines compared to current findings, that may be due to the different methods to assess the IC50 value in the proliferation assay (cell counting vs MTT assay) as will be discussed in Chapter 5.

For clonogenic data (Section 2.4.2.2); unlike GM that showed difference between IC50's obtained from proliferation vs clonogenic survival endpoints, the clonogenic IC50's for IQs were in the same range as those obtained from proliferation assessments. The clonogenic IC50's of IQ9 and IQ10 at 48 hours treatment for MIA Paca-2 cells were 250 and 240 nM respectively; while the clonogenic IC50's for BxPc-3 cells are expected to be higher than 1000 nM for both IQs. In contrast to the current finding, the initial study of ES936 analogues against PC cells (Yan et al., 2009) showed that clonogenic IC50's of IQ9 for BxPc-3 after 4 and 72 hours' treatments were 70 and 10 nM respectively. IQ9 has never previously been evaluated against MIA Paca-2 cells for clonogenic survival, however, analogues of ES396 (IQ1-IQ8) exhibited clonogenic IC50's between 1 and 400 nM after 72 hours' treatment. Analogues of ES396 have never previously been evaluated against PANC-1 for clonogenic survival.

Generally, IQs exhibit potent *in vitro* cytotoxicity on PC cell lines, with IC50 values in the nanomolar range, which are much lower than other characterized TrxR inhibitors such as nitrosureas (IC50=430 μM), gold thiosugars (IC50=0.8–2.4 μM), platinum complexes pt (IC50=25 μM), organochalcogenides (IC50=10.4 μM), polyphenols resveratrol

(IC50>50 µM), pleurotin (IC50>50 µM) and naphthoquinone (IC50=1-3.1 µM) (Urig and Becker, 2006).

AUR is a well-characterised TrxR inhibitor, and used as a positive control to evaluate the TrxR inhibitory effect of IQs on PC cell lines, as shown later in Chapter 3. Generally, the IC50's of AUR for PC cell lines were higher than GM and IQs (Section 2.4.2.1). After 24, 48 and 72 hours' treatment, AUR exhibited IC50's of 2000, 900, and 700 nM for PANC-1 cells, 1050, 750 and 400 nM for MIA Paca-2 cells and 2550, 1100 and 500 nM for BxPc-3 cells respectively. Current data are comparable with the published studies but for other types of cancer; the estimated IC50 of AUR, after 24, 48 and 72 hours' treatment, for Hela cervical cancer cells were 2500, 1500 and 900 nM respectively (You et al., 2015), while the estimated IC50 values of AUR, after 24 hours treatment, for RPMI8226, U266 and OPM2 myeloma cancer cell lines were between 1 and 2 µM (Raninga et al., 2016). However, certain cancer cell lines are documented as being resistant to AUR; the IC50 of AUR after 24 hours' treatment for A549 lung cancer cell line was 9.1 µM (Bhatia et al., 2016).

MDA-MB-231 BC cell line, used as a positive control cell line and comparator, showed intermediate sensitivity to IQs and AUR. The IC50 of AUR for MDA-MB-231 cells at 48 hours' treatment was 900 nM (Section 2.4.2.1). A recent study investigated the inhibition effect of TrxR on MDA-MB-231 cells showed that the IC50 of AUR after 24 hours treatment, using the MTT assay, was 5.1 µM (Bhatia et al., 2016). As discussed previously, differences in IC50 values for AUR between current findings and the previous study may be due to the different of AUR treatment times and the sensitivity of the MTT assay vs cell counting.

In terms of radioresponse, current data (Section 2.4.3.1) show that SF2 values for PANC-1 (8 experiments), MIA Paca-2 (5 experiments) and BxPc-3 (6 experiments) cells were 0.41, 0.33 and 0.29 respectively. Previous studies have shown a wide variation in SF2 values in clonogenic survival of PC cell lines. One study evaluated the radiation sensitivity of PC cells showing SF2 values for MIA Paca-2 and BxPc-3 cells of 0.57 and

0.45 respectively (Alcock et al., 2002), while Burner and colleagues reported SF2 values for PANC-1 and MIA Paca-2 and BxPc-3 cells of 0.5, 0.5 and 0.4 respectively (Brunner et al., 2005). A recent study has shown a mean SF2 value of MIA Paca-2 cells, from four independent experiments, was 0.27 (Purvinienė et al., 2009), which is comparable to current data. In contrast to current finding, Morak and colleagues observed that MIA Paca-2 and PANC-1 cells were resistant to irradiation, with SF2 values of 0.77 and 0.70 respectively (Morak et al., 2011).

When combining IQs treatment with radiation, current data (Section 2.4.3.2) show a significant increase in radiosensitisation at 6 GY in PANC-1 and BxPc-3 cells treated with IQs for 48 hours. However, SER values, for both cell lines, were low (SER≤1.13). The radiosensitising effect of ES936 analogues has never been studied, however, several studies have investigated the implication of inhibiting the Trx system on radiotherapeutic efficacy and cell cycle progression in cancer cells. Current findings are comparable to a recent study that showed significant radiosensitivity at 2 and 5 Gy for lung cancer cells (U1810) treated with a novel TrxR inhibitor; phosphine gold(I) compound [Au(SCN)(PEt3)] for 48 hours. Although the radiosensitivity at 2 and 5 Gy was significant, the SER values also seem low; the SF2 and SF5 values of control cells were decreased from 0.94 and 0.65 to 0.71 and 0.51 in treated cells respectively (Selenius et al., 2012). Furthermore, the latter study showed an increase in G2/M phase in U1819 cells treated with phosphine gold(I) compound for 24, 48 and 72 hours compared to control (no significant statistics were provided). A recent study showed a significant radiosensitisation at 6 Gy in EMT-6 and 4T1 mouse breast carcinoma cancer cells treated with 5 or 7.5 or 10 µM of AUR for 2 hours before irradiation (Wang et al., 2017). However, EMT-6 cells treated with 10 µM of AUR showed only ~50% increase of radiosensitivity at 6 Gy, which is comparable to current findings. Rodman and colleagues observed a marginal radiation sensitivity of MDA-MB-231 cells treated with AUR, BSO (a GSH inhibitor) and AUR+BSO, with SER values of 1.12, 1.13 and 1.15 respectively, which is comparable to our SER values (1.03-1.13) (Rodman et al., 2016). Current radiosensitisation data suggest that IQ's have the potential to radiosensitise PC cells,

with levels of sensitisation being comparable to other TrxR inhibitors in other cancer types. It may be, however, that improved sensitisation could be achieved by altering treatment parameters – this will be the focus of the subsequent chapter.

In terms of cell cycle progression (Section 2.4.4), PANC-1 and BxPc-3 control cells displayed typical cell cycle distributions of 35% and 61% in the G0-G1 phase, 44% and 32% in the S-phase, and 21% and 7% in the G2-M phase respectively. Current findings are comparable to published studies; a recent study showed that BxPc-3 cells displayed a typical cell cycle distribution of 55% in the G0-G1 phase, 30% in the S-phase, and 15% in the G2-M phase (Ma et al., 2015), while another two recent studies showed that PANC-1 cells displayed a cell cycle distribution of 45% and 43% in the G0-G1 phase, 35% and 30% in the S-phase, and 20% and 27% in the G2-M phase respectively (Duong et al., 2012, Maftouh et al., 2014). In contrast to the current findings, a recent study showed that PANC-1 and BxPc-3 cells have identical cell cycle distribution of 85% in the G0-G1 phase, 5% in the S-phase, and 10% in the G2-M phase (Qiao et al., 2016).

Current data show a significant cell cycle arrest at G0/G1 of PANC-1 cells treated with IC50 of IQ9 for 48 hours, while no effect was observed for BxPc-3 cells. Effect of IQs on cell cycle progression has never been studied. As mentioned earlier, in Chapter 1, previous studies have shown varying results in terms of cell cycle arrest following Trx system inhibition. Certain studies have shown that inhibition of the Trx system can cause a significant arrest in G1/S phase (Laurent et al., 1964), a G1 arrest (Mochizuki et al., 2009b), or G2/M arrest (Selenius et al., 2012, You et al., 2014). Theoretically, inhibition of the Trx system could lead to G1/S arrest due to the involvement of reduced-Trx in DNA synthesis through the reduction/activation of s-ribonucleotide reductase, an enzyme that reduces ribonucleotides to deoxyribonucleotide (Laurent et al., 1964). A recent study has shown that inhibition of the Trx system by metformin, in MCF-7 and MDA-MB-231 BC cell lines, did not seem to affect cell cycle progression (Zhang, 2014). In contrast to current data, a novel TrxR inhibitor (BBSKE, a novel organoselenium compound) showed a cell cycle arrest in S-phase for PC-3 and DU145 human prostate cancer cell lines (Shi et al., 2003). Lu and colleagues observed an S-phase arrest in A549

lung cancer cells treated with a flavonoid-based TrxR inhibitor (quercetin), with an accumulation of cells in sub-G1 phase (Lu et al., 2006). The varying results of cell cycle arrest induced by novel TrxR inhibitors may due to potential off-target effects of these inhibitors that can affect multiple cellular processes but may also reflect inherent differences in how different cancer cell types respond to inhibition of the Trx system.

In conclusion, IQs are effective on PC cell lines as single agents, with IC50 values in the low nanomolar range. However, IQs was less potent than GM and more potent than AUR. The hypothesis of the current chapter (radiosensitivity and cell cycle arrest of PC cells can be modulated by treatment with IQs novel agents) has been proven but in key pre-clinical in-vitro cell models. Although the current chapter addressed a number of important areas, with drug efficacy having been shown (albeit to variable levels) a number of questions remain to be addressed i.e. is the cytotoxic effect of IQs on PC cell lines correlated with the inhibition of TrxR activity/protein expression, ROS overproduction, different treatment exposure times and altering O_2 levels? These questions will be the focus of the subsequent chapters.

Chapter 3: Evaluation of mechanisms of action of IQs on the Trx/TrxR system in pancreatic cancer cell lines

3.1 Abstract

Background: IQ9 and IQ10 (IQs) are novel TrxR inhibitors being trialled as drugs against PC cell lines. Chapter 2 showed that IQs were highly cytotoxic across all PC cell lines as single agents, can arrest progression through the cell cycle and increase, albeit slightly, radiotherapeutic efficacy in certain PC cell lines. The current chapter sought to investigate the related mechanisms of action of IQs in the Trx/TrxR system by examining their effects at different treatment times on intracellular ROS levels, on the protein expression of Trx system family members, protein expression of reductase enzymes, TrxR activity and radiation sensitivity. As IQs are bioreductive agents, the current chapter also sought to study the effect of IQs on proliferation and clonogenic survival of PC cell lines under hypoxia.

Methods: All cell lines and tissue culture methodologies were described in Chapter 2. The cellular ability of PC cells to cope with oxidative stress was evaluated by measuring ROS levels, by flow cytometry, following IQ treatment +/- H_2O_2 exposure. Western blotting was used to assess the expression of Trx system members and reductase enzymes in PC cell lines treated with/without IQs under normoxic or hypoxic conditions. An insulin reduction assay was used to assess TrxR activity in PC cell lines treated with IQs for 4 or 48 hours. For radiosensitivity evaluations, PC cells were treated with IQs for 4 hours or with AUR, as a comparator, for 4 or 48 hours, then, irradiated with 1, 2, 4, 6 or 8 Gy of X-rays and plated for clonogenic survival. To evaluate the effect of IQs on the proliferation of PC cell lines in hypoxia (1% O_2), cells were incubated in hypoxic conditions for 24 hours then, cells were treated, whilst still under hypoxia, with a range of IQ9 (0-1000 nM) for 48 hours. Then, cells were trypsinised, counted and plotted as a percentage of control. To evaluate the effect of IQs on clonogenic survival of PC cell lines in hypoxia, cells were incubated in hypoxia (1% O_2) for 24 hours then, cells were treated, whilst still under hypoxia, with a range of IQ9 (0-1000 nM) for 4 or 48 hours. Then, cells were trypsinised, counted, and plated for clonogenic survival.

Results: PC cells treated with IC50 doses of IQs in combination with H_2O_2 showed an increase in ROS levels over treatment with H_2O_2 alone, with a maximum fold increase of 2. Western blots only showed reduced expression of Trx in BxPc-3 cells treated with the IC50's of IQs for 48 hours, with no notable changes in expression of TrxR and TxNIP. PANC-1 and MIA Paca-2 cell lines treated with IQs for 48 hours showed no alteration in the expression of any of the Trx system proteins. PANC-1 and BxPc-3 cells treated with IQs showed a substantial decrease in TrxR activity, in a dose-dependent manner, with 4 hours' treatment giving greater inhibition than 48 hours' treatment. A significant increase in radiosensitisation at 6 and 8 Gy was observed in PANC-1 cells treated with IQ9 or AUR for 4 hours, but with a small increase in SER values (SER≤1.13) making the biological relevance of IQs as radiosensitisers somewhat questionable. PANC-1 and BxPc-3 hypoxic cells were sensitive to IQ9, in terms of proliferation and clonogenic survival, than normoxic cells, but with a small increase in hypoxia cytotoxicity ratio (HCR) (HCR=1.2-2.4), suggesting marginal biological significance of IQs in PC hypoxic cells. IQ9 treatment does not alter the endogenous expression of reductase enzymes such as NQO1 and CPR enzymes in PANC-1 and BxPc-3 cells either in normoxic or hypoxic conditions.

Conclusion: TrxR may be a useful potential target in PC. IQs showed high efficacy in terms of inhibiting TrxR activity and increasing ROS levels under oxidative stress. IQs showed a marginal increase in radiation sensitivity in certain PC cell lines, with 4 hours' treatment giving greater radiosensitising effect than 48 hours' treatment, suggesting that IQs seem to have a short half-life than long half-life. Hypoxia increases, albeit slightly, the cytotoxic efficacy of IQs on PC cell lines, with no effect on the protein expression of any of the Trx system proteins or reductase enzymes. Current findings suggest marginal biological significance of IQs in PC cells.

3.2 Introduction and aims

Chapter 2 showed that IQs were highly cytotoxic against PC cell lines as single agents, with IC50 values in the low nanomolar range. Also, IQs treatment caused cell cycle arrest and enhanced, albeit slightly, radiotherapeutic efficacy in certain PC cell lines. The current chapter is an extension of the previous chapter, and it aims to evaluate the related mechanisms of action of IQs, by examining their effects on intracellular ROS levels, protein expression of Trx system family members and reductase enzymes, TrxR activity and radiation sensitivity. As IQs are bioreductive agents, hypoxic conditions may increase the reduction/activity of IQs in PC cells. Therefore, the current chapter also sought to evaluate the effect of IQs on proliferation and clonogenic survival of PC cell lines under hypoxia.

The introduction of the current chapter discusses hypoxia in solid cancers, specifically in PC, and the effect of hypoxia on the Trx system.

3.2.1 Hypoxia in tumour cells

3.2.2.1 Definitions and causative mechanisms of hypoxia

Hypoxia, a reduction in the normal level of tissue oxygen tension, is a characteristic feature of 50-60% of locally advanced solid cancers, and it occurs when there is an imbalance between the cellular O_2 consumption rate and the O_2 supply to the cells (Harris, 2002, Vaupel et al., 2002). The common unit used to measure O_2 concentration (pO_2) is a millimetre of mercury (mmHg), which is equal to 0.13% O_2. The normal level of O_2 (normoxia) varies in different organs, and ranges between pO_2=25 mmHg (3.25 $\%O_2$) in muscle and pO_2=72 mmHg (9.5 $\%O_2$) in kidney (Hammond et al., 2014). The common method to measure O_2 levels in solids cancers is the computerized polarographic needle electrode system (oxygen tension [pO_2] histography), that provides rapid and reliable measurement of pO_2 values, allowing it to evaluate and characterise the hypoxic status in tumours and its clinical relevance (Höckel et al., 1991,

Vaupel et al., 1991). Within a solid tumour, O_2 levels are extremely heterogeneous and can include mild hypoxia (2% O_2), severe hypoxia (<0.1% O_2) and anoxia (0% O_2) (Hammond et al., 2014).

In solid tumours, O_2 delivery to the respiring neoplastic and stromal cells is frequently reduced by three causes (Vaupel and Harrison, 2004):

1- Acute hypoxia (perfusion-related); caused by the temporary closing of tumour blood vessels around the tumour due to the severe structural and functional abnormalities of tumour microvasculature such as disorganised vascular network, dilations, elongated and tortuous shape, incomplete endothelial lining, lack of physiological/pharmacological receptors, absence of flow regulation and intermittent stasis (Vaupel and Harrison, 2004).

2- Chronic hypoxia (diffusion-related); caused by an increase in diffusion distances between O_2 and blood vessels due to tumour expansion. Chronic hypoxia was initially thought to arise in cells distant more than 100 µm from the nutritive blood vessels (Bussink et al., 1999, Rijken et al., 2000). However, *in vivo* study showed that chronic hypoxia can occur in cells within 20-50 µm from the blood vessels for a long period of time (Ljungkvist et al., 2002).

3- Anaemic hypoxia; caused by tumour-associated or therapy-induced anaemia. Experimental studies showed that the level of hypoxia is intensified at haemoglobin levels below 10-12 g/dl (Vaupel et al., 2001a, Vaupel et al., 2001b).

Oxygen enhancement ratio (OER), SER and hypoxia cytotoxicity ratio (HCR) are three main concepts describing the effect of hypoxia during chemotherapy or radiotherapy. OER is the ratio of radiation doses to produce the same biologic effect under hypoxic against aerobic conditions (Zeman, 2000), with the following formula:

$$OER = Radiation\ dose\ in \frac{hypoxia}{normoxia}$$

The definition of SER was described in Chapter 2. However, in terms of hypoxia, SER is the dose ratio for an isoeffect under hypoxic conditions alone versus under hypoxic conditions in the presence of the hypoxic cell sensitiser (Zeman, 2011), with the following formula at 1% of survival:

$$SER = \left(\frac{Radiation\ dose\ at\ 1\%\ of\ survival\ of\ untreated\ hypoxic\ cells}{Radiation\ dose\ at\ 1\%\ of\ survival\ of\ treated\ hypoxic\ cells}\right)$$

The HCR can be defined as a drug concentration ratio that required to produce equal cytotoxicity under normoxia relative to hypoxia (Koumenis et al., 2016), with the following formula at IC50 dose:

$$HCR = IC50\ dose\ in \frac{normoxia}{hypoxiaa}$$

3.2.2.2 Cellular responses to hypoxic states

Hypoxia induces proteomic and genomic changes within tumour cells that can influence tumour cells either by impairing cell proliferation and causing cell death (apoptosis and necrosis) or by stimulating malignant progression and increasing resistance to chemotherapy and radiotherapy (Vaupel and Harrison, 2004). The proteomic changes by hypoxia lead to growth stability, cell-cycle arrest, differentiation, apoptosis and necrosis (Vaupel and Harrison, 2004). The main response of tumour cells to low O_2 levels is activation of hypoxia-inducible transcription factor 1 (HIF-1), the master transcriptional factor which stimulates a group of downstream genes, such as vascular endothelial growth factor (VEGF), that are responsible for malignant progression (Maynard and Ohh, 2007). HIF-1 has two protein subunits: HIF-1β and HIF-1α, with both subunits ~~are~~ expressed in normal and hypoxic conditions. However, HIF-1α is rapidly degraded by the proteasome in normoxia, while is stabilised and accumulated in hypoxia (Huang et al., 1998). The accumulation of HIF-1 in hypoxic cells acts as a master regulator to initiate adaptive responses in solid cancer cells to cope with low O_2 levels, which is discussed later in Section 3.2.2.4.

Severe hypoxia ($pO_2 \leq 0.7$ mmHg) can promote genomic instability; exposing Chinese hamster ovary cells to severe hypoxia for 72 hours caused an amplification of dihydrofolate reductase gene leading to increase cells' resistance to chemotherapy agents such as methotrexate (Young et al., 1988). Furthermore, hypoxia has been shown to impair cellular DNA repair functions by downregulating certain DNA repair genes involved in different DNA repair pathways such as homologous recombination (HR) pathway's genes e.g. BRCA1, BRCA2, RAD51 (Bindra et al., 2005, Bindra and Glazer, 2007, Fanale et al., 2013), mismatch repair (MMR) pathway's genes e.g. MLH1 and MSH2 (Mihaylova et al., 2003) and base excision repair (BER) pathway's genes e.g. APE1, OGG1, MYH, NEIL2, and MTH1 (Chan et al., 2014). Interestingly, hypoxia has been shown to upregulate genes involved in non-homologous end joining (NHEJ) pathway (one of the two major double-strand break repair pathways) such as Ku70, Ku80, DNA-PKcs, and DNA Ligase IV (Madan et al., 2012, Ren et al., 2012). Therefore, targeting NHEJ pathway seems to be a potential target to decrease the resistance of hypoxic cells in solid tumours to conventional cancer treatments such as radiotherapy (Jorgensen, 2009).

3.2.2.3 Tumour hypoxia and treatment resistance

Tumour hypoxia has long been identified as a critical issue in oncology as it making cells more resistant to conventional cancer therapies such as chemotherapy and radiotherapy. In chemotherapy, hypoxia decreases the efficacy of chemotherapy agents by direct and indirect pathways. Low O_2 levels can directly reduce the maximal efficacy of alkylating chemotherapeutic agents, such as cisplatin and melphalan, in cancer cells (Teicher, 1994). These agents are electrophilic compounds, with a mechanism of action based on transferring alkyl groups to nucleophilic positions of the DNA base during cell division to induce alkylation DNA damage leading to prevent subsequent DNA synthesis (Teicher, 1994). However, alkylating agents seem less effective in hypoxia due to overproduction of nucleophilic substances, such as GSH, that compete with targeted DNA for alkylation (Vaupel et al., 2001b). Also, hypoxia indirectly reduces the efficacy of chemotherapeutic agents by arresting cell cycle, inducing proteomic/genomic changes,

initiating angiogenesis and changing pH conditions in cancer cells. Generally, hypoxia causes slow cell cycle progression, however, extreme hypoxia increases protein expression of the cyclin-dependent kinase inhibitors p21 and p27 leading to pre DNA-synthetic (pre-S phase) arrest at G1/S transition (Gardner et al., 2001). As most chemotherapeutic agents, such as alkylating agents and antimetabolites, causes DNA damage during S-phase, cell cycle arrest at pre-S phase decreases the efficacy of these agents (Rang et al., 2003). Also, Hypoxia increases activity of DNA repair enzymes, such as human AP endonuclease-1 (HAP1) (Walker et al., 1994), upregulates chemoresistance-related proteins such as metallothioneins (Murphy et al., 1994, Ebert et al., 2000) and amplifies chemoresistance-related genes such as dihydrofolate reductase gene (DHFR) (Comerford et al., 2002). In terms of angiogenesis, arteriovenous shunts and dysfunctional blood vessels cause poor and heterogeneous blood flow in hypoxic regions of solid tumours leading to poor delivery of chemotherapeutic agents to the tumour tissue or an uneven distribution of these agents within tumour tissue (Airley et al., 2000, Vaupel et al., 2001b). The high rate of aerobic glycolysis in hypoxic tumours, as discussed later in Section 3.2.2.4, increases lactic acid (lactate) production and subsequently increases the acidity in hypoxic cells (PH=7.05) compared to normoxic cells (PH=7.4) (Helmlinger et al., 1997, Hockel and Vaupel, 2001). In addition to lactate, overexpression of the enzyme carbonic anhydrase 9 (CA9) on the surface of hypoxic cells can catalyse the extracellular trapping of acid by hydrating cell-generated CO_2 into HCO^-_3 and H^+, leading to increasing the acidity in tumour cells (Swietach et al., 2007). Low PH negatively impacts the uptake of weak base chemotherapeutic agents by creating a physiological barrier for the cellular uptake and, subsequently, inhibits the intracellular accumulation of these weak bases drugs, which known as '*ion-trapping phenomenon*' (Raghunand and Gillies, 2000, Wojtkowiak et al., 2011).

In radiotherapy, tumour hypoxia is a severe problem since it rapidly increases cells' resistance to ionising radiation (Gray et al., 1953). Fractionated radiotherapy can oxygenate hypoxic cells and subsequently sensitise them to radiation as previously indicated in Section 1.1.6.3.3. Oxygen is a potent radiation sensitiser, it can react with

free radicals, resulting from radiolysis of cellular water, to form oxygen free radicals. The oxygen free radicals are organic peroxides that can change the chemical composition of the target molecules (mainly DNA) and fix these changes, which known as *oxygen fixation hypothesis.* However, in the absence of O_2 during radiation, the target molecules in irradiated cells can repair the radiation damages and recover the ability to function normally (Gray et al., 1953).

Furthermore, hypoxia induces proteomic and genomic changes that can increase cells' resistance to radiation. These changes including overexpression of NHEJ genes, as indicated earlier, heat-shock proteins (hsps) (Samali and Cotter, 1996) or by increasing number of cells with diminished apoptotic potential (Graeber et al., 1996, Kim et al., 1997) that have been linked to radioresistance in hypoxic cells (Samali and Cotter, 1996, Zhivotovsky et al., 1999).

3.2.2.4 Hypoxia in pancreatic cancer

A major reason for the aggressive behaviour of PC is the tumour microenvironment characterised by extensive desmoplasia and hypoxia (Erkan et al., 2016). By using pO2 histography in 359 cancer patients, PC (pO_2=2 mmHg) was the most hypoxic tumour out of 9 different solid tumours (pO_2=6-32 mmHg) (Vaupel et al., 2007). Intraoperative measurement of pO_2 values of seven resectable PCs showed a mean pO_2 of 2.5 mmHg (0-5.3 mmHg), while the mean pO_2 of normal pancreatic tissues of the same patients was 57.1 mmHg (24.3-92.7 mmHg) (Koong et al., 2000).

Abnormal vasculature in PC is a major cause of hypoxia that limits blood supply to all sites in tumour tissues. Two previous studies have investigated vascular structures in PC, and detected vessels only in a small area of the tumour mass using angiographic and colour flow sonographic assessments (Ranniger and Saldino, 1966, Yassa et al., 1997). PC cells show high expression of angiogenic substances such as VEGF, but also they expressed high levels of anti-angiogenic factors such as angiostatin and endostatin that can inhibit angiogenesis and subsequently develop hypoxic regions due to low oxygen supply (O'Mahony et al., 1998, Kisker et al., 2001).

Stroma is a complex network of glycoproteins and proteoglycans, and it is primarily made of extracellular matrix (ECM), a non-cellular component present within all tissues and organs (Frantz et al., 2010). Stroma accounts >90% of the total volume of PC, and may contribute to hypoxia either by amplifying the production of antiangiogenic factors or by the physical compressing on the capillaries through ECM deposition in the periacinar spaces (Erkan et al., 2016).

Pancreatic stellate cells (PSC) are the main source of fibrosis in stroma, and they interact with tumour cells to create a tumour facilitatory environment that stimulates local tumour growth and distant metastasis. PC cells interact with stromal cells and PSC to initiate a cascade of events resulting in deposition of ECM. ECM compromises blood supply by producing antiangiogenic factors and, consequently, creating hypoxic regions within the tumour tissues. In response to ECM, stromal cells and PSC proliferate and sustain ECM deposition leading to create new hypoxic regions. This vicious cycle, between stromal cells/PSC and ECM, accumulates hypoxic regions within tumour tissues and, consequently, increases HIF-1 activity (Figure 3.1) (Phillips, 2012).

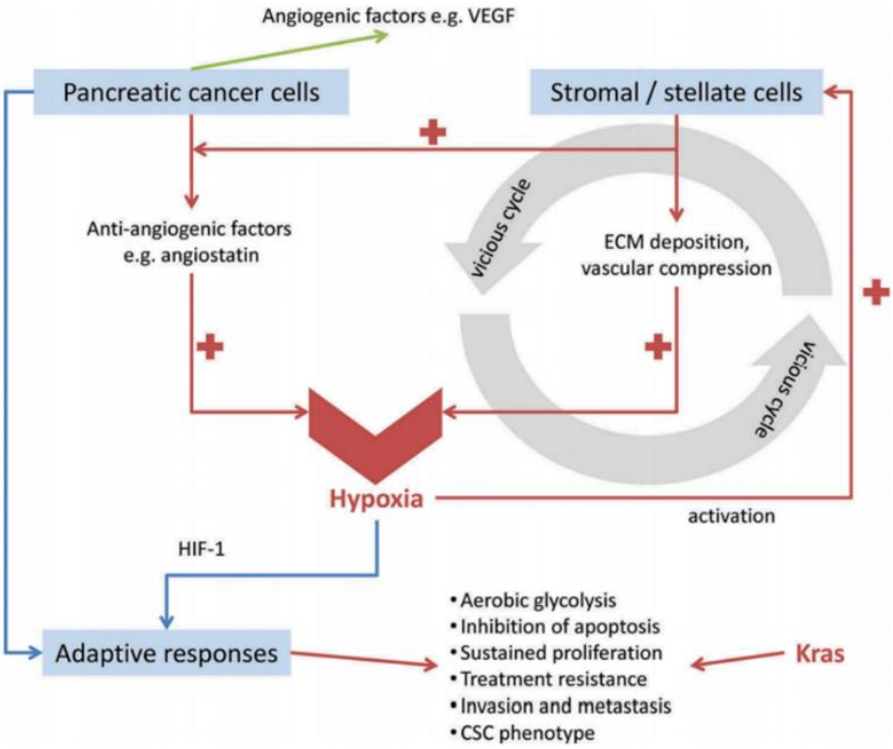


Figure 3.1: The vicious cycle of hypoxia and stroma in PC. The interaction between PC cells and stromal cells/PSC initiates a cascade of events resulting in depositing of the ECM causing hypoxia. In response to hypoxia, stromal cells/PSC sustain ECM deposition resulting in formation of new hypoxic regions. Source: Erkan, M., Kurtoglu, M. & Kleeff, J. 2016. The role of hypoxia in pancreatic cancer: a potential therapeutic target? *Expert review of gastroenterology & hepatology,* 10, 301-31; used with permission.

HIF-1 transcription factor acts as the master regulator to initiate adaptive responses of hypoxic cancer cells allowing them to survive by enhancing aerobic glycolysis, arresting cell cycle, inhibiting apoptosis, sustaining proliferation, regulating cancer stem cell (CSC) and promoting invasion and metastasis (Semenza, 2003). Several studies have shown a correlation between HIF-1 expression and prognosis of PC patients. Analysis of HIF-1 expression in tumour tissues from 41 PC patients showed that high expression of HIF-1α was significantly associated with poor overall survival (Hoffmann et al., 2008). A recent meta-analysis of 8 clinical studies involving 557 patients confirmed the previous findings, and showed that overexpression of HIF-1α was significantly associated with poor overall survival, lymph node metastasis and advanced tumour stage (Ye et al., 2014). In PC pathogenesis, the association between HIF-2α and PanIN is unclear. However, a recent *in vivo* study showed that HIF-2α loss mice model exhibited high number of low-grade

PanIN lesions. However, these lesions failed to progress to high-grade PanIN and showed an exclusive loss of SMAD. The association between HIF-2α and Smad4 was confirmed *in vitro*, where silencing of HIF-2α reduced Smad4 transcript levels (Criscimanna et al., 2013). Such findings suggest that HIF-2α is dispensable for initiation of PanINs, but it is required for PanIN progression.

Switching from oxidative phosphorylation to glycolysis is a critical metabolic change in PC cells to adapt to hypoxic conditions. HIF-1 upregulates several glycolytic genes that can increase conversion of glucose to pyruvate and, subsequently, to lactate (Semenza, 2013). In addition to activating glycolytic genes, HIF-1 also actively inhibits oxidative phosphorylation by directly trans-activating the gene encoding pyruvate dehydrogenase kinase 1 (PDK1). PDK1 inactivates the enzyme pyruvate dehydrogenase (PDH) by phosphorylating it using adenosine triphosphate (ATP) and, subsequently, inhibits oxidative phosphorylation (Kim et al., 2006).

A major consequence of inhibiting oxidative phosphorylation is a decrease in the endogenous level of ROS in hypoxic cells. Glucose in hypoxic cells is actively shunted away from mitochondria to limit the potential for ROS production resulting from the conversion of glucose to pyruvate (Liemburg-Apers et al., 2015). A recent study showed TxNIP seems to suppress cellular glucose uptake in different cancer cells either directly, by binding to the glucose transporter 1 (GLUT1, a glucose transporter that facilitates the transport of glucose across the plasma membranes of cells) leading to induce GLUT1 internalization through clathrin-coated pits, or indirectly by reducing the level of GLUT1 mRNA (Wu et al., 2013). The latter study also showed that inhibition of TxNIP caused an increase in glucose metabolism by upregulation of GLUT1 mRNA, leading to increasing oxidative stress in cancer cells. Therefore, inhibiting the Trx system in hypoxic cancer cells may be a good strategy to stimulate aerobic metabolism and, subsequently, increase oxidative stress and radiotherapeutic response in these cells. The association between hypoxia in tumour cells and the Trx system is discussed below.

3.2.2.5 Tumour hypoxia and the Trx system

Several studies have investigated the effect of overexpression of HIF-1α on the Trx system in hypoxic tumour cells. Berggren and colleagues showed that incubation of HT-20 colon cancer cells in hypoxia caused a 4- and 14-fold increase in TrxR mRNA and Trx mRNA respectively (Berggren et al., 1996). Stable transfection of Trx-1 in the MCF-7 BC cell line caused a significant increase in HIF-1α expression in normoxic (2.3-fold) and hypoxic (2.1-fold) cells compared with empty vector control cells ($P \leq 0.001$ in both conditions) (Welsh et al., 2002). Another study showed that MCF-7 BC cells incubated 16 hours under hypoxic conditions and subsequently treated with 10 uM of PX-12 showed a significant decrease in expression of HIF-1α compared to untreated cells (Welsh et al., 2003). In the same study, MCF-7 cells were grown as xenografts in SCID mice and subsequently were treated with/without 12 mg/kg of PX-12. The intensity of the immunohistochemical staining of HIF-1α in treated tissues was significantly decreased ($P \leq 0.001$) compared to controls (Welsh et al., 2003). Stable transfection of Trx-1 in BEAS-2B normal human bronchial epithelial cells caused a significant overexpression of HIF-1α under normoxic conditions (Csiki et al., 2006). Baker and colleagues showed that AsPC-1, BxPC-3 and MIA Paca-2 PC cell lines incubated in hypoxia for 16 hours showed a significant increase in TxNIP expression (Baker et al., 2008). A recent study showed that expression of TxNIP was significantly correlated with HIF1-α expression in 70 patients with non-small cell lung cancer carcinoma (Li et al., 2015). The above studies suggest that inhibiting the Trx system in hypoxic tumour cells may be a suitable strategy to stimulate aerobic metabolism in these cells and subsequently decrease their resistance to conventional cancer therapies. The current chapter sets out to evaluate the potential mechanism of action of IQs in normoxic conditions, and also to examine the selectivity of IQs, as bioreductive agents, toward hypoxic PC cells by addressing the hypotheses mentioned below.

3.2.2 Hypotheses

1. IQs treatment impairs PC cells' ability to maintain redox status.
2. IQs treatment inhibits the protein expression and activity of TrxR in PC cell lines in a dose-and time-dependent fashion.
3. By using the appropriate concentration and exposure time of IQs, radiosensitive effect of IQs on PC cell lines can be maximised.
4. Hypoxia increases the cytotoxic efficacy of IQs on PC cell lines.

3.2.3 Aims

1. Assess the effect of IQs pre- and post-H_2O_2 treatment on intracellular ROS levels in PC cell lines.
2. Assess the effect of IQs treatment, at different exposure times, on expression of the Trx system proteins and TrxR activity in PC cell lines.
3. Examine the radioresponse of PANC-1 PC cell line treated with IQs for short-time treatment (4 hours) or with AUR, as a comparator, for 4 and 48 hours.
4. Observe the effect of hypoxia pre- and post-IQs treatment on proliferation, clonogenic survival, protein expression of Trx system members and reductase enzymes in PC cell lines.

3.3 Materials and methods

3.3.1 Cell lines, culture conditions and drug preparation

All cell lines, tissue culture methodologies and drug preparation were described in Chapter 2.

3.3.2 Measurement of intracellular reactive oxygen species (ROS) levels

In ROS level measurement, H_2O_2 (Sigma) was used as positive control to induce oxidative stress in cells, while MDA-MB-231 BC cell line was used as a positive control cell line as it was well-studied previously in terms of ROS levels assessment (Zhang, 2014), as discussed later in Section 3.5. To select the appropriate concentration of H_2O_2 (a concentration that can increase ROS levels without dramatic cell killing of PC cells as discussed later in Section 3.5) to use in ROS level assessment, the proliferation of PC cells and MDA-MB-231 BC cells was assessed against 25, 50, 100 and 200 mM of H_2O_2 for 1 hour, with 0 mM as control.

The membrane permeable dye 2',7'-dichlorodihydrofluorescein diacetate (H_2DCF-DA) (Invitrogen, NY, USA) is a molecular probe able to detect intracellular ROS levels and is not fluorescent until the acetate groups are removed by intracellular ROS (Hancock, 2008). 100 µM of H_2DCF-DA was dissolved in DMSO immediately before use. For each cell line; cells treated with dH_2O, with the same dilution ratio as IQs in complete cell culture medium, for 30 minutes were set as a negative control. Cells treated with 1 µM of H_2DCF-DA for 30 minutes for 30 minutes in complete cell culture medium were set as a positive control. For tested samples, each PC cell line was treated with the proliferation IC50 values (IC50s at 48 hours treatment, Table 2.4) of IQ9 and IQ10 for 1, 4, 24 or 48 hours with/without subsequent H_2O_2 treatment for 1 hour. For each PC cell line, a certain concentration of H_2O_2 was selected based on the cytotoxic effect of H_2O_2 against PC cell lines, as shown later in Section 3.4.1. The treatment with IQs alone aimed to examine the ability of IQs to induce oxidative stress when delivered as single agents. The

combination of IQs and H_2O_2 examined the ability of the PC cells to cope with oxidative stress following drug treatment.

After washing once with PBS, all flasks were incubated with 1 µM of H_2DCF-DA in fresh medium for 30 minutes, at 37˚C in a humidified incubator with 5% CO_2. After incubation, cells were trypsinised, centrifuged at 170 x g for 5 minutes, washed with PBS, centrifuged again at 170 x g for 5 minutes to remove all H_2O_2 and H_2DCF-DA, and resuspended in PBS at a concentration of 1 x 10^6 cells/ml. The intracellular ROS levels were determined by measurement of the fluorescence (FL1 at 525 nm) using a Beckman Coulter FC500 MCL flow cytometer system (Beckman Coulter). A gate was set to include the living cells in the flow cytometer analysis only and gate out the dead cells. Data exported from the flow cytometer were analysed using FlowJo7.6.1 software (Tree Star) to obtain the median fluorescence intensity (MFI) of each group representing the intracellular ROS level. The MFI of each sample was normalised to the control. As PC cell lines treated with H_2O_2 showed a marginal increase in ROS level (as shown later), MDA-MB-231 BC cells treated with 1 mM was run along with each PC experiment as positive control, to validate the flow cytometry assessment.

3.3.3 Western blot

As the expression of Trx system proteins in MCF-7 and MDA-MB-231 BC cells was well-studied in published literature (Berggren and Powis, 2001, Farina et al., 2011, Sun et al., 2012, Zhang, 2014), both cell lines were set as positive controls to assess the endogenous expression of the Trx system proteins in PC cell lines.

To investigate the effect of IQs on the expression of the Trx system proteins in PC cell lines, cells were treated with 100, 250, 500 and 1000 of IQs for 48 hours or with estimated clonogenic IC50's of IQs (except BxPc-3 cells were treated with 500 nM of IQs, Section 2.4.3.2) for 48 hours, with 0 nM as control. Then, cells were trypsinised and centrifuged at 170 x g for 5 minutes. The cell pellet was resuspended with PBS and counted, then centrifuged again at 170 x g for 5 minutes. After the supernatant was

removed, 1 ml of ice-cold RIPA cell lysate solution (970 µl RIPA Buffer (Sigma) + 10 µl phosphatase inhibitor cocktail (Thermo) + 10 µl protease inhibitor cocktail (Thermo) + 10 µl 0.5 M EDTA solution (Thermo)) was used to lyse $5x10^6$ cells. Tubes were left on ice for 30 minutes with vortexing every 10 minutes, and then cell lysates were frozen at -20˚C or -70˚C for long-term storage. Lysates were clarified by centrifuging at 14,000 x g for 10 minutes at 4°C to separate the total protein (supernatant) from the cell debris (pellet) after the first time thawing. The supernatants containing the soluble protein were used for Western blot, and the remaining samples were aliquoted and stored at -20˚C or -70˚C for long-time storage. Thawed lysates were kept on ice prior to use, and repeat freeze-thaw cycles avoided.

For Western blot, 18 µl of each lysate (~25 µg) was mixed with 6 µl of loading buffers (100 µl of loading buffer contains 80 µl of gel loading dye (Sigma) and 20 µl of 2-mercaptoethanol (Sigma)). 24 µl of each sample was incubated at 95^{o}C for 5 minutes before loading to sodium dodecyl sulfate poly-acrylamide gel electrophoresis (SDS-PAGE), and then put on ice for further use. Buffers needed for Western blot were prepared as described in Table 3.1.

Buffer	Reagent	Source
Running Buffer (1 litre)	50 ml of Running Buffer (20x) + 950 dH_2O	NP0001, Novex
PBS/Tween (1 litre)	10 PBS tablet + 1 ml Tween20 + 999 ml dH_2O	BR0014G, OXOID P2287, Sigma
Transfer Buffer (500 ml)	25 ml of Transfer Buffer (20x) + 50 ml absolute Methanol + 375 ml dH_2O	NP0006-1, Novex Sigma (Cat# 32213) *NA*
Block solution (50 ml)	2.5 g of dried milk + 50 ml of PBS/Tween	*NA*

Table 3.1: Western blot buffers.

A mixture (3 µl) of magic marker (1.5 µl) (Invitrogen) and rainbow marker (1.5 µl) (Amersham) were added to the first well of the gel to enable the determination of the protein transfer and protein size. SDS-PAGE was applied to separate the mixtures of total proteins in each cell lysate sample based purely on protein size. SDS-PAGE gels were prepared by filling Invitrogen cassettes (NC2010) with 12% SDS-PAGE resolving gel solution to ¾ of the cassette at first. A comb was inserted on the top of cassettes into the stacking gel solution to form sample loading wells. At least 30 minutes was allowed at room temperature to let the gel set. The comb was removed before SDS-PAGE. XCell SureLock™ Mini-Cell Electrophoresis System (Invitrogen) was used for SDS-PAGE. The SDS-PAGE gel cassette was loaded, and running buffer was filled into the tank according to the product manual. Then the system was run at 125V for 90 minutes. After SDS-PAGE, separated protein bands in the gel were transferred onto a nitrocellulose membrane in transfer buffer using the same XCell SureLock™ Mini-Cell Electrophoresis System at 25V for 90 minutes. After transfer, the nitrocellulose membrane was incubated in blocking buffer at room temperature for 1 hour and then in primary antibody solution at 4°C overnight. The primary and secondary antibodies used in the project with their dilution ratios and host species are listed in Table 3.2.

Targeted protein	Source	Catalogue number	Host specious	Dilution
Trx	Abcam	Ab133524	Rabbit	1:5000
TrxR	Abcam	Ab16847	Mouse	1:1000
TxNIP	Abcam	Ab188865	Rabbit	1:1000
NQO1	Cell signalling	3187	Mouse	1:1000
P450	Abcam	ab180597	Rabbit	1:1000
CA9	Absolute Antibody	Ab00414-1.1	Mouse	1:1000
β-actin	Abcam	Ab8226	Mouse	1:2000
β-actin	Abcam	Ab8227	Rabbit	1:2000
Anti-moues	DAKO	P00260	Rabbit	1:1000
Anti-rabbit	DAKO	P00448	Goat	1:1000
Li-COR Anti-Mouse	Li-COR	925-68072	Donkey	3:10000
Li-COR Anti-Rabbit	Li-COR	926-32213	Donkey	3:10000

Table 3.2: Primary and secondary antibodies for Western blot.

In the second day, Western blot was carried out either by using enhanced chemiluminescence (ECL) assay (Amersham) in order to determine antibodies' specificity as shown later in Chapter 4, or by using two-colour Western blot detection with infrared fluorescence assay (LI-COR Biosciences) to quantify protein expression as shown in the current chapter.

For the ECL assay, in the second day, after a 3 x 5 minutes wash with 0.1% PBS/Tween, the membrane was incubated with horseradish peroxidase (HRP)-conjugated secondary antibody solution (1:1000 diluted in blocking buffer), according to the host species of the primary antibody (i.e. anti-mouse or anti-rabbit HRP-conjugated antibody, all from Dako, Glostrup, Denmark), at room temperature for 1 hour. Following another 3 x 5 minutes wash with 0.1% PBS/Tween, a mixture of Amersham ECL reagent (GE

Healthcare) was spread onto the membrane for 1 minute. Then an Amersham hyperfilm ECL (GE Healthcare) was exposed on top of the membrane for a certain amount of time (varying from 30 seconds to 15 minutes according to the chemiluminescence signal from the membrane) and developed to visualise protein bands. In the current project, β-actin was used as the housekeeping protein.

For the Li-COR assay, in the second day, the membrane was washed for 3 x 5 minutes with 0.1% PBS/Tween then incubated with primary housekeeping antibody (β-actin) for 1 hour. Following another membrane wash of 3 x 5 minutes with 0.1% PBS/Tween, the membrane was incubated for 1 hour with two different species of IRDye secondary antibodies, simultaneously, in the dark. Infrared fluorescent secondary antibodies (LI-COR) are listed in Table 3.2. Then, the membrane was washed for 3 x 5 minutes with 0.1% PBS/Tween, dried and then processed using the LI-COR machine (LI-COR Biosciences) to image all protein bands in the membrane. Odyssey Image Studio Software (LI-COR) was used to quantify the signal value of each protein band in the membrane.

To calculate the normalised protein expression of each tested sample, the following formula was used: the signal value of tested protein expression / normalised signal value of β-actin of same tested sample. The normalised signal value of β-actin can be calculated by the following formula: the signal value of β-actin of the tested sample/ the highest signal of β-actin in the Western blot membrane.

As shown later in Section 3.4.2.2, quantification of Trx, TrxR, TxNIP and β-actin protein expression of each PC cell lines can be analysed from a single membrane. The membrane was cut into two pieces at a weight of 24 KD. The lower part of the membrane (<24 KD) was processed independently to quantify Trx protein expression (12 KD). The upper part of the membrane was processed to quantify TrxR (55 KD) and β-actin (42 KD) simultaneously. After quantification of TrxR and β-actin was analysed, the membrane was stripped for 30 minutes in restore Western blot stripping buffer (Thermo) to remove all the primary and secondary antibodies. Following 3 x 5 minutes wash with 0.1%

PBS/Tween, the membrane was incubated in blocking buffer at room temperature for 1 hour, then incubated with anti-TxNIP overnight. In the third day, the upper part of the membrane was processed to quantify TxNIP (50 KD).

3.3.4 Thioredoxin reductase activity

PANC-1 and BxPc-3 cells were selected to investigate the inhibitory effect of IQs on TrxR activity, as both cell lines showed an increase in radiosensitivity after IQs treatment as shown in Chapter 2, while AUR was selected as a comparator. PANC-1 and BxPc-3 cells were treated with 100, 250, 500 and 1000 nM of IQs or with 1000 nM of AUR for 4 or 48 hours, with 0 mM as control. Cells were then lysed as mentioned in Section 3.3.3**.** The total protein concentration of each cell lysate sample was determined, on the day of use, by detergent compatible (DC) Protein Assay (Bio-Rad, UK) based on the Bradford assay (Bradford, 1976) to ensure equal protein concentration for each tested sample. Six dilutions of a protein standard, from 0 mg/ml to 1 mg/ml bovine serum albumin (BSA) (Sigma), were prepared before measurement. For optimal results, the standard protein samples were prepared in the same buffer as the tested samples. Briefly, 25µl of solution A, prepared by adding 20 µl of reagent S to 1 ml of reagent A, was added to each well of a 96-well plate. Then, 5µl of tested samples or protein standard samples was added to 96-well plate in duplicate. Finally, 200 µl of reagent B was added to each well of a 96-well plate, and the plate was incubated at room temperature for 15-30 minutes. Absorbance at 650 nm in each well was measured using a microplate reader. The concentration of the tested protein samples was interpolated by linear regression, which was produced by plotting a standard curve of the known protein concentrations against their measured absorbance, considering the dilution factor of each sample.

The insulin reduction assay was used to determine the functional activity of TrxR according to the method adapted from Kunkel et al (Kunkel et al., 1997). Trx is involved in transferring thiol groups to a wide variety of substrates in the cell, one of them being insulin. The assay depends on the availability of the active reduced form of Trx to reduce

protein disulphides in insulin. The reduced form of insulin then reduces the substrate DTNB (5, 5'-dithiobis-2-nitrobenzoic acid) to TNB (5'-thionitrobenzoic acid), measured by the absorbance of the coloured substrate at 405 nm. The cell-free enzyme assay for TrxR uses DTNB as a substrate in the following reaction:

$$DTNB + NAPDH + H^{+} \xrightarrow[TrxR]{} 2TNB + NAPD^{+}$$

The experiment was run in 96 well-plate format. To conduct a standard curve of TNB concentrations, six different concentrations (25, 50, 100, 250, 500, 750 and 1000 nM) of TrxR (Sigma) was added in two sets of wells, with 0 nM as control. The first set included seven wells with the seven different concentrations of TrxR in a final volume of 100 µl (a mixture of Hepes buffer (100 mM, Sigma), EDTA (5 mM, Sigma), insulin (10 mg/ml, Sigma) and Trx (20 uM, Sigma)). The second set included the same seven different concentrations of TrxR in seven wells in a final volume of 100 µl (a mixture of Hepes buffer (100 mM), EDTA (5mM) and insulin (10mg/ml)), with no Trx was added to the mixture of the second set.

For the tested samples, in the same 96 well-plate, 80 µg of each sample was added in duplicate on top of two sets; the first set contained a mixture the following in a final volume of 90 µl:

HE buffer (100mM HEPES, pH 7.2; 5mM EDTA)	70 µl
Trx (20 uM)	10 µl
Bovine insulin (10mg/ml)	10 µl

While the second set contained a mixture the following in a final volume of 90 µl (no Trx was added to the mixture of the second set):

HE buffer (100mM HEPES, pH 7.2; 5mM EDTA)	80 µl
Bovine insulin (10mg/ml)	10 µl

10 µl of NADPH (10mM, Sigma) was added to all wells as the last step to allow the reaction to start at time 0 minute. After NAPDH was added, the 96 well-plate was incubated at 37°C for 60 minutes, then 150 µl of DTNB/guanidine (10 mM DTNB (Sigma) + 6M guanidine (Sigma)) was added to each well to stop the reaction. The TNB colour of each well, resulting from the reaction, was determined at an absorbance of 406 nm. The differences of the TNB reading between the two sets (-/+ Trx) of the tested sample were applied to the linear TNB standard curve to calculate the TrxR activity of each sample, considering the dilution factor of each sample. Then, the TrxR activity of each sample was plotted as a percentage of control.

3.3.5 Drug-radiation combination clonogenic assay

Based on the results of ROS level assessment and TrxR activity (as to be shown later), PANC-1 and MIA Paca-2 cells were selected for the drug-radiation clonogenic, which was previously described in Section 2.3.7.2.3. In the current chapter, PANC-1 cells were treated with 900 nM of IQ9 (estimated clonogenic IC50 of IQ9 after 48 hours' treatment) for 4 hours, and MIA Paca-2 cells were treated with 260 nM and 240 nM of IQ9 and IQ10 respectively for 1 hour (estimated clonogenic IC50's of IQ9 and IQ10 for 48 hours' treatment respectively). Then cells were irradiated and plated for clonogenic survival as protocol described previously. Also, the drug-radiation combination clonogenic assay was performed for PANC-1 cells treated with the estimated proliferation IC50 of AUR for 4 or 48 hours, as positive control comparator.

3.3.6 Cytotoxicity experiments of PC cell lines in hypoxic conditions

3.3.6.1 Proliferation and clonogenic survival

Subconfluent PANC-1, MIA Paca-2 and BxPc-3 cells were trypsinised and resuspended as single cells in complete cell culture medium. 1×10^5 cells of each cell line (2×10^5 for MIA Paca-2) were plated in each well of a 6-well plate (3 wells/time point) and incubated overnight to allow attachment. Plates were then incubated at 37°C, 5% CO_2 and 1% O_2

in an INVIVO2400 hypoxic workstation (Baker Ruskinn, Sanford, ME, USA) for 24, 48 and 72 hours. Cells were then trypsinised and cell number counted using a haemocytometer. Cell counts were recorded, analysed and plotted over a 72-hour time course. To assess the growth delay of hypoxic cells over normoxic cells at each time points, a parallel normoxic set of wells of each cell line was added to the experiment. For both sets, the experiments were repeated independently three times.

For assessment of clonogenic survival, the remaining cells from the above proliferation assay assessments were diluted at appropriate concentrations and plated into T25cm^2 tissue culture flasks (3 flasks/time point) and incubated for three weeks at 37°C and 5% CO_2 to allow colony formation. The clonogenic experiments were repeated independently two times.

To confirm hypoxic conditions, following a hypoxic incubation, cells were collected and lysed for Western blot, according to the protocol in Section 3.3.3, to observe the expression of anti-Human carbonic anhydrase 9 (CA9) as a hypoxic marker (Leek et al., 2016). The characteristics of CA9 antibody (Absolute Antibody Company) used in the current study are listed in Table 3.2. Briefly, CA9 is a member of the tumour-associated transmembrane CAs that catalyse the reversible hydration of carbon dioxide to carbonic acid, providing a potential link between metabolism and pH regulation (Pastorek et al., 1994, Sly and Hu, 1995). CA9 is tightly regulated by HIF-1 and strongly induced by hypoxia in various cancer cells (Wykoff et al., 2000, da Motta et al., 2017).

3.3.6.2 Proliferation and clonogenic survival following IQ9 treatment in hypoxic conditions

PANC-1 and BxPc-3 PC cell lines treated with IQs showed radiation sensitivity compared to control, as shown in Chapter 2, and so both cell lines were selected to investigate their sensitivity to IQ9 in hypoxia. In addition, as IQ9 exhibited higher inhibitory effect on TrxR activity than IQ10 in PANC-1 and BxPc-3 cells (to be shown later in Section 3.3.4),

it was selected to investigate its cytotoxic effect on PANC-1 and BxPc-3 under hypoxic conditions.

PANC-1 and BxPc-3 PC cell lines were incubated at 37^{o}C, 5% CO_2 and 1% O_2 for 24 hours. Then, whilst still under hypoxia, cells were treated with 50, 100, 250, 500 or 1000 nM of IQ9 for 48 hours, with 0 mM as control (total hypoxic incubation time was 72 hours). Cells were then trypsinised and counted using a haemocytometer. Cell counts were recorded, analysed and plotted as a percentage of control. A set of six wells for each cell line were treated under normoxic conditions as comparators; 3 wells as controls and 3 wells were treated with the proliferation IC50 of IQ9. The results of the normoxic set were compared with previous findings, in Section 2.4.2.1, as a positive control.

For clonogenic survival, PANC-1 and BxPc-3 PC cell lines were incubated at 37^{o}C, 5% CO_2 and 1% O_2 for 24 hours. Then, whilst still under hypoxia, cells were treated with 50, 100, 250, 500 or 1000 nM of IQ9 for 4 or 48 hours, with 0 mM as a control (total hypoxic incubation times was 28 and 72 hours respectively). Cells were then trypsinised, counted, diluted at appropriate concentrations and plated into T25cm^2 tissue culture flasks (3 flasks/time point) and incubated for three weeks at 37°C and 5% CO_2 to allow colony formation. The clonogenic experiments were repeated independently two times. A set of six flasks for each cell line were treated under normoxic conditions as comparators; 3 flasks as controls and 3 flasks were treated with the clonogenic IC50 of IQ9. The results of the normoxic set were compared with previous findings, in Section 2.4.2.2, as a positive control.

3.3.6.3 Expression of Trx, TrxR, NQO1 and CPR in PC cell lines treated with IQs under the normoxic and hypoxic conditions

The effect of IQ9 on the endogenous expression of Trx and TrxR in PC cells under normoxia was shown in Section 3.4.2.1. However, the current experiment aims to study the effect of hypoxia on altering the endogenous expression of Trx and TrxR in PC cells with/without IQ9 treatment. PANC-1 and BxPc-3 cells were treated with the same procedure as above (Section 3.3.6.2). However, following IQ9 treatment, cells were

lysed and assessed for protein expression by Western analysis as described in Section 3.3.3**.** Western blot was conducted to observe the effect of hypoxia on the endogenous expression of Trx, TrxR, NQO1, CPR and CA9 proteins in PANC-1 and BxPc-3 cells, in addition to study the effect of IQ9 treatment for 4 or 48 hours on altering the expression of these proteins in normoxic or hypoxic conditions.

3.3.7 Statistical analysis and graph design

Statistical analysis and graph design were described in Chapter 2.

3.4 Results

3.4.1 Effect of IQs on intracellular ROS levels

An initial optimisation was performed to explore the cytotoxic effect of H_2O_2 on PC cells and MDA-MB-231 BC cells. As shown in Figure 3.2, current data suggest that PC cell lines are exceptionally sensitive (IC50=30-40 mM) to H_2O_2 compared to MDA-MB-231 BC cells (IC50=100 mM). BxPc-3 (IC50=30 mM), MIA Paca-2 (IC50=30 mM) and PANC-1 cells (IC50=40 mM) cells seem to have similar sensitivities to each other. The current results are comparable with published studies as discussed in Section 3.5.

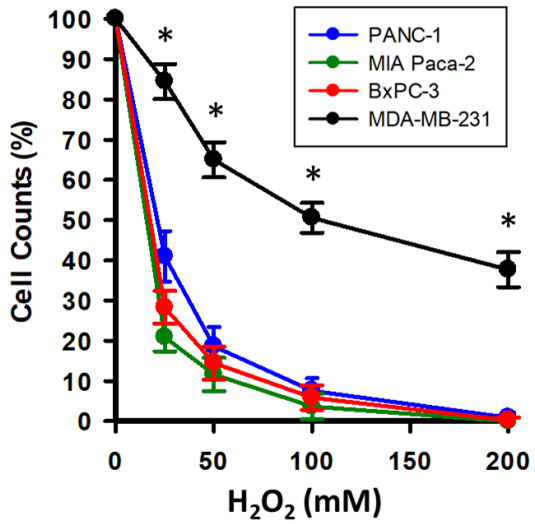


Figure 3.2: Effect of H_2O_2 on proliferation of PC cell lines and MDA-MB 231 BC cell line. PANC-1, BxPc-3 and MIA Paca-2 PC cell lines were treated with H_2O_2 (50-200 mM) for 1 hour. Data represent the mean ± standard deviation of pooled data of three independent experiments, with each experiment performed in triplicate, which are analysed using the Student T-test. * P<0.05 vs MDA-MB-231 cells.

Several H_2O_2 optimisations, by flow cytometry, were conducted in order to select the appropriate concentration of H_2O_2 of each cell line that could induce ROS level more than 4-fold over control, whilst ensuring a sufficient number of living cells to run subsequent ROS assessments (10,000 living cells were needed in each run). For MDA-MB-231 BC cells, 1 mM of H_2O_2 for 1 hour was the most appropriate concentration since it induced ROS level more than 4-fold over control with a sufficient number of living cells to run the assessment (Figure 3.3).

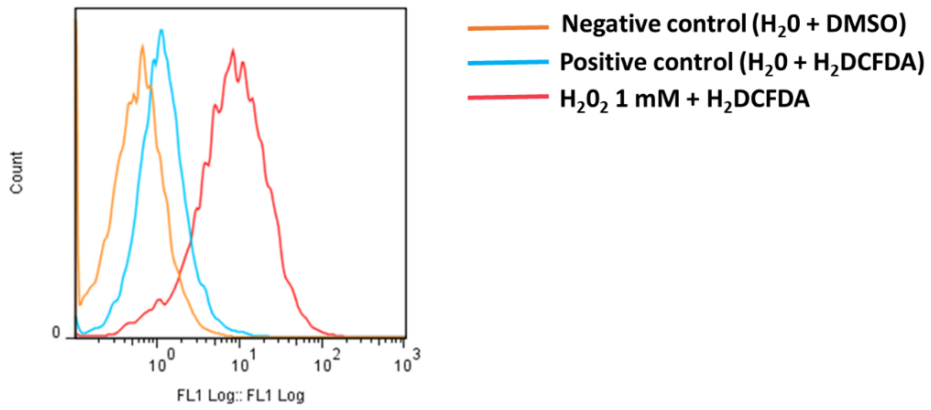


Figure 3.3: Optimization of H_2DCF-DA and H_2O_2 concentration in ROS level assessment. MDA-MB-231 BC cells treated with H_2O and DMSO as a negative control (orange) or with 1 µM H_2DCF-DA alone as a positive control (blue) or with 1 mM of H_2O_2 for one hour followed by 1 µM H_2DCF-DA for 30 minutes (red) were collected for intracellular ROS level analysis.

Initial experiments showed that 1 mM of H_2O_2 for 1 hour was extremely toxic to the PC cells, causing an insufficient number of cells to run the ROS level assessment. After several optimisations of H_2O_2 with PC cell lines, concentrations of 0.4, 0.3 and 0.3 mM of H_2O_2 for 1 hour for PANC-1, MIA Paca-2 and BxPc-3 cells respectively, were selected to use in ROS level assessments. The selected concentration of H_2O_2 against each cell line caused a 1.2-1.4-fold increase in ROS level over control in PC cell lines. The selection criteria of H_2O_2 concentration for each PC cell line in ROS level assessment is discussed in Section 3.5.

As shown in Figure 3.4, PC cell lines treated with IQs alone showed a marginal increase (<25%) in ROS levels over untreated cells. However, cells treated with IQs in combination with H_2O_2 showed an increase in ROS levels over treatment with H_2O_2 alone, with a maximum fold increase of 2. PANC-1 and BxPc-3 cells treated with IQ9 for 48 hours in combination with H_2O_2 showed a 1.6- and 2-fold increase in ROS levels over treatment with H_2O_2 alone respectively. While MIA Paca-2 cells treated with IQ9 for 1 hour in combination with H_2O_2 showed a 2.2-fold increase in ROS levels over treatment with H_2O_2 alone, suggesting that cells were less able to deal with oxidative stress in presence of IQs, giving support that assessing the radiation sensitivity of MIA Paca-2 cells treated with IQs for 1 hour might be worthwhile, as shown in Section 3.4.4.

The initial plan for ROS level assessments was to perform three experiments for each cell line for each drug, with each experiment performed in a single T25 flask. However, after the second experiment for each cell line, unfortunately, the flow cytometer machine was broken for a long period of time. Therefore, current data, in Figure 3.4 and Figure 3.5, represent the average of only two independent experiments. No statistical analysis was performed for results of ROS level assessments (Figure 3.4 and Figure 3.5) since these results came from only two experiments (Section 2.3.9).

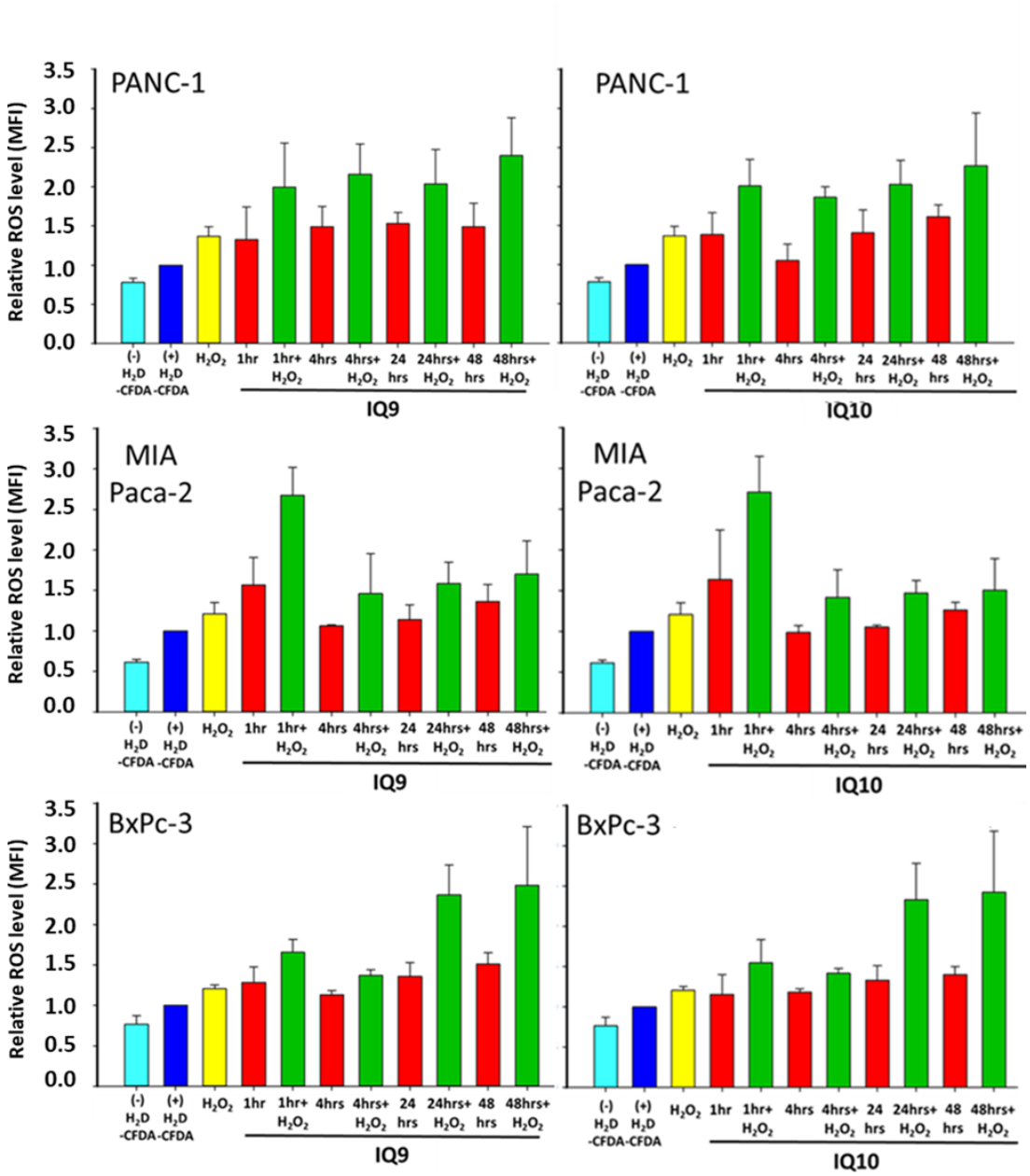


Figure 3.4: Effect of IQs on intracellular ROS level of PC cell lines. PC cells treated with IQs, either with (green bars) or without (red bars) H_2O_2, were subjected to intracellular ROS level analysis. Cells without drug treatment were set as negative control (light blue) or as positive control (blue). Data represent the mean ± standard deviation of two independent experiments, with each experiment performed in a single T25 flask.

As shown in Figure 3.5, AUR shows no effect on ROS levels production in PC cell lines or MDA-MB-231 BC cells either alone or combined with H_2O_2. The effect of AUR on ROS levels in PC and MDA-MB-231 cells was comparable with published studies as discussed in Section 3.5.

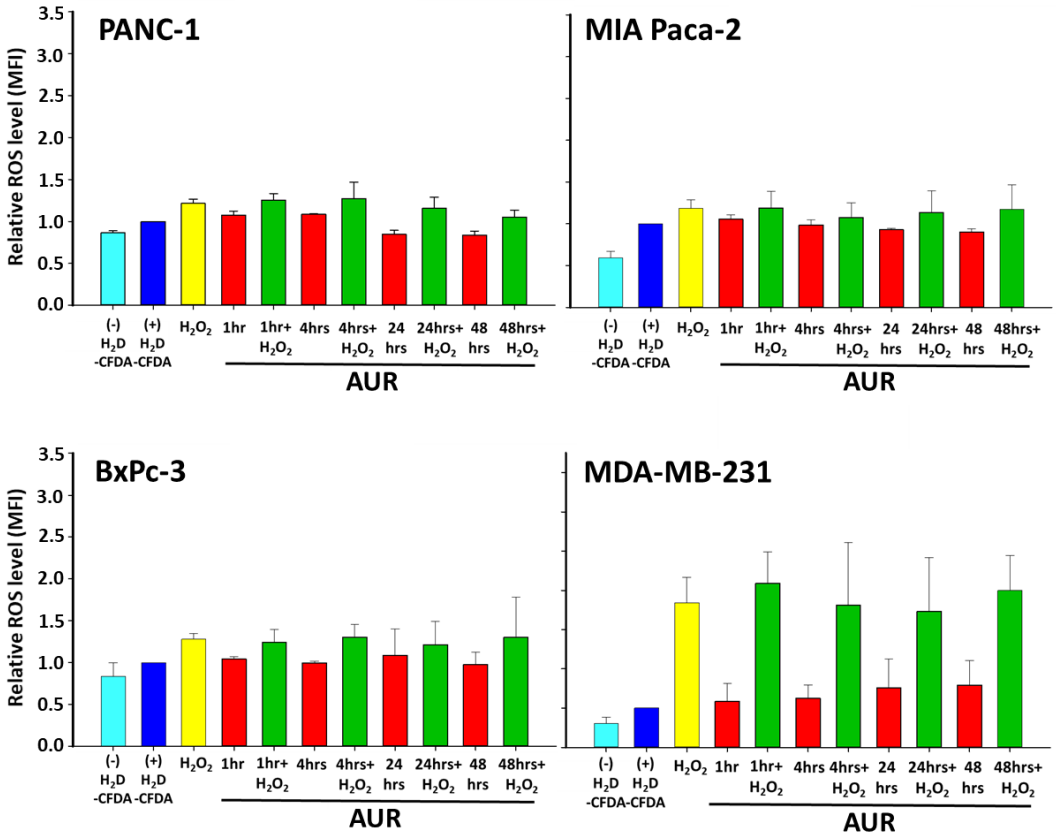


Figure 3.5: Effect of AUR on intracellular ROS level of PC cell lines and MDA-MB-231 BC cell line. PANC-1, MIA Paca-2, BxPc-3 and MDA-MB-231 cells treated with AUR, either with (green) or without (red) H_2O_2, were subjected to intracellular ROS level analysis. Cells without drug treatment were set as negative control (light blue) or as positive control (blue). Data represent the mean ± standard deviation of two independent experiments, with each experiment performed in a single T25 flask.

3.4.2 Effect of IQs on the expression of Trx system in PC cell lines

3.4.2.1 The endogenous expression of Trx, TrxR and TxNIP in PC cell lines

To quantify the expression of Trx system proteins in PC cell lines, three independent Western blots using separate lysates each time from cells cultured at different times were performed. As shown in Figure 3.6, MCF-7 and MDA-MB-231 cells showed low endogenous expression of TrxR and TxNIP, while the endogenous expression of Trx was expressed. The endogenous protein expression of Trx in BxPc-3 cells was higher than MIA Paca-2 (P=0.055) and PANC-1 (P=0.179) cells. In contrast, endogenous protein

expression of TrxR in BxPc-3 cells was significantly lower than PANC-1 (P=0.008) and MIA Paca-2 (P=0.036) cells.

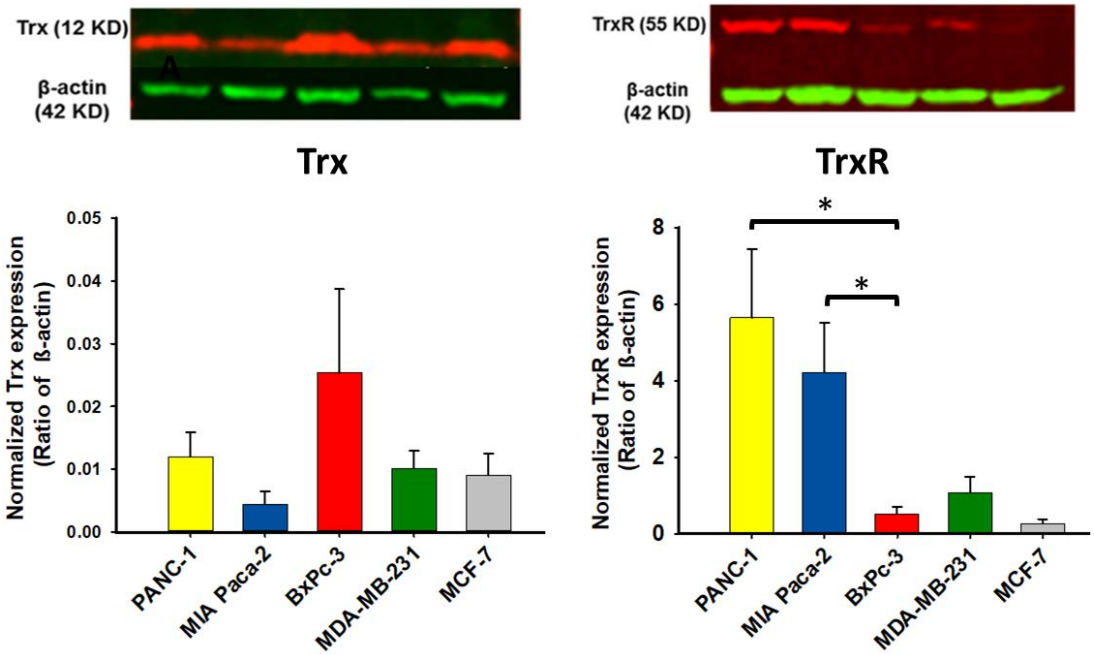


Figure 3.6: Quantification of the endogenous expression of Trx and TrxR in PC and BC cell lines. The bar plots show the quantified protein expression of Trx and TrxR in PANC-1, MIA Paca-2 and BxPc-3 PC cell lines and MCF-7 and MDA-MB-231 BC cell lines. Western blot image represents one of the three independent experiments of each protein. Data represent the average of three independent experiments with a standard deviation (SD), which are analysed using the Student T-test. * P<0.05

As shown in Figure 3.7, the endogenous expression of TxNIP in PANC-1 cells was lower than BxPc-3 cells (P=0.007) and MIA Paca-2 (P=0.057) cells. The current results of the endogenous expression of Trx system proteins in PC and BC cell lines are comparable to the published studies as discussed in Section 3.5.

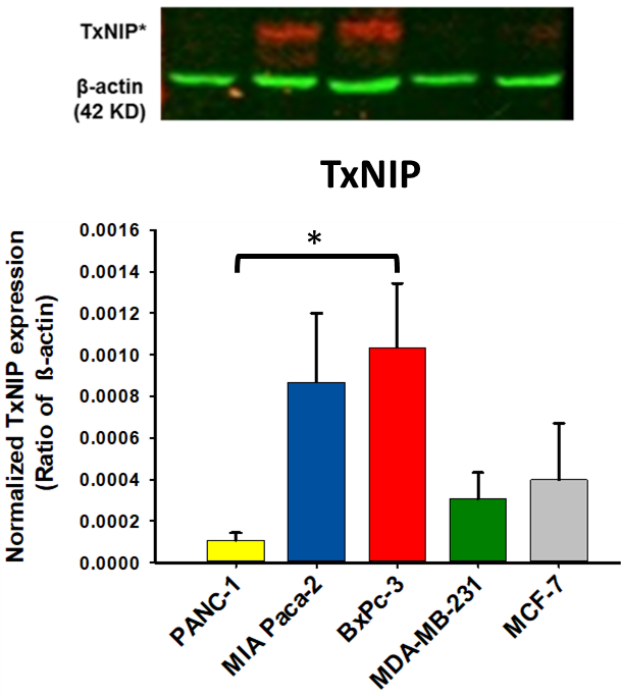


Figure 3.7: Quantification of the endogenous expression of TxNIP in PC and BC cell lines. The bar plot shows the quantification expression of TxNIP protein in PANC-1, MIA Paca-2 and BxPc-3 PC cell lines and MCF-7 and MDA-MB-231 BC cell lines, while Western blot image represents one of the three independent experiments of TxNIP expression. Data represent the average of three independent experiments with a standard deviation (SD), which are analysed using the Student T-test. * $P<0.05$

3.4.2.2 Effect of IQs on protein expression of the Trx system

To quantify the effect of IQs on the expression of TrxR protein, PC cell lines were treated with IQs (0-1000 nM) for 48 hours, three independent Western blots were performed, using separate lysates each time from cells cultured at different times. As shown in Figure 3.8, IQ9 and IQ10 showed no effect on the endogenous expression of TrxR across all PC cell lines.

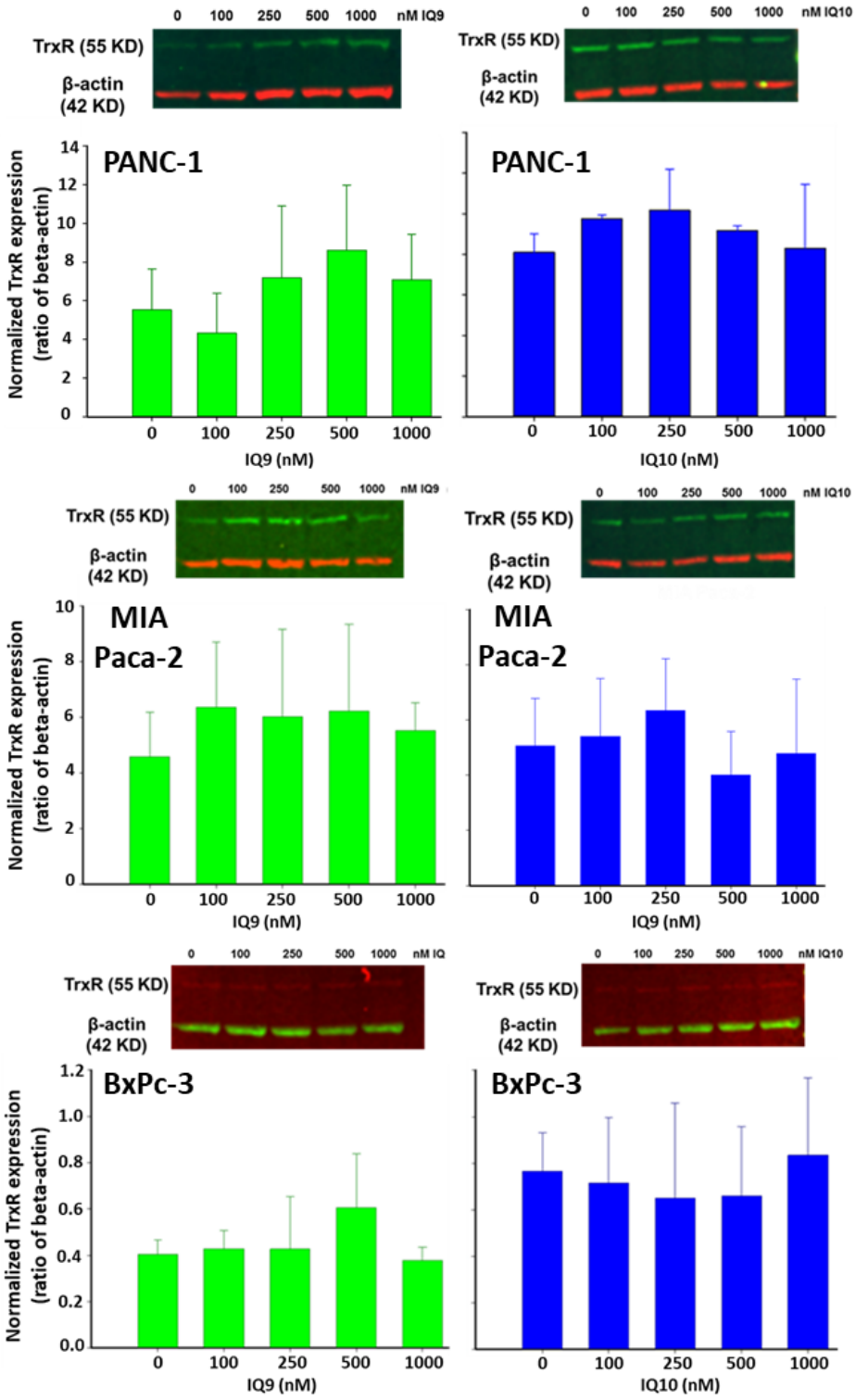


Figure 3.8: Effect of IQs on the expression of TrxR in PC cell lines. PANC-1, MIA Paca-2 and BxPc-3 cells treated with IQ9 (green) or IQ10 (blue) for 48 hours showed no effect on the endogenous expression of TrxR compared to control. The bar plots show the quantification expression of TrxR, while the Western blot images represent one of the three independent experiments of each protein. Data represent the average of three independent experiments with a standard deviation (SD).

To quantify the effect of IQs on the protein expression of other Trx system members in PANC-1, MIA Paca-2 and BxPc-3 PC cell lines treated with IQs for 48 hours, three independent Western blots were conducted, using separate lysates each time from cells cultured at different times. As shown in Figure 3.9, Western blot showed a significant decrease in the expression of Trx protein in BxPc-3 cells treated with clonogenic IC50's of IQ9 (P=0.014) or IQ10 (P=0.01) for 48 hours compared to control, with no alteration in the expression of TxNIP protein was observed. No altered expression of Trx, TrxR or TxNIP proteins was observed in either PANC-1 (Figure 3.10) or MIA Paca-2 (Figure 3.11) cells treated with clonogenic IC50's of IQ9 or IQ10.

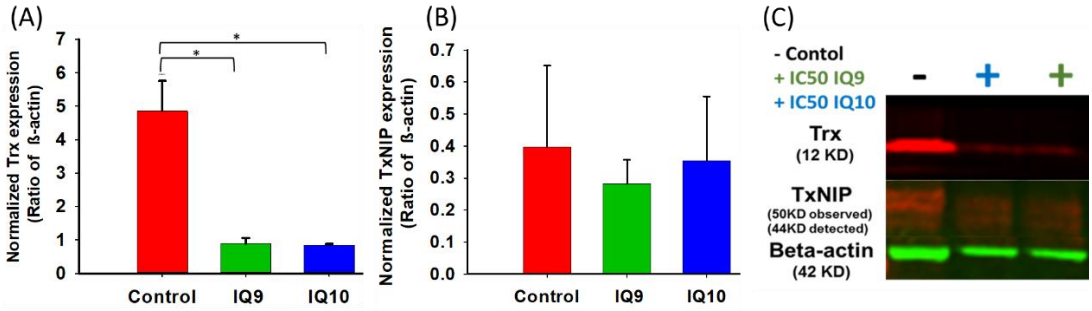


Figure 3.9: Effect of IQs on the expression of Trx and TxNIP proteins in BxPc-3 PC cell line. BxPc-3 cells treated with 500 nM of IQ9 (green) or IQ10 (blue) for 48 hours showed a significant decrease in the expression of Trx protein (A) compared to control, while no altered expression of TxNIP protein (B) was observed. The image (C) represents one of the three independent experiments of Western blot. Data represent the average of three independent experiments with a standard deviation (SD), which are analysed using the Student T-test. * P<0.05

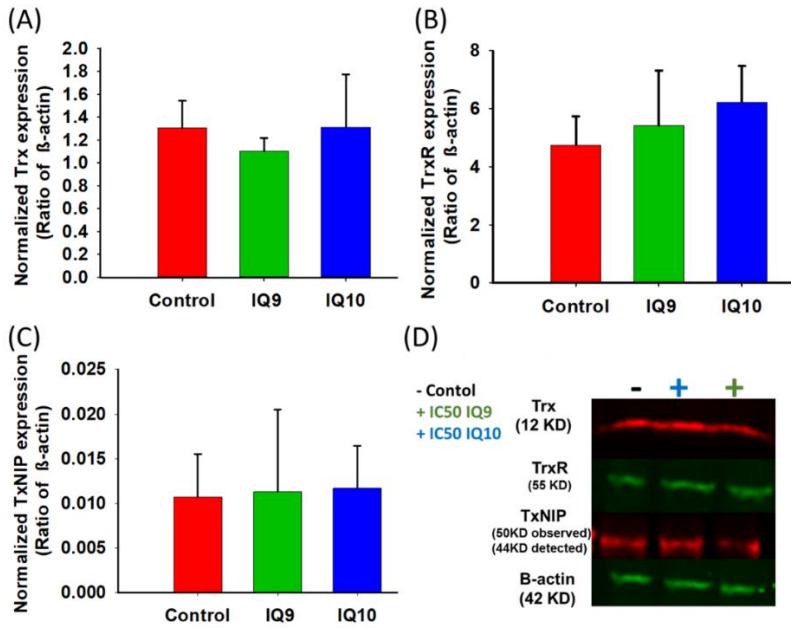


Figure 3.10: Effect of IQs on the expression of Trx system in PANC-1 PC cell line. PANC-1 cells treated with IC50's of IQ9 (green) or IQ10 (blue) for 48 hours showed no alteration in the expression of Trx (A), TrxR (B) or TxNIP (C) proteins compared to control (red). The image (D) represents one of the three independent experiments of Western blot. Data represent the average of three independent experiments with a standard deviation (SD).

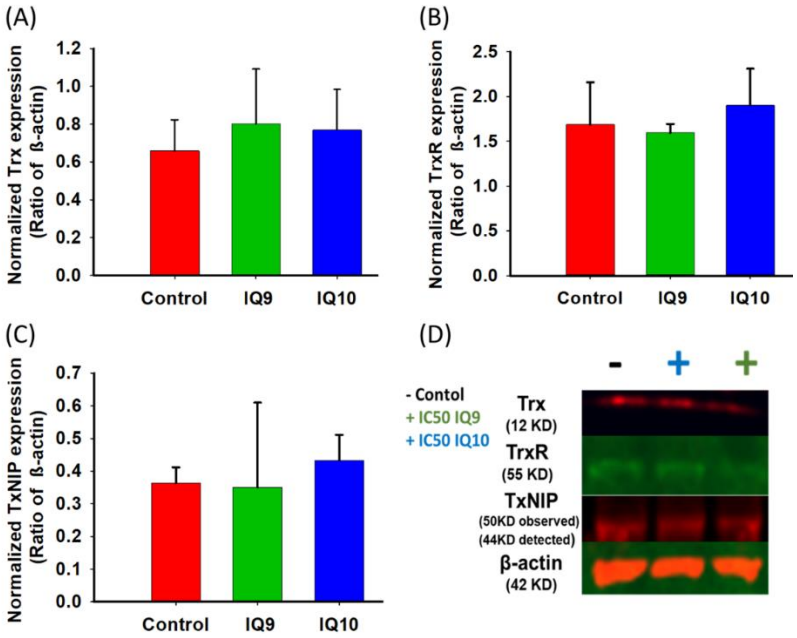


Figure 3.11: Effect of IQs on the expression of Trx system proteins in MIA Paca-2 PC cell line. MIA Paca-2 cells treated with IC50's of IQ9 (green) or IQ10 (blue) for 48 hours showed no alteration in the expression of Trx (A), TrxR (B) or TxNIP (C) proteins compared to controls (red). The blot image (D) represents one of the three independent experiments of Western blot. Data represent the average of three independent experiments with a standard deviation (SD).

3.4.3 Effect of IQs on TrxR activity

PANC-1 cells treated with IQs showed a substantial decrease in TrxR activity in a dose-dependent manner, with 4 hours' treatment giving greater inhibition than 48 hours' treatment. As shown in Figure 3.12, the activity of TrxR in PANC-1 cells treated with 1000 nM of IQ9 or IQ10 or AUR was decreased by 72%, 61% and 81% respectively, compared to control. For 48 hours' treatment, the activity of TrxR in PANC-1 cells was decreased 55%, 45% and 30% after treated with 1000 nM of IQ9 or IQ10 or AUR respectively, compared to control (Figure 3.12). No statistical analysis was performed for TrxR activity results since they came from only two independent experiments (Section 2.3.9).

IQs seem to be more effective at inhibiting the activity of TrxR in PANC-1 cells after 4 hours' treatment than 48 hours' treatment, suggesting that future assessments of radiation sensitivity of PANC-1 cells treated with IQs for 4 hours would be worthwhile, as shown later in Section 3.4.4. Also, as AUR seems to also inhibit the activity of TrxR in PANC-1 cells, it was also thought worthwhile to assess the radiation sensitivity of PANC-1 cells treated with AUR for 4 and 48 hours, as shown in Section 3.4.4. The current results of TrxR inhibition by AUR are comparable to published studies as shown in Section 3.5.

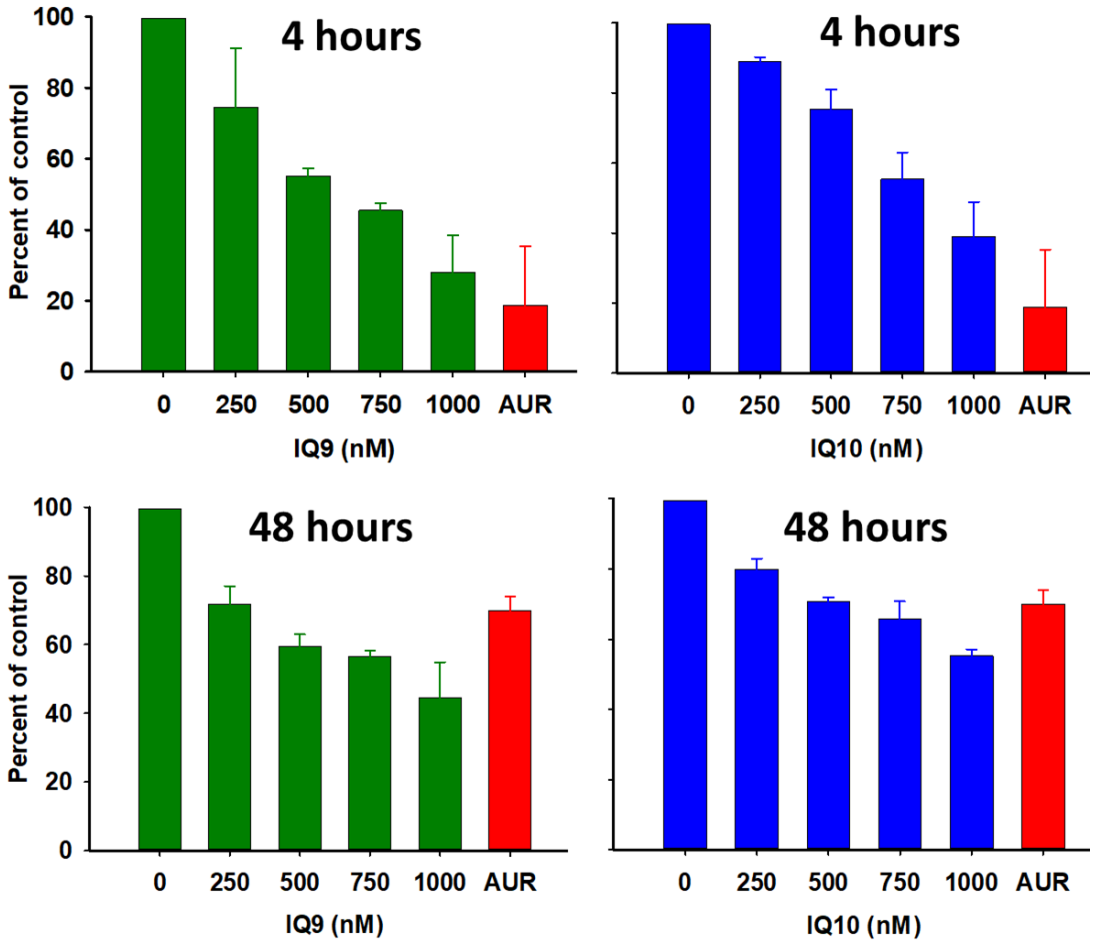


Figure 3.12: Effect of IQs on TrxR activity in PANC-1 PC cell line. PANC-1 cells treated with IQ9 (green) or IQ10 (blue) or AUR (red) for 4 or 48 hours showed a decrease, in a dose-dependent manner, in TrxR activity. TrxR enzyme activity of PANC-1 cells treated with 1000 nM of IQ9 or IQ10 or AUR for 4 hours was decreased by 72%, 61% and 81% respectively, while PANC-1 cells treated with 1000 nM of IQ9 or IQ10 or AUR for 48 hours was decreased by 55%, 45% and 30% respectively. Data represent the average of two independent experiments with a standard deviation (SD), with each experiment performed in duplicate.

As shown in Figure 3.13, BxPc-3 cells treated with IQ9 or IQ10 or AUR for 4 or 48 hours showed a dramatic decrease, in a dose-dependent manner, in TrxR activity. The activity of TrxR in BxPc-3 treated with 1000 nM of IQ9 or IQ10 or AUR for 4 hours was decreased by 98% 99% and 100% respectively, compared to control. For 48 hours' treatment, TrxR activity following treatment with 1000 nM of IQ9 or IQ10 or AUR was decreased by 94%, 74% and 95% respectively (Figure 3.13). AUR and IQs showed similar inhibitory effects in BxPc-3 cells following 4 or 48 hours' treatment.

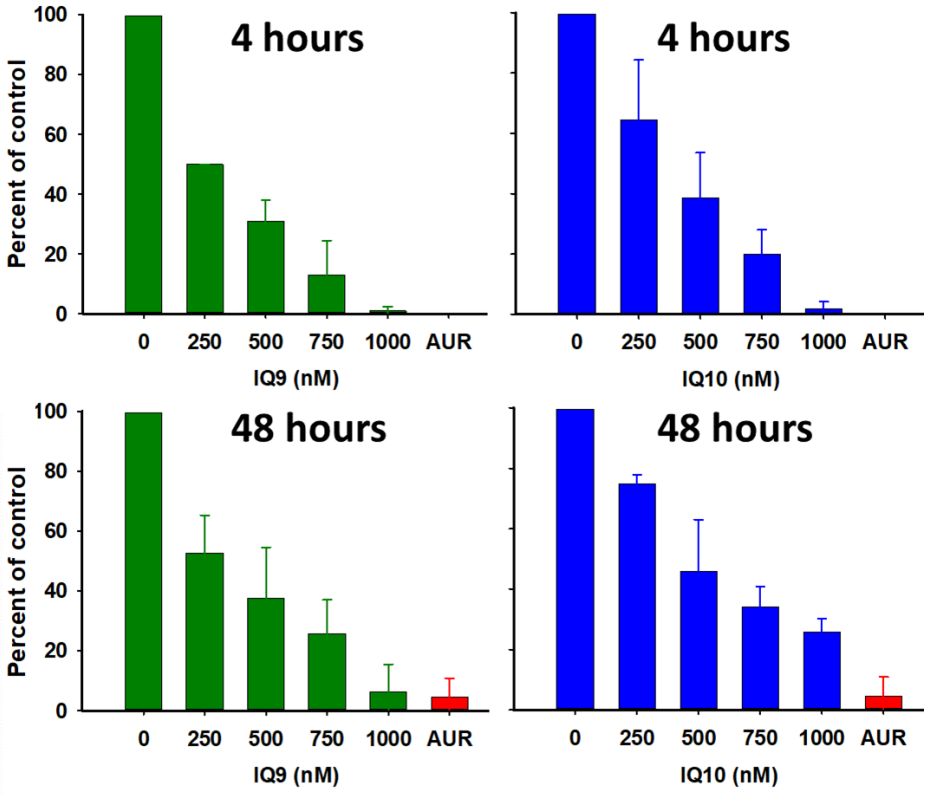


Figure 3.13: Effect of IQs on the activity of TrxR in BxPC-3 PC cells. BxPC-3 cells treated with IQ9 (green) or IQ10 (blue) or AUR (red) for 4 or 48 hours showed a dramatic decrease, in a dose-dependent manner, in TrxR activity. TrxR enzyme activity of BxPc-3 cells treated with 1000 nM of IQ9 or IQ10 or AUR for 4 hours was decreased by 98% 99% and 100% respectively compared to control, while BxPc-3 cells treated with 1000 nM of IQ9 or IQ10 or AUR for 48 hours was decreased by 94%, 74% and 95% respectively. Data represent the average of two independent experiments with a standard deviation (SD), with each experiment performed in duplicate.

3.4.4 Drug-radiation combination - clonogenic survival

The ROS level assessment of MIA Paca-2 cells treated with a combination of IQs, for 1 hour, and H_2O_2 showed approximately a 2-fold increase in ROS levels over treatment with H_2O_2 alone. Thus, an initial assessment of radiation sensitivity of MIA Paca-2 cells treated with IQ9 and IQ10 for 1 hour was performed. As shown in Figure 3.14, no radiation sensitivity was observed following the 1 hour treatment with IQ9 or IQ10, with SER values of 1.05 and 1.06 respectively. Data represent a single experiment, performed in triplicate, with no statistical analysis and SD analysis were applied (Section 2.3.9).

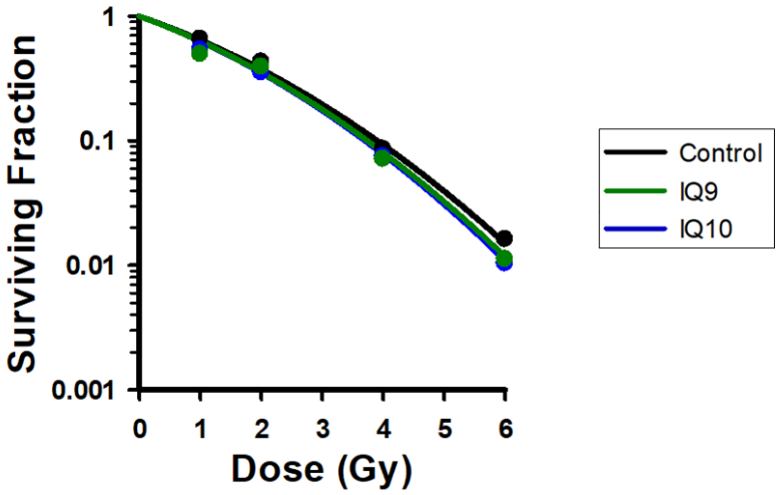


Figure 3.14: Effect of IQs on radiosensitivity of MIA Paca-2 PC cell line following 1 hour treatment. MIA Paca-2 cells were treated with IC50's of IQ9 (green) and IQ10 (blue) for 1 hour, then irradiated with a single dose of 1, 2, 4 or 6 Gy. Control is radiation alone (black). Average PE: MIA Paca-2=44%. Data represent a single experiment, performed in triplicate.

PANC-1 cells treated with AUR for 48 hours showed 30% inhibition of TrxR activity. Thus, an assessment of radiation sensitivity of PANC-1 cells treated with 1000 nM of AUR for 48 hours was performed. As shown in Figure 3.15, no radiation sensitivity was observed after 48 hour's treatment with AUR, with SER value of 1. Data represent the average of two independent experiments each performed in triplicate.

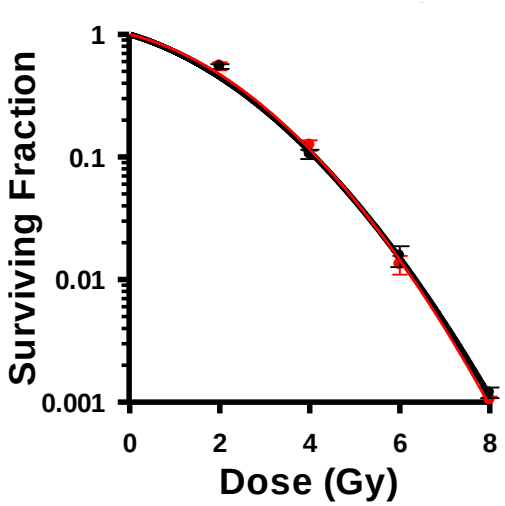


Figure 3.15: Effect of AUR on radiosensitivity of PANC-1 PC cell line following 48 hours treatment. PANC-1 cells were treated with 1000 nM of AUR (red) for 48 hours, then irradiated with a single dose of 2, 4, 6 or 8 Gy. Control is radiation alone (black). Average PE: PANC-1=28%. Data represent the mean ± standard deviation of pooled data of two independent experiments, with each experiment performed in triplicate.

As the inhibition of TrxR activity of PANC-1 cells treated with IQ9 and AUR treatments for 4 hours was substantially higher than 48 hours' treatment, radiation sensitivity of PANC-1 cells treated with the clonogenic IC50 of IQ9 (900 nM) or 1000 nM of AUR for 4 hours was assessed. As shown in Figure 3.16, a significant increase in radiosensitisation at 6 and 8 Gy was observed in PANC-1 cells treated with IQ9 (53% increase at 6 Gy ($P< 0.001$) and 71% increase at 8 Gy ($P< 0.0001$)) or AUR (36% increase at 6 Gy ($P< 0.001$) and 55% increase at 8 Gy ($P< 0.0001$)). The SER values of PANC-1 cells treated with IQ9 or AUR for 4 hours were 1.12 and 1.08 respectively. Results represent the mean ± standard deviation of three independent experiments were performed in triplicate. Although significant differences in radiosensitivity were observed, the relatively small increases in SER make the biological relevance of IQs as radiosensitisers somewhat questionable – discussed further in Section 3.5.

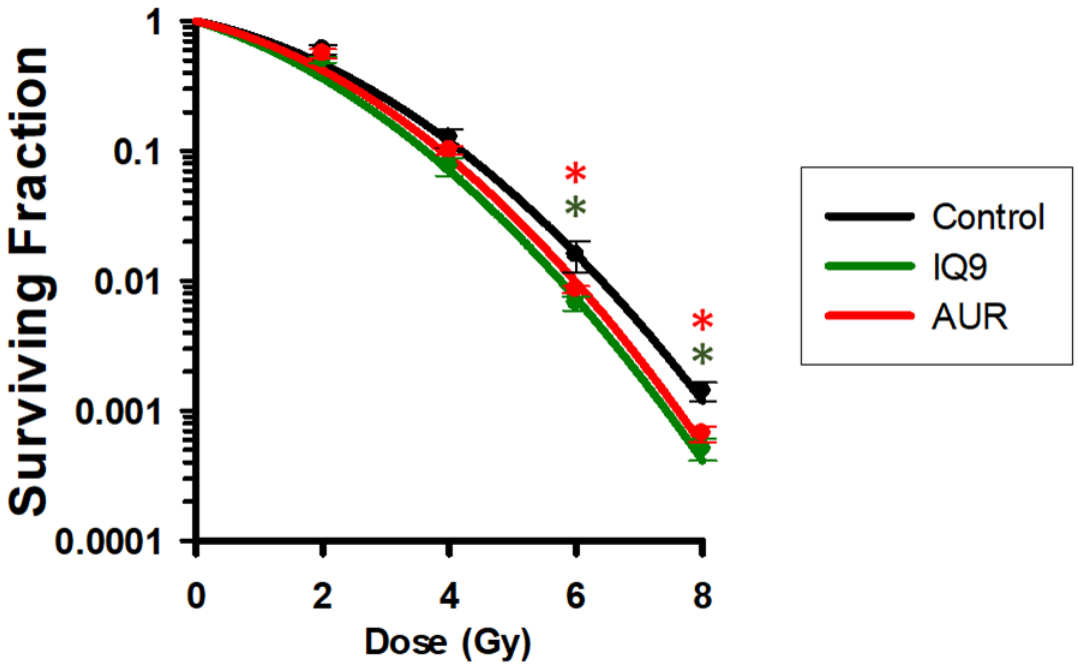


Figure 3.16: Effect of IQ9 and AUR on radiosensitivity of PANC-1 PC cell line following 4 hours treatment. PANC-1 cells were treated with the clonogenic IC50 of IQ9 (green) or 1000 nM of AUR (red) for 4 hours, then irradiated with a single dose of 2, 4, 6 or 8 Gy. Control is radiation alone (black). Average PE: PANC-1=27%. Data represent the average of pooled data of three independent experiments with a standard deviation (SD), with each experiment performed in triplicate, which are analysed using the Student T-test. * $P<0.001$

3.4.5 Influence of hypoxia on IQs cytotoxicity

3.4.5.1 Effect of hypoxia on proliferation and clonogenic survival

Effect of hypoxia on the proliferation of the PC cell lines was examined by determining the growth delay of hypoxic cells over normoxic cells as described in Section 3.3.6.1. As shown in Figure 3.17, 72 hours of hypoxic incubation caused a significant growth delay by 37% (P<0.001), 34% (P<0.001) and 36% (P<0.001) in PANC-1, MIA Paca-2 and BxPc-3 cell lines respectively, compared to normoxic cells. No significant growth delay was observed after 24 and 48 hours of hypoxic incubation. PC cell lines showed overexpression of CA9 after 24, 48 and 72 hours of hypoxic incubation, while no overexpression of CA9 in PC cells was observed after normoxic incubation. Results represent the mean ± standard deviation of three independent experiments with each experiment performed in triplicate.

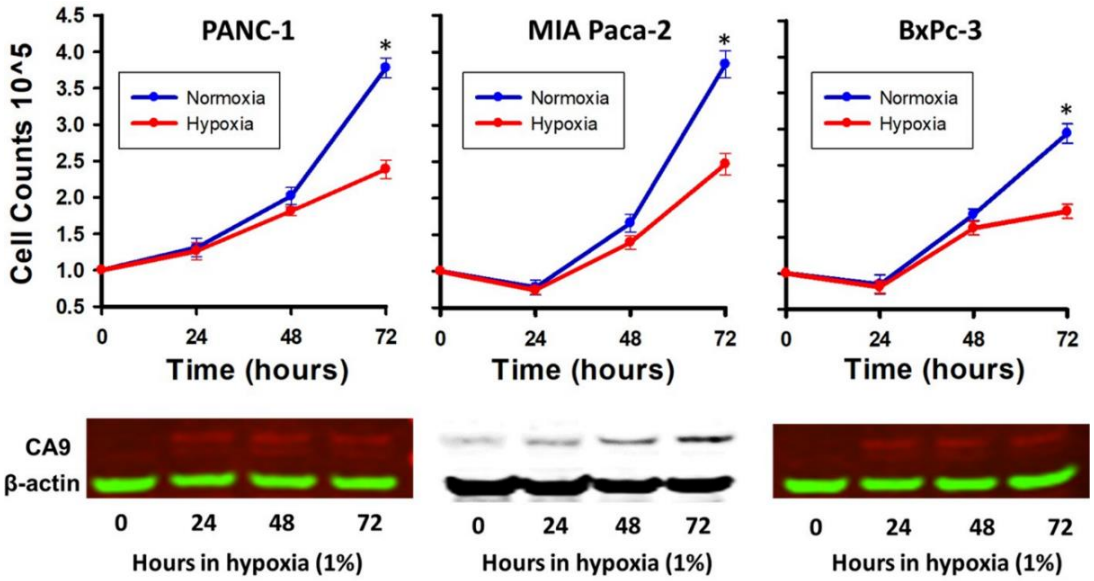


Figure 3.17: Effect of hypoxia on the proliferation of PC cell lines. PC cells were incubated in normoxia (blue) or hypoxia (red) for 24, 48 and 72 hours. Western blot image showed overexpression of CA9 in each PC cell lines at 24, 48 and 72 hours of hypoxic incubation. Results represent the average of pooled data of three independent experiments with a standard deviation (SD), with each experiment performed in triplicate, which are analysed using the Student T-test. * P<0.001

To assess the hypoxic effect on survival of PC cell lines, the remaining cells from the proliferation assay were diluted and plated for clonogenic survival as described in Section 3.3.6.1. As shown in Figure 3.18, clonogenic survival of PANC-1, MIA Paca-2 and BxPc-3 cells was decreased by 10%, 20% and 5% after 24 hours; 23%, 31% and 8% after 48 hours; 51%, 55% and 29% after 72 hours of hypoxic incubation respectively, compared to normoxic control. BxPc-3 cells seem less sensitive to hypoxia than PANC-1 and MIA Paca-2 cells. PANC-1 cells showed moderate sensitivity to hypoxia, while MIA Paca-2 cells were the most sensitive cells to hypoxia amongst the PC cell lines. Results represent the average of two independent experiments with each experiment performed in triplicate, with no statistical analysis was performed as these results came from only two experiments (Section 2.3.9). The current results of hypoxia effect on the proliferation and clonogenic survival of PC cell lines are comparable with published studies as discussed in Section 3.5.

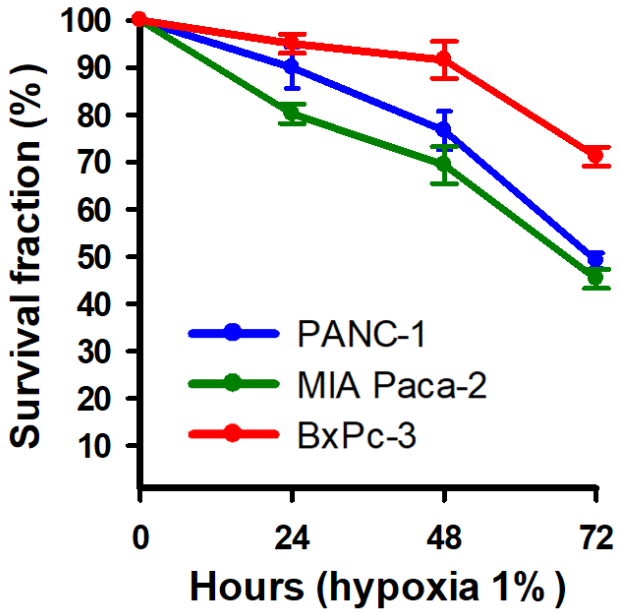


Figure 3.18: Effect of hypoxia on clonogenic survival of PC cell lines. PANC-1 (blue), MIA Paca-2 (green) and BxPc-3 (red) cells were incubated in hypoxia for 0, 24, 48 and 72 hours. Then, cells were trypsinised and plated for clonogenic survival. Results represent the average of pooled data of two independent experiments with each experiment performed in triplicate.

3.4.5.2 Effect of IQ9 on proliferation and clonogenic survival under hypoxia

As shown in Figure 3.19, proliferation of PANC-1 and BxPc-3 cells seem more sensitive to IQ9 (48 hours treatment) in hypoxia (IC50's=340 and 290 nM respectively) than normoxia (IC50's=470 and 350 nM respectively), with HCR value of 1.4 and 1.2 respectively. The positive control of each cell line under normoxic conditions was comparable with previous findings shown in Chapter 2. Thus, for each cell line, the current hypoxic results are combined with the previous normoxic results (Section 2.4.2.1) as shown in Figure 3.19. The remaining cells from each cell line were either lysed to observe the expression of CA9 hypoxic marker or plated for clonogenic survival as showed later on. For each cell line, overexpression of CA9 was observed after 72 hours of hypoxia (24 hours pre-IQ9 treatment and 48 hours post-IQ9 treatment) compared to control. Results represent the mean ± standard deviation of three independent experiments were performed in triplicate.

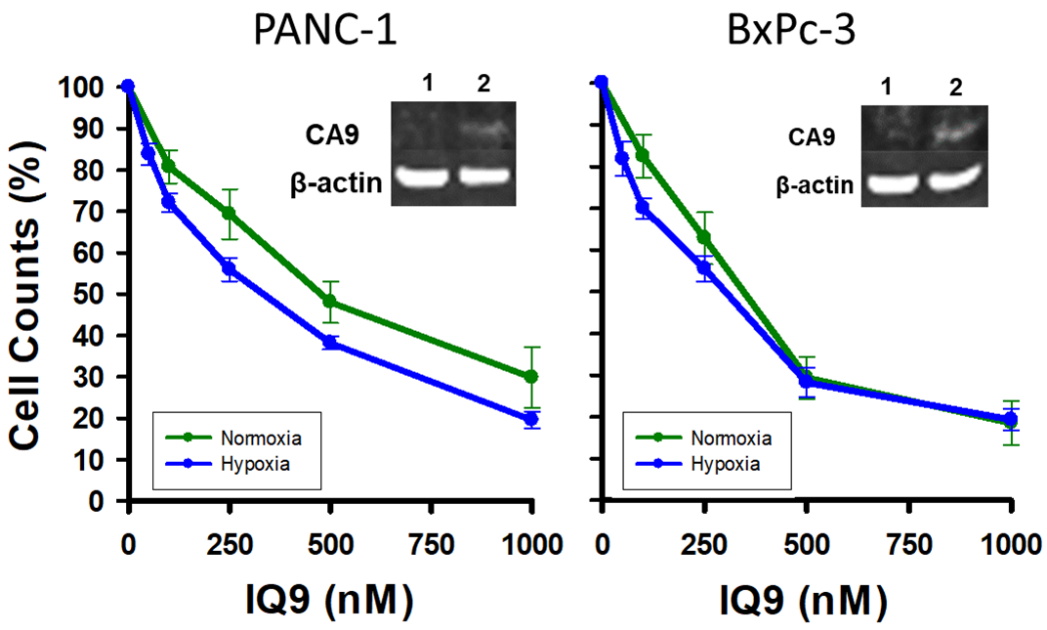


Figure 3.19: Effect of IQ9 on the proliferation of PC cell lines under hypoxic and normoxic conditions. PANC-1 and BxPc-3 cells were incubated in normoxia (green) or hypoxia (blue) for 24 hours. Then, cells were treated, in normoxia or hypoxia, with IQ9 for 48 hours. Cell counting was plotted as a percentage of control (0 nM) for each time point. For each cell line, overexpression of CA9 was observed after 72 hours of hypoxia (2) compared to normoxia (1). Results represent the mean ± standard deviation of pooled data of three independent experiments were performed in triplicate.

In terms of clonogenic survival, as shown in Figure 3.20, PANC-1 (IC50=600 nM) and BxPc-3 (IC50=640 nM) hypoxic cells seem more sensitive to IQ9 (for 48 hours treatment) compared to normoxic cells (IC50=900 nM for PANC-1 and >1000 nM for BxPc-3). The HCR value of PANC-1 treated with IQ9 for 48 hours was 1.5. The positive control of each cell line under normoxic conditions showed comparable survival fraction with previous findings in Section 2.4.2.2. Thus, for each cell line, the current hypoxic findings were combined with the previous normoxic results as shown in Figure 3.20. Results represent the average of two independent experiments with each experiment performed in triplicate, with no statistical analysis was performed as these results came from only two experiments (Section 2.3.9).

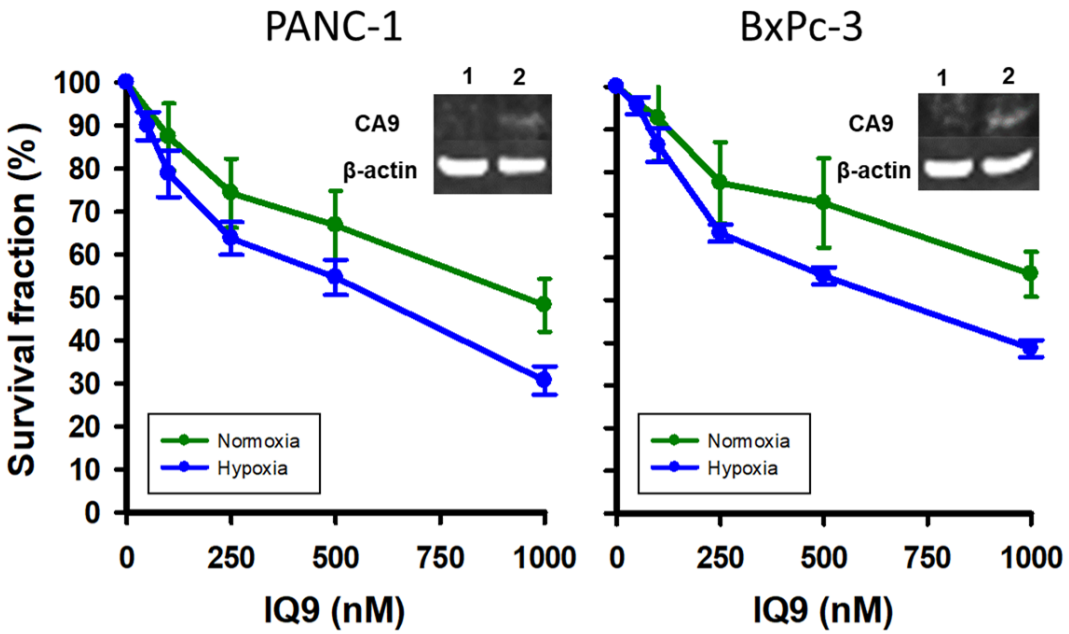


Figure 3.20: Effect of IQ9 treatment for 48 hours on clonogenic survival of PC cell lines under hypoxic conditions. PANC-1 and BxPc-3 cells were incubated in normoxia (green) or hypoxia (blue) for 24 hours. Then cells were treated, in normoxia or hypoxia, with IQ9 for 48 hours, with 0 mM as control. Then, cells were plated for clonogenic survival. For each cell line, overexpression of CA9 was observed after 72 hours of hypoxia (2) compared to normoxia (1). Results represent the mean ± standard deviation of pooled data of two independent experiments were performed in triplicate.

As described in Section 3.3.6.2, the cytotoxicity effect of IQ9 for 4 hours on PANC-1 and BxPc-3 cells under normoxic or hypoxic conditions was assessed only by the clonogenic

survival assay. As shown in Figure 3.21, PANC-1 hypoxic cells (IC50=250 nM) were more sensitive to IQ9 (for 4 hours treatment) compared to normoxic cells (IC50=610 nM). BxPc-3 hypoxic cells (IC50=440 nM) showed marginal sensitivity to IQ9 compared to normoxic cells (IC50=570 nM). The HCR values of PANC-1 and BxPc-3 treated with IQ9 for 4 hours were 2.4 and 1.3 respectively. For each cell line, overexpression of CA9 was observed after 28 hours of hypoxic condition (24 hours pre-treatment and 4 hours post-treatment with IQ9). Results represent the average of two independent experiments were performed in triplicate, with no statistical analysis was performed as these results came from only two experiments (Section 2.3.9). Although changes with HCR values are seen, the level of these changes suggests a marginal biological significance of IQs on hypoxic cell as discussed in Section 3.5.

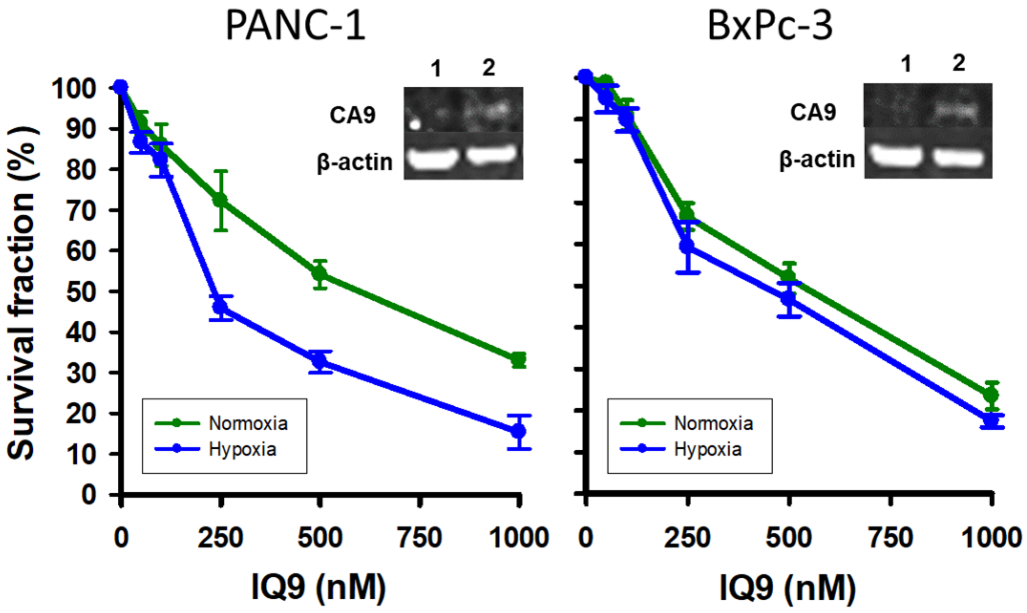


Figure 3.21: Effect of IQ9 treatment for 4 hours on clonogenic survival of PC cell lines under hypoxic and normoxic conditions. PANC-1 and BxPc-3 cells were incubated in normoxia (green) or hypoxia (blue) for 24 hours. Then, cells were treated, under normoxia or hypoxia, with IQ9 for 4 hours, with 0 mM as control. Then, cells were plated for clonogenic survival. For each cell line, overexpression of CA9 was observed after 28 hours of hypoxia (2) compared to normoxia (1). Results represent the mean ± standard deviation of pooled data of two independent experiments were performed in triplicate.

3.4.5.3 Effect of hypoxia on the expression of Trx and TrxR proteins under hypoxia

Figure 3.22 shows that hypoxia does not alter the expression of Trx and TrxR in PANC-1 or BxPc-3 cells treated with/without IQ9 for 4 or 48 hours. Furthermore, current results confirmed the previous ones, in Section 3.4.2.2, that showed a significant inhibition of Trx expression in BxPc-3 cells treated with IQ9 for 48 hours, with no effect after 4 hours' treatment.

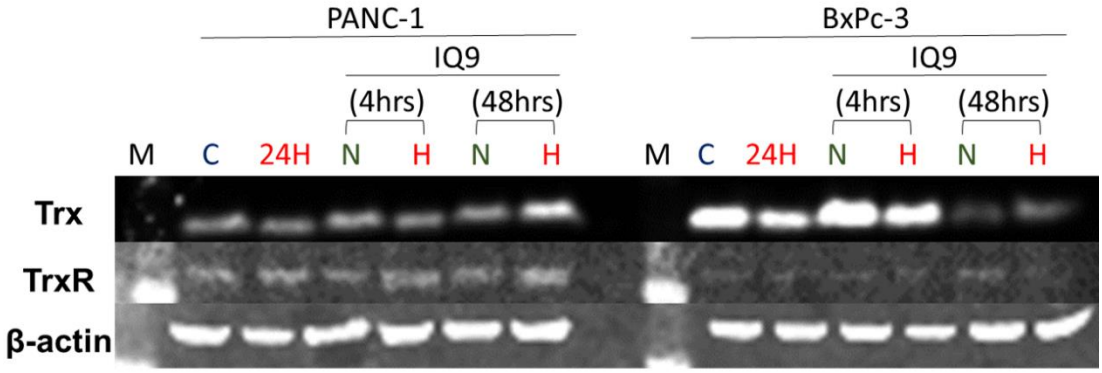


Figure 3.22: Effect of hypoxia on the expression of Trx and TrxR proteins in PC cell lines under hypoxic conditions. PANC-1 and BxPc-3 cells were treated with IQ9 for 4 or 48 hours either under normoxic or hypoxic conditions. Results showed that hypoxia does not alter the protein expression of Trx and TrxR after IQ9 treatment. Abbreviations; M=marker, C=control, 24H=cells incubated for 24 hours in hypoxia, N=normoxia, H=hypoxia.

3.4.5.4 Effect of IQ9 on the expression of NQO1 and CPR proteins under hypoxic and normoxic conditions

By using the same lysates of PANC-1 and BxPc-3 cells from Section 3.4.5.3, the effect of IQ9 on the expression of NQO1, CPR and CA9 proteins in PC cell lines under hypoxic and normoxic conditions was assessed. As shown in Figure 3.23, overexpression of CA9 was observed in hypoxic samples. PANC-1 and BxPc-3 cells showed lack and moderate endogenous expression of NQO1 protein respectively, with no effect of hypoxia or IQ9 treatment on altering the endogenous expression of NQO1 in both cell lines. The CPR protein was endogenously expressed in both cell lines, with no effect of hypoxia or IQ9 treatment on altering the endogenous expression of CPR. Some experimental errors

(e.g. air bubbles) occurred during protein transferring procedure that caused unreliable results of some proteins - these errors are marked with red circles in Figure 3.23.

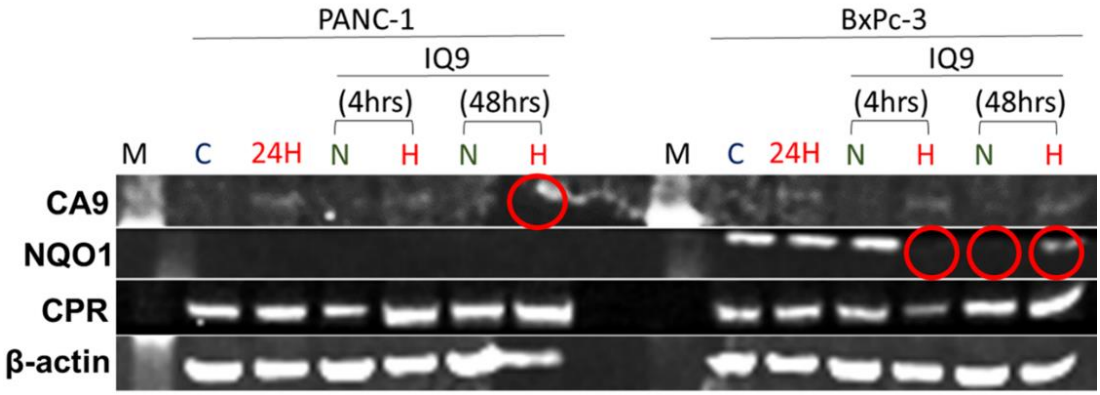


Figure 3.23: Effect of IQ9 on the expression of CPR and NQO1 proteins in PC cell lines under normoxic and hypoxic conditions. PANC-1 and BxPc-3 cells were treated with IQ9 for 4 or 48 hours either under normoxic or hypoxic conditions. Results showed no effect of hypoxia or IQ9 treatment on altering the endogenous expression of both NQO1 and CPR proteins. Red circles represent unreliable results due to experimental errors. Abbreviations; M=marker, C=control, 24H=cells incubated for 24 hours in hypoxia, N=normoxia, H=hypoxia.

In conclusion, IC50 doses combined with subsequent H_2O_2 exposure increased the oxidative stress ~2 fold in PC cells over treatment with H_2O_2 alone. IQs seem to have no effect on the expression of TrxR proteins and reductase enzymes. However, IQs are more effective at inhibiting TrxR activity in PC cell lines, with 4 hours' treatment giving greater inhibition than 48 hours' treatment. A significant increase in radiosensitisation was observed in PANC-1 cells treated with IQ9, but with low SER values. Hypoxic PC cell lines seem more sensitive to IQ9 than normoxic cells, but with low HCR values. The small increase in SER and HCR values in PC cell lines following IQs treatment making the biological relevance of IQs as potentials radiosensitisers or hypoxic cytotoxins becomes somewhat questionable as discussed in Section 3.5.

3.5 Discussion

To explore potential factors involved in regulation of radiosensitivity of PC cell lines treated with IQs, different mechanisms were examined including assessment of oxidative stress via intracellular ROS levels, and of TrxR activity following IQs treatment. The current chapter also studied effect of IQs, under hypoxic and normoxic conditions, on the expression of Trx system proteins, protein expression of reductase enzymes, proliferation and survival of PC cell lines.

Inhibiting the redox system allows accumulation of ROS molecules, resulting in DNA oxidative damage, compromising protein structure and causing lipid peroxidation (Section 1.2.1.1). As the Trx system is a main family of redox proteins, inhibiting it by targeting TrxR could increase ROS levels in PC cells. Therefore, assessment of ROS levels of PC cells treated with IQs was an important parameter to evaluate the mechanisms behind the inhibitory and cytotoxic effects of IQs. The treatment with IQs alone aimed to examine the ability of IQs to induce oxidative stress when delivered as single agent. The combination of IQs with H_2O_2 examined the ability of the PC cells to cope with oxidative stress following drug treatment. H_2O_2 was used as an alternative to radiation to cause oxidative stress in PC cells due to its stability compared with other ROS molecules, such as $OH^{\bullet}$, produced by the radiolysis of cellular water. The hydroxyl radical is one of the main ROS molecules resulting from the indirect effect of radiation, and responsible for two-thirds of the x-ray damage to DNA in mammalian cells (Eric J. Hall, 2012). However, $OH^{\bullet}$ molecules resulted from cell irradiation are not detectable by conventional flow cytometry due to the very short biological half-life and high reactivity with any biological molecule as it can abstract a hydrogen atom ($OH^{\bullet}$ has a lifespan less that one second (10^{-9} seconds)) (Eric J. Hall, 2012). H_2O_2 is widely used as an inducer of oxidative stress. Although some studies (Luo et al., 2013, Cho et al., 2015) have used a combination of radiation and radiosensitiser to demonstrate overproduction of ROS molecules detected by flow cytometry, this combination may be fundamentally flawed. However, recent studies suggested that quantification of cellular oxidative stress can be

conducted by other means, such as protein carbonyl quantification (Suzuki et al., 2010, Fedorova et al., 2014), which set as a future plan for the current project as discussed in Chapter 5.

An initial optimisation was performed to evaluate the potency of H_2O_2 against PC cell lines and MDA-MB BC cells (Section 3.4.1). The results suggest that PC cell lines are substantially more sensitive to H_2O_2 (IC50=40 mM for PANC-1, IC50=30 mM for MIA Paca-2 and IC50=30 mM for BxPc-3) than MDA-MB-231 BC cells (IC50=100 mM). Current results are comparable to a study examining the effect of H_2O_2 resulting from the oxidation of pharmacological concentrations of ascorbate that inhibited viability in certain cancer cell lines. The study showed that BC cell lines, including MDA-MB-231 cells, were less sensitive to ascorbate among 5 different cancer cell lines including lymphoma, melanoma, kidney, lung and colorectal cancer cell lines (Chen et al., 2005). Five years later, another study investigated, for the first time, the cytotoxic effect of pharmacological ascorbate on PC cell lines (Du et al., 2010). The study showed that 10 mM of ascorbate for 1 hour caused 85% decrease in cell viability of both MIA Paca-2 and BxPc-3 cells, assessed by the MTT assay, while current results showed that 50 mM of H_2O_2 for 1 hour caused 88% and 86% decreased in cell viability of MIA Paca-2 and BxPc-3 cell line respectively, using a cell counts based assay. The direct cytotoxic effect of H_2O_2 against PC cell lines does not seem to have been previously studied. However, the difference between our findings and the previous study may be due to the different methods to assess cytotoxicity (direct cytotoxicity of H_2O_2 using the cell counting assay vs cytotoxicity of H_2O_2 resulting from ascorbate oxidation using the MTT assay).

A previous study used 1 mM of H_2O_2 in ROS level assessment in MDA-MB-231 cells, and showed more than a 4-fold induction of ROS over control (Zhang, 2014). In PC cells, two concentrations of H_2O_2 (0.3 for MIA Paca-2 and BxPc-3 cells and 0.4 mM for PANC-1 cells) were selected for ROS levels assessment in PC cells. The selection of these two concentrations was for two main reasons. Firstly, initial experiments showed that any concentration higher than 0.4 mM of H_2O_2 was dramatically toxic to cells, and produced insufficient number of cells to run the experiment (10,000 cells required for each run).

Although the IC50's of H_2O_2 for the PC cell lines were between 30 and 40 mM, the dramatic toxicity at 0.3-0.4 mM of H_2O_2 following the 10 minutes of centrifugation, required for the FACS analysis, is still unknown. However, the physical stress caused by centrifugation for 10 minutes seems to increase ROS levels in mammalian cells (Shekarriz et al., 1995, Kim et al., 2013), and this may contribute to the dramatic cell killing of PC cells following H_2O_2 treatment. Secondly, a previous study used 1 mM of H_2O_2 to induce ROS level more than 4-fold over control in MDA-MB-231 cells (Zhang, 2014); the concentration of 1 mM represents 1% of the cytotoxic IC50 value of H_2O_2 against MDA-MB-231 cells (IC50=100 mM). In PC cell lines, the selected concentrations of 0.4, 0.3 and 0.3 mM of H_2O_2 represent 1% of the cytotoxic IC50 values of H_2O_2 against PANC-1 (IC50=40 mM), MIA Paca-2 (IC50=30 mM) and BxPc-3 (IC50=30 mM) cells respectively.

To explore the impact that inhibiting the cells ability to deal with oxidative stress might have on radiation sensitivity, PC cell lines were treated with IC50 values of IQs, with/without H_2O_2, for 48 hours, which is the same concentration and time treatment that used to assess the effect of IQs on radiation sensitivity, as discussed in Chapter 2. Additionally, treatment times of 1, 4 and 24 hours were added to the ROS assessment of PC cells. The effect of IQs (analogues of ES396) on the ROS levels of PC cell lines has never been previously studied. Current findings (Section 3.4.1) show that PC cell lines treated with IC50's of IQs alone showed a marginal increase (<25%) in ROS levels over control, whilst PC cells treated with IQs then exposed to oxidative stress, caused by H_2O_2 exposure, showed approximately a 1.5-2.3-fold increase over treatment with H_2O_2 alone. The increase, albeit marginal, in ROS levels following treatment with IQs alone may be due to the inhibitory effect of IQs on TrxR expression/activity of PC cells, as discussed later, or to expression of another redox system, such as the GSH system, that could compensate for the inhibition of the Trx system as discussed in Chapter 5.

Current findings of the ~1.5-fold increase in ROS levels in PANC-1 cells treated with IC50 of IQs for 48 hours in combination H_2O_2 may explain the ~50% increase in radiosensitivity

of PANC-1 cells treated with IC50's of IQs at 6 Gy (as shown in Chapter 2). Current data prove the first hypothesis of this chapter, and show that IQs treatment impairs PC cells' ability to maintain oxidative stress.

As MCF-7 and MDA-MB-231 BC cells have been well-studied in the literature, in terms of studying the Trx system in cancer cells (Berggren and Powis, 2001, Farina et al., 2011, Sun et al., 2012, Zhang, 2014), both cell lines were used as positive controls in this project. In both cell lines, current data (Section 3.4.2.1) show low endogenous expression of TrxR and TxNIP, while the endogenous expression of Trx was expressed. The current findings are comparable to published studies; two studies showed that MDA-MB-231 cells exhibited lack endogenous expression of TxNIP, while Trx was expressed (Turturro et al., 2007, Farina et al., 2011). Another two findings showed that Trx was expressed in MCF-7 cells (Berggren and Powis, 2001, Sun et al., 2012), whilst, in another, Trx was expressed at low levels (Hsieh et al., 2010). In contrast to the current BC findings, a previous study showed that the endogenous protein expression of Trx, TrxR and TxNIP was expressed in MCF-7 and MDA-MB-231 BC cells (Zhang, 2014). For PC cell lines, current data (Section 3.4.2.1) showed that the endogenous expression of Trx in BxPc-3 cells was higher than MIA Paca-2 ($P=0.055$) and PANC-1 ($P=0.179$) cells, while the endogenous expression of TrxR in BxPc-3 cells was significantly lower than PANC-1 ($P=0.008$) and MIA Paca-2 ($P=0.036$) cells. The endogenous expression of TxNIP of PANC-1 cells was lower than BxPc-3 ($P=0.007$) and MIA Paca-2 ($P=0.057$) cells. The current data can be compared with two studies showing low endogenous expression of Trx in PANC-1 and MIA Paca-1 cells (Zhang et al., 2012), and one in which TxNIP was expressed in MIA Paca-2 cells (Baker et al., 2008), whilst, in contrast to our findings, BxPc-3 exhibited low expression of Trx (Pramanik and Srivastava, 2012).

As shown in Section 3.4.2.2, MIA Paca-2 and PANC-1 cells treated with IQs for 48 hours showed no alteration in the protein expression of Trx, TrxR and TxNIP, whilst BxPc-3 cells treated with IC50's of IQ9 ($P=0.014$) or IQ10 ($P=0.01$) for 48 hours showed a significant decrease in Trx expression, with no effect on the expression of TrxR and TxNIP compared to control. The effect of IQs (analogues of ES396) on the endogenous expression in PC

cell lines has never been studied. However, MIA Paca-2 cells treated with two analogues of ES396 (IQ1 and IQ2) for 1 hour exhibited an increase in oxidised Trx expression and a decrease in reduced Trx expression, compared to control, using native protein gel electrophoresis to separate both proteins (Yan et al., 2012). As current results showed that IQs have little, if any, effect on the expression of TrxR in PC cells, the effect of IQs on the enzyme activity of TrxR was determined.

Current data (Section 3.4.3) shows that PANC-1 cells treated with 1000 nM of IQs for 4 hours strongly inhibits TrxR activity (61-72%) compared to treatment for 48 hours (45-55%), suggesting that it would be more appropriate to assess the effect IQs on radiation sensitivity after 4 hours' treatment. However, TrxR activity of BxPc-3 cells treated with IQs for 4 or 48 hours was dramatically decreased compared to PANC-1 cells yet with no effect on radiosensitivity - discussed later. Only two studies have investigated the effect of the new generation of IQs (analogues of ES396) on PC cells. The first study showed 99% and 95% of TrxR inhibition in MIA Paca-2 cells after 4 hours' treatment with 1000 nM of IQ3 and IQ9 respectively (Yan et al., 2009). In the second study, MIA Paca-2 cells treated with 1000 nM of IQ1 and IQ9 for 1 hour exhibited inhibition in TrxR activity by 90% and 95% respectively (Yan et al., 2012). Although current results did not investigate 1 hour, the effect of IQ9 on the TrxR activity of MIA Paca-2 cells, PANC-1 and BxPc-3 cells treated with IQ9 for 4 hours showed 94% and 98% decrease in TrxR activity respectively, which is comparable between both studies. The second hypothesis of the current chapter (IQs treatment inhibits the protein expression and activity of TrxR in PC cell lines in a dose-and time-dependent fashion) was disproven in terms of protein expression and was proven in terms of TrxR activity.

Current results (Section 3.4.4) show that PANC-1 cells treated with IQ9 (900 nM) for 4 hours exhibited 53% and 71% increase in radiosensitivity at 6 and 8 Gy respectively, with SER value of 1.12, whilst, as shown in Chapter 2, treatment with IQ9 for 48 hours showed 47% increase in radiosensitivity at 6 Gy, with SER value of 1.08. The marginal increase in PANC-1 radiosensitivity treated with IQ9 for 4 hours (Figure 3.16) over 48 hours (Figure 2.13) may be due to the marginal increase in the inhibition of TrxR activity after

treatment with IQ9 for 4 hours over 48 hours (Figure 3.12). Current data suggest determining the stability (half-life) of IQ9 in cell culture medium as discussed later in Chapter 5.

Although the radiosensitivity in PANC-1 cells treated with IQs for 4 or 48 hours was significant, the SER values are rather low (1.08-1.12), making the biological relevance of IQs as radiosensitisers somewhat questionable. As shown in Chapter 2, IQs exhibited a marginal increase in radiosensitivity of BxPc-3 cells although results of BxPc-3 cells in the current chapter showed that IQ9 exhibited a significant decrease in Trx expression, a dramatic decrease in TrxR activity and a 2-fold increase in ROS levels. The limited effect of IQs on radiosensitisation on BxPc-3 cells may be due to the low endogenous expression of TrxR in BxPc-3 cells or to the low IQs concentration ~~has~~ used (500 nM) to assess the radiosensitivity (clonogenic IC50's value of IQs for BxPc-3 cells is >1000 nM).

In summary, exposing PC cell lines to IQs for 4 hours can slightly increase the radiosensitive effect of IQs on PC cell lines compared to 48 hours' treatment, which somewhat proves the third hypothesis of the current chapter (using the appropriate concentration and exposure time of IQs, radiosensitive effect of IQs on PC cell lines can be maximised). Unfortunately, no substantial increase in radiation sensitivity in PC cells treated with IQs was observed. Many reasons may involve to such findings including insufficient inhibition of TrxR activity by IQs, expression of another redox system, such as the GSH system, low endogenous level of the enzyme (TrxR) or the substrate (Trx) in certain PC cells or to other potential reasons as discussed in Chapter 5.

AUR, as a single agent or combined with H_2O_2, showed no effect on altering ROS levels in PC cell lines (Section 3.4.1). PANC-1 cells treated with 1000 nm of AUR for 48 hours showed low inhibition of TrxR activity (30%) and no increase in ROS levels, which may explain the lack of radiation sensitivity in PANC-1 cells after AUR treatment for 48 hours (SER=1) (Section 3.4.4). Although PANC-1 cells treated with AUR for 4 hours showed no increase in ROS levels, they exhibited high inhibition of TrxR activity (81%), with a significant radiosensitisation at 6 and 8 Gy but with low SER value (SER=1.08). Such

results are comparable to a recent study that showed a significant inhibition in TrxR activity in murine mammary adenocarcinoma EMT-6 and 4T1 cells treated with 1000 nM of AUR for 2 hours, with no significant increase in ROS levels of both cell lines (Wang et al., 2017a). In the same study, a significant ROS overexpression in both cell lines was detected only after 7500 nM of AUR for 2 hours, with a significant increase in radiation sensitivity (SER>2). However, the current study uses much lower concentrations of AUR (1000 nM) than the previous study. In contrast to the current results, MIA Paca-2 cells treated with 1000 nM of AUR for 1 hour caused only 55% inhibition of TrxR activity (Yan et al., 2012), while current findings show that PANC-1 and BxPc-3 cells treated with 1000 nM of AUR for 4 hours showed 81% and 100% inhibition of TrxR activity respectively.

Initial optimisations were performed to examine the effect of hypoxia alone on proliferation and clonogenic survival of PC cell lines. Current findings (Section 3.4.5.1) show that 72 hours of 1% O_2 caused a significant growth delay by 37%, 34% and 36% in PANC-1, MIA Paca-2 and BxPc-3 cell lines respectively, compared to the growth of normoxic cells. No significant growth delay was observed in any of the PC lines at 24 or 48 hours of hypoxic incubation. Hypoxic incubation of PANC-1, MIA Paca-2 and BxPc-3 showed a decrease in clonogenic survival by 51%, 55% and 29% after 72 hours respectively, compared to normoxic cells.

Hypoxia has been reported to induce growth inhibition but not cell death of PC cells, including MIA Paca-2 cells (Akakura et al., 2001). Different cancer cell line types show different proliferation responses to hypoxic incubation. D566 and U251 glioblastoma cancer cell lines exhibited stability in cell viability after 24 and 48 hours of hypoxic incubation. However, the growth delay of both cell lines was observed only after 72 hours of hypoxic incubation (Richards et al., 2016), which is comparable to our findings. In the same study, U87 glioblastoma cancer cell line showed stability in proliferation up to 96 hours of hypoxic incubation. MCF-7 and MDA-MB-231 BC cells were resistant to hypoxia, with no growth delay was observed up to 72 hours of hypoxic incubation (Huang et al., 2017). The current results of the effects of hypoxia on the proliferation of PC cell lines are comparable to published studies.

Hypoxic PANC-1 cells seem slightly more sensitive to IQ9 at 48 hours than normoxic cells, with an HCR value of 1.4, while BxPc-3 cells treated with IQ9 for 48 hours showed less sensitivity to hypoxia, with an HCR value of 1.2 (Section 3.4.5.2). No proliferation assay was conducted after 4 hours' treatment with IQ9 since IQ9 with/without hypoxia was not expected to induce cell death due to the short time of treatment. In terms of clonogenic survival, PANC-1 and BxPc-3 hypoxic cells treated with IQ9 for 48 hours seem more sensitive to IQ9 compared to normoxic cells, with PANC-1 HCR value of 1.5 (HCR value of BxPc-3 cells is not available as clonogenic IC50 value of IQ9 for BxPc-3 cells in normoxic conditions was not observed (IC50>1000 nM)). Following 4 hours treatment, PANC-1 hypoxic cells showed increased sensitivity to IQ9 compared to normoxic cells, with an HCR value of 2.4, while BxPc-3 hypoxic cells exhibited a smaller increased sensitivity compared to normoxic cells, with an HCR value of 1.3. Although increased hypoxic sensitivity is seen, the biological significance of the level of change, as with SER's, may be marginal.

The effect of the new generation of IQs (analogues of ES396) on the cytotoxicity of PC cell lines in hypoxia has never been studied. However, comparing to EO9, our findings were relevant to a study that showed MDA-MB-231 cells treated with EO9 for 3 hours achieved a HCR value of 4 (Saunders et al., 2000), while the highest a HCR value in the current data is 2.4. It is important to note that EO9 hypoxia sensitisation is very dependent on the types of the cancer cell line and the level of reductases enzymes expressed endogenously or induced by hypoxia (Robertson et al., 1994). Nevertheless, HCR values achieved by IQ9 or EO9 are much lower than a well-characterised bioreductive drug such as achiral phosphoramidate mustards (Duan et al., 2008). The analogues of achiral phosphoramidate mustards against HT29 colorectal and H460 lung cancer cell lines can achieve clonogenic HCR values of 200 and 300 respectively.

In the clonogenic assay (Section 3.4.5.2), as shown in Table 3.3, IQ9 seem more effective on PC cell lines given short exposures (4 hours) than longer treatment times (48 hours) either under normoxic or hypoxic conditions.

	IC50 value of IQ9 in normoxia (nM)		IC50 value of IQ9 in hypoxia (nM)	
Cel line/ treatment time	PANC-1	BxPc-3	PANC-1	BxPc-3
4 hours	610	570	250	440
48 hours	900	> 1000	600	640

Table 3.3: Clonogenic IC50 values of IQ9 for PANC-1 and BxPc-3 in normoxic and hypoxic conditions.

In contrast to the current findings, MIA Paca-2 and BxPc-3 cells treated with IQs (analogues of ES396) for 72 hours showed high inhibition of clonogenic survival compared to treatment for 4 hours (Yan et al., 2009). In the previous study, the estimated clonogenic IC50 value of IQ9 for BxPc-3 cells were 70 and 10 nM after 4 and 72 hours' treatment respectively, while in the current findings, the IC50 values of IQs for BxPc-3 cells were 570 and >1000 nM after 4 and 48 hours' treatment respectively. The reasons for the substantial differences in the IC50 values between the current findings and the previous study are unknown. However, it is important to note that protocols used to assess clonogenic survival in both studies are different, which may somewhat affect the results; the previous study plated 800 cells (fixed number) in complete medium into 100-mm tissue culture plates and allowed to attach for 16 hours. Then, cells were exposed to IQs for 4 or 72 hours. The medium was then replaced with fresh medium and cells incubated at 37°C for only 10 days. In summary, as shown in Table 3.3, hypoxia increases, albeit slightly, the cytotoxic efficacy of IQs on PC cell lines, which proves the fourth hypothesis of the current chapter (hypoxia increases the cytotoxic efficacy of IQs on PC cell lines).

Hypoxia seems to have little/no effect on altering expression of Trx or TrxR protein in PANC-1 cells treated with IQ9 for 4 or 48 hours (Section 3.4.5.3). Furthermore, PANC-1 cells exhibited lack of the endogenous expression of NQO1, while the endogenous level of CPR was expressed either in normoxic or hypoxic conditions. No alteration of the endogenous expression of NQO1 or CPR after IQ9 treatment was observed.

As shown previously in Section 3.4.5.2, PANC-1 showed an increase in sensitivity to IQ9 in hypoxia compared to normoxia. Current findings were comparable with EO9 studies that showed EO9 was selectively cytotoxic, under hypoxic conditions, only against the cancer cell lines that lacked expression of NQO1 (e.g. PANC-1 cells), suggesting that the one-electron reductases such as CPR and xanthine oxidase play a critical role in the hypoxia selectivity of bioreductive drugs (Robertson et al., 1992, Plumb et al., 1994a, Plumb et al., 1994b). Four studies were comparable to the current findings; three studies showed a lack endogenous expression of NQO1 in PANC-1 cells (Mayor-López et al., 2014, Probst et al., 2015, Hong et al., 2010), while a single study showed that the endogenous expression of CPR in PANC-1 cells was well expressed (Koliopanos et al., 2002).

NQO1 and CPR were expressed in BxPc-3 cells in both normoxic and hypoxic conditions, with no alteration of the endogenous expression of NQO1 or CPR after IQ9 treatment (Section 3.4.5.4). As shown previously, BxPc-3 hypoxic cells showed marginal sensitivity to IQ9 compared to normoxic cells. Current findings were comparable with EO9 studies that showed low cytotoxic effect of EO9 on NQO1-rich cell lines (e.g. BxPc-3 cells) under hypoxic conditions (Workman, 1994). A recent study confirms current data and showed high endogenous expression of NQO1 in BxPc-3 cells (Mayor-López et al., 2014), while another study exhibited lack expression of NQO1 (Probst et al., 2015). Two studies have shown that CPR is expressed in BxPc-3 cells (Dehn et al., 2006, Borowa-Mazgaj et al., 2017). The expression of the reductases enzymes has never been studied on PC cell line treated with the analogues of ES396. However, a study showed that the parent drug (ES396) showed no effect on the expression of NQO1 in BxPc-3 and MIA Paca-2 cells, which is comparable to our findings (Dehn et al., 2006). In summary, IQs showed no substantial hypoxic sensitisation against PC cell line, suggesting to determine the activity of reductase enzymes, assess the expression/activity of another redox system (e.g. GSH system) and evaluate the stability of IQ9 in cell culture medium in normoxic/hypoxic conditions. These assays, which set as future work in Chapter 5, may explain the marginal hypoxic sensitisation of IQs against PC cell lines.

In conclusion, TrxR may be a useful potential target in PC. IQs showed no effect on the expression of TrxR across all PC cell lines, with significant inhibition of Trx expression in BxPc-3. However, IQs seem to inhibit TrxR activity in PC cell lines, with 4 hours' treatment giving greater inhibition than 48 hours' treatment. IQs doses combined with subsequent H_2O_2 exposure were significantly increased the oxidative stress a 1.5-2.3 fold in PC cell lines compared with H_2O_2 treatment alone. PANC-1 cells treated with IQ9 or AUR for 4 hours showed higher radiosensitisation than 48 hours' treatment but with low SER values. Furthermore, PANC-1 and BxPc-3 hypoxic seem to be more sensitive to IQ9 compared to normoxic cells. IQ9 showed no effect on the expression the Trx system proteins or reductases enzymes under hypoxic conditions. IQ9 was more potent, under hypoxic conditions, in cells with lack expression of NQO1, such as PANC-1 cells, than NQO1-rich cell lines, such as BxPc-3 cells. Therefore, PANC-1 cell line seems to be a good target for any further radiosensitisation studies in hypoxic conditions.

Chapter 4: Thioredoxin system protein expression in carcinomas of the pancreas, bile duct and ampulla

4.1 Abstract

Background: The activity of redox proteins plays an important role in regulating the radioresponse and chemoresponse of tumour cells in both *in vitro* tissue culture and *in vivo* tumour models. Several studies suggested that expression of redox proteins, including the Trx system, in cancer is correlated with the prognosis of cancer treatment. The current chapter investigates the relationship of Trx system redox protein expression with clinicopathological variables and clinical outcome of patients with pancreatic, bile duct and ampullary cancers.

Methods: The expression of Trx, TrxR and TxNIP was assessed in two cancer patient cohorts using immunohistochemistry (IHC) on tissue microarrays. The first cohort was composed of 85 pancreatic adenocarcinomas (PAD) and the second cohort was composed of 145 cancers of the bile duct and ampulla.

Results: In the PAD cohort, high cytoplasmic TrxR expression was significantly associated with lymph node metastasis (P=0.033). High expression of cytoplasmic (P=0.018) and nuclear (P=0.006) Trx were significantly associated with better overall survival, with nuclear Trx expression remaining significantly associated with survival in multivariate Cox-regression (Hazard Ratio (HR)=0.316; 95% Confidence Interval (95% CI)=0.174-0.573; P<0.0001) when potentially confounding factors were included (gender, age, tumour size, tumour grade, tumour stage, lymph node status, perineural and venous invasion).

In cancers of the bile duct and ampulla, high expression of nuclear TrxR (P=0.024) and high cytoplasmic TxNIP (P=0.049) were associated with patients aged above 60 years. Associations were also observed between high nuclear TrxR expression and the presence of venous (P=0.001) and perineural (P=0.021) invasion. Low cytoplasmic TxNIP expression was also associated with the presence of perineural invasion (P=0.025). High expression of cytoplasmic TxNIP was significantly associated with better overall survival (P=0.0002), which remains significant in multivariate Cox-regression analysis (HR=0.548;

95% CI=0.340-0.882; P=0.013) when potentially confounding factors were included (tumour grade, stage, lymph node status, perineural and venous invasion). Further analysis showed that low nuclear with high cytoplasmic (low nuclear/high cytoplasmic) expression of Trx showed longer overall survival than the other three subgroups (low nuclear/low cytoplasmic, high nuclear/low cytoplasmic and high nuclear/high cytoplasmic) expression; either against each separate subgroup (P=0.017) or when the three subgroups were combined together (P=0.002).

Conclusion: Current findings show that the Trx family protein expression can be used prognostically in patients with pancreatic, bile duct and ampullary cancers, and may influence cancer cell susceptibility to anticancer agents. The findings of this chapter warrant a larger follow-up study.

4.2 Introduction, hypothesis and aims

As shown in previous chapters, the Trx system plays an important role in regulating cell growth, proliferation, apoptosis and redox homeostasis. Numerous studies showed that the activity of redox proteins play an important role in regulating the radioresponse and chemoresponse of tumour cells in both *in vitro* tissue culture and *in vivo* tumour models, and suggested that expression of redox proteins in cancer is correlated with the outcome of cancer treatment. Results of Chapter 3 showed that the Trx system may be a useful potential target in PC. The current chapter investigates the relationship of Trx system protein expression with clinicopathological variables and clinical outcome of patients with pancreatic, bile duct and ampullary cancers.

4.2.1 Role of expression of redox proteins in clinicopathological criteria and clinical outcome of cancer patients

The distribution of redox proteins, including the Trx system, between normal and cancer tissues has been widely studied. Cullen and colleagues showed that cytoplasmic expression of MnSOD, catalase and glutathione peroxidase were significantly lower in PC tissues (n=10) compared to normal pancreas tissues (n=5) ($P<0.05$) (Cullen et al., 2003a). The expression of Trx1 ($P=0.0044$), Trx2 ($P<0.0001$) and Grx5 ($P=0.019$) were significantly higher in 25 hepatocellular carcinomas (HCCs) compared to the respective surrounding normal liver cells. Additionally, the latter study found that expression of Grx3 in colorectal carcinoma liver metastases was higher than the primary tumour (Mollbrink et al., 2014). A recent report also showed that Trx protein expression was significantly higher in 18 basal cell carcinomas (BCCs) than 18 controls ($P=0.018$) (Sobhani et al., 2016). Another recent study showed that Trx expression was significantly higher in 228 tissues of patients with clinical colorectal cancer (CRC) than normal tissues ($P<0.001$) (Lou et al., 2017a).

Several studies investigated the association between redox proteins expression and clinical characteristics of different cancers including breast, ovarian, gastro-oesophageal

and colorectal cancers. Woolston and colleagues investigated the relationship between 5 redox proteins (Trx, TrxR, TxNIP, metallothionein and glutathione S-transferase) and the clinical outcome of 145 ovarian cancer patients treated with platinum-based chemotherapy (Woolston et al., 2010). Results showed no significant association between the expression of TrxR, TxNIP and glutathione S-transferase and patients' clinical features. However, authors observed that low cytoplasmic Trx (P=0.032) and negative nuclear expression of metallothionein (P=0.04) were significantly correlated with better progression-free survival. Low cytoplasmic of Trx, when combined with high nuclear expression of Trx, was significantly associated with better progression-free survival (P=0.003) and overall survival (P=0.004). Also, negative nuclear expression of metallothionein, when combined with negative cytoplasmic expression of metallothionein, was associated with better progression-free survival (P=0.038). Further analysis showed that low cytoplasmic expression of Trx, when combined with negative nuclear expression of metallothionein, was significantly associated with better progression-free survival (P=0.026), but not with overall survival (P=0.072) (Woolston et al., 2010).

The same group investigated the associations between the expression of nine redox proteins (glutathione, glutathione reductase, glutaredoxin, glutathione peroxidase 1, 3, and 4, and glutathione S-transferase-θ, -π, and -α) and the response to radiotherapy in 224 early-stage breast cancer patients (Woolston et al., 2011a). Results showed that high cytoplasmic glutathione S-transferase-θ expression was associated with greater risk of local recurrence (P=0.008) and worse overall survival (P=0.009). High cytoplasmic glutathione S-transferase-θ expression, when combined with low nuclear expression, became a strong independent predictive factor for local recurrence (P=0.002). Additionally, high nuclear (P=0.005) and cytoplasmic (P=0.001) glutathione peroxidase 4 expression were significantly correlated with low-grade tumours (Woolston et al., 2011a).

By using the same cohort of the latter study, Woolston and colleagues studied the relationship of the expression of Trx system (Trx, TrxR and TxNIP) and peroxiredoxin (Prx

I-VI) with clinicopathological variables and clinical outcomes (Woolston et al., 2011b). Results showed that high nuclear expression of Trx (P=0.046) and TrxR (P=0.046) was associated with better overall survival in BC patients under 40 years. High nuclear expression of Prx VI was borderline correlated with worse overall survival (P=0.065). However, when high nuclear expression of Prx VI combined with low cytoplasmic expression of Prx VI, the association became significant (P=0.004). Also, high cytoplasmic expression of Prx III (P=0.029) was associated with higher risk of local recurrence. Furthermore, results showed that high cytoplasmic expression of Prx I was strongly associated with higher risk of local recurrence either alone (P=0.009) or combined with low nuclear expression of Prx I (P=0.005) (Woolston et al., 2011b).

The same group studied the associations between the expression of eight redox proteins (Trx, TrxR, TxNIP, GST π, θ and α, catalase and manganese superoxide dismutase) and clinical characteristics of 98 locally advanced pre-chemotherapy breast cancer specimens. Results showed that high expression of GST π (P=0.05) and low expression of catalase (P=0.045) were associated with complete pathological response in pre-chemotherapy biopsy samples. Additionally, high TxNIP (P=0.021) and TrxR (P=0.021) were associated with improved distant metastasis-free survival (Woolston et al., 2012). In a subsequent study, Woolston and colleagues revealed significant associations between TxNIP expression and clinical features of 140 gastro-oesophageal adenocarcinomas patients (Woolston et al., 2013). The latter study found that high expression of TxNIP was significantly associated with lack of lymph node involvement (P=0.005), absence of perineural invasion (P=0.03), well/moderate tumour differentiation (P=0.033) and better disease-free survival (P=0.002).

Another group investigated the associations between the expression of 6 redox proteins (Trx1-2, Grx1-3 and Grx5) and the clinical outcome of 25 patients with HCC and 15 patients with colorectal cancer liver metastasis (CRLM) (Mollbrink et al., 2014). Authors observed that Trx1 (P=0.0044), Trx2 (P<0.0001) and Grx5 (P=0.019) were significantly overexpressed in the HCC tumours compared to the surrounding normal liver tissues. Also, results showed that expression of Trx1 (P=0.0001), Trx2 (P=0.0002), Grx1 (P=0.01),

Grx3 (P=0.0001) and Grx5 (P=0.0005) was significantly higher in CRC liver metastases than normal colorectal tissues. Further analysis showed that high expression of Trx1 was correlated with cell proliferation (P<0.05) and micro-vascular invasion (P=0.057), while high expression of Trx2 was significantly associated with decreased tumour size (P<0.05) (Mollbrink et al., 2014).

A recent study showed that high expression of TxNIP in meningioma tissues from 65 patients was associated with longer recurrence-free survival (P=0.003) and low tumour grade (P<0.001) (Cai et al., 2017). Another recent study showed that high expression of Trx was significantly associated with better failure-free survival of 174 Hodgkin lymphoma patients (P=0.049), with no significant association with any of clinicopathological parameters (P. Vassilakopoulos et al., 2017).

All the above studies showed the role of expression of redox proteins in clinicopathological criteria and clinical outcome of cancer patients. Nevertheless, expression of the Trx system has never been previously assessed, in a simultaneous fashion, in a large cohort of PC patients. Only one study indicated a possible association between Trx and Grx with the malignant potential of PDAC in a small number of patients (n=32). Authors observed that PDAC tissues were immunohistochemically more positive for Trx (75%, 24/32 cases) and Grx (91%, 29/32 cases) than pancreatic cystadenocarcinoma or normal pancreatic tissue (Nakamura et al., 2000).

Expression Trx-related proteins such as Prx have been investigated in PC patients. A recent study evaluated the expression of five isoforms of Prx (Prx 1-3, 5-6) in pre-treatment samples from 69 patients with PDAC. In patients with tumours of T3-4 class, high expression of Prx I was associated with longer relapse-free survival (RFS) (P=0.041), while high expression of Prx VI was associated with longer disease-free survival (P=0.0037). Stronger intensity of cytoplasmic Prx III expression was associated with node-negative status (P=0.007) and better tumour differentiation (P=0.033), while high cytoplasmic Prx V expression was associated with smaller tumour size (P=0.029) and node-negative status (P=0.003) (Isohookana et al., 2016). Another recent study

confirmed the previous study and showed that high nuclear Prx I was associated with longer survival in 60 patients with PC (P=0.001) (Schultz et al., 2017).

The current chapter sets out to investigate the relationship of the Trx system protein expression in carcinomas of the pancreas, bile duct and ampulla with clinicopathological criteria and patient survival outcomes by addressing the hypothesis mentioned below.

4.2.2 Hypothesis

Elevated protein expression of Trx and TrxR is an adverse prognostic factor for overall survival in patients with pancreatic, bile duct and ampullary cancers.

4.2.3 Aims

Investigate the relationship of Trx system protein expression with clinicopathological criteria and patient survival outcomes, using conventional immunohistochemistry (IHC), in 230 tumours from PAD, bile duct and ampullary cancer patients.

4.3 Materials and methods

4.3.1 Clinical samples

Investigation of Trx system protein expression in patients' specimens was conducted using a tissue microarray (TMA) with tissue collected from cancer patients treated at Nottingham University Hospitals between 1993 and 2013. This study has ethical approval from the Nottingham Research Ethics Committee and was conducted according to REMARK (REporting recommendations for tumour MARKer prognostic studies) criteria (McShane et al., 2006). REMARK was established to address widespread deficiencies in the reporting of reports on tumour markers in oncology. The REMARK checklist consists of 20 items to report for published tumour marker prognostic studies, with providing positive examples and giving empirical evidence of the quality of reporting (McShane et al., 2006).

A total of 230 cancer patients were included in the current study, and were divided into two cohorts; the first cohort was composed of 85 PAD patients and the second cohort was composed of 145 cancers of the bile duct and ampulla. In PAD patients, 61% of were male (52/85) and the age of the patients ranged from 35 years to 81 years with a median age of 66. In patients with bile duct and ampullary tumours, 56% were male (81/145) and the age of the patients ranged from 39 years to 85 years with a median age of 65. Table 4.1 shows the full clinicopathological characteristics of both cohorts.

For both cohorts, survival was calculated from the date of surgery to the date of death, or from the date of surgery to the last date known to be alive for those patients censored. The median survival time was 18.2 months for PAD cohort and 18.0 months for bile duct and ampullary tumours cohort. In the PAD cohort, 53.7% (36/67) of patients received adjuvant chemotherapy (data was not available for 18 patients), of the 36 patients that did receive adjuvant chemotherapy 52.8% (19/36) received 5FU/folinic acid and 13.8% (5/36) received GM chemotherapy. In the bile duct and ampullary cohort, 28.7% (27/94) of patients received adjuvant chemotherapy (data was not

available for 51 patients), of the 27 patients that did receive adjuvant chemotherapy 48.1% (13/27) received 5FU/folinic acid and 18.5% (5/27) received GM chemotherapy in the context of clinical trials.

Characteristics	PAD cohort=(85)	Bile duct and Ampullary cancer cohort (n=145)
	Frequencies (%)	Frequencies (%)
Age		
≤ 60 years	27 (31.8)	46 (31.7)
> 60 years	56 (65.9)	98 (67.6)
Missed	2 (2.4)	1 (0.7)
Gender		
Male	52 (61.2)	81 (55.9)
Female	33 (38.8)	64 (44.1)
Missed	0 (0)	0 (0)
Tumour size		
≤ $2cm^2$	6 (7.1)	56 (38.6)
> $2cm^2$	77 (90.6)	87 (60)
Missed	2 (2.4)	2 (1.4)
Tumour stage		
I	1 (1.2)	3 (2.1)
II	18 (21.2)	30 (20.7)
III	62 (72.9)	106 (73.1)
IV	3 (3.5)	5 (3.4)
Missed	1 (1.2)	1 (0.7)
Lymph node stage		
Negative	28 (32.9)	52 (35.9)
Positive	54 (63.5)	85 (58.6)
Missed	3 (3.5)	8 (5.5)
Venous invasion		
Absent	30 (35.3)	55 (37.9)
Present	54 (63.5)	88 (60.7)
Missed	1 (1.2)	2 (1.4)
Prenural invasion		
Absent	15 (17.6)	60 (41.4)
Present	69 (81.2)	84 (57.9)
Missed	1 (1.2)	1 (0.7)

Table 4.1: Clinicopathological variables of the PAD cohort of 85 patients and the bile duct and ampullary cohort of 145 patients.

4.3.2 Optimization of antibodies for immunohistochemistry (IHC)

The specificity of the Trx, TrxR and TxNIP antibodies were determined prior to immunohistochemical staining of patients' specimen using ECL-Western blot, described in Section 3.3.3, with pancreatic cell lysates of PANC-1, MIA Paca-2 and BxPc-3 and BC cell lysates of MDA-MB-231 and MCF-7 made following procedures described in Section 3.3.3. Antibodies yielding expected bands without nonspecific bands were applicable for IHC. Then, antibody concentrations to be used in IHC were optimised using three PC tissues representing three PC types i.e. 3 pancreatic adenocarcinomas, 3 ductal adenocarcinomas and 3 ampullary adenocarcinomas. The optimization of antibody concentration was carried out using a Novolink Novocastra polymer detection kit (Leica, Denmark), each using three different concentrations, including one as recommended by the manufacturer in their datasheet. Additional concentrations were tried if initial concentrations did not give appropriate immunohistochemical staining. As antibodies of the Trx system were previously optimized in BC tissues (Zhang, 2014), breast tissue sections were used as a positive control for optimisation. Negative controls omitted the primary antibody from the procedure. By comparing staining patterns from each marker with the negative control, the staining specificity of the antibody can be determined. The primary and secondary antibodies used in the current chapter with their dilution ratios and host species were previously listed in Table 3.2.

4.3.3 IHC

IHC was performed on 4-µm paraffin-embedded sections that were mounted on Superfrost^{+} microscope slides (Menzel-Glaser, Germany) then quick-dried at 37 °C overnight (by Mr Christopher Nolan, Department of Histopathology, School of Medicine, University of Nottingham). PC sections slides were placed on a 60°C hotplate for 10 minutes and then allowed to cool before deparaffinising and rehydrating, which were conducted automatically using a Leica Autostainer XL Staining System ST5010 (Minnesota, USA). Each slide was deparaffinised with two xylene baths (5 minutes)

followed by rehydration with three industrial methylated spirit (IMS) baths (2 minutes), and a 5 minute wash in running tap water. Antigen retrieval was performed, based on microwave irradiation (Taylor et al., 1994), using 0.01 mol/L sodium citrate buffer (pH 6) in a microwave, 750 watts for 10 minutes followed by 450 watts for 10 minutes. Following microwaving, slides were washed immediately under running tap water to stop the retrieval process. The slides were then loaded onto a sequenza slide rack (ThermoFisher Scientific, NY, USA) and a Novolink Novocastra polymer detection kit was applied on the tissue sections according to instructions. Briefly, for the Novolink Novocastra polymer detection kit 100 µl peroxidase block was added onto each slide for 5 minutes at room temperature to block the endogenous hydrogen peroxidase activity and then washed 2 x 5 minutes with Tris buffered saline (TBS). 100 µl of protein block was then added for another 5 minutes at room temperature, which serves as a general protein block to minimize the nonspecific interactions of the subsequent detection reagents, and washing was carried out as above, before the addition of 100 µl of antibody solution for 1 hour at room temperature. The slides were then washed 2 x 5 minutes. 100 µl of post primary block was added for 30 minutes at room temperature, washed and 100 µl of Novolink polymer was added for another 30 minutes at room temperature followed by 2 x 5 minutes wash. DAB (3,3'-diaminobenzidine) solution (1:20 DAB chromogen in DAB substrate buffer) was applied to the slides for 5 minutes followed by another 2 x 5 minutes wash. The slides were then stained with Novolink haematoxylin for another 6 minutes at room temperature, removed from the sequenza trays, and place in a Leica autostainer for dehydration programme: 5 minutes running tap water wash followed by 3 x 2 minutes IMS bath and then 2 x 5 minutes xylene bath. Sections were mounted with DPX mounting medium, a mixture of distyrene (a polystyrene), a plasticiser (tricresyl phosphate), and xylene, (Leica, Germany) and were left to dry overnight. Breast tumour slides were included as positive and negative controls with each run, with the negative control having primary antibody substituted by Leica antibody diluent.

4.3.4 Assessment of expression

All cores were assessed semi-quantitatively using an immunohistochemical H-score using a HPF Nikon Eclipse E600 at 200x magnification. Staining intensity was assessed as; none (0), weak (1), medium (2) and strong (3) over the percentage area of each staining intensity. H-scores were calculated by multiplying the percentage of positive tumour cells by the staining intensity (i.e. (0 x negatively stained tumour %) + (1 x weakly stained tumour %) + (2 x moderately stained tumour %) and (3 X strongly stained tumour %)), giving a score ranging between 0 and 300. Each core was assessed, at same time, by two individuals, including one pathologist (Dr. Abed M. Zaitoun, Department of Pathology, Nottingham University Hospitals, Queen's Medical Centre, Nottingham, UK) and myself. An average H-score was generated by taking the mean H-score of the three cores (n=187) or two cores (n=43) available for each patient included in the current study (n=230). Figure 4.1 shows representative photomicrographs of staining of Trx system protein expression from the carcinomas of the pancreas, bile duct and ampulla TMAs. Figure 4.2 shows representative photomicrographs of different staining patterns of Trx system protein expression from PAD TMAs.

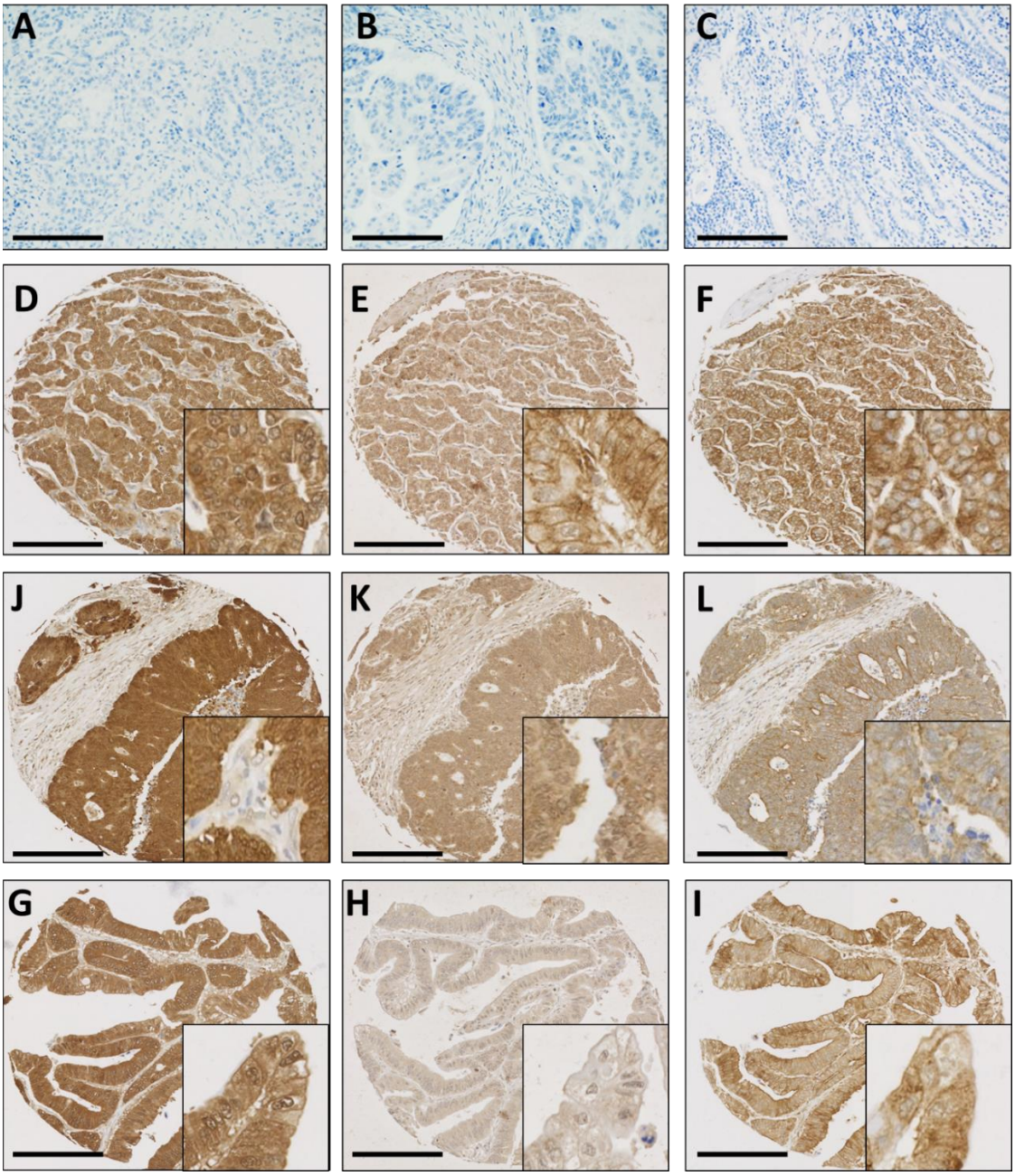


Figure 4.1: **Representative photomicrographs of Trx system protein expression from the carcinomas of the pancreas, bile duct and ampulla.** A,B and C are negative controls of PC tissue sections representing three PC types; PAD, bile ductal and ampullary carcinomas respectively. D,E and F are expression of Trx, TrxR and TxNIP in PADs respectively. G,H and I are expression of Trx, TrxR and TxNIP in bile ductal carcinomas respectively. J, K and L are expression of Trx, TrxR and TxNIP in ampullary carcinomas respectively. Photomicrographs are at 10x magnification with 20x magnification inset box where scale bar shows 200µm.

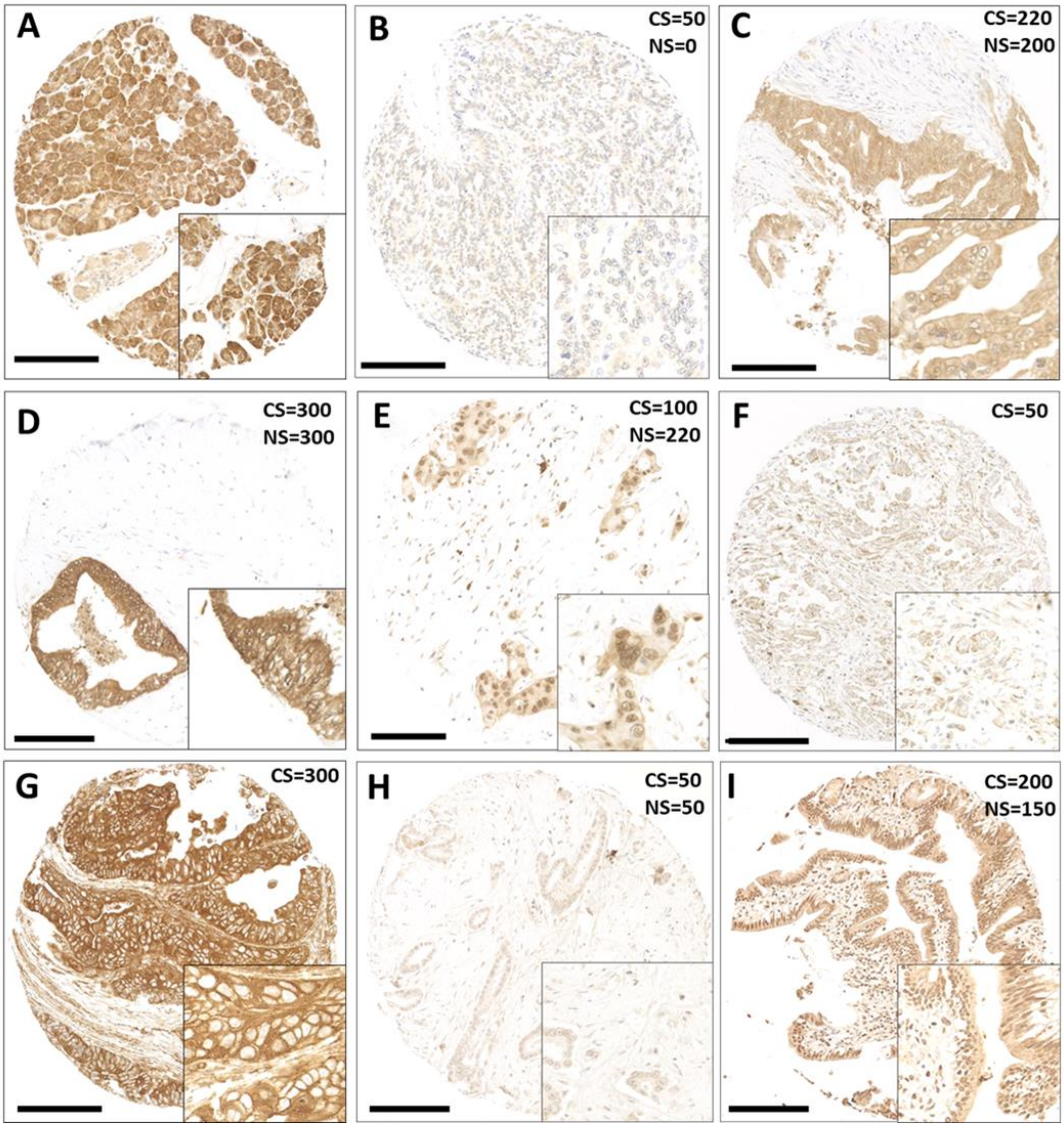


Figure 4.2: **Representative photomicrographs of different staining patterns of Trx system protein expression from PAD TMAs.** (A) benign pancreatic tissue, (B) weak staining of Trx, (C) moderate staining of Trx, (D) strong staining of Trx, (E) low cytoplasmic staining with moderate nuclear staining of Trx, (F) weak cytoplasmic staining of TxNIP, (G) strong cytoplasmic staining of TxNIP, (H) weak staining of TrxR, (I) moderate staining of TrxR. Photomicrographs are at 10x magnification with 20x magnification inset box where scale bar shows 200µm. Abbreviation: CS=Cytoplasmic H-score, NS= Nuclear H-score.

4.3.5 Statistical analysis

The relationship between categorised protein expression and clinicopathological variables was assessed using Pearson Chi Square (χ^2) test of association. Survival curves were plotted according to the Kaplan-Meier method and significance determined using the log-rank test. Multivariate survival analysis was performed by Cox Proportional Hazards regression model. All differences were deemed statistically significant at the level of $P<0.05$. Statistical analysis was performed using SPSS 23.0 software (IBM Corporation). Stratification cut points were determined using X-Tile software (Yale School of Medicine) and were determined prior to statistical analysis (Camp et al., 2004). X-tile is a graphical method that generates an unbiased cut-point selection by illustrating the presence of substantial tumour subpopulations and showing the robustness of the relationship between a biomarker and outcome by construction of a two-dimensional projection of every possible subpopulation.

4.4 Results

4.4.1 Optimizations of Trx, TrxR and TxNIP primary antibodies for IHC

As mentioned in Section 4.3.2, the specificity of Trx, TrxR and TxNIP antibodies were determined using ECL-Western blot with pancreatic and breast cell lysates. The Trx, TrxR and TxNIP antibodies were directed against total Trx protein with molecular weight of 12 kDa, TrxR protein with molecular weight of 55 kDa and TxNIP protein with molecular weight of 44 (observed 50 kDa) respectively. In the current project, β-actin was used as the housekeeping protein, with a molecular weight of 42 kDa.

Figure 4.3 shows that Trx and TrxR detected a single band, in all lysates, of the expected size of 12 and 55 kDa respectively. TxNIP antibody detected a single band of the expected size of 44 kDa (observed 50 kDa) in MIA Paca-2, BxPc-3 and MCF-7 lysates, with no bands were detected in PANC-1 and MDA-MB-231 lysates.

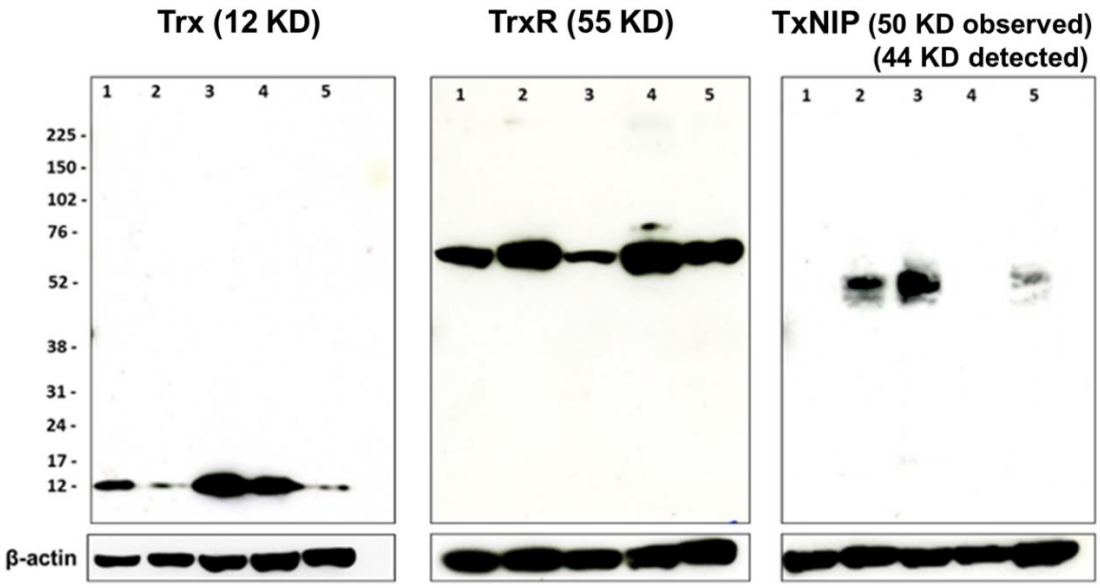


Figure 4.3: **Assess the specificity of Trx, TrxR and TxNIP antibodies.** Lysates from (1) PANC-1, (2) MIA Paca-2 and (3) BxPc-3, (4) MDA-MB-231 and (5) MCF-7 cancer cell lines were subjected to ECL-Western blot to assess the specificity of Trx, TrxR and TxNIP antibodies.

These Western blot results suggested that Trx, TrxR and TxNIP antibodies were specific and detected the correct protein band, so they were eligible for immunohistochemical

staining of patients' specimens using IHC. The concentration of the Trx system antibodies applied in IHC was optimised in PC sections with breast tumour composite tissues used as positive controls as described in Section 4.3.2. A dilution of 1:2000 (1 hour, RT), 1:100 (overnight, 4°C) and 1:250 (1 hour, RT) for anti-Trx, anti-TrxR and anti-TxNIP respectively, was determined to give the optimal staining on the PC tissue sections. The positive staining for anti-Trx and anti-TrxR in PC tissues were detected in the cytoplasm and the nucleus, while anti-TxNIP was detected only in the cytoplasm.

4.4.2 Expression of Trx, TrxR and TxNIP in the PAD cohort and the bile duct and ampullary carcinoma cohort

In the PAD cohort, cytoplasmic Trx had a median H-score of 210 and ranged from 100 to 300; nuclear Trx had a median H-score of 225 and ranged from 50 to 300; cytoplasmic TxNIP had a median H-score of 150 and ranged from 0 to 267; cytoplasmic TrxR had a median H-score of 75 and ranged from 0 to 225; and nuclear TrxR had a median H-score of 75 and ranged from 0 to 225 (Appendix A, Figure A.1). In the bile duct and ampullary carcinoma cohort, cytoplasmic Trx had a median H-score of 150 and ranged from 0 to 300; nuclear Trx had a median H-score of 166.7 and ranged from 0 to 300; cytoplasmic TxNIP had a median H-score of 166.7 and ranged from 0 to 300; cytoplasmic TrxR had a median H-score of 66.7 and ranged from 0 to 250; and nuclear TrxR had a median H-score of 66.7 and ranged from 0 to 250 (Appendix A, Figure A.2).

Bioinformatics software X-tile (Camp et al., 2004) was used to obtain an optimal H-score cut-off point for each protein, which stratified H-scores of tumour samples into low- vs high-expression. The X-tile cut-point values, for each marker in both cohorts, are summarised in Table 4.2.

Staining/ X-tile	The PAD cohort		
	X-tile cut-off point	Cases lower cut-off point (%)	Cases higher cut-off point (%)
Cytoplasmic Trx	160	13 (17.6%)	61 (82.4%)
Nuclear Trx	234	40 (54.8%)	33 (45.2%)
Cytoplasmic TrxR	58	29 (38.2%)	47 (61.2%)
Nuclear TrxR	58	29 (38.2%)	47 (61.2%)
Cytoplasmic TxNIP	217	66 (82.5%)	14 (17.5%)

Staining/ X-tile	The bile duct and ampullary carcinoma cohort		
	X-tile cut-off point	Cases lower cut-off point (%)	Cases higher cut-off point (%)
Cytoplasmic Trx	142	51 (39.8%)	77 (60.2%)
Nuclear Trx	133	47 (36.7%)	81 (63.3%)
Cytoplasmic TrxR	167	117 (89.3%)	14 (10.7%)
Nuclear TrxR	75	70 (52.6%)	63 (47.4%)
Cytoplasmic TxNIP	85	32 (24.4%)	99 (75.6%)

Table 4.2: The X-tile cut-point values of Trx, TrxR and TxNIP in the PAD cohort and bile duct and ampullary carcinoma cohorts. The number/percentage of cases lower/higher cut-point for each staining, cytoplasmic Trx, nuclear Trx, cytoplasmic TrxR, nuclear TrxR and cytoplasmic TxNIP, is shown for PAD cohort (upper) and bile duct and ampullary carcinoma cohorts (lower).

The correlation between expression levels of the proteins with one another was assessed using the Spearman rank correlation coefficient. In the PAD cohort, cytoplasmic TxNIP expression had a statistically significant correlation with cytoplasmic TrxR (r=0.234, P=0.038) and nuclear TrxR expression (r=0.241, P=0.032). Cytoplasmic TrxR expression was strongly correlated with nuclear TrxR expression (r=0.711,

P<0.001). Nuclear expression of Trx was strongly correlated with cytoplasmic Trx expression (r=0.549, P<0.001).

In the bile duct and ampullary tumours, cytoplasmic Trx expression was strongly correlated with nuclear Trx expression (r=0.653, P<0.001), cytoplasmic TrxR expression (r=0.436, P<0.001) and nuclear TrxR expression (r=0.328, P<0.001). In addition, nuclear Trx expression had a statistically significant correlation with cytoplasmic TrxR expression (r=0.2, P=0.25) and nuclear TrxR expression (r=0.376, P<0.001). Cytoplasmic TrxR expression was strongly correlated with nuclear TrxR expression (r=0.653, P<0.001).

4.4.3 Relationship of Trx, TrxR and TxNIP expression with clinicopathological variables in the PAD cohort and the bile duct and ampullary carcinoma cohort

In the PAD cohort, an association was observed between high cytoplasmic TrxR expression and lymph node metastasis (χ^2=4.533, d.f.=1, P=0.033), while protein expression of Trx and TxNIP showed no association with clinicopathological variables. The full relationship of the Trx system expression with clinicopathological variables in the PAD cohort is listed in Tables 4.3 (for Trx and TxNIP) and 4.4 (for TrxR).

Variable	Trx (cytoplasmic)			Trx (nuclear)			TxNIP		
	Low	High	P-value	Low	High	P-value	Low	High	P-value
Age									
≤ 60 years	3 (3.9)	24 (31.6)	0.521*	15 (20.0)	11 (14.7)	0.701	22 (27.2)	5 (6.2)	0.669
> 60 years	9 (11.8)	40 (52.6)		26 (34.7)	23 (30.7)		46 (56.8)	8 (9.9)	
Gender									
Male	11 (14.3)	38 (49.4)	0.117*	24 (31.6)	24 (31.6)	0.227	44 (53.0)	7 (8.4)	0.335
Female	2 (2.6)	26 (33.8)		18 (23.7)	10 (13.2)		25 (30.1)	7 (8.4)	
Tumour size									
≤ 2cm²	1 (1.3)	5 (6.6)	1.000*	2 (2.7)	4 (5.3)	0.401*	6 (7.4)	0 (0.0)	0.582*
> 2cm²	12 (15.8)	58 (76.3)		39 (52.0)	30 (40.0)		62 (76.5)	13 (16.0)	
Tumour stage									
1	1 (1.3)	0 (0)	0.063	1 (1.3)	0 (0.0)	0.057	1 (1.2)	0 (0.0)	0.398
2	1 (1.3)	16 (20.8)		12 (15.8)	4 (5.3)		17 (20.7)	1 (1.2)	
3	11 (14.3)	45 (58.4)		26 (34.2)	30 (39.5)		48 (58.5)	12 (14.6)	
4	0 (0.0)	3 (3.9)		3 (3.9)	0 (0.0)		3 (3.7)	0 (0.0)	
Node status									
Negative	4 (5.3)	21 (28.0)	1.000*	13 (17.6)	12 (16.2)	0.674	25 (31.3)	3 (3.8)	0.526*
Positive	9 (12.0)	41 (54.7)		28 (37.8)	21 (28.4)		42 (52.5)	10 (12.5)	
Venous Invasion									
Absent	4 (5.2)	22 (28.6)	1.000*	17 (22.4)	8 (10.5)	0.118	24 (29.3)	5 (6.1)	0.799
Present	9 (11.7)	42 (54.5)		25 (32.9)	26 (34.2)		45 (54.9)	8 (9.8)	
Perineural Invasion									
Absent	4 (5.2)	9 (11.7)	0.216*	8 (10.5)	5 (6.6)	0.617	11 (13.4)	4 (4.9)	0.243*
Present	9 (11.7)	55 (71.4)		34 (44.7)	29 (38.2)		58 (70.7)	9 (11.0)	

Table 4.3: Associations between Trx and TxNIP protein expression and various clinicopathological variables in the PAD cohort. The number of observations for the cohort is shown for each clinicopathological variable; the table does not include the number of observations where clinicopathological data were not available. The frequency of observed clinicopathological variables is noted next to the variable subgroup. The P-values are resultant from Pearson Chi Square test of association (χ^2) or Fisher's Exact test in a 2×2 table if a cell count was less than 5 (indicated by *). Significant P-values are indicated by bold font.

Variable	TrxR (cytoplasmic)			TrxR (nuclear)		
	Low	High	P-value	Low	High	P-value
Age						
≤ 60 years	9 (11.7)	18 (23.4)	0.565	9 (11.7)	18 (23.4)	0.457
> 60 years	20 (26.0)	30 (39.0)		21 (27.3)	29 (37.7)	
Gender						
Male	19 (24.1)	31 (39.2)	0.995	19 (24.1)	31 (39.2)	0.767
Female	11 (13.9)	18 (22.8)		12 (15.2)	17 (21.5)	
Tumour size						
≤ 2cm²	2 (2.6)	4 (5.2)	1.000*	3 (3.9)	3 (3.9)	0.680*
> 2cm²	28 (36.4)	43 (55.8)		28 (36.4)	43 (55.8)	
Tumour stage						
1	1 (1.3)	0 (0.0)	0.304	1 (1.3)	0 (0.0)	0.228
2	6 (7.7)	11 (14.1)		6 (7.7)	11 (14.1)	
3	23 (25.9)	34 (43.6)		24 (30.8)	33 (42.3)	
4	0 (0.0)	3 (3.8)		0 (0.0)	3 (3.8)	
Node status						
Negative	15 (19.7)	12 (15.8)	**0.033**	13 (17.1)	14 (18.4)	0.333
Positive	15 (19.7)	34 (44.7)		18 (23.7)	31 (40.8)	
Venous Invasion						
Absent	7 (9.0)	20 (25.6)	0.098	11 (14.1)	16 (20.5)	0.896
Present	23 (29.5)	28 (35.9)		20 (26.5)	31 (39.7)	
Perineural Invasion						
Absent	5 (6.4)	9 (11.5)	0.816	5 (6.4)	9 (11.5)	0.734
Present	25 (32.1)	39 (50.0)		26 (33.3)	38 (48.7)	

Table 4.4: Associations between TrxR protein expression and various clinicopathological variables in the PAD cohort. The number of observations for the cohort is shown for each clinicopathological variable; the table does not include the number of observations where clinicopathological data were not available. The frequency of observed clinicopathological variables is noted next to the variable subgroup. The P-values are resultant from Pearson Chi Square test of association (χ^2) or Fisher's Exact test in a 2×2 table if a cell count was less than 5 (indicated by *). Significant P-values are indicated by bold font.

In bile duct and ampullary cancers, high expression of nuclear TrxR and cytoplasmic TxNIP were associated with patients aged above 60 years (χ2=5.091, d.f.=1, P=0.024) (χ2=3.892, d.f.=1, P=0.049) respectively. Associations were observed between high nuclear TrxR expression and the presence of venous invasion (χ^2= 10.548, d.f.=1, P=0.001) and the presence of perineural invasion (χ^2= 5.314, d.f.=1, P=0.021). Low cytoplasmic TxNIP expression was associated with the presence of perineural invasion (χ^2=5.044, d.f.=1, P=0.025), while expression of Trx and cytoplasmic TrxR protein showed no association with clinicopathological variables. The full relationship of the Trx system expression with clinicopathological variables in the bile duct and ampullary carcinoma cohort is listed in Tables 4.5 (for Trx and TxNIP) and 4.6 (for TrxR).

Variable	Trx (cytoplasmic)			Trx (nuclear)			TxNIP		
	Low	High	P-value	Low	High	P-value	Low	High	P-value
Age									
≤ 60 years	17 (13.1)	25 (19.2)	0.865	18 (13.8)	24 (18.5)	0.401	16 (11.9)	30 (22.4)	**0.049**
> 60 years	37 (28.5)	51 (39.2)		31 (23.8)	57 (43.8)		17 (12.7)	71 (53.0)	
Gender									
Male	26 (19.8)	47 (35.9)	0.144	25 (19.1)	48 (36.6)	0.402	17 (12.6)	57 (42.2)	0.514
Female	28 (21.4)	30 (22.9)		24 (18.3)	34 (26.0)		17 (12.6)	44 (32.6)	
Tumour size									
≤ 2cm²	16 (12.3)	32 (24.6)	0.187	18 (13.8)	30 (23.1)	0.917	11 (8.20)	39 (29.1)	0.489
> 2cm²	37 (28.5)	45 (34.6)		30 (23.1)	52 (40.0)		23 (17.2)	61 (45.5)	
Tumour stage									
1	1 (0.8)	2 (1.5)	0.778	2 (1.5)	1 (0.8)	0.329	0 (0.0)	3 (2.2)	0.497
2	11 (8.4)	16 (12.2)		12 (9.2)	15 (11.5)		5 (3.7)	23 (17.0)	
3	41 (31.3)	55 (42.0)		32 (24.4)	64 (48.9)		28 (20.7)	71 (52.6)	
4	1 (0.8)	4 (3.1)		3 (2.3)	2 (1.5)		1 (0.7)	4 (3.0)	
Node status									
Negative	17 (13.5)	29 (23.0)	0.456	17 (13.5)	29 (23.0)	0.937	27 (20.9)	22 (17.1)	0.573
Positive	35 (27.8)	45 (35.7)		29 (23.0)	51 (40.5)		40 (31.0)	40 (31.0)	
Venous Invasion									
Absent	21 (16.2)	29 (22.3)	0.821	22 (16.9)	28 (21.5)	0.186	11 (8.2)	41 (30.6)	0.371
Present	32 (24.6)	48 (36.9)		26 (20.0)	54 (41.5)		23 (17.2)	59 (44.0)	
Perineural Invasion									
Absent	21 (16.0)	36 (27.5)	0.371	26 (19.8)	31 (23.7)	0.088	9 (6.7)	49 (36.3)	**0.025**
Present	33 (25.2)	41 (31.3)		23 (17.6)	51 (38.9)		25 (18.5)	52 (38.5)	

Table 4.5: Associations between Trx and TxNIP protein expression and various clinicopathological variables in the bile duct and ampullary carcinoma cohort. The number of observations for the cohort is shown for each clinicopathological variable; the table does not include the number of observations where clinicopathological data were not available. The frequency of observed clinicopathological variables is noted next to the variable subgroup. The P-values are resultant from Pearson Chi Square test of association (χ^2) or Fisher's Exact test in a 2×2 table if a cell count was less than 5 indicated by *). Significant P-values are indicated by bold font.

Variable	TrxR (cytoplasmic)			TrxR (nuclear)		
	Low	High	P-value	Low	High	P-value
Age						
≤ 60 years	41 (30.6)	4 (3.00)	0.773*	30 (22.4)	15 (11.2)	**0.024**
> 60 years	79 (59.0)	10 (7.50)		41 (30.6)	48 (35.8)	
Gender						
Male	68 (50.4)	8 (5.90)	0.946	37 (27.4)	39 (28.9)	0.219
Female	53 (39.3)	6 (4.40)		35 (25.9)	24 (17.8)	
Tumour size						
≤ 2cm²	47 (35.1)	5 (3.70)	0.802	30 (22.4)	22 (16.4)	0.385
> 2cm²	73.1 (54.5)	9 (6.70)		41 (30.6)	41 (30.6)	
Tumour stage						
1	3 (2.2)	0 (0.0)	0.100	2 (1.5)	1 (0.7)	0.461
2	23 (17.0)	4 (3.0)		14 (10.4)	13 (9.6)	
3	92 (68.1)	8 (5.9)		55 (40.7)	45 (33.3)	
4	3 (2.2)	2 (1.5)		1 (0.7)	4 (3.0)	
Node status						
Negative	9 (7.0)	38 (29.5)	0.326	43 (33.3)	6 (4.7)	0.522
Positive	22 (17.1)	60 (46.5)		73 (56.6)	7 (5.4)	
Venous Invasion						
Absent	44 (32.8)	5 (3.7)	0.944	35 (26.1)	14 (10.4)	**0.001**
Present	76 (56.7)	9 (6.7)		36 (26.9)	49 (36.3)	
Perineural Invasion						
Absent	48 (36.5)	9 (6.7)	0.077	37 (27.4)	20 (14.8)	**0.021**
Present	73 (54.1)	5 (3.7)		35 (25.9)	43 (31.9)	

Table 4.6: Associations between TrxR protein expression and various clinicopathological variables in the bile duct and ampullary carcinoma cohort. The number of observations for the cohort is shown for each clinicopathological variable; the table does not include the number of observations where clinicopathological data were not available. The frequency of observed clinicopathological variables is noted next to the variable subgroup. The P-values are resultant from Pearson Chi Square test of association (χ^2) or Fisher's Exact test in a 2×2 table if a cell count was less than 5 (indicated by *). Significant P-values are indicated by bold font.

4.4.4 Relationship of the Trx, TrxR and TxNIP protein expression with clinical outcome in the PAD cohort and the bile duct and ampullary carcinoma cohort

In the PAD cohort, high expression of cytoplasmic Trx (Figure 4.4A) and nuclear Trx (Figure 4.4B) was significantly associated with better overall survival (P=0.018 and P=0.006 respectively). Cytoplasmic TrxR (Figure 4.4C), nuclear TrxR (Figure 4.4D) and cytoplasmic TxNIP (Figure 4.5A) expression showed no association with overall survival (P=0.239, P=0.180 and P=0.174 respectively).

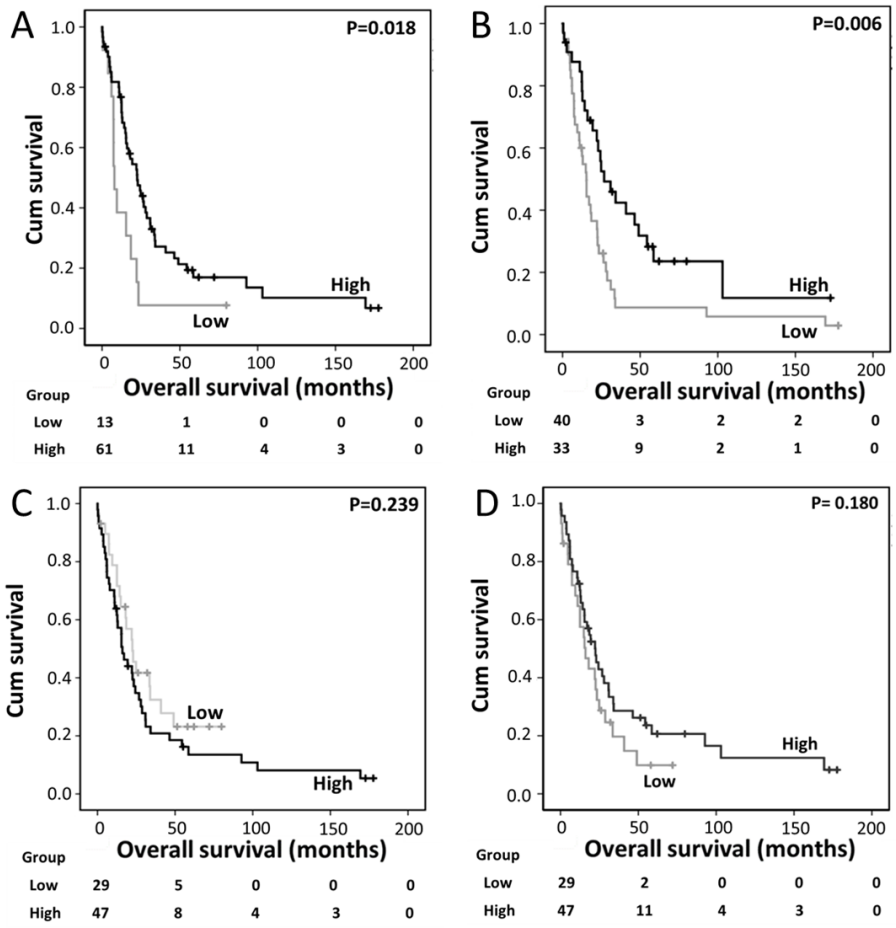


Figure 4.4 Kaplan-Meier analysis of association between Trx and TrxR expression and overall survival in PAD cohort. Kaplan-Meier analysis of overall survival showing the impact of Trx and TrxR expression in PAD cohort of 85 patients with significance determined using the log-rank test. High expression of cytoplasmic Trx (A) and nuclear Trx (B) was significantly associated with better overall survival (P=0.018 and P=0.006 respectively). Cytoplasmic TrxR (C) and nuclear TrxR (D) expression showed no association with overall survival (P=0.239 and P=0.180 respectively).

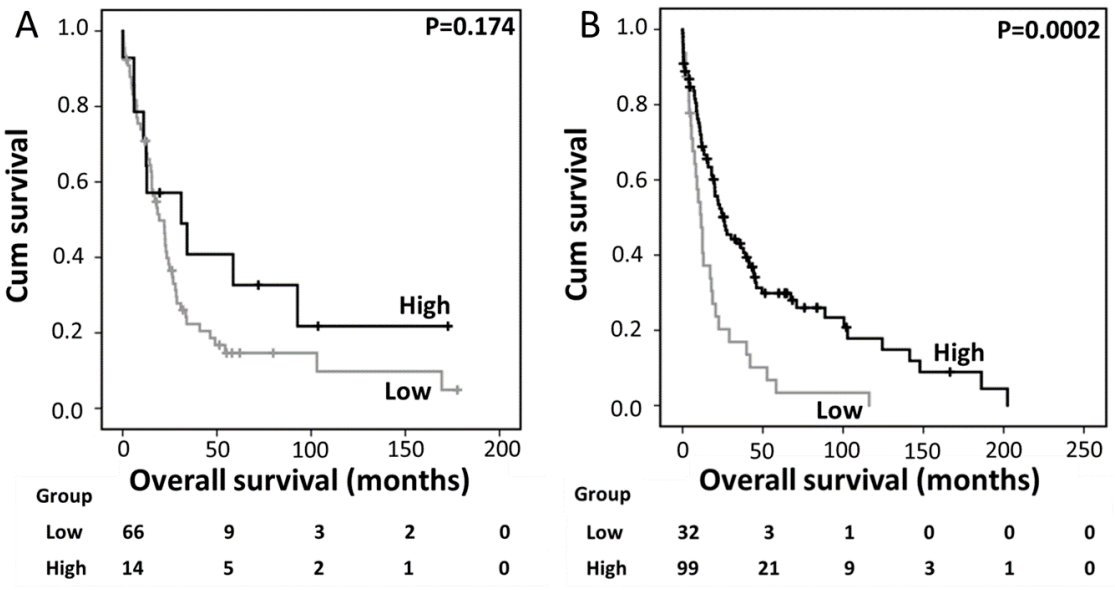


Figure 4.5: Kaplan-Meier analysis of association between TxNIP expression and overall survival in the carcinomas of the pancreas, bile duct and ampulla. Kaplan-Meier analysis of overall survival showing the impact of TxNIP expression in PAD cohort of 85 patients (A) and bile duct and ampullary carcinoma cohort of 145 patients (B) with significance determined using the log-rank test. Cytoplasmic TxNIP expression in PAD cohort (A) showed no association with overall survival (P=0.174), while high expression of cytoplasmic TxNIP in bile duct and ampullary carcinoma cohort (B) was significantly associated with better overall survival (P=0.0002).

Nuclear Trx expression remained significant for survival in multivariate Cox-regression analysis (Hazard Ratio (HR)=0.316; 95% confidence Interval (95% CI)=0.174-0.573; P<0.0001), while cytoplasmic Trx was not significant (HR=0.5; 95% CI=0.218-1.146; P=0.102) (Table 4.7).

In the multivariate Cox-regression, all the potentially confounding factors were included; even though none of these factors was independently associated with survival, discussed later in Section 4.5. Gender, age, tumour size, tumour grade, tumour stage, lymph node status, perineural invasion and venous invasion were included; with individual Kaplan-Meier statistics of P=0.380, P=0.694 P=0.419, P=0.820, P=0.349, P=0.063, P=0.163 and P=0.491 respectively.

A

PAD cohort	P value	EXP(B)	95.0% CI for EXP(B)	
			Lower	Upper
Cytoplasmic Trx expression	0.102	0.5	0.218	1.146
Gender	0.579	1.178	0.662	2.096
T stage	0.493	0.772	0.368	1.619
Node status	0.113	1.727	0.878	3.398
Venous invasion	0.833	1.068	0.581	1.962
Prenural invasion	0.305	1.521	0.682	3.392
Tumour size	0.221	1.825	0.697	4.784
Patient age	0.804	0.929	0.518	1.666
Grade	0.874	1.045	0.608	1.796

B

PAD cohort	P value	EXP(B)	95.0% CI for EXP(B)	
			Lower	Upper
Nuclear Trx expression	**<0.0001**	0.324	0.177	0.592
Gender	0.182	1.482	0.831	2.64
T stage	0.99	1.004	0.497	2.031
Node status	0.015	2.353	1.178	4.698
Venous invasion	0.292	1.412	0.744	2.679
Prenural invasion	0.985	1.008	0.458	2.217
Tumour size	0.132	2.202	0.788	6.155
Patient age	0.601	1.176	0.642	2.154
Grade	0.644	1.135	0.664	1.94

C

Bile duct and ampullary cancer cohort	P value	EXP(B)	95.0% CI for EXP(B)	
			Lower	Upper
TxNIP expression	**0.013**	0.548	0.34	0.882
T stage	0.063	1.634	0.974	2.741
Node status	0.054	1.586	0.992	2.537
Venous invasion	0.916	0.975	0.606	1.568
Prenural invasion	0.251	1.309	0.827	2.073
Grade	0.05	1.5	0.999	2.251

Table 4.7: Multivariate Cox Regression analysis of factors associated with overall survival in the carcinomas of the pancreas, bile duct and ampulla. Cox proportional hazards analysis for overall survival for cytoplasmic Trx expression (A) and nuclear Trx expression (B) in the PAD cohort. Cox proportional hazards analysis for overall survival for cytoplasmic TxNIP expression in the bile duct and ampullary cancer cohort (C).

In cancers of the bile duct and ampulla, high expression of cytoplasmic TxNIP (Figure 4.5B) was significantly associated with better overall survival (P=0.0002), which remained significant in multivariate Cox-regression analysis (HR=0.548; 95% CI=0.340-0.882; P=0.013) (Table 4.7C). This finding is comparable to the published studies as

discussed later in Section 4.5. Cytoplasmic Trx (Figure 4.6A), nuclear Trx (Figure 4.6B), cytoplasmic TrxR (Figure 4.6C) and nuclear TrxR (Figure 4.6D) showed no association with overall survival (P=0.08, P=0.144, P=0.144 and P=0.174 respectively). In the multivariate Cox-regression the potential confounding factors of patient grade, stage, lymph node status, perineural and venous invasion were significantly associated with survival (with individual Kaplan-Meier statistics of P=0.011, P=0.004, P=0.003 P=0.001 and P=0.012 respectively).

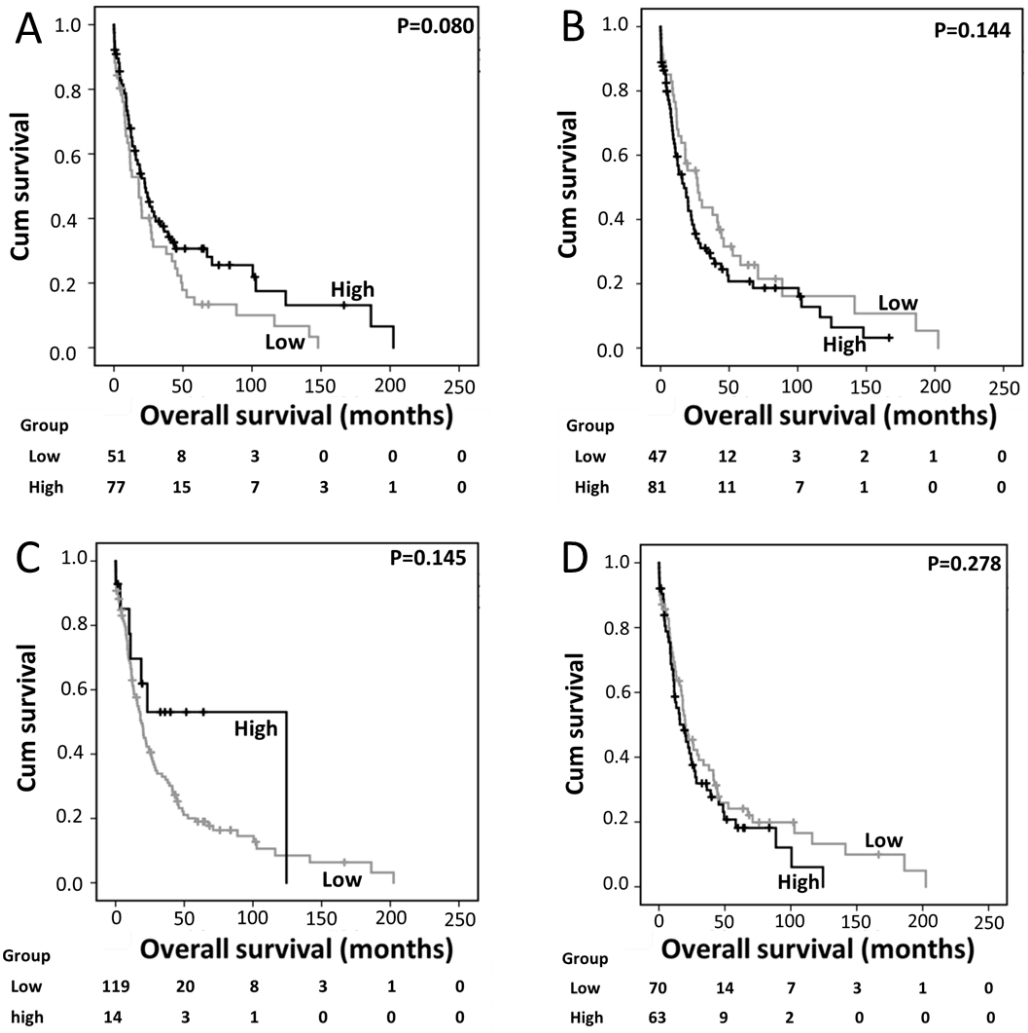


Figure 4.6: Kaplan-Meier analysis of association between Trx and TrxR expression and overall survival in bile duct and ampullary carcinoma cohort. Kaplan-Meier analysis of overall survival showing the impact of Trx and TrxR expression in bile duct and ampullary carcinoma cohort of 145 patients with significance determined using the log-rank test. Cytoplasmic Trx (A), nuclear Trx (B), cytoplasmic TrxR (C) and nuclear TrxR (D) expression showed no association with overall survival (P=0.080, P=0.144, P=0.145 and P=0.278 respectively).

As Trx and TrxR were expressed in both nucleus and cytoplasm, data were also analysed by grouping patients into combinations based upon expression profiles, i.e. low nuclear staining with low cytoplasmic, low nuclear with high cytoplasmic, high nuclear with low cytoplasmic and high nuclear with high cytoplasmic. In the PAD cohort, no significant correlation was observed in the combination analysis between nuclear and cytoplasmic expression of Trx or TrxR.

Further analysis in the bile duct and ampullary carcinoma cohort showed no significant correlation in the combination analysis between nuclear and cytoplasmic expression of TrxR. However, low nuclear with high cytoplasmic expression of Trx (n=14) showed longer overall survival than other three subgroups (n=114); either against each separate subgroup (P=0.017) (Figure 4.7A) or when the three subgroups were combined together (P=0.002) (Figure 47B).

Although there were only a limited number in the low nuclear/high cytoplasmic expressing subgroup (n=14, with 9 deaths/event), this finding is in contrast to a study that showed high nuclear with low cytoplasmic expression showed longer overall survival and progression-free survival in ovarian cancer patients (Woolston et al., 2010), as discussed later in Section 4.5.

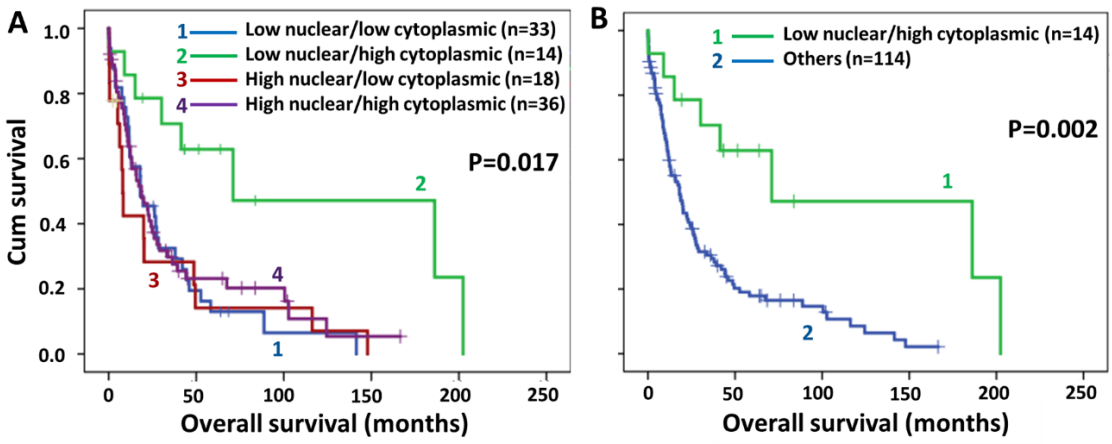


Figure 4.7: Kaplan–Meier overall survival analysis between different subgroups of Trx expression in the bile duct and ampullary cohort. Kaplan-Meier analysis of overall survival based upon expression profiles. Low nuclear/high cytoplasmic expression showed longer overall survival than other three subgroups either against each separate subgroup (A) or when the three subgroups were combined (B).

In conclusion, in the PAD cohort, an association was observed between high cytoplasmic TrxR expression and lymph node metastasis, while in bile duct and ampullary cancers, the high expression of nuclear TrxR and cytoplasmic TxNIP was associated with patients aged above 60 years. Associations were also observed between high nuclear TrxR expression and the presence of venous invasion and the presence of perineural invasion. Furthermore, low cytoplasmic TxNIP expression was associated with the presence of perineural invasion.

In terms of patients' survival, in the PAD cohort, high expression of cytoplasmic Trx and nuclear Trx was significantly associated with better overall survival, with nuclear Trx expression remained significantly associated with survival in multivariate Cox-regression analysis. In cancers of the bile duct and ampulla, expression of cytoplasmic TxNIP was significantly associated with better overall survival, which remained significant in multivariate Cox-regression analysis. Further analysis showed that low nuclear with high cytoplasmic expression of Trx showed longer overall survival than other expression profiles in the bile duct and ampullary carcinoma cohort.

4.5 Discussion

The Trx system regulates the redox state of different signalling molecules, and by regulating their redox state, can regulate cell growth, apoptosis, gene transcription, cell cycle progression and ROS levels (Sen and Packer, 1996, Saitoh et al., 1998, Mochizuki et al., 2009a). As shown earlier in Section 4.2, numerous studies have investigated the relationship of Trx system protein expression with clinicopathological criteria and patient survival outcomes in different types of cancer, including ovarian, breast, gastro-oesophageal, colorectal and brain cancers (Woolston et al., 2010, Woolston et al., 2011b, Woolston et al., 2012, Woolston et al., 2013, Mollbrink et al., 2014, Cai et al., 2017, Schultz et al., 2017). Nevertheless, expression of the Trx system has never been previously associated with clinical characteristics of PC patients. Only one study demonstrated that PDAC tissues were immunohistochemically more positive for Trx expression (24/32 cases) than pancreatic cystadenocarcinoma or normal pancreas tissues (Nakamura et al., 2000).

Current findings (Section 4.4.3) show that expression of Trx and TxNIP protein show no association with clinicopathological variables of the PAD cohort. However, high cytoplasmic TrxR expression was associated with lymph node metastasis (P=0.049). In contrast to the current findings, a previous study has described an association between low TrxR expression and lymph node metastasis (P=0.027) in 50 patients with oral squamous cell carcinoma (Iwasawa et al., 2011). In the bile duct and ampulla cancer cohort, current data (Section 4.4.3) show that high nuclear TrxR expression was associated with the presence of venous (P=0.001) and perineural invasion (P=0.021). In addition, low cytoplasmic TxNIP expression was significantly associated with the presence of perineural invasion (P=0.025). In agreement with current findings, a previous study has reported an association between high TxNIP and absence of perineural invasion (P=0.030) in 140 gastro-oesophageal adenocarcinoma patients (Woolston et al., 2013).

Current findings (Section 4.4.4) demonstrate that high expression of cytoplasmic Trx (P=0.018) and nuclear Trx (P=0.006) is significantly associated with better overall survival in the PAD patients, with nuclear Trx expression remains in multivariate Cox-regression (P<0.0001) while cytoplasmic Trx expression did not (P=0.102). This was perhaps unexpected as previous findings have indicated that high expression of Trx is associated with poor overall survival in certain tumour types. Raffle and colleagues observed that high expression of Trx was significantly associated with poor overall survival (P=0.004) in 12 colorectal cancer patients (Raffel et al., 2003). In 154 ovarian cancer patients, low cytoplasmic expression of Trx was significantly associated with better progression-free survival (P=0.032), whereas Trx nuclear expression did not (P=0.455) (Woolston et al., 2010). Another study showed that high expression of Trx was significantly associated with poor recurrence-free survival (P=0.008) and poor overall survival (P=0.015) in 65 gastric cancer patients (Lim et al., 2012). However, one study was comparable with the current findings and showed that high cytoplasmic expression of Trx was associated with better failure-free survival (P=0.049) in 174 Hodgkin lymphoma patients, which remained significant in multivariate Cox-regression analysis (P=0.023) (P. Vassilakopoulos et al., 2017), while another two studies showed no association between Trx expression and patients' survival in lung or breast cancers (Azuma et al., 2007, Woolston et al., 2012). Current data also show no relationship of cytoplasmic and nuclear TrxR expression with overall survival, unlike a study that showed that high expression of TrxR (P=0.021) and TxNIP (P=0.021) were significantly associated with better distant metastasis-free survival in 98 locally advanced breast cancer (Woolston et al., 2012).

Furthermore, the study showed that none of the tumour size, tumour grade, tumour stage, lymph node status, perineural invasion and venous invasion these factors was associated with survival of PAD patients. Although another study showed similar findings using the same two cohorts (Storr et al., 2012), this findings seem to be unusual as several studies showed PC survival was significantly influenced by, at least one or

more, tumour size, tumour grade, tumour stage and/or lymph node status (Sperti et al., 1996, Gebhardt et al., 2000, Cleary et al., 2004, Jamieson et al., 2013).

In conclusion, the current results of the PAD cohort show that high Trx expression seems to have a potential favourable impact on patients' prognosis, which disprove the hypothesis of Chapter 4. This unexpected finding as it shows that low Trx expression is an adverse prognostic factor for overall survival in PAD patients, while the main hypothesis of the *in vitro* assays, in Chapter 2 and 3, claims that inhibiting the Trx system shows adverse effects on PC cells. It is important to note, however, that immunohistochemical detection, and the Trx antibodies that are currently available, can detect only the total Trx expression in PC tissues, and is not able to discriminate between reduced, functional, Trx and oxidised, non-functional, Trx expression in archival material, which makes interpretation challenging. For example, Woolston and colleagues observed that high expression of TrxR and TxNIP were significantly associated with better distant metastasis-free survival although the biological functions of TrxR and TxNIP are opposed (TrxR reduces Trx while TxNIP inhibits the reducing activity of Trx) (Woolston et al., 2012). Therefore, the redox status of Trx protein in PAD cohort need to be identified by specific immunoassays such as the Trx redox status assay (Sun and Rigas, 2008, Yan et al., 2012) as discussed in Chapter 5.

In the bile duct and ampulla carcinoma cohort, current data (Section 4.4.4) reveal a strong association between high cytoplasmic TxNIP expression and better overall survival, which remained significant in multivariate Cox-regression analysis. As TxNIP is the endogenous inhibitor of the Trx system, current findings of the bile duct and ampulla carcinoma cohort confirmed the hypothesis of the current chapter, and are comparable with a previous study that showed high expression of TxNIP was significantly associated with distant metastasis-free survival (P=0.021) and overall survival (P=0.037) in 98 locally advanced breast cancer (Woolston et al., 2012). Also, Lim and colleagues observed a significant correlation between high expression of TxNIP and longer relapse-free survival (P=0.036) in 65 gastric cancer patients (Lim et al., 2012). Furthermore, a third study showed that high expression of TxNIP was significantly associated with a better disease

specific survival (P=0.016) in 66 gastro-oesophageal adenocarcinomas patients (Woolston et al., 2013). A recent study also showed that high-grade meningioma patients with strong TXNIP expression (n=37) had longer recurrence-free time (P=0.02) than those with weak expression of TxNIP (n=28) (Cai et al., 2017).

The bile duct and ampullary cancers were included in the current project as they are gastrointestinal cancers mostly treated as PC. The bile duct and ampullary cancers represent 5% of all gastrointestinal tract cancers, with ampullary cancers occur more frequently than distal common bile duct cancer with a ratio of 1:12 (Beger et al., 1999).

In the current project, PAD patients were categorised in a single cohort as they have much lower survival rate than the bile duct and ampullary patients (five-year survival were ~5%, 27.3% and 37% respectively), this variation in survival rates may be most likely explained by the differences between both cohorts in terms of tumour resectability rate (tumour resectability rates were 10-20%, 49.4% and 77.7% respectively) (Beger et al., 1999, Launois et al., 1999, De Castro et al., 2004, CancerResearchUK, 2017b). Early diagnosis due to early symptoms may explain the higher resectability rate and better survival outcomes of bile duct and ampullary patients compared with PAD patients. However, after tumour resection, several factors (such as genetic, embryologic, anatomic and histologic factors) have been related to survival for pancreatic, bile duct and ampullary cancer patients, with high tumour stage, large tumour size and lymph node metastases seem to adversely affect survival regardless of the origin of these cancers (Sarmiento et al., 2001).

As shown in Section 4.4.4, both cohorts showed differences between one another regarding the relationship of the Trx and TxNIP protein expression with patient survival outcomes, however, TrxR protein expression shows no association with patients' survival in both cohorts. Such unusual findings can be validated by reanalysing the current data by an extensive bioinformatics approach such as Artificial Neural Networks (ANNs). ANNs work in a nonlinear fashion that may better describe the interactions between health risk factors than traditional statistical models such as Kaplan-Meier survival (Cross et al., 1995). ANNs have been applied in complex medical decision making

and prediction of patients' prognosis in certain cancer types including breast, oesophagal and colorectal cancers (Lundin et al., 1999, Sato et al., 2005, Dolgobrodov et al., 2007). A previous study developed an ANN model for predicting survival in PDAC patients and showed that ANN survival predictions and Kaplan-Meier survival curves were identical (Ansari et al., 2013). The latter study suggested incorporating biomarkers such as genes, microRNAs, or proteins to increase the predictive ability of ANN. Therefore, analysing the current data by ANNs seems to be worthwhile to validate the current findings produced by Kaplan-Meier survival.

Further analysis in the bile duct and ampullary carcinoma cohort, showed that low nuclear with high cytoplasmic expression of Trx showed longer overall survival than other three subgroups; either against each subgroup (P=0.017) or when the three subgroups were combined (P=0.002) (Section 4.4.4). In contrast to the current findings, Woolston and colleagues investigated the associations between Trx expression and ovarian cancer patients' survival, and they observed that high nuclear with low cytoplasmic expression of Trx demonstrated a significantly better overall survival either against each separate subgroup (P=0.04) or when the three subgroups were combined together (P=0.004). Furthermore, high nuclear with low cytoplasmic expression of Trx were associated with better progression-free survival either against each separate subgroup (P=0.025) or when the three subgroups were combined together (P=0.003) (Woolston et al., 2010).

Numerous studies explained the differences in the subcellular localization of Trx protein in the mammalian cell, and showed that Trx protein was in reduced state within the nucleus more than in the cytoplasm, and it imported from the cytoplasm into the nucleus during oxidative stress either in normal or cancer cells (Hirota et al., 1999, Wei et al., 2000, Schroeder et al., 2007, Spielberger et al., 2008, Go and Jones, 2010). Furthermore, a previous study has demonstrated that nuclear Trx protein offers better protection against oxidative stress than cytoplasmic or mitochondrial Trx protein in human colonic epithelial cells (Go et al., 2007).

In summary, this study demonstrates that high nuclear and high cytoplasmic expression of Trx is associated with better overall survival in PAD patients, and high cytoplasmic TxNIP expression is associated with better survival in bile duct and ampullary cancer patients. Trx system protein expression is important in pancreatic, bile duct and ampullary cancers, and may influence disease progression and cancer cell susceptibility to anticancer agents. The current findings warrant a larger follow-up study with increased numbers of patients.

Chapter 5: General discussion

5.1 General discussion

Targeting the Trx system, by inhibiting TrxR, has been studied in terms of the role it plays in regulating a radioresponse of cancer cells; with the intent to modulate intracellular ROS levels and induce lethal effects. The main aim of the current project is to investigate the involvement of the Trx system in PC radioresponse using novel TrxR inhibitors (IQ9 and IQ10) produced at the University of Nottingham as potential anti-cancer agents (Yan et al., 2009, Yan et al., 2012). In addition, the current project aimed to evaluate the related mechanisms of action of IQs on the Trx system by examining their effects on intracellular ROS levels, TrxR activity and protein expression of Trx system family members. As IQs are a class of bioreductive agents, the current project also sought to examine the cytotoxic effect of IQs on PC cell lines under hypoxic conditions. Moreover, the current study investigated the relationship between protein expression of Trx system family members with clinicopathological criteria and patient survival outcome, using IHC, in 230 PC cancer patients.

In order to explore the role of IQs in PC cancer, the present study first screened the cytotoxic effect of IQs (in terms of cell proliferation and clonogenic survival) on three PC cancer cell lines (PANC-1, MIA Paca-2 and BxPc-3 cell lines), with two of them (PANC-1 and BxPc-3 cell lines) being selected to examine the effect of IQs on TrxR activity level.

In terms of proliferation assay, IQs were effective against proliferation of all three PC cell lines as single agents, with IC50 values in the low nanomolar range (IC50=90-920 nM). However. current proliferation IC50 values of IQs for PC cell lines were found to be higher than published studies (IC50=18-270 nM) using a high-throughput screening short-term assay, MTT assay (Yan et al., 2009, Yan et al., 2012). The MTT assay is a commonly used assay to determine cell viability, rather than cell numbers, based on enzymatic reduction of the water soluble tetrazolium dye (yellow) to water insoluble formazan crystals (purple) by dehydrogenases occurring mainly in the outer side of mitochondrial inner membranes (90%) and other organelles (10%) such as endoplasmic reticulum (Slater et al., 1963, Berridge and Tan, 1993). Therefore, MTT assay has also

been used to measure mitochondrial function rather than cell viability (Rago et al., 1991, Vukmanović and Zamoyska, 1991). As inhibition of the Trx system causes significant mitochondrial dysfunction and endoplasmic reticulum stress in cancer cells (Fiskus et al., 2014, Zou et al., 2015), the MTT assay may not be a suitable method to assess the cytotoxicity of agents, such as IQs, relying on mitochondrial function in their mechanism of action. Therefore, any changes in mitochondria activity pre-tetrazolium treatment may change the rate of MTT reduction, and consequently alter the result of cell counting. Other short-term assays, such as the SRB assay, may be more accurate to measure the viability of cells treated with redox protein inhibitors, as the method is based on measuring total protein mass of cells, which is directly proportional to cell number (Skehan et al., 1990, Vichai and Kirtikara, 2006).

Although short-term assays can provide an indication of cellular apoptosis and distinct cellular morphological changes post drug treatment, these assays measure only early functional changes, with no information of overall toxicity of treatment (Woolston and Martin, 2011). Therefore, the present study also evaluated the cytotoxicity of IQs against PC by using a long-term assay - clonogenic survival. In contrast to short-term assays, clonogenic survival can evaluate multiple mediators of cell killing and investigate the end result of treatment which can either be cell death or recovery. Furthermore, the clonogenic assay has particular relevance to the radiotherapy of tumours as it can evaluate the further growth (recurrence) of cancer cells, in particular cancer stem cells, following radiotherapy (Eric J. Hall, 2012). Therefore, the clonogenic assay has become the ‘gold standard’ for assessing cellular sensitivity to anti-cancer agents and irradiation (Brown and Wouters, 1999, Franken et al., 2006, Woolston and Martin, 2011).In terms of clonogenic survival, PC cell lines were treated with IQs for two exposure times of 4 and 48 hours (MIA Paca-2 cells were treated only for 48 hours) before plating them for clonogenic survival. Clonogenic survival showed that MIA Paca-2 cells (IC50 240-260 nM) were more sensitive to IQs than PANC-1 (IC50 730-900 nM) and BxPc-3 cells (IC50 >1000 nM).

As shown in Chapter 2, PANC-1 and BxPc-3 cells treated with clonogenic IC50 of IQs for 48 hours showed an increase in radiosensitisation, but with low SER values (1.08-1.13). It may be, however, that improved sensitisation could be achieved by altering treatment parameters (such as changing exposure time or O_2 levels) and investigating related mechanisms of action of IQs (such as effect of IQs on intracellular ROS level, protein expression of Trx system family members and TrxR activity) – which was the main aim of Chapter 3 as discussed below.

Current results showed that PC cell lines treated with IQs alone showed an increase, albeit marginal, in ROS levels, with a maximum fold increase of 1.25. On the other hand, PC cells treated with IQs in combination with H_2O_2 showed an increase in ROS levels, with a maximum fold increase of 1.5 to 2.3, indicating that cells were less able to deal with the induced oxidative stress in the presence of IQs. The effect of IQs on intracellular ROS levels in PC cell lines has never been studied. However, current assessment of ROS levels has many limitations, practically and theoretically, which are discussed later in Section 5.2.

As shown in Chapter 3, the current study also sought to investigate the effect of IQs on TrxR protein expression in PANC-1, MIA Paca-2 and BxPc-3 PC cells. Results showed that IQ9 and IQ10 had no effect on TrxR protein expression across all PC cell lines. Therefore, the effect of IQs on the activity of TrxR was determined.

In the TrxR activity assay, PANC-1 and BxPc-3 cells treated with IQs showed a substantial decrease in TrxR activity in a dose-dependent manner, with 4 hours of treatment giving a greater inhibition than 48 hours of treatment, making the stability of IQs in culture medium perhaps questionable, as discussed later in Section 5.2.2. Therefore, assessment of radiation sensitivity of PANC-1 cells treated with IQs for 4 hours was performed, with the intent to maximise the effect of IQs on radiosensitivity in PANC-1 cells, as discussed below.

PANC-1 cells treated with the clonogenic IC50 of IQ9 (900 nM) for 4 hours showed a significant increase in radiosensitisation at 6 and 8 Gy (53% increase at 6 Gy ($P< 0.001$)

and 71% increase at 8 Gy (P< 0.0001)), with SER values of 1.12. Although, there is a marginal increase in PANC-1 radiosensitivity treated with IQ9 for 4 hours (SER=1.12) compared to 48 hours (SER=1.08), SER values for both exposure times were very low, making the biological relevance of IQs as radiosensitisers somewhat questionable.

Several assumptions may explain the marginal effect of IQs and AUR on radiation sensitivity of PC cells. A major assumption is the potential expression of other redox systems, such as the glutathione system, that may compensate the inhibition of the Trx system and subsequently maintain intracellular ROS levels induced by radiation. Recently, dual inhibition of both systems has been highlighted in several recent studies that showed lethal synergistic effect, as single agents or combined with radiation, in different types of cancer cells (Hwang et al., 2015, Harris et al., 2015, Kiebala et al., 2015, Rodman et al., 2016, Wang et al., 2017). Therefore, dual inhibition of both systems in PC cells is a possible approach to be considered for future work with this project as discussed in Section 5.2.2.

Also, the stability of IQs in cell culture medium is a potential important factor that could reduce the efficacy of IQs against PC cells. Current data shows that IQ9 treatment for 4 hours strongly inhibits the clonogenic survival and TrxR activity in BxPc-3 cells compared to treatment for 48 hours (Table 3.3 and Figure 3.13), suggesting that IQs have a short half-life rather than a long half-life. Similarly, PANC-1 cells also seem slightly sensitive to IQ9 after 4 hours treatment compared to 48 hours' treatment in terms of clonogenic survival (IC50 values: 610 nM vs 900 nM) and radiation sensitivity (SER values 1.12 vs 1.08). The half-life of IQs in cell culture medium has never been studied – this is actively being examined by the group.

As IQs are bioreductive agents, theoretically, low O_2 levels may increase the reduction/activity of IQs against PC cells. Therefore, the current study sought to evaluate the cytotoxic effect of IQs on proliferation and clonogenic survival of PC cell lines under hypoxic conditions. In terms of proliferation assay, PANC-1 and BxPc-3 seem sensitive to IQ9, at 48 hours treatment, than normoxic cells, with HCR values of 1.4 and

1.2 respectively. In terms of clonogenic survival, PANC-1 and BxPc-3 hypoxic cells seem sensitive to IQ9 compared to normoxic PANC-1 cells either after 4 hours' treatment or 48 hours' treatment. Although both cell lines seem more sensitive to IQs in hypoxia than normoxia, the HCR values of both cell lines were much lower (HCR≤2.4) than well-characterised hypoxic sensitisers, such as SR tirapazamine (HCR=50-200) (Zeman et al., 1986) or achiral phosphoramidate mustards (HCR=200-300) (Duan et al., 2008), making the biological significance of IQs as potential hypoxic cytotoxins doubtful. However, the main aim of assessing the effect of IQs on PC cell lines in hypoxia was to determine the IC50 of IQs for both cell lines in hypoxia, and subsequently performing a drug-radiation clonogenic survival assay in hypoxic conditions, which has unfortunately not been achieved due to a lack of time and technical problems - this has been set as future work in this project as discussed in Section 5.2.2.

In vitro results were almost comparable to *in vivo* results that were obtained by our collaborator, Professor Kaye J Williams at the Division of Pharmacy & Optometry, School of Biology, Medicine and Health at the University of Manchester. As indicated earlier, BxPc-3 and PANC-1 cell lines and the IQ10 agent were selected for *in vivo* evaluation. In summary, xenografts were established from PANC-1 and BxPc-3 cell lines. Once palpable tumours were established, volume measurements were taken at least 3 times a week using callipers. When tumours reach a volume of approximately 250 mm^3, treatments of IQ10 alone, radiation alone or a drug-radiation combination were applied. Based on a previous *in vivo* study (Yan et al., 2009), the initial treatment plan for drug alone treatment was scheduled to be 6 doses of IQ9 administrated via oral gavage at a dose of 1 mg/kg daily, with the first dose initiated after 24 hours before the start of 5 daily fractions of 2 Gy. On radiation days, IQ10 was given 60 minutes prior to radiotherapy. However, unexpectedly, toxicity was observed in some animals, which resulted in a revised protocol whereby IQ10 was given on days 1, 3 and 5 of the radiation therapy schedule. As shown in Figure 5.1, results showed that IQ10 alone induced a 4 day growth delay (mean = 26.8 days) in BxPc-3 xenografts (n=6) (time for volume to quadruple post-treatment compared with controls (n=13, mean=22.2 days)). However, IQ10 alone had

no effect on PANC-1 xenografts (n=2, mean=24 days) compared to control (n=9, mean=23 days) (Figure 5.1). A significant enhancement in growth delay was observed using radiation alone in both BxPc-3 (9 days, mean= 31.2 days, n=9, P=0.002) and PANC-1 (17 days, mean= 41 days, n=6, P=0.0005) xenografts (Figure 5.1). Unfortunately, this radiation-induced effect was not significantly altered by coincidental IQ10 treatment either in BxPc-3 (n=5, mean=30.2 days) or PANC-1 (n=6, mean= 40 days) xenograft models (Figure 5.1).

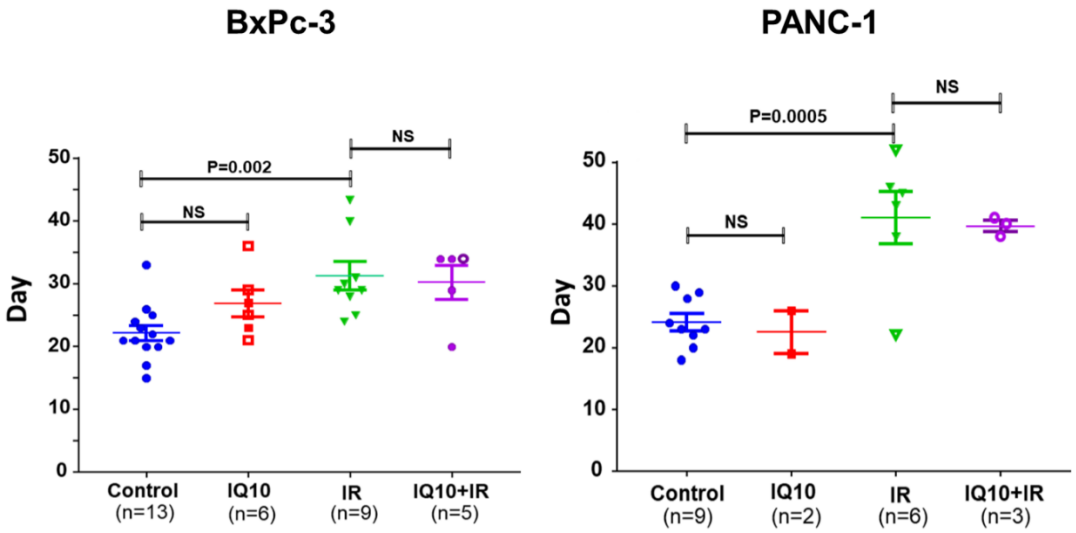


Figure 5.1: Effect of IQ10 on growth delay of BxPc-3 and PANC-1 xenograft models. Xenografts were established from BxPc-3 and PANC-1 cell lines. Results showed that IQ10 alone induced a 4 day growth delay in BxPc-3 xenografts, but had no effect on PANC-1 xenografts. Radiation alone caused a significant growth delay in both BxPc-3 and PANC-1 xenografts. A combination of IQ10 and radiation showed no effect on both xenograft models compared to the treatment with radiation alone.

Differences between *in vitro* and *in vivo* data may be expected, as *in vitro* systems measure the direct effect of IQs on PC cells, but *in vivo* system IQs are exposed to variable levels of multiple metabolic processes in different tissues. In terms of drug alone treatment, *in vivo* results of PANC-1 cells were not directly comparable to *in vitro* results and showed that IQ10 exhibited potent cytotoxicity on PANC-1 cell lines, with IC50 values in the nanomolar range, while *in vivo* results of BxPc-3 cells were comparable with the *in vitro* findings (Section 2.4.2). In terms of radiation alone, *in vivo* results were comparable to *in vitro* results and showed that both cell lines responded to radiation

treatment (Section 2.4.3.1). In drug-radiation combination assay, the *in vivo* protocol was based on multiple doses of IQs (1mg/kg) prior to fractionated radiation exposure (5 daily fractions of 2 Gy), while *in vitro* protocol was based on exposing PC cells to a single dose (IC50) of IQs for 48 hours followed by a single radiation dose of 0, 1, 2, 4, 6 or 8 Gy. Regardless of the differences between both protocols, *in vitro* radiosensitisation at 6 Gy was observed in both cells treated with IQ10, while no radiosensitisation was observed with *in vivo* experiments. It is important to note that the radiosensitising effect of IQs, *in vitro* or *in vivo*, on PC cell lines has never before been studied.

A previous *in vivo* study by Yan and colleagues (Yan et al., 2009) observed that MIA PaCa-2 xenografts treated with IQ8 and IQ9 at 1.0 or 2.5 mg/kg every other day for 20 days showed significant growth inhibition in a dose-dependent manner compared to control. This potentially conflicting data may be a result of the different dosing regimen between both studies, however, Yan and colleagues also applied different IQs (IQ8 and IQ9) and used a different PC cell line (MIA Paca-2), whereas the current *in vivo* study used fewer doses, and IQ10 against PANC-1 and BxPc-3 xenograft tumours.

Furthermore, both studies showed no information regarding IQs delivery to tumours, IQs distribution within tumours or stability of IQs in the biological system. The stability of IQs in the biological system was a main concern of two IQ-related anti-cancer agents that were evaluated in clinical trials; PX-12 and EO9. As indicated in Section 1.2.3.2.2, the rapid metabolism of PX-12 in plasma proteins was a potential cause of the failure of PX-12 in clinical trials (Ramanathan et al., 2007), whilst the rapid clearance EO9 (Section 2.2.2.2.1) was a main cause of the failure of EO9 in clinical evaluations. Therefore, evaluating the IQs stability may help to explain such *in vivo* results as discussed in Section 5.2.2.

Several studies investigated the association between redox proteins expression, including protein expression of Trx system family members, and clinical characteristics of different cancers including breast, ovarian, gastro-oesophageal, colon, lymphoma and brain cancers (Woolston et al., 2010, Woolston et al., 2011a, Woolston et al., 2011b,

Woolston et al., 2012, Woolston et al., 2013, Mollbrink et al., 2014, Cai et al., 2017, P. Vassilakopoulos et al., 2017). To our knowledge, the current study is the first time that the expression of Trx system proteins has been assessed, in a simultaneous fashion, in a large cohort of cancer patients (n=230); 85 PAD patients and 145 cancers of the bile duct and ampulla. Although bile duct and ampulla cancers show a higher resectability rate (48% and 50% of patients respectively) and a better prognosis (five-year survival were 28.6% and 41.7% respectively) than PC, these cancers were included in the current study as they are surgically and chemotherapeutically treated as PC (Wade et al., 1997, Sarmiento et al., 2001, Riall et al., 2006).

As shown in Chapter 4, high protein expression of cytoplasmic (P=0.018) and nuclear Trx (P=0.06) are significantly associated with better overall survival in PAD patients (remaining significant in multivariate Cox-regression (P<0.0001)), with no association observed between TrxR and TxNIP protein expression and PAD patient survival. Current results differ from with certain published literature which show that protein expression of Trx is associated with a worse overall survival in different cancers (Raffel et al., 2003, Woolston et al., 2010, Lim et al., 2012), whilst two studies are consistent with current findings (Woolston et al., 2011b, P. Vassilakopoulos et al., 2017) and two further studies that show no association with the protein expression of Trx expression cancer patients' survival (Azuma et al., 2007, Woolston et al., 2012).

Current *in vitro* results suggest that inhibition of the Trx/TrxR system may be a useful potential target in PC, while the immunohistochemical analysis showed that high Trx expression was significantly associated with better overall survival in PC patients (high Trx expression is a good prognosis) This conflict between the in vitro results and the immunohistochemical analysis may be explained by the limitation of the current antibodies used in immunohistochemical detection to discriminate between oxidised or reduced states of Trx protein. Trx exists in the cellular system in two forms, oxidised form (inactive form) and reduced form (active form). Current antibodies applied in IHC can detect only the total Trx expression in PC tissues, and is unable to discriminate between reduced Trx and oxidised Trx expression in archival material. However, a

specific technique such as the Trx redox status assay may be able to identify the redox state of Trx by determining the relative abundance of oxidized and reduced Trx in cellular lysates (Sun and Rigas, 2008, Yan et al., 2012). However, this technique is based on native protein gel electrophoresis, which is more suitable to apply to lysates extracted from cultured cell lines rather than these from archival tissue material (e.g. TMAs).

5.2 Limitations, future work and conclusions

5.2.1. Practical limitations for *in vitro* models

Several practical limitations were identified for *in vitro* assays including experimental design, number of experiments, number of replicates for each experiment and statistical analysis of certain results.

Although the initial plan for this project was to repeat each experiment three times, certain experiments were performed as single experiments or in duplicate due to the lack of time or technical difficulties. In detail, two initial/optimisation experiments were performed as single experiments; optimisation of HU in cell cycle analysis (Figure 2.14) and the effect of IQs on radiosensitivity of MIA Paca-2 cells following 1 hour treatment (Figure 3.14). Furthermore, certain cytotoxicity, clonogenic and radiosensitivity experiments were performed in duplicate (Figures 2.8, 2.9, 2.10, 2.11, 2.13B, 3.4, 3.5, 3.12, 3.13, 3.15, 3.18, 3.20 and 3.21) due to a lack of time or to other factors or challenges.

In ROS level assessments (Figures 3.4 and 3.5), the initial plan was to conduct three experiments for each cell line for each drug (IQ9, IQ10 or AUR). However, after the second experiment for each cell line, the flow cytometer system was broken for a long period of time. Therefore, only two independent experiments were performed. Due to the nature of protocol of ROS level assessments (Section 3.3.2), each experiment was performed in a single T25 flask (10^6 cells in a single T25 flask were needed for each drug/time exposure with/without H_2O_2 to complete a single experiment). In TrxR activity assay, only two experiments were performed due to a lack of time, with each experiment performed, according to the protocol in Section 3.3.4, in duplicate.

In drug-radiation - clonogenic survival assay (Sections 2.4.3.2 and 3.4.4), the statistical method used to demonstrate the significant effect of IQs on radiation sensitivity between treated cells and control cells was based on calculating the statistical differences at a single radiation dose, i.e. 6 or 8 Gy, rather than calculating the statistical

differences between both curves, which is a statistical limitation. However, the statistical comparison of both curves in an LQ model has been a challenge for a long time. A recent software (LQ-Script) created by Eberhard Karls University (Germany) is dedicated to analysing radiosensitivity measured by survival fractions in the LQ model, with a statistical and graphical comparison between treated and control curves by evaluating confidence intervals and prediction bounds (Marzec et al., 2018).

5.2.2. Theoretical limitation for *in vitro* models and future work

In the ROS level assessment, as indicated in Section 3.5, H_2O_2 was used as an alternative to radiation to induce cellular oxidative stress in order to evaluate the ability of PC cells to cope with oxidative stress in the presence of IQs. Although this simulation seems reasonable, it has certain limitations due to several assumptions. Firstly, PC cells are exceptionally sensitive (IC50=30-40 mM, Figure 3.2) to H_2O_2 compared to other types of cancer cell lines (Chen et al., 2005, Du et al., 2010). Due to the hypersensitivity of PC cells to H_2O_2, the maximum cellular ROS level post H_2O_2 treatment was 1.2 to 1.4-fold over control, whilst MDA-MB-231 BC cells treated with H_2O_2 showed more than 4-fold in ROS over control (Figure 3.3). The marginal increase in ROS levels in PC cells post H_2O_2 treatment may limit the ability of this technique to evaluate IQs effect on PC cells under oxidative stress.

Secondly, it is a challenge to quantify the exact amount of ROS in the biological system by conventional flow cytometry due to the unstable reactivity status of ROS molecules as they rapidly react with oxidised adjacent molecules in the cellular system. For example, $OH^{\bullet}$ is a main ROS molecule, responsible for two-thirds of the x-ray damage to DNA in mammalian cells, and has a biological half-life of less than 10^{-9} seconds (Eric J. Hall, 2012). Therefore, recent studies have suggested a unique assay such as protein carbonyl quantification to quantify damages induced by ROS rather than quantify ROS per say (Suzuki et al., 2010, Fedorova et al., 2014).

The biomolecule carbonylation has been known as a major hallmark of oxidative stress (Dalle-Donne et al., 2006, Yao and Rahman, 2011). Briefly, ROS molecules induced from oxidative stress react/oxidise with amino acids in proteins to form carbonyl groups (e.g. aldehydes, ketones, and lactams), and then, carbonyl groups are reduced by 2,4-Dinitrophenylhydrazine (DNPH) to form detectable DNP groups. DNP levels can then be determined either by spectrophotometer at an absorbance of 360 nm (Levine et al., 1990), Western blot (oxyblot technique) (Goto et al., 1999), IHC (Astruc et al., 2007) or enzyme-linked immunosorbent assay (ELISA) (Jung et al., 2006). For future work, applying a protein carbonylation assay to the current study may give a better understanding of IQs effect on cellular ROS levels rather than conventional flow cytometry.

Certain results in the current study, such as those from the TrxR activity assay and the clonogenic assay, suggest that IQs have a short half-life. However, the half-life of the parent compound ES936 or its analogues (IQs), either *in vitro* or *in vivo,* has never been studied, which is a major limitation to the current study. Determination of the half-life of anti-cancer agents is important to evaluate as the pharmacokinetic characteristics of such drugs and their mechanism of action, may explain variations in results between preclinical and clinical studies. For example, EO9 showed a significant antitumor activity with *in vitro* studies (Section 2.2.2.2.2), with a half-life of 6.3 hours in culture medium (Phillips et al., 1992a). However, EO9 failed to demonstrate a significant antitumor activity in clinical trials due to its poor stability in the biological system, with a biological half-life between 1.9 and 3 minutes in mice, and between 0.8 to 19 minutes in humans (Workman et al., 1992, Schellens et al., 1994).

As mentioned earlier, the marginal effect of IQs on radiation sensitivity as well as the different responses to IQs between PC cell lines may be due to the expression of another redox system, mainly the GSH system. The GSH system may compensate for the inhibition of the Trx system following IQs treatment. Therefore, as mentioned earlier, dual inhibition of the Trx and GSH systems seems to be a promising strategy used by several recent studies with intent to achieve optimum ROS levels and subsequently

induce lethal effects on cancer cells. Two novel studies used AUR, and BSO (well-characterised inhibitors of the GSH system) to induce dual inhibition of Trx and GSH systems in MDA-MB-231 breast cancer cell line and various malignant B-cell lines respectively (Harris et al., 2015, Kiebala et al., 2015). The latter studies showed synergistic cancer cell death with high ROS levels observed with *in vitro* and *in vivo* models. Furthermore, a recent study showed a dual inhibition of TrxR and GR by using a single herbal product, plumbagin (5-hydroxy-2-methyl-1, 4-naphthoquinone) (Hwang et al., 2015). This study found that plumbagin has dual inhibition functions; it acts as a competitive inhibitor to TrxR by preventing it from reacting with oxidised Trx (TrxR reduced plumbagin instead of oxidised Trx) in addition to acting as a direct inhibitor to GR. The study showed that plumbagin caused high ROS levels and high apoptosis induction in the liver, lungs and cervical cancer cell lines leading to synergistic cell death (Hwang et al., 2015). Recently, a novel curcumin analogue (dimethoxycurcumin) exhibited dual inhibition effects on the Trx and GSH systems in lung, prostate and breast cancer cells causing a significant increase in the cellular radiosensitisation, apoptosis and mitotic cell death (Jayakumar et al., 2016). Only one study investigated the effect of dual inhibition of both systems on radiation sensitivity (Rodman et al., 2016). The latter study showed a significant increase in radiation sensitivity of BC cancer stem cells (*in vivo* and *in vitro*) after dual inhibition of Trx and GSH systems by AUR and BSO respectively. To our knowledge, dual inhibition of the Trx and GSH systems, with/without radiation, in PC cells has never been studied, therefore, it has been proposed for future work in the current project.

Although several inhibitors of the Trx system were evaluated or are currently being investigated in clinical trials for cancer treatment (Section 1.2.3.2.2), none of these inhibitors seem to be specific to the Trx system in the cellular system (Zhang et al., 2017a). Therefore, a major challenge in developing therapeutic drugs inhibitors of the Trx system is the lack of specific inhibitors. In detail, most of the TrxR inhibitors in the literature are based on the strong nucleophilicity or metal affinity of the Sec residue within the C terminus of TrxR. Another residue existing within the C terminal of TrxR is

Cys residue, which may react with these inhibitors, but with a weak reactivity compared to the Sec residue (Zhang et al., 2017a). Although more than 20 genes encoding selenoproteins, including TrxR, have been identified in human cells (Bulteau and Chavatte, 2015), targeting Sec residue in TrxR is more reactive and accessible than the other proteins. This is due to the fact that Sec residue in TrxR is exposed at the surface of the enzyme, whilst Sec residue in other proteins are buried within the proteins. In general, the main challenge for TrxR inhibitors is to avoid reacting with cellular thiols, especially ones that are much more abundant than selenols (Zhang et al., 2017a). In terms of IQs, Yan and colleagues investigated the specificity of IQs to TrxR by determining the activity assay of two related-TrxR enzymes (GR and GPx) in MIA Paca-2 cells treated with IQs (IQ3 and IQ9) (Yan et al., 2012). It is important to note that GR has no Sec residue, whilst GPx has Sec residue but it is not as exposed as that in TrxR (Ren et al., 1997). Authors observed that IQs showed no effect on the activity of GR and GPx, and they stated that 'these data also demonstrated that the IQ compounds are relatively specific inhibitors of TR1 in human pancreatic cells', which seems unconvincing in terms of TrxR specificity as a recent report showed that more than 20 genes encoding selenoproteins existed in human cells (Bulteau and Chavatte, 2015). As current data shows that IQs were more toxic than AUR across all PC cell lines, it therefore appeared worthwhile to examine if IQs have other potential molecular targets in the cellular system rather than TrxR. Therefore, for future work, knocking down TrxR, using siRNA or shRNA, in PC cells, then examining the cytotoxic effect of IQs on PC cells seems to be a good strategy to evaluate the specificity of IQs against TrxR.

As the current data in Section 3.4.5 shows that PANC-1 and BxPc-3 hypoxic cells seem slightly more sensitive to IQ9 than normoxic cells, it will be interesting, as a long-term future study, to perform an IQ-radiation combination - clonogenic survival assay under hypoxic conditions. Also, to mimic *in vivo* models, it will be worthwhile to investigate the effect of IQs on PC cells -/+ hypoxia using spheroid 3D models treated with fractionated radiation.

Moreover, as shown in Chapter 4, high nuclear TrxR protein expression was associated with the presence of venous invasion (P=0.001) and perineural invasion (P=0.021), while low cytoplasmic TxNIP expression was associated with the presence of perineural invasion (P=0.025) in bile duct and ampullary carcinoma cohorts. Such results suggest that the Trx system is involved in invasion and metastasis of the bile duct and ampullary carcinomas. Therefore, it would be interesting to evaluate, in future work, the role of the Trx system in modulating migration and invasion of the bile duct and ampullary carcinomas, and whether this can be modulated by TrxR inhibitors such as IQs.

5.2.3. Conclusion

In conclusion, the current study suggests that targeting the Trx system, by IQs, may be a useful potential strategy for treating PC. Current findings show that IQs are effective in PC cell lines as single agents, with IC50 values in the low nanomolar range. However, IQs were less potent than GM, as standard first-line chemotherapy in PC, and more potent than AUR, as a well-characterised TrxR inhibitor. IQs arrest the cell cycle and enhance radiotherapeutic efficacy in certain PC cell lines, but with low SER values, making the biological relevance of IQs as radiosensitisers somewhat questionable. The first hypothesis of the current study (Section 1.3.1) has been proven but only in certain PC cell lines and, as a result, therefore there is little potential for clinical impact. Also, the current study evaluates the related mechanisms of action of IQs on the Trx/TrxR system and shows that IQs exhibited high efficacy to inhibit TrxR activity and increase ROS levels under oxidative stress, with no notable changes in protein expression of TrxR. Therefore, the second hypothesis of this study has been proven but again, only in certain PC cell lines. Hypoxia increases, albeit slightly with low HCR values, the cytotoxic efficacy of IQs on PC cell lines, which proves the third hypothesis of the current study. However, hypoxia seems to have no effect on the expression of any of the Trx system proteins or related reductase enzymes. Certain results in the current study, such as TrxR activity assay, clonogenic assay and drug-radiation combination assay, suggest that IQs have a short half-life rather than a long half-life. With *in vivo* models, kindly performed by a co-

investigator in this project, it was shown that IQs caused a significant growth delay in certain PC xenograft models as single agents. There was no radiosensitising effect observed, suggesting a marginal biological significance of IQs on PC with *in vivo* models. Although the current results suggests that inhibition of the Trx/TrxR system by IQs exhibit potent *in vitro* cytotoxicity against PC cell lines, high protein expression of Trx protein expression was significantly associated with a worse overall survival in the PAD cohort, which rejects the fourth hypothesis in the current study. However, a high expression of cytoplasmic TxNIP was significantly associated with a better overall survival, which proves the fourth hypothesis of the current study. In summary, the Trx family protein expression can be used prognostically in patients with pancreatic, bile duct and ampullary cancers, and may influence cancer cell susceptibility to anticancer agents. Table 5.1 summarises the main hypotheses of the current study (Section 1.3.1), and discusses in detail the expected and observed results of each hypothesis for each cell line or marker.

In order to maximise the effect of IQs as single agents or in combination with radiation, several assays were considered for future work with the intention of studying certain related mechanisms of action of IQs on the Trx system. These could be protein carbonyl quantification assay or dual inhibition of the Trx and GSH systems, or to investigate certain pharmacokinetic characteristics of IQs in terms of specificity or stability.

Hypothesis	Expected results according to hypothesis	Cell line /marker	Observed results	The hypothesis has been
1- Radiosensitivity and cell cycle progression of PC cells are altered by treatment with IQs.	1.1. PC cells treated with IQs show a significant increase in radiation sensitivity compared to control.	PANC-1	A significant increase in radiation sensitivity, but with low SER.	proven
		BxPc-3		
		MIA Paca-2	No radiosensitivity effect.	disproven
	1.2. PC cells treated with IQs show a significant effect of IQs on cell cycle progression.	PANC-1	A significant arrest at G0/G1 phase.	proven
		BxPc-3	No significant effect on cell cycle progression.	disproven
2- IQ treatment impairs the function of the Trx system in PC cell lines.	2.1. IQs treatment impairs PC cells' ability to maintain oxidative stress.	PANC-1	IC50 combined with H_2O_2 increased the oxidative stress ~2 fold over treatment with H_2O_2 alone.	proven
		BxPc-3		
		MIA Paca-2		
	2.2. IQs treatment inhibits the protein expression of TrxR in PC cell lines.	PANC-1	IQs showed no effect on TrxR expression across all PC cell lines.	disproven
		BxPc-3		
		MIA Paca-2		
	2.3. IQs treatment inhibits the TrxR activity in PC cell lines.	PANC-1	A substantial decrease in TrxR activity in a dose-dependent manner.	proven
		BxPc-3		
3- Hypoxia increases the cytotoxic efficacy of IQs on PC cell lines.	3.1. In terms of proliferation and clonogenic survival, PC cells seem more sensitive to IQ9 in hypoxia than normoxia.	PANC-1	Hypoxic PC cells seem more sensitive to IQ9 than normoxia, but with low HCR.	proven
		BxPc-3		
4- Elevated protein expression of Trx and TrxR is an adverse prognostic factor for overall survival in patients with pancreatic, bile duct and ampullary cancers.	High protein expression of Trx and TrxR and low protein expression of TxNIP are associated with worse overall survival in tumours from PAD patients.	Trx	High cytoplasmic and nuclear expression of Trx was significantly associated with better overall survival.	disproven
		TrxR	No association.	disproven
		TxNIP	No association.	disproven
	High protein expression of Trx and TrxR and low protein expression of TxNIP are associated with worse overall survival in tumours from bile duct and ampullary carcinoma patients.	Trx	No association.	disproven
		TrxR	No association.	disproven
		TxNIP	High expression of TxNIP was significantly associated with better overall survival.	proven

Table 5.1: Summary of the main hypotheses, expected results and observed results of each cell line/marker applied to the current study

References

ADSAY, N. V., PIERSON, C., SARKAR, F., ABRAMS, J., WEAVER, D., CONLON, K. C., BRENNAN, M. F. & KLIMSTRA, D. S. 2001. Colloid (Mucinous Noncystic) Carcinoma of the Pancreas. *The American Journal of Surgical Pathology,* 25**,** 26-42.

AGGARWAL, G., KAMADA, P. & CHARI, S. T. 2013. Prevalence of diabetes mellitus in pancreatic cancer compared to common cancers. *Pancreas,* 42**,** 198-201.

ALCOCK, R. A., DEY, S., CHENDIL, D., INAYAT, M. S., MOHIUDDIN, M., HARTMAN, G., CHATFIELD, L. K., GALLICCHIO, V. S. & AHMED, M. M. 2002. Farnesyltransferase inhibitor (L-744,832) restores TGF-β type II receptor expression and enhances radiation sensitivity in K-ras mutant pancreatic cancer cell line MIA PaCa-2. *Oncogene,* 21**,** 7883.

ALLEN, V. B., GURUSAMY, K. S., TAKWOINGI, Y., KALIA, A. & DAVIDSON, B. R. 2016. Diagnostic accuracy of laparoscopy following computed tomography (CT) scanning for assessing the resectability with curative intent in pancreatic and periampullary cancer. *The Cochrane Library*.

ALSTON, E., BAE, S. & ELTOUM, I. A. 2014. Atypical cytologic diagnostic category in EUS-FNA of the pancreas: follow-up, outcomes, and predictive models. *Cancer Cytopathol,* 122**,** 428-34.

ANATHY, V., ROBERSON, E. C., GUALA, A. S., GODBURN, K. E., BUDD, R. C. & JANSSEN-HEININGER, Y. M. W. 2011. Redox-Based Regulation of Apoptosis: S-Glutathionylation As a Regulatory Mechanism to Control Cell Death. *Antioxidants & Redox Signaling,* 16**,** 496-505.

ANDREADOU, I., ILIODROMITIS, E. K., FARMAKIS, D. & KREMASTINOS, D. T. 2009. To prevent, protect and save the ischemic heart: antioxidants revisited. *Expert Opinion on Therapeutic Targets,* 13**,** 945-56.

ANSARI, D., NILSSON, J., ANDERSSON, R., REGNÉR, S., TINGSTEDT, B. & ANDERSSON, B. 2013. Artificial neural networks predict survival from pancreatic cancer after radical surgery. *The American Journal of Surgery,* 205**,** 1-7.

ANTWI, S. O., ECKERT, E. C., SABAQUE, C. V., LEOF, E. R., HAWTHORNE, K. M., BAMLET, W. R., CHAFFEE, K. G., OBERG, A. L. & PETERSEN, G. M. 2015. Exposure to environmental chemicals and heavy metals, and risk of pancreatic cancer. *Cancer Causes & Control,* 26**,** 1583-1591.

ARNER, E. S. & HOLMGREN, A. 2000. Physiological functions of thioredoxin and thioredoxin reductase. *European Journal of Biochemistry,* 267**,** 6102-9.

ASTRUC, T., MARINOVA, P., LABAS, R., GATELLIER, P. & SANTÉ-LHOUTELLIER, V. 2007. Detection and localization of oxidized proteins in muscle cells by fluorescence microscopy. *Journal of agricultural and food chemistry,* 55**,** 9554-9558.

AWWAD, H. 2013. *Radiation oncology: radiobiological and physiological perspectives: the boundary-zone between clinical radiotherapy and fundamental radiobiology and physiology*, Springer Science & Business Media.

AZUMA, K., KOMOHARA, Y., SASADA, T., TERAZAKI, Y., IKEDA, J., HOSHINO, T., ITOH, K., YAMADA, A. & AIZAWA, H. 2007. Excision repair cross-complementation group 1

predicts progression-free and overall survival in non-small cell lung cancer patients treated with platinum-based chemotherapy. *Cancer science,* 98**,** 1336-1343.

BACHMANN, J., MICHALSKI, C. W., MARTIGNONI, M. E., BÜCHLER, M. W. & FRIESS, H. 2006. Pancreatic resection for pancreatic cancer. *HPB : The Official Journal of the International Hepato Pancreato Biliary Association,* 8**,** 346-351.

BAILEY, H. H., RIPPLE, G., TUTSCH, K. D., ARZOOMANIAN, R. Z., ALBERTI, D., FEIERABEND, C., MAHVI, D., SCHINK, J., POMPLUN, M., MULCAHY, R. T. & WILDING, G. 1997. Phase I Study of Continuous-Infusion l - S,R -Buthionine Sulfoximine With Intravenous Melphalan. *JNCI: Journal of the National Cancer Institute,* 89**,** 1789-1796.

BAILEY, S. M., LEWIS, A. D., PATTERSON, L. H., FISHER, G. R., KNOX, R. J. & WORKMAN, P. 2001. Involvement of NADPH: cytochrome P450 reductase in the activation of indoloquinone EO9 to free radical and DNA damaging species. *Biochemical pharmacology,* 62**,** 461-468.

BAKER, A., ADAB, K., RAGHUNAND, N., CHOW, H., STRATTON, S., SQUIRE, S., BOICE, M., PESTANO, L., KIRKPATRICK, D. & DRAGOVICH, T. 2013. A phase IB trial of 24-hour intravenous PX-12, a thioredoxin-1 inhibitor, in patients with advanced gastrointestinal cancers. *Investigational new drugs,* 31**,** 631-641.

BAKER, A., PAYNE, C. M., BRIEHL, M. M. & POWIS, G. 1997. Thioredoxin, a gene found overexpressed in human cancer, inhibits apoptosis in vitro and in vivo. *Cancer Res,* 57**,** 5162-7.

BANIN, S., MOYAL, L., SHIEH, S., TAYA, Y., ANDERSON, C. W., CHESSA, L., SMORODINSKY, N. I., PRIVES, C., REISS, Y., SHILOH, Y. & ZIV, Y. 1998. Enhanced phosphorylation of p53 by ATM in response to DNA damage. *Science,* 281**,** 1674-7.

BARDEESY, N. & DEPINHO, R. A. 2002. Pancreatic cancer biology and genetics. *Nature Reviews Cancer,* 2**,** 897.

BARENDSEN, G. 1968. RESPONSES OF CULTURED CELLS, TUMOURS, AND NORMAL TISSUES TO RADIATIONS OF DIFFERENT LINEAR ENERGY TRANSFER. Health Research Organization TNO, Rijswijk, Netherlands.

BASU, A. K. & MARNETT, L. J. 1983. Unequivocal demonstration that malondialdehyde is a mutagen. *Carcinogenesis,* 4**,** 331-333.

BEDFORD, J. S. 1991. Sublethal damage, potentially lethal damage, and chromosomal aberrations in mammalian cells exposed to ionizing radiations. *International Journal of Radiation Oncology* Biology* Physics,* 21**,** 1457-1469.

BEGER, H. G., TREITSCHKE, F., GANSAUGE, F., HARADA, N., HIKI, N. & MATTFELDT, T. 1999. Tumor of the ampulla of Vater: experience with local or radical resection in 171 consecutively treated patients. *Archives of surgery,* 134**,** 526-532.

BEN, Q., XU, M., NING, X., LIU, J., HONG, S., HUANG, W., ZHANG, H. & LI, Z. 2011. Diabetes mellitus and risk of pancreatic cancer: A meta-analysis of cohort studies. *European Journal of Cancer* 47**,** 1928-37.

BERGGREN, M. M. & POWIS, G. 2001. Alternative splicing is associated with decreased expression of the redox proto-oncogene thioredoxin-1 in human cancers. *Archives of biochemistry and biophysics,* 389**,** 144-149.

BERRIDGE, M. V. & TAN, A. S. 1993. Characterization of the cellular reduction of 3-(4, 5-dimethylthiazol-2-yl)-2, 5-diphenyltetrazolium bromide (MTT): subcellular localization, substrate dependence, and involvement of mitochondrial electron transport in MTT reduction. *Archives of biochemistry and biophysics,* 303**,** 474-482.

BERROZPE, G., SCHAEFFER, J., PEINADO, M. A., REAL, F. X. & PERUCHO, M. 1994. Comparative analysis of mutations in the p53 and K-ras genes in pancreatic cancer. *International Journal of Cancer,* 58**,** 185-91.

BHATIA, M., MCGRATH, K. L., DI TRAPANI, G., CHAROENTONG, P., SHAH, F., KING, M. M., CLARKE, F. M. & TONISSEN, K. F. 2016. The thioredoxin system in breast cancer cell invasion and migration. *Redox Biology,* 8**,** 68-78.

BIAGLOW, J. E., CLARK, E. P., EPP, E. R., MORSE-GUADIO, M., VARNES, M. E. & MITCHELL, J. B. 1983. Nonprotein thiols and the radiation response of A549 human lung carcinoma cells. *Int J Radiat Biol Relat Stud Phys Chem Med,* 44**,** 489-95.

BIAGLOW, J. E. & MILLER, R. A. 2005. The thioredoxin reductase/thioredoxin system: novel redox targets for cancer therapy. *Cancer biology & therapy,* 4**,** 13-20.

BIANKIN, A., BIANKIN, S., KENCH, J., MOREY, A., LEE, C., HEAD, D., ECKSTEIN, R., HUGH, T., HENSHALL, S. & SUTHERLAND, R. 2002. Aberrant p16INK4A and DPC4/Smad4 expression in intraductal papillary mucinous tumours of the pancreas is associated with invasive ductal adenocarcinoma. *Gut,* 50**,** 861-868.

BILIMORIA, K. Y., BENTREM, D. J., KO, C. Y., STEWART, A. K., WINCHESTER, D. P. & TALAMONTI, M. S. 2007. National failure to operate on early stage pancreatic cancer. *Annals of Surgery,* 246**,** 173-80.

BLACKFORD, A., PARMIGIANI, G., KENSLER, T. W., WOLFGANG, C., JONES, S., ZHANG, X., PARSONS, D. W., LIN, J. C., LEARY, R. J., ESHLEMAN, J. R., GOGGINS, M., JAFFEE, E. M., IACOBUZIO-DONAHUE, C. A., MAITRA, A., KLEIN, A., CAMERON, J. L., OLINO, K., SCHULICK, R., WINTER, J., VOGELSTEIN, B., VELCULESCU, V. E., KINZLER, K. W. & HRUBAN, R. H. 2009. Genetic mutations associated with cigarette smoking in pancreatic cancer. *Cancer Research,* 69**,** 3681-8.

BLOCK, K. I., KOCH, A. C., MEAD, M. N., TOTHY, P. K., NEWMAN, R. A. & GYLLENHAAL, C. 2008. Impact of antioxidant supplementation on chemotherapeutic toxicity: a systematic review of the evidence from randomized controlled trials. *International Journal of Cancer,* 123**,** 1227-1239.

BO, Z., YONGPING, S., FENGCHAO, W., GUOPING, A. & YONGJIANG, W. 2005. Identification of differentially expressed proteins of gamma-ray irradiated rat intestinal epithelial IEC-6 cells by two-dimensional gel electrophoresis and matrix-assisted laser desorption/ionisation-time of flight mass spectrometry. *Proteomics,* 5**,** 426-432.

BOIVIN, A., HANOT, M., MALESYS, C., MAALOUF, M., ROUSSON, R., RODRIGUEZ-LAFRASSE, C. & ARDAIL, D. 2011. Transient alteration of cellular redox buffering before irradiation triggers apoptosis in head and neck carcinoma stem and non-stem cells. *PLoS One,* 6**,** e14558.

BOSMAN, F. T., CARNEIRO, F., HRUBAN, R.H., THEISE, N.D 2010. WHO Classification of Tumours of the Digestive System. 4th edition ed. Lyon: International Agency for Research on Cancer (IARC).

BOUFFARD, D. Y., LALIBERTÉ, J. & MOMPARLER, R. L. 1993. Kinetic studies on 2', 2'-difluorodeoxycytidine (Gemcitabine) with purified human deoxycytidine kinase and cytidine deaminase. *Biochemical pharmacology,* 45**,** 1857-1861.

BRAGG, W. H. & KLEEMAN, R. 1905. XXXIX. On the α particles of radium, and their loss of range in passing through various atoms and molecules. *The London, Edinburgh, and Dublin Philosophical Magazine and Journal of Science,* 10**,** 318-340.

BROWN, C. O., SALEM, K., WAGNER, B. A., BERA, S., SINGH, N., TIWARI, A., CHOUDHURY, A., BUETTNER, G. R. & GOEL, A. 2012. Interleukin-6 counteracts therapy-induced cellular oxidative stress in multiple myeloma by up-regulating manganese superoxide dismutase. *Biochemical Journal,* 444**,** 515-27.

BROWN, J. M. & WILSON, W. R. 2004. Exploiting tumour hypoxia in cancer treatment. *Nature Reviews Cancer,* 4**,** 437.

BROWN, J. M. & WOUTERS, B. G. 1999. Apoptosis, p53, and tumor cell sensitivity to anticancer agents. *Cancer research,* 59**,** 1391-1399.

BRUNNER, T. B., CENGEL, K. A., HAHN, S. M., WU, J., FRAKER, D. L., MCKENNA, W. G. & BERNHARD, E. J. 2005. Pancreatic Cancer Cell Radiation Survival and Prenyltransferase Inhibition: The Role of K-Ras. *Cancer Research,* 65**,** 8433.

BUCHS, N. C., BUHLER, L., BUCHER, P., WILLI, J. P., FROSSARD, J. L., ROTH, A. D., ADDEO, P., ROSSET, A., TERRAZ, S., BECKER, C. D., RATIB, O. & MOREL, P. 2011. Value of contrast-enhanced 18F-fluorodeoxyglucose positron emission tomography/computed tomography in detection and presurgical assessment of pancreatic cancer: a prospective study. *Journal of Gastroenterology and Hepatology,* 26**,** 657-62.

BULTEAU, A.-L. & CHAVATTE, L. 2015. Update on selenoprotein biosynthesis. *Antioxidants & redox signaling,* 23**,** 775-794.

BURRELL, M. M. 1993. RNase A (EC 3.1. 27.5). *Enzymes of Molecular Biology***,** 263-270.

BURT, B. A. 2001. Definitions of risk. *Journal of Dental Education,* 65**,** 1007-8.

C. XAVIER, H. W. A. X. L. 2015. Inhibition of the Glutaredoxin System Increases Doxorubicin Sensitivity in Hepatocellular Carcinoma by Impairing the Nrf2-dependent Antioxidant Response. *Research Appreciation Day* UNT Health Science Center , Texax.

CAI, Z., ZHANG, C., ZOU, Y., LU, C., HU, H., QIAN, J., JIANG, L. & HU, G. 2017. Tissue thioredoxin-interacting protein expression predicted recurrence in patients with meningiomas. *International journal of clinical oncology,* 22**,** 660-666.

CALDAS, C., HAHN, S. A., DA COSTA, L. T., REDSTON, M. S., SCHUTTE, M., SEYMOUR, A. B., WEINSTEIN, C. L., HRUBAN, R. H., YEO, C. J. & KERN, S. E. 1994. Frequent somatic mutations and homozygous deletions of the p16 (MTS1) gene in pancreatic adenocarcinoma. *Nature Genetics,* 8**,** 27-32.

CALDAS, C. & KERN, S. E. 1995. K-ras mutation and pancreatic adenocarcinoma. *International journal of pancreatology,* 18**,** 1-6.

CALVERT, P., YAO, K.-S., HAMILTON, T. C. & O'DWYER, P. J. 1998. Clinical studies of reversal of drug resistance based on glutathione. *Chemico-biological interactions,* 111**,** 213-224.

CAMERON, J. L., RIALL, T. S., COLEMAN, J. & BELCHER, K. A. 2006. One thousand consecutive pancreaticoduodenectomies. *Annals of surgery,* 244**,** 10-5.

CAMP, R. L., DOLLED-FILHART, M. & RIMM, D. L. 2004. X-tile: a new bio-informatics tool for biomarker assessment and outcome-based cut-point optimization. *Clin Cancer Res,* 10**,** 7252-9.

CANCERRESEARCHUK. 2017a. *Cancer Stats: Cancer Statistics for the UK* [Online]. Available: http://www.cancerresearchuk.org/cancer-info/cancerstats/.

CANCERRESEARCHUK. 2017b. *Pancreatic cancer statistics, Cancer Research UK.* [Online]. Available: http://www.cancerresearchuk.org/health-professional/cancer-statistics/statistics-by-cancer-type/pancreatic-cancer#heading-Two.

CAO, J., YANG, J., RAMACHANDRAN, V., ARUMUGAM, T., DENG, D., LI, Z., XU, L. & LOGSDON, C. D. 2015. TM4SF1 promotes gemcitabine resistance of pancreatic cancer in vitro and in vivo. *PloS one,* 10**,** e0144969.

CASINI, A., KELTER, G., GABBIANI, C., CINELLU, M. A., MINGHETTI, G., FREGONA, D., FIEBIG, H.-H. & MESSORI, L. 2009. Chemistry, antiproliferative properties, tumor selectivity, and molecular mechanisms of novel gold (III) compounds for cancer treatment: a systematic study. *JBIC Journal of Biological Inorganic Chemistry,* 14**,** 1139-1149.

CERDA, M. B., LLOYD, R., BATALLA, M., GIANNONI, F., CASAL, M. & POLICASTRO, L. 2017. Silencing peroxiredoxin-2 sensitizes human colorectal cancer cells to ionizing radiation and oxaliplatin. *Cancer Letters,* 388**,** 312-319.

CHAKRABORTI, P. K., GARABEDIAN, M. J., YAMAMOTO, K. R. & SIMONS, S. S., JR. 1992. Role of cysteines 640, 656, and 661 in steroid binding to rat glucocorticoid receptors. *The Journal of biological chemistry,* 267**,** 11366-73.

CHARI, S. T., KELLY, K., HOLLINGSWORTH, M. A., THAYER, S. P., AHLQUIST, D. A., ANDERSEN, D. K., BATRA, S. K., BRENTNALL, T. A., CANTO, M., CLEETER, D. F., FIRPO, M. A., GAMBHIR, S. S., GO, V. L., HINES, O. J., KENNER, B. J., KLIMSTRA, D. S., LERCH, M. M., LEVY, M. J., MAITRA, A., MULVIHILL, S. J., PETERSEN, G. M., RHIM, A. D., SIMEONE, D. M., SRIVASTAVA, S., TANAKA, M., VINIK, A. I. & WONG, D. 2015. Early detection of sporadic pancreatic cancer: summative review. *Pancreas,* 44**,** 693-712.

CHELIKANI, P., FITA, I. & LOEWEN, P. C. 2004. Diversity of structures and properties among catalases. *Cellular and molecular life sciences,* 61**,** 192-208.

CHEN, D., NIU, M., JIAO, X., ZHANG, K., LIANG, J. & ZHANG, D. 2012. Inhibition of AKT2 enhances sensitivity to gemcitabine via regulating PUMA and NF-κB signaling pathway in human pancreatic ductal adenocarcinoma. *International journal of molecular sciences,* 13**,** 1186-1208.

CHEN, Q., ESPEY, M. G., KRISHNA, M. C., MITCHELL, J. B., CORPE, C. P., BUETTNER, G. R., SHACTER, E. & LEVINE, M. 2005. Pharmacologic ascorbic acid concentrations selectively kill cancer cells: action as a pro-drug to deliver hydrogen peroxide to

tissues. *Proceedings of the national academy of sciences of the United States of America,* 102**,** 13604-9.

CHEN, Q., ESPEY, M. G., SUN, A. Y., LEE, J.-H., KRISHNA, M. C., SHACTER, E., CHOYKE, P. L., POOPUT, C., KIRK, K. L., BUETTNER, G. R. & LEVINE, M. 2007. Ascorbate in pharmacologic concentrations selectively generates ascorbate radical and hydrogen peroxide in extracellular fluid in vivo. *Proceedings of the National Academy of Sciences,* 104**,** 8749-8754.

CHEN, W. C., MCBRIDE, W. H., IWAMOTO, K. S., BARBER, C. L., WANG, C. C., OH, Y. T., LIAO, Y. P., HONG, J. H., DE VELLIS, J. & SHAU, H. 2002. Induction of radioprotective peroxiredoxin-I by ionizing irradiation. *Journal of neuroscience research,* 70**,** 794-8.

CHEW, E.-H., LU, J., BRADSHAW, T. D. & HOLMGREN, A. 2008a. Thioredoxin reductase inhibition by antitumor quinols: a quinol pharmacophore effect correlating to antiproliferative activity. *The FASEB Journal,* 22**,** 2072-2083.

CHEW, E. H., LU, J., BRADSHAW, T. D. & HOLMGREN, A. 2008b. Thioredoxin reductase inhibition by antitumor quinols: a quinol pharmacophore effect correlating to antiproliferative activity. *The FASEB Journal,* 22**,** 2072-83.

CHIOREAN, E. G. & COVELER, A. L. 2015. Pancreatic cancer: optimizing treatment options, new, and emerging targeted therapies. *Drug Design, Development and Therapy,* 9**,** 3529-3545.

CHUI, C. S., CHAN, M. F., YORKE, E., SPIROU, S. & LING, C. C. 2001. Delivery of intensity-modulated radiation therapy with a conventional multileaf collimator: Comparison of dynamic and segmental methods. *Medical Physics,* 28**,** 2441-2449.

CLEARY, S. P., GRYFE, R., GUINDI, M., GREIG, P., SMITH, L., MACKENZIE, R., STRASBERG, S., HANNA, S., TAYLOR, B. & LANGER, B. 2004. Prognostic factors in resected pancreatic adenocarcinoma: analysis of actual 5-year survivors. *Journal of the American College of Surgeons,* 198**,** 722-731.

COLLARD, J., MATTHEW, A. M., DOUBLE, J. A. & BIBBY, M. C. 1995. EO9: relationship between DT-diaphorase levels and response in vitro and in vivo. *British journal of cancer,* 71**,** 1199-203.

COMITO, T., COZZI, L., CLERICI, E., FRANZESE, C., TOZZI, A., IFTODE, C., NAVARRIA, P., D'AGOSTINO, G., RIMASSA, L., CARNAGHI, C., PERSONENI, N., TRONCONI, M. C., DE ROSE, F., FRANCESCHINI, D., ASCOLESE, A. M., FOGLIATA, A., TOMATIS, S., SANTORO, A., ZERBI, A. & SCORSETTI, M. 2017. Can Stereotactic Body Radiation Therapy Be a Viable and Efficient Therapeutic Option for Unresectable Locally Advanced Pancreatic Adenocarcinoma? Results of a Phase 2 Study. *Technology in cancer research & treatment,* 16**,** 295-301.

CONNER, J. R., MARIÑO-ENRÍQUEZ, A., MINO-KENUDSON, M., GARCIA, E., PITMAN, M. B., SHOLL, L. M., SRIVASTAVA, A. & DOYLE, L. A. 2017. Genomic Characterization of Low- and High-Grade Pancreatic Mucinous Cystic Neoplasms Reveals Recurrent KRAS Alterations in “High-Risk” Lesions. *Pancreas,* 46**,** 665-671.

CONRAD, M., JAKUPOGLU, C., MORENO, S. G., LIPPL, S., BANJAC, A., SCHNEIDER, M., BECK, H., HATZOPOULOS, A. K., JUST, U., SINOWATZ, F., SCHMAHL, W., CHIEN, K.

R., WURST, W., BORNKAMM, G. W. & BRIELMEIER, M. 2004. Essential role for mitochondrial thioredoxin reductase in hematopoiesis, heart development, and heart function. *Molecular and cellular biology,* 24**,** 9414-23.

CONROY, T., DESSEIGNE, F., YCHOU, M., BOUCHÉ, O., GUIMBAUD, R., BÉCOUARN, Y., ADENIS, A., RAOUL, J.-L., GOURGOU-BOURGADE, S., DE LA FOUCHARDIÈRE, C., BENNOUNA, J., BACHET, J.-B., KHEMISSA-AKOUZ, F., PÉRÉ-VERGÉ, D., DELBALDO, C., ASSENAT, E., CHAUFFERT, B., MICHEL, P., MONTOTO-GRILLOT, C. & DUCREUX, M. 2011. FOLFIRINOX versus Gemcitabine for Metastatic Pancreatic Cancer. *New England Journal of Medicine,* 364**,** 1817-1825.

CRANE, C. H. 2016. Hypofractionated ablative radiotherapy for locally advanced pancreatic cancer. *Journal of Radiation Research,* 57**,** i53-i57.

CRANE, C. H., ABBRUZZESE, J. L., EVANS, D. B., WOLFF, R. A., BALLO, M. T., DELCLOS, M., MILAS, L., MASON, K., CHARNSANGAVEJ, C., PISTERS, P. W., LEE, J. E., LENZI, R., VAUTHEY, J. N., WONG, A. B., PHAN, T., NGUYEN, Q. & JANJAN, N. A. 2002. Is the therapeutic index better with gemcitabine-based chemoradiation than with 5-fluorouracil-based chemoradiation in locally advanced pancreatic cancer? *International journal of radiation oncology, biology, physics,* 52**,** 1293-302.

CRANE, C. H., VARADHACHARY, G. R., YORDY, J. S., STAERKEL, G. A., JAVLE, M. M., SAFRAN, H., HAQUE, W., HOBBS, B. D., KRISHNAN, S., FLEMING, J. B., DAS, P., LEE, J. E., ABBRUZZESE, J. L. & WOLFF, R. A. 2011. Phase II trial of cetuximab, gemcitabine, and oxaliplatin followed by chemoradiation with cetuximab for locally advanced (T4) pancreatic adenocarcinoma: correlation of Smad4(Dpc4) immunostaining with pattern of disease progression. *Journal of clinical oncology,* 29**,** 3037-43.

CRIPPA, S., SALVIA, R., WARSHAW, A. L., DOMINGUEZ, I., BASSI, C., FALCONI, M., THAYER, S. P., ZAMBONI, G., LAUWERS, G. Y., MINO-KENUDSON, M., CAPELLI, P., PEDERZOLI, P. & CASTILLO, C. F. 2008. Mucinous cystic neoplasm of the pancreas is not an aggressive entity: lessons from 163 resected patients. *Annals of surgery,* 247**,** 571-9.

CRISSMAN, H. A. & HIRONS, G. T. 1994. Staining of DNA in live and fixed cells. *Methods in cell biology,* 41**,** 195-209.

CROSS, S. S., HARRISON, R. F. & KENNEDY, R. L. 1995. Introduction to neural networks. *The Lancet,* 346**,** 1075-1079.

CULLEN, J. J., MITROS, F. A. & OBERLEY, L. W. 2003a. Expression of Antioxidant Enzymes in Diseases of the Human Pancreas: Another Link Between Chronic Pancreatitis and Pancreatic Cancer. *Pancreas,* 26**,** 23-27.

CULLEN, J. J., WEYDERT, C., HINKHOUSE, M. M., RITCHIE, J., DOMANN, F. E., SPITZ, D. & OBERLEY, L. W. 2003b. The role of manganese superoxide dismutase in the growth of pancreatic adenocarcinoma. *Cancer Research,* 63**,** 1297-303.

CUMMING, G., FIDLER, F. & VAUX, D. L. 2007. Error bars in experimental biology. *The Journal of cell biology,* 177**,** 7-11.

CUNNINGHAM, D., CHAU, I., STOCKEN, D. D., VALLE, J. W., SMITH, D., STEWARD, W., HARPER, P. G., DUNN, J., TUDUR-SMITH, C., WEST, J., FALK, S., CRELLIN, A., ADAB, F., THOMPSON, J., LEONARD, P., OSTROWSKI, J., EATOCK, M., SCHEITHAUER, W.,

HERRMANN, R. & NEOPTOLEMOS, J. P. 2009. Phase III Randomized Comparison of Gemcitabine Versus Gemcitabine Plus Capecitabine in Patients With Advanced Pancreatic Cancer. *Journal of Clinical Oncology,* 27**,** 5513-5518.

CURTIN, J. F., DONOVAN, M. & COTTER, T. G. 2002. Regulation and measurement of oxidative stress in apoptosis. *Journal of Immunological Methods,* 265**,** 49-72.

DAHIYA, P., KAMAL, R., GUPTA, R., BHARDWAJ, R., CHAUDHARY, K. & KAUR, S. 2013. Reactive oxygen species in periodontitis. *Journal of Indian Society of Periodontology,* 17**,** 411-416.

DALLE-DONNE, I., ALDINI, G., CARINI, M., COLOMBO, R., ROSSI, R. & MILZANI, A. 2006. Protein carbonylation, cellular dysfunction, and disease progression. *Journal of cellular and molecular medicine,* 10**,** 389-406.

DARBY WEYDERT, C. J., SMITH, B. B., XU, L., KREGEL, K. C., RITCHIE, J. M., DAVIS, C. S. & OBERLEY, L. W. 2003. Inhibition of oral cancer cell growth by adenovirusMnSOD plus BCNU treatment. *Free radical biology & medicine,* 34**,** 316-29.

DAVIES, M. J. 2016. Protein oxidation and peroxidation. *The Biochemical journal,* 473**,** 805-25.

DE CASTRO, S., VAN HEEK, N., KUHLMANN, K. F., BUSCH, O. R., OFFERHAUS, G., VAN GULIK, T. M., OBERTOP, H. & GOUMA, D. 2004. Surgical management of neoplasms of the ampulla of Vater: local resection or pancreatoduodenectomy and prognostic factors for survival. *Surgery,* 136**,** 994-1002.

DE LA SANTA, L. G., RETORTILLO, J. A. P., MIGUEL, A. C. & KLEIN, L. M. 2014. Radiology of pancreatic neoplasms: An update. *World Journal of Gastrointestinal Oncology,* 6**,** 330-343.

DE LANEY, T. F. & KOOY, H. M. 2008. *Proton and charged particle radiotherapy*, Lippincott Williams & Wilkins.

DE SOUSA CAVALCANTE, L. & MONTEIRO, G. 2014. Gemcitabine: metabolism and molecular mechanisms of action, sensitivity and chemoresistance in pancreatic cancer. *European journal of pharmacology,* 741**,** 8-16.

DEER, E. L., GONZALEZ-HERNANDEZ, J., COURSEN, J. D., SHEA, J. E., NGATIA, J., SCAIFE, C. L., FIRPO, M. A. & MULVIHILL, S. J. 2010. Phenotype and genotype of pancreatic cancer cell lines. *Pancreas,* 39**,** 425-35.

DEHN, D. L., SIEGEL, D., SWANN, E., MOODY, C. J. & ROSS, D. 2003. Biochemical, Cytotoxic, and Genotoxic Effects of ES936, a Mechanism-Based Inhibitor of NAD(P)H:quinone Oxidoreductase 1, in Cellular Systems. *Molecular Pharmacology,* 64**,** 714-720.

DEHN, D. L., SIEGEL, D., ZAFAR, K. S., REIGAN, P., SWANN, E., MOODY, C. J. & ROSS, D. 2006. 5-Methoxy-1, 2-dimethyl-3-[(4-nitrophenoxy) methyl] indole-4, 7-dione, a mechanism-based inhibitor of NAD (P) H: quinone oxidoreductase 1, exhibits activity against human pancreatic cancer in vitro and in vivo. *Molecular Cancer Therapeutics,* 5**,** 1702-1709.

DEL RIO, D., STEWART, A. J. & PELLEGRINI, N. 2005. A review of recent studies on malondialdehyde as toxic molecule and biological marker of oxidative stress. *Nutrition, metabolism and cardiovascular diseases,* 15**,** 316-328.

DEMPLE, B. & HARRISON, L. 1994. Repair of oxidative damage to DNA: enzymology and biology. *Annual review of biochemistry,* 63**,** 915-48.

DENNING, T. L., TAKAISHI, H., CROWE, S. E., BOLDOGH, I., JEVNIKAR, A. & ERNST, P. B. 2002. Oxidative stress induces the expression of Fas and Fas ligand and apoptosis in murine intestinal epithelial cells. *Free radical biology & medicine,* 33**,** 1641-50.

DIRIX, L. Y., TONNESEN, F., CASSIDY, J., EPELBAUM, R., TEN BOKKEL HUININK, W. W., PAVLIDIS, N., SORIO, R., GAMUCCI, T., WOLFF, I., TE VELDE, A., LAN, J. & VERWEIJ, J. 1996. EO9 phase II study in advanced breast, gastric, pancreatic and colorectal carcinoma by the EORTC Early Clinical Studies Group. *European Journal of Cancer and Clinical Oncology,* 32A**,** 2019-22.

DISCHE, S., CHASSAGNE, D., HOPE-STONE, H., DAWES, P., ROBERTS, J., YOSEF, H., BEY, P., HORIOT, J.-C., JACOBSON, A. & FRANKENDAL, B. 1993. A trial of Ro 03-8799 (pimonidazole) in carcinoma of the uterine cervix: an interim report from the Medical Research Council Working Party on advanced carcinoma of the cervix. *Radiotherapy and Oncology,* 26**,** 93-103.

DIZDAROGLU, M. 1993. Chemistry of free radical damage to DNA and nucleoproteins. *DNA and Free Radicals*.

DOHERTY, G. J., TEMPERO, M. & CORRIE, P. G. 2018. HALO-109–301: a Phase III trial of PEGPH20 (with gemcitabine and nab-paclitaxel) in hyaluronic acid-high stage IV pancreatic cancer. *Future Oncology,* 14**,** 13-22.

DOLGOBRODOV, S., MOORE, P., MARSHALL, R., BITTERN, R., STEELE, R. & CUSCHIERI, A. 2007. Artificial neural network: predicted vs. observed survival in patients with colonic cancer. *Diseases of the colon & rectum,* 50**,** 184-191.

DREVET, J. R. 2006. The antioxidant glutathione peroxidase family and spermatozoa: A complex story. *Molecular and Cellular Endocrinology,* 250**,** 70-79.

DU, J., MARTIN, S. M., LEVINE, M., WAGNER, B. A., BUETTNER, G. R., WANG, S.-H., TAGHIYEV, A. F., DU, C., KNUDSON, C. M. & CULLEN, J. J. 2010. Mechanisms of Ascorbate-Induced Cytotoxicity in Pancreatic Cancer. *Clinical Cancer Research,* 16**,** 509-520.

DU, T., BILL, K. A., FORD, J., BARAWI, M., HAYWARD, R. D., ALAME, A. & BERRI, R. N. 2017. The diagnosis and staging of pancreatic cancer: A comparison of endoscopic ultrasound and Computed Tomography with pancreas protocol. *The American Journal of Surgery*.

DUONG, H.-Q., HWANG, J. S., KIM, H. J., SEONG, Y.-S. & BAE, I. 2012. BML-275, an AMPK inhibitor, induces DNA damage, G2/M arrest and apoptosis in human pancreatic cancer cells. *International journal of oncology,* 41**,** 2227-2236.

EDGE, S. B. & COMPTON, C. C. 2010. The American Joint Committee on Cancer: the 7th edition of the AJCC cancer staging manual and the future of TNM. *Annals of surgical oncology,* 17**,** 1471-4.

EKLUND, H., CAMBILLAU, C., SJOBERG, B. M., HOLMGREN, A., JORNVALL, H., HOOG, J. O. & BRANDEN, C. I. 1984. Conformational and functional similarities between glutaredoxin and thioredoxins. *The EMBO journal,* 3**,** 1443-9.

EL SHAFIE, R. A., HABERMEHL, D., RIEKEN, S., MAIRANI, A., ORSCHIEDT, L., BRONS, S., HABERER, T., WEBER, K.-J., DEBUS, J. & COMBS, S. E. 2013. In vitro evaluation of

photon and raster-scanned carbon ion radiotherapy in combination with gemcitabine in pancreatic cancer cell lines. *Journal of radiation research,* 54**,** i113-i119.

ELLIS, H. R. & POOLE, L. B. 1997. Roles for the two cysteine residues of AhpC in catalysis of peroxide reduction by alkyl hydroperoxide reductase from Salmonella typhimurium. *Biochemistry,* 36**,** 13349-56.

ERIC J. HALL, A. J. G. 2012. *Radiobiology for the Radiologist,* Philadelphia, Pennsylvania, United States, Radiobiology for the Radiologist.

ESCHWÈGE, F., SANCHO-GARNIER, H., CHASSAGNE, D., BRISGAND, D., GUERRA, M., MALAISE, E. P., BEY, P., BUSUTTI, L., CIONINI, L. & N'GUYEN, T. 1997. Results of a European randomized trial of etanidazole combined with radiotherapy in head and neck carcinomas. *International Journal of Radiation Oncology* Biology* Physics,* 39**,** 275-281.

ESER, S., MESSER, M., ESER, P., VON WERDER, A., SEIDLER, B., BAJBOUJ, M., VOGELMANN, R., MEINING, A., VON BURSTIN, J., ALGUL, H., PAGEL, P., SCHNIEKE, A. E., ESPOSITO, I., SCHMID, R. M., SCHNEIDER, G. & SAUR, D. 2011. In vivo diagnosis of murine pancreatic intraepithelial neoplasia and early-stage pancreatic cancer by molecular imaging. *Proceedings of the National Academy of Sciences of the United States of America,* 108**,** 9945-50.

ESTERBAUER, H., SCHAUR, R. J. & ZOLLNER, H. 1991. Chemistry and biochemistry of 4-hydroxynonenal, malonaldehyde and related aldehydes. *Free radical Biology and medicine,* 11**,** 81-128.

ESTRELA, J. M., ORTEGA, A. & OBRADOR, E. 2006. Glutathione in cancer biology and therapy. *Critical reviews in clinical laboratory sciences,* 43**,** 143-181.

ETSUO, N., JYUNICHI, T., RITSUKO, T. & YOSHIO, K. 1982. REGENERATION OF VITAMIN E FROM α-CHROMANOXYL RADICAL BY GLUTATHIONE AND VITAMIN C. *Chemistry Letters,* 11**,** 789-792.

EVERHART, J. & WRIGHT, D. 1995. Diabetes mellitus as a risk factor for pancreatic cancer: A meta-analysis. *JAMA,* 273**,** 1605-1609.

FARINA, A. R., CAPPABIANCA, L., DESANTIS, G., IANNI, N. D., RUGGERI, P., RAGONE, M., MEROLLE, S., TONISSEN, K. F., GULINO, A. & MACKAY, A. R. 2011. Thioredoxin stimulates MMP-9 expression, de-regulates the MMP-9/TIMP-1 equilibrium and promotes MMP-9 dependent invasion in human MDA-MB-231 breast cancer cells. *FEBS letters,* 585**,** 3328-3336.

FATTMAN, C. L., SCHAEFER, L. M. & OURY, T. D. 2003. Extracellular superoxide dismutase in biology and medicine. *Free radical biology & medicine,* 35**,** 236-56.

FEDOROVA, M., BOLLINENI, R. C. & HOFFMANN, R. 2014. Protein carbonylation as a major hallmark of oxidative damage: update of analytical strategies. *Mass spectrometry reviews,* 33**,** 79-97.

FERLAY, J., SOERJOMATARAM, I., DIKSHIT, R., ESER, S., MATHERS, C., REBELO, M., PARKIN, D. M., FORMAN, D. & BRAY, F. 2014. Cancer incidence and mortality worldwide: Sources, methods and major patterns in GLOBOCAN 2012. *International journal of cancer*.

FISKUS, W., SABA, N., SHEN, M., GHIAS, M., LIU, J., GUPTA, S. D., CHAUHAN, L., RAO, R., GUNEWARDENA, S. & SCHORNO, K. 2014. Auranofin induces lethal oxidative and endoplasmic reticulum stress and exerts potent preclinical activity against chronic lymphocytic leukemia. *Cancer research***,** canres. 2033.2013.

FOLDES, F. F. 1978. *Enzymes in Anesthesiology,* New York, Springer Science & Business Media.

FRANKEN, N. A., RODERMOND, H. M., STAP, J., HAVEMAN, J. & VAN BREE, C. 2006. Clonogenic assay of cells in vitro. *Nature protocols,* 1**,** 2315.

FREI, B., KIM, M. C. & AMES, B. N. 1990. Ubiquinol-10 is an effective lipid-soluble antioxidant at physiological concentrations. *Proceedings of the National Academy of Sciences of the United States of America,* 87**,** 4879-83.

FREISLEBEN, H. J. & PACKER, L. 1993. Free-radical scavenging activities, interactions and recycling of antioxidants. *Biochemical Society transactions,* 21**,** 325-30.

FRIC, P., ŠKRHA, J., ŠEDO, A., BUŠEK, P., LACLAV, M., BUNGANIC, B. & ZAVORAL, M. 2017. Precursors of pancreatic cancer. *European Journal of Gastroenterology & Hepatology,* 29**,** e13-e18.

FRITSCHI, L., BENKE, G., RISCH, H. A., SCHULTE, A., WEBB, P. M., WHITEMAN, D. C., FAWCETT, J. & NEALE, R. E. 2015. Occupational exposure to N-nitrosamines and pesticides and risk of pancreatic cancer. *Occupational and environmental medicine*.

GANDHI, V., LEGHA, J., CHEN, F., HERTEL, L. W. & PLUNKETT, W. 1996. Excision of 2′, 2′-difluorodeoxycytidine (gemcitabine) monophosphate residues from DNA. *Cancer research,* 56**,** 4453-4459.

GAO, M. C., JIA, X. D., WU, Q. F., CHENG, Y., CHEN, F. R. & ZHANG, J. 2011. Silencing Prx1 and/or Prx5 sensitizes human esophageal cancer cells to ionizing radiation and increases apoptosis via intracellular ROS accumulation. *Acta Pharmacologica Sinica,* 32**,** 528-36.

GAO, Z., SARSOUR, E. H., KALEN, A. L., LI, L., KUMAR, M. G. & GOSWAMI, P. C. 2008. Late ROS accumulation and radiosensitivity in SOD1-overexpressing human glioma cells. *Free Radical Biology and Medicine,* 45**,** 1501-9.

GARCIA-CARRACEDO, D., YU, C.-C., AKHAVAN, N., FINE, S. A., SCHÖNLEBEN, F., MAEHARA, N., KARG, D. C., XIE, C., QIU, W., FINE, R. L., REMOTTI, H. E. & SU, G. H. 2015. Smad4 Loss Synergizes with TGFα Overexpression in Promoting Pancreatic Metaplasia, PanIN Development, and Fibrosis. *PLoS ONE,* 10**,** e0120851.

GEBHARDT, C., MEYER, W., REICHEL, M. & WÜNSCH, P. H. 2000. Prognostic factors in the operative treatment of ductal pancreatic carcinoma. *Langenbeck's archives of surgery,* 385**,** 14-20.

GENKINGER, J. M., SPIEGELMAN, D., ANDERSON, K. E., BERNSTEIN, L., VAN DEN BRANDT, P. A., CALLE, E. E., ENGLISH, D. R., FOLSOM, A. R., FREUDENHEIM, J. L., FUCHS, C. S., GILES, G. G., GIOVANNUCCI, E., HORN-ROSS, P. L., LARSSON, S. C., LEITZMANN, M., MANNISTO, S., MARSHALL, J. R., MILLER, A. B., PATEL, A. V., ROHAN, T. E., STOLZENBERG-SOLOMON, R. Z., VERHAGE, B. A., VIRTAMO, J., WILLCOX, B. J., WOLK, A., ZIEGLER, R. G. & SMITH-WARNER, S. A. 2011. A pooled analysis of 14

cohort studies of anthropometric factors and pancreatic cancer risk. *International journal of cancer,* 129**,** 1708-17.

GHOSH, N., DAS, A., CHAFFEE, S., ROY, S. & SEN, C. K. 2018. Chapter 4 - Reactive Oxygen Species, Oxidative Damage and Cell Death A2 - Chatterjee, Shampa. *In:* JUNGRAITHMAYR, W. & BAGCHI, D. (eds.) *Immunity and Inflammation in Health and Disease.* Academic Press.

GILES, G. I. 2006. The redox regulation of thiol dependent signaling pathways in cancer. *Current pharmaceutical design,* 12**,** 4427-43.

GILLEN, S., SCHUSTER, T., MEYER ZUM BUSCHENFELDE, C., FRIESS, H. & KLEEFF, J. 2010. Preoperative/neoadjuvant therapy in pancreatic cancer: a systematic review and meta-analysis of response and resection percentages. *PLoS Med,* 7**,** e1000267.

GILMORE, T. D., KOEDOOD, M., PIFFAT, K. A. & WHITE, D. W. 1996. Rel/NF-kappaB/IkappaB proteins and cancer. *Oncogene,* 13**,** 1367-78.

GIROTTI, A. W. 1985. Mechanisms of lipid peroxidation. *Journal of free radicals in biology & medicine,* 1**,** 87-95.

GIROUX, V., MALICET, C., BARTHET, M., GIRONELLA, M., ARCHANGE, C., DAGORN, J.-C., VASSEUR, S. & IOVANNA, J. L. 2006. p8 Is a New Target of Gemcitabine in Pancreatic Cancer Cells. *Clinical Cancer Research,* 12**,** 235-241.

GO, Y.-M. & JONES, D. P. 2010. Redox control systems in the nucleus: mechanisms and functions. *Antioxidants & redox signaling,* 13**,** 489-509.

GO, Y. M., ZIEGLER, T. R., JOHNSON, J. M., GU, L., HANSEN, J. M. & JONES, D. P. 2007. Selective protection of nuclear thioredoxin-1 and glutathione redox systems against oxidation during glucose and glutamine deficiency in human colonic epithelial cells. *Free Radic Biol Med,* 42**,** 363-70.

GOGGINS, M., OFFERHAUS, G. J., HILGERS, W., GRIFFIN, C. A., SHEKHER, M., TANG, D., SOHN, T. A., YEO, C. J., KERN, S. E. & HRUBAN, R. H. 1998. Pancreatic adenocarcinomas with DNA replication errors (RER+) are associated with wild-type K-ras and characteristic histopathology. Poor differentiation, a syncytial growth pattern, and pushing borders suggest RER+. *The American journal of pathology,* 152**,** 1501-7.

GOLDBERG, S. F., MIELE, M. E., HATTA, N., TAKATA, M., PAQUETTE-STRAUB, C., FREEDMAN, L. P. & WELCH, D. R. 2003. Melanoma metastasis suppression by chromosome 6: evidence for a pathway regulated by CRSP3 and TXNIP. *Cancer Research,* 63**,** 432-40.

GÖNENÇ, A., ÖZKAN, Y., TORUN, M. & ŞIMŞEK, B. 2001. Plasma malondialdehyde (MDA) levels in breast and lung cancer patients. *Journal of clinical pharmacy and therapeutics,* 26**,** 141-144.

GORRINI, C., HARRIS, I. S. & MAK, T. W. 2013. Modulation of oxidative stress as an anticancer strategy. *Nature Reviews Drug Discovery,* 12**,** 931.

GOTO, S., NAKAMURA, A., RADAK, Z., NAKAMOTO, H., TAKAHASHI, R., YASUDA, K., SAKURAI, Y. & ISHII, N. 1999. Carbonylated proteins in aging and exercise: immunoblot approaches. *Mechanisms of ageing and development,* 107**,** 245-253.

GROMER, S., URIG, S. & BECKER, K. 2004. The thioredoxin system—From science to clinic. *Medicinal Research Reviews,* 24**,** 40-89.

GUO, H., SEIXAS-SILVA JR, J. A., EPPERLY, M. W., GRETTON, J. E., SHIN, D. M., BAR-SAGI, D., ARCHER, H. & GREENBERGER, J. S. 2003. Prevention of radiation-induced oral cavity mucositis by plasmid/liposome delivery of the human manganese superoxide dismutase (SOD2) transgene. *Radiation research,* 159**,** 361-370.

GURKA, M. K., COLLINS, S. P., SLACK, R., TSE, G., CHARABATY, A., LEY, L., BERZCEL, L., LEI, S., SUY, S. & HADDAD, N. 2013. Stereotactic body radiation therapy with concurrent full-dose gemcitabine for locally advanced pancreatic cancer: a pilot trial demonstrating safety. *Radiation Oncology,* 8**,** 44.

HAMMEL, P., HUGUET, F., VAN LAETHEM, J. & ET AL. 2016. Effect of chemoradiotherapy vs chemotherapy on survival in patients with locally advanced pancreatic cancer controlled after 4 months of gemcitabine with or without erlotinib: The lap07 randomized clinical trial. *JAMA,* 315**,** 1844-1853.

HAMMOND, E., ASSELIN, M.-C., FORSTER, D., O'CONNOR, J. P., SENRA, J. & WILLIAMS, K. 2014. The meaning, measurement and modification of hypoxia in the laboratory and the clinic. *Clinical oncology,* 26**,** 277-288.

HAN, S. H., JEON, J. H., JU, H. R., JUNG, U., KIM, K. Y., YOO, H. S., LEE, Y. H., SONG, K. S., HWANG, H. M., NA, Y. S., YANG, Y., LEE, K. N. & CHOI, I. 2003. VDUP1 upregulated by TGF-β1 and 1,25-dihydorxyvitamin D3 inhibits tumor cell growth by blocking cell-cycle progression. *Oncogene,* 22**,** 4035.

HANAHAN, D. & WEINBERG, R. A. 2000. The Hallmarks of Cancer. *Cell,* 100**,** 57-70.

HANAHAN, D. & WEINBERG, ROBERT A. 2011. Hallmarks of Cancer: The Next Generation. *Cell,* 144**,** 646-674.

HANSON, J. R. 2001. *Functional group chemistry*, Royal Society of chemistry.

HAREWOOD, G. C. & WIERSEMA, M. J. 2002. Endosonography-guided fine needle aspiration biopsy in the evaluation of pancreatic masses. *The American journal of gastroenterology,* 97**,** 1386-91.

HARRIS, A. L. 2002. Hypoxia—a key regulatory factor in tumour growth. *Nature Reviews Cancer,* 2**,** 38.

HARRIS, I. S., TRELOAR, A. E., INOUE, S., SASAKI, M., GORRINI, C., LEE, K. C., YUNG, K. Y., BRENNER, D., KNOBBE-THOMSEN, C. B., COX, M. A., ELIA, A., BERGER, T., CESCON, D. W., ADEOYE, A., BRUSTLE, A., MOLYNEUX, S. D., MASON, J. M., LI, W. Y., YAMAMOTO, K., WAKEHAM, A., BERMAN, H. K., KHOKHA, R., DONE, S. J., KAVANAGH, T. J., LAM, C. W. & MAK, T. W. 2015. Glutathione and thioredoxin antioxidant pathways synergize to drive cancer initiation and progression. *Cancer Cell,* 27**,** 211-22.

HASSAN, M. M., BONDY, M. L., WOLFF, R. A., ABBRUZZESE, J. L., VAUTHEY, J.-N., PISTERS, P. W., EVANS, D. B., KHAN, R., CHOU, T.-H., LENZI, R., JIAO, L. & LI, D. 2007. Risk Factors for Pancreatic Cancer: Case-Control Study. *The American Journal Of Gastroenterology,* 102**,** 2696.

HAYASHI, T., UENO, Y. & OKAMOTO, T. 1993. Oxidoreductive regulation of nuclear factor kappa B. Involvement of a cellular reducing catalyst thioredoxin. *The Journal of biological chemistry,* 268**,** 11380-8.

HEINEMANN, V., HERTEL, L. W., GRINDEY, G. B. & PLUNKETT, W. 1988. Comparison of the cellular pharmacokinetics and toxicity of 2′, 2′-difluorodeoxycytidine and 1-β-D-arabinofuranosylcytosine. *Cancer research,* 48**,** 4024-4031.

HEINEMANN, V., XU, Y.-Z., CHUBB, S., SEN, A., HERTEL, L. W., GRINDEY, G. B. & PLUNKETT, W. 1992. Cellular elimination of 2′, 2′-difluorodeoxycytidine 5′-triphosphate: a mechanism of self-potentiation. *Cancer research,* 52**,** 533-539.

HERMAN, J. M., CHANG, D. T., GOODMAN, K. A., DHOLAKIA, A. S., RAMAN, S. P., HACKER-PRIETZ, A., IACOBUZIO-DONAHUE, C. A., GRIFFITH, M. E., PAWLIK, T. M. & PAI, J. S. 2015. Phase 2 multi-institutional trial evaluating gemcitabine and stereotactic body radiotherapy for patients with locally advanced unresectable pancreatic adenocarcinoma. *Cancer,* 121**,** 1128-1137.

HERRMANN, R., BODOKY, G., RUHSTALLER, T., GLIMELIUS, B., BAJETTA, E., SCHÜLLER, J., SALETTI, P., BAUER, J., FIGER, A., PESTALOZZI, B., KÖHNE, C.-H., MINGRONE, W., STEMMER, S. M., TÀMAS, K., KORNEK, G. V., KOEBERLE, D., CINA, S., BERNHARD, J., DIETRICH, D. & SCHEITHAUER, W. 2007. Gemcitabine Plus Capecitabine Compared With Gemcitabine Alone in Advanced Pancreatic Cancer: A Randomized, Multicenter, Phase III Trial of the Swiss Group for Clinical Cancer Research and the Central European Cooperative Oncology Group. *Journal of Clinical Oncology,* 25**,** 2212-2217.

HIDALGO, M. 2012. New insights into pancreatic cancer biology. *Annals of Oncology,* 23**,** x135-x138.

HINGORANI, S. R., HARRIS, W. P., BECK, J. T., BERDOV, B. A., WAGNER, S. A., PSHEVLOTSKY, E. M., TJULANDIN, S. A., GLADKOV, O. A., HOLCOMBE, R. F. & KORN, R. 2016. Phase Ib study of PEGylated recombinant human hyaluronidase and gemcitabine in patients with advanced pancreatic cancer. *Clinical Cancer Research,* 22**,** 2848-2854.

HIROTA, K., MURATA, M., SACHI, Y., NAKAMURA, H., TAKEUCHI, J., MORI, K. & YODOI, J. 1999. Distinct roles of thioredoxin in the cytoplasm and in the nucleus a two-step mechanism of redox regulation of transcription factor NF-κB. *Journal of Biological Chemistry,* 274**,** 27891-27897.

HÖCKEL, M., SCHLENGER, K., KNOOP, C. & VAUPEL, P. 1991. Oxygenation of carcinomas of the uterine cervix: evaluation by computerized O2 tension measurements. *Cancer Research,* 51**,** 6098-6102.

HOLMGREN, A. 1989. Thioredoxin and glutaredoxin systems. *The Journal of biological chemistry,* 264**,** 13963-6.

HOOS, W. A., JAMES, P. M., RAHIB, L., TALLEY, A. W., FLESHMAN, J. M. & MATRISIAN, L. M. 2013. Pancreatic cancer clinical trials and accrual in the United States. *Journal of Clinical Oncology,* 31**,** 3432-3438.

HOSHIKAWA, H., INDO, K., MORI, T. & MORI, N. 2011. Enhancement of the radiation effects by D-allose in head and neck cancer cells. *Cancer letters,* 306**,** 60-6.

HOSHINO, Y., NISHIDA, J., KATSUNO, Y., KOINUMA, D., AOKI, T., KOKUDO, N., MIYAZONO, K. & EHATA, S. 2015. Smad4 Decreases the Population of Pancreatic Cancer–Initiating Cells through Transcriptional Repression of ALDH1A1. *The American Journal of Pathology,* 185**,** 1457-1470.

HRUBAN, R. H., MOLINA, J. M., REDDY, M. N. & BOITNOTT, J. K. 1987. A neoplasm with pancreatic and hepatocellular differentiation presenting with subcutaneous fat necrosis. *American journal of clinical pathology,* 88**,** 639-45.

HSIUNG-STRIPP, D. C., MCDONOUGH, J., MASTERS, H. M., LEVIN, W. P., HAHN, S. M., JONES, H. A. & METZ, J. M. 2001. Comparative treatment planning between proton and X-ray therapy in pancreatic cancer. *Medical Dosimetry,* 26**,** 255-259.

HUANG, Q., ZHOU, H. J., ZHANG, H., HUANG, Y., HINOJOSA-KIRSCHENBAUM, F., FAN, P., YAO, L., BELARDINELLI, L., TELLIDES, G., GIORDANO, F. J., BUDAS, G. R. & MIN, W. 2015. Thioredoxin-2 Inhibits Mitochondrial ROS Generation and ASK1 Activity to Maintain Cardiac Function. *Circulation,* 131**,** 1082-1097.

HUBER, K., PATEL, P., ZHANG, L., EVANS, H., WESTWELL, A. D., FISCHER, P. M., CHAN, S. & MARTIN, S. 2008. 2-[(1-methylpropyl) dithio]-1H-imidazole inhibits tubulin polymerization through cysteine oxidation. *Molecular cancer therapeutics,* 7**,** 143-151.

HUGUET, F., ANDRÉ, T., HAMMEL, P., ARTRU, P., BALOSSO, J., SELLE, F., DENIAUD-ALEXANDRE, E., RUSZNIEWSKI, P., TOUBOUL, E., LABIANCA, R., GRAMONT, A. D. & LOUVET, C. 2007. Impact of Chemoradiotherapy After Disease Control With Chemotherapy in Locally Advanced Pancreatic Adenocarcinoma in GERCOR Phase II and III Studies. *Journal of Clinical Oncology,* 25**,** 326-331.

HUTCHISON, K. A., MATIC, G., MESHINCHI, S., BRESNICK, E. H. & PRATT, W. B. 1991. Redox manipulation of DNA binding activity and BuGR epitope reactivity of the glucocorticoid receptor. *The Journal of biological chemistry,* 266**,** 10505-9.

HWANG, G. H., RYU, J. M., JEON, Y. J., CHOI, J., HAN, H. J., LEE, Y.-M., LEE, S., BAE, J.-S., JUNG, J.-W., CHANG, W., KIM, L. K., JEE, J.-G. & LEE, M. Y. 2015. The role of thioredoxin reductase and glutathione reductase in plumbagin-induced, reactive oxygen species-mediated apoptosis in cancer cell lines. *European Journal of Pharmacology,* 765**,** 384-393.

IACOBUZIO-DONAHUE, C. A. 2012. Genetic evolution of pancreatic cancer: lessons learnt from the pancreatic cancer genome sequencing project. *Gut,* 61**,** 1085-94.

ISOHOOKANA, J., HAAPASAARI, K.-M., SOINI, Y. & KARIHTALA, P. 2016. Loss of peroxiredoxin expression is associated with an aggressive phenotype in pancreatic adenocarcinoma. *Anticancer research,* 36**,** 427-433.

IWASAWA, S., YAMANO, Y., TAKIGUCHI, Y., TANZAWA, H., TATSUMI, K. & UZAWA, K. 2011. Upregulation of thioredoxin reductase 1 in human oral squamous cell carcinoma. *Oncology reports,* 25**,** 637-644.

IYANAGI, T. & YAMAZAKI, I. 1970. One-electron-transfer reactions in biochemical systems. V. Difference in the mechanism of quinone reduction by the NADH dehydrogenase and the NAD(P)H dehydrogenase (DT-diaphorase). *Biochimica et Biophysica Acta (BBA)-Bioenergetics,* 216**,** 282-94.

JAMES, R. D., GLYNNE-JONES, R., MEADOWS, H. M., CUNNINGHAM, D., MYINT, A. S., SAUNDERS, M. P., MAUGHAN, T., MCDONALD, A., ESSAPEN, S., LESLIE, M., FALK, S., WILSON, C., GOLLINS, S., BEGUM, R., LEDERMANN, J., KADALAYIL, L. & SEBAG-MONTEFIORE, D. 2013. Mitomycin or cisplatin chemoradiation with or without maintenance chemotherapy for treatment of squamous-cell carcinoma of the

anus (ACT II): a randomised, phase 3, open-label, 2 x 2 factorial trial. *Lancet Oncology,* 14**,** 516-24.

JAMIESON, N. B., CHAN, N. I., FOULIS, A. K., DICKSON, E. J., MCKAY, C. J. & CARTER, C. R. 2013. The prognostic influence of resection margin clearance following pancreaticoduodenectomy for pancreatic ductal adenocarcinoma. *Journal of Gastrointestinal Surgery,* 17**,** 511-521.

JAYAKUMAR, S., KUNWAR, A., SANDUR, S. K., PANDEY, B. N. & CHAUBEY, R. C. 2014. Differential response of DU145 and PC3 prostate cancer cells to ionizing radiation: role of reactive oxygen species, GSH and Nrf2 in radiosensitivity. *Biochimica et Biophysica Acta (BBA)-General Subjects,* 1840**,** 485-94.

JAYAKUMAR, S., PATWARDHAN, R. S., PAL, D., SHARMA, D. & SANDUR, S. K. 2016. Dimethoxycurcumin, a metabolically stable analogue of curcumin enhances the radiosensitivity of cancer cells: Possible involvement of ROS and thioredoxin reductase. *Biochemical and Biophysical Research Communications,* 478**,** 446-454.

JIAO, L., MITROU, P. N., REEDY, J., GRAUBARD, B. I., HOLLENBECK, A. R., SCHATZKIN, A. & STOLZENBERG-SOLOMON, R. 2009. A combined healthy lifestyle score and risk of pancreatic cancer in a large cohort study. *Archives of internal medicine,* 169**,** 764-70.

JOHANSSON, C., LILLIG, C. H. & HOLMGREN, A. 2004. Human mitochondrial glutaredoxin reduces S-glutathionylated proteins with high affinity accepting electrons from either glutathione or thioredoxin reductase. *The Journal of biological chemistry,* 279**,** 7537-43.

JONES, D. T., PUGH, C. W., WIGFIELD, S., STEVENS, M. F. & HARRIS, A. L. 2006. Novel thioredoxin inhibitors paradoxically increase hypoxia-inducible factor-α expression but decrease functional transcriptional activity, DNA binding, and degradation. *Clinical cancer research,* 12**,** 5384-5394.

JONES, S., ZHANG, X., PARSONS, D. W., LIN, J. C., LEARY, R. J., ANGENENDT, P., MANKOO, P., CARTER, H., KAMIYAMA, H., JIMENO, A., HONG, S. M., FU, B., LIN, M. T., CALHOUN, E. S., KAMIYAMA, M., WALTER, K., NIKOLSKAYA, T., NIKOLSKY, Y., HARTIGAN, J., SMITH, D. R., HIDALGO, M., LEACH, S. D., KLEIN, A. P., JAFFEE, E. M., GOGGINS, M., MAITRA, A., IACOBUZIO-DONAHUE, C., ESHLEMAN, J. R., KERN, S. E., HRUBAN, R. H., KARCHIN, R., PAPADOPOULOS, N., PARMIGIANI, G., VOGELSTEIN, B., VELCULESCU, V. E. & KINZLER, K. W. 2008. Core signaling pathways in human pancreatic cancers revealed by global genomic analyses. *Science,* 321**,** 1801-6.

JORDAN, B. F., RUNQUIST, M., RAGHUNAND, N., GILLIES, R. J., TATE, W. R., POWIS, G. & BAKER, A. F. 2005. The Thioredoxin-1 Inhibitor 1-Methylpropyl 2-Imidazolyl Disulfide (PX-12) Decreases Vascular Permeability in Tumor Xenografts Monitored by Dynamic Contrast Enhanced Magnetic Resonance Imaging. *Clinical Cancer Research,* 11**,** 529.

JUNG, T., ENGELS, M., KAISER, B., POPPEK, D. & GRUNE, T. 2006. Intracellular distribution of oxidized proteins and proteasome in HT22 cells during oxidative stress. *Free Radical Biology and Medicine,* 40**,** 1303-1312.

KANDA, M., MATTHAEI, H., WU, J., HONG, S. M., YU, J., BORGES, M., HRUBAN, R. H., MAITRA, A., KINZLER, K., VOGELSTEIN, B. & GOGGINS, M. 2012. Presence of somatic mutations in most early-stage pancreatic intraepithelial neoplasia. *Gastroenterology,* 142**,** 730-733 e9.

KANDA, M., SADAKARI, Y., BORGES, M., TOPAZIAN, M., FARRELL, J., SYNGAL, S., LEE, J., KAMEL, I., LENNON, A. M., KNIGHT, S., FUJIWARA, S., HRUBAN, R. H., CANTO, M. I. & GOGGINS, M. 2013. Mutant TP53 in duodenal samples of pancreatic juice from patients with pancreatic cancer or high-grade dysplasia. *Clinical gastroenterology and hepatology,* 11**,** 719-30 e5.

KATZ, M. H., TAYLOR, T. H., AL-REFAIE, W. B., HANNA, M. H., IMAGAWA, D. K., ANTON-CULVER, H. & ZELL, J. A. 2011. Adenosquamous versus adenocarcinoma of the pancreas: a population-based outcomes analysis. *Journal of gastrointestinal surgery,* 15**,** 165-74.

KAUSHIK, N. K., KAUSHIK, N., PARK, D. & CHOI, E. H. 2014. Altered antioxidant system stimulates dielectric barrier discharge plasma-induced cell death for solid tumor cell treatment. *PLoS One,* 9**,** e103349.

KEALL, P. 4-dimensional computed tomography imaging and treatment planning. Seminars in radiation oncology, 2004. Elsevier, 81-90.

KEAN, W. & KEAN, I. 2008. Clinical pharmacology of gold. *Inflammopharmacology,* 16**,** 112-125.

KELSEN, D. P., PORTENOY, R., THALER, H., TAO, Y. & BRENNAN, M. 1997. Pain as a predictor of outcome in patients with operable pancreatic carcinoma. *Surgery,* 122**,** 53-9.

KENNEDY, K. A., ROCKWELL, S. & SARTORELLI, A. C. 1980. Preferential activation of mitomycin C to cytotoxic metabolites by hypoxic tumor cells. *Cancer Research,* 40**,** 2356-60.

KEYES, S. R., ROCKWELL, S. & SARTORELLI, A. C. 1985. Enhancement of mitomycin C cytotoxicity to hypoxic tumor cells by dicoumarol in vivo and in vitro. *Cancer research,* 45**,** 213-216.

KHALED, S. & HELD, K. D. 2012. Radiation biology: a handbook for teachers and students. Taylor & Francis.

KIEBALA, M., SKALSKA, J., CASULO, C., BROOKES, P. S., PETERSON, D. R., HILCHEY, S. P., DAI, Y., GRANT, S., MAGGIRWAR, S. B. & BERNSTEIN, S. H. 2015. Dual Targeting of the Thioredoxin and Glutathione Anti-Oxidant Systems in Malignant B-cells; A Novel Synergistic Therapeutic Approach. *Experimental hematology,* 43**,** 89-99.

KIRKPATRICK, D. L., KUPERUS, M., DOWDESWELL, M., POTIER, N., DONALD, L. J., KUNKEL, M., BERGGREN, M., ANGULO, M. & POWIS, G. 1998. Mechanisms of inhibition of the thioredoxin growth factor system by antitumor 2-imidazolyl disulfides. *Biochemical pharmacology,* 55**,** 987-994.

KIRKPATRICK, D. L., WATSON, S., KUNKEL, M., FLETCHER, S., ULHAQ, S. & POWIS, G. 1999. Parallel syntheses of disulfide inhibitors of the thioredoxin redox system as potential antitumor agents. *Anti-cancer drug design,* 14**,** 421-432.

KLEIN, A. P., BRUNE, K. A., PETERSEN, G. M., GOGGINS, M., TERSMETTE, A. C., OFFERHAUS, G. J., GRIFFIN, C., CAMERON, J. L., YEO, C. J., KERN, S. & HRUBAN, R.

H. 2004. Prospective risk of pancreatic cancer in familial pancreatic cancer kindreds. *Cancer Res,* 64**,** 2634-8.

KLEIN, E. A., THOMPSON, I. M., TANGEN, C. M. & ET AL. 2011. Vitamin e and the risk of prostate cancer: The selenium and vitamin e cancer prevention trial (select). *JAMA,* 306**,** 1549-1556.

KOMATSU, M., KURODA, M., WANG, Y., ST CLAIR, D., URANO, M., AKAKI, S., ASAUMI, J., KAWASAKI, S., HIRAKI, Y. & KANAZAWA, S. 2005. Manganese superoxide dismutase overexpression changes plating efficiency bidirectionally according to change in redox for SaOS2 human osteosarcoma cell line. *International journal of oncology,* 26**,** 853-62.

KOONG, A. C., CHRISTOFFERSON, E., LE, Q.-T., GOODMAN, K. A., HO, A., KUO, T., FORD, J. M., FISHER, G. A., GRECO, R., NORTON, J. & YANG, G. P. 2005. Phase II study to assess the efficacy of conventionally fractionated radiotherapy followed by a stereotactic radiosurgery boost in patients with locally advanced pancreatic cancer. *International Journal of Radiation Oncology*Biology*Physics,* 63**,** 320-323.

KOONG, A. C., LE, Q. T., HO, A., FONG, B., FISHER, G., CHO, C., FORD, J., POEN, J., GIBBS, I. C., MEHTA, V. K., KEE, S., TRUEBLOOD, W., YANG, G. & BASTIDAS, J. A. 2004. Phase I study of stereotactic radiosurgery in patients with locally advanced pancreatic cancer. *International Journal of Radiation Oncology*Biology*Physics,* 58**,** 1017-1021.

KOULOURIS, A. I., BANIM, P. & HART, A. R. 2017. Pain in Patients with Pancreatic Cancer: Prevalence, Mechanisms, Management and Future Developments. *Digestive Diseases and Sciences,* 62**,** 861-870.

KOZAK, K. R., KACHNIC, L. A., ADAMS, J., CROWLEY, E. M., ALEXANDER, B. M., MAMON, H. J., FERNANDEZ-DEL CASTILLO, C., RYAN, D. P., DELANEY, T. F. & HONG, T. S. 2007. Dosimetric feasibility of hypofractionated proton radiotherapy for neoadjuvant pancreatic cancer treatment. *International Journal of Radiation Oncology* Biology* Physics,* 68**,** 1557-1566.

KRISHNAIAH, P. R. 1980. *Handbook of Statistics*, Motilal Banarsidass

KRISHNAN, S., CHADHA, A. S., SUH, Y., CHEN, H.-C., RAO, A., DAS, P., MINSKY, B. D., MAHMOOD, U., DELCLOS, M. E., SAWAKUCHI, G. O., BEDDAR, S., KATZ, M. H., FLEMING, J. B., JAVLE, M. M., VARADHACHARY, G. R., WOLFF, R. A. & CRANE, C. H. 2016. Focal Radiation Therapy Dose Escalation Improves Overall Survival in Locally Advanced Pancreatic Cancer Patients Receiving Induction Chemotherapy and Consolidative Chemoradiation. *International Journal of Radiation Oncology*Biology*Physics,* 94**,** 755-765.

LAGENDIJK, J. J., RAAYMAKERS, B. W., RAAIJMAKERS, A. J., OVERWEG, J., BROWN, K. J., KERKHOF, E. M., VAN DER PUT, R. W., HÅRDEMARK, B., VAN VULPEN, M. & VAN DER HEIDE, U. A. 2008. MRI/linac integration. *Radiotherapy and Oncology,* 86**,** 25-29.

LANE, D. A., FIELDER, S. S., TOWNSEND, S. J., BUNCE, N. J., ZHU, J., LIU, L., WIENS, B. & POND, P. 1996. Atmospheric Photochemistry of Naphthalene: a Practical and Theoretical Approach. *Polycyclic Aromatic Compounds,* 9**,** 53-59.

LASNITZKI, I. 1947. A quantitative analysis of the direct and indirect action of X radiation on malignant cells. *The British journal of radiology,* 20**,** 240-247.

LAUNOIS, B., TERBLANCHE, J., LAKEHAL, M., CATHELINE, J. M., BARDAXOGLOU, E., LANDEN, S., CAMPION, J. P., SUTHERLAND, F. & MEUNIER, B. 1999. Proximal bile duct cancer: high resectability rate and 5-year survival. *Annals of surgery,* 230**,** 266.

LAURENT, T. C., MOORE, E. C. & REICHARD, P. 1964. Enzymatic synthesis of deoxyribonucleotides. IV. isolation and characterization of thioredoxin, the hydrogen donor from escherichia coli B. *Journal of Biological Chemistry,* 239**,** 3436-44.

LEVINE, R. L., GARLAND, D., OLIVER, C. N., AMICI, A., CLIMENT, I., LENZ, A.-G., AHN, B.-W., SHALTIEL, S. & STADTMAN, E. R. 1990. [49] Determination of carbonyl content in oxidatively modified proteins. *Methods in enzymology.* Elsevier.

LI, D., DAY, R. S., BONDY, M. L., SINHA, R., NGUYEN, N. T., EVANS, D. B., ABBRUZZESE, J. L. & HASSAN, M. M. 2007. Dietary mutagen exposure and risk of pancreatic cancer. *Cancer epidemiology, biomarkers & prevention,* 16**,** 655-61.

LI, G., GAO, K., CHI, Y., ZHANG, X., MITSUI, T., YAO, J. & TAKEDA, M. 2016. Upregulation of connexin43 contributes to PX-12-induced oxidative cell death. *Tumor Biology,* 37**,** 7535-7546.

LIANG, Y.-W., ZHENG, J., LI, X., ZHENG, W. & CHEN, T. 2014. Selenadiazole derivatives as potent thioredoxin reductase inhibitors that enhance the radiosensitivity of cancer cells. *European journal of medicinal chemistry,* 84**,** 335-342.

LILLEMOE, K. D., YEO, C. J. & CAMERON, J. L. 2000. Pancreatic cancer: state-of-the-art care. *CA: a cancer journal for clinicians,* 50**,** 241-68.

LILLIG, C. H., BERNDT, C. & HOLMGREN, A. 2008. Glutaredoxin systems. *Biochimica et Biophysica Acta (BBA) - General Subjects,* 1780**,** 1304-1317.

LIM, J. Y., YOON, S. O., HONG, S. W., KIM, J. W., CHOI, S. H. & CHO, J. Y. 2012. Thioredoxin and thioredoxin-interacting protein as prognostic markers for gastric cancer recurrence. *World journal of gastroenterology: WJG,* 18**,** 5581.

LIN, A. J., COSBY, L. A., SHANSKY, C. W. & SARTORELLI, A. C. 1972. Potential bioreductive alkylating agents. 1. Benzoquinone derivatives. *Journal of medicinal chemistry,* 15**,** 1247-1252.

LO, M., LING, V., WANG, Y. Z. & GOUT, P. W. 2008. The x(c)(−) cystine/glutamate antiporter: a mediator of pancreatic cancer growth with a role in drug resistance. *British Journal of Cancer,* 99**,** 464-472.

LOEFFLER, J. S. & DURANTE, M. 2013. Charged particle therapy—optimization, challenges and future directions. *Nature reviews Clinical oncology,* 10**,** 411.

LÖHR, M., KLÖPPEL, G., MAISONNEUVE, P., LOWENFELS, A. B. & LÜTTGES, J. 2005. Frequency of K-ras Mutations in Pancreatic Intraductal Neoplasias Associated with Pancreatic Ductal Adenocarcinoma and Chronic Pancreatitis: A Meta-Analysis. *Neoplasia (New York, N.Y.),* 7**,** 17-23.

LOU, M., LIU, Q., REN, G., ZENG, J., XIANG, X., DING, Y., LIN, Q., ZHONG, T., LIU, X. & ZHU, L. 2017a. Physical interaction between human ribonucleotide reductase large

subunit and thioredoxin increases colorectal cancer malignancy. *Journal of Biological Chemistry,* 292**,** 9136-9149.

LOU, M., LIU, Q., REN, G., ZENG, J., XIANG, X., DING, Y., LIN, Q., ZHONG, T., LIU, X., ZHU, L., QI, H., SHEN, J., LI, H. & SHAO, J. 2017b. Physical interaction between human ribonucleotide reductase large subunit and thioredoxin increases colorectal cancer malignancy. *The Journal of biological chemistry,* 292**,** 9136-9149.

LOUKOPOULOS, P., KANETAKA, K., TAKAMURA, M., SHIBATA, T., SAKAMOTO, M. & HIROHASHI, S. 2004. Orthotopic transplantation models of pancreatic adenocarcinoma derived from cell lines and primary tumors and displaying varying metastatic activity. *Pancreas,* 29**,** 193-203.

LOWENFELS, A. B., MAISONNEUVE, P., DIMAGNO, E. P., ELITSUR, Y., GATES, L. K., JR., PERRAULT, J. & WHITCOMB, D. C. 1997. Hereditary pancreatitis and the risk of pancreatic cancer. International Hereditary Pancreatitis Study Group. *Journal of the National Cancer Institute,* 89**,** 442-6.

LU, G., GREENE, E. L., NAGAI, T. & EGAN, B. M. 1998. Reactive oxygen species are critical in the oleic acid-mediated mitogenic signaling pathway in vascular smooth muscle cells. *Hypertension,* 32**,** 1003-10.

LU, J., PAPP, L. V., FANG, J., RODRIGUEZ-NIETO, S., ZHIVOTOVSKY, B. & HOLMGREN, A. 2006. Inhibition of mammalian thioredoxin reductase by some flavonoids: implications for myricetin and quercetin anticancer activity. *Cancer research,* 66**,** 4410-4418.

LUCAS, A. L., TARLECKI, A., VAN BECK, K., LIPTON, C., ROYCHOUDHURY, A., LEVINSON, E., KUMAR, S., CHUNG, W. K., FRUCHT, H. & GENKINGER, J. M. 2017. Self-Reported Questionnaire Detects Family History of Cancer in a Pancreatic Cancer Screening Program. *Journal of Genetic Counseling,* 26**,** 806-813.

LUCHINI, C., CAPELLI, P. & SCARPA, A. 2016. Pancreatic ductal adenocarcinoma and its variants. *Surgical pathology clinics,* 9**,** 547-560.

LUNDIN, M., LUNDIN, J., BURKE, H., TOIKKANEN, S., PYLKKÄNEN, L. & JOENSUU, H. 1999. Artificial neural networks applied to survival prediction in breast cancer. *Oncology,* 57**,** 281-286.

MA, J., ZHANG, Z. & WANG, J. 2015. Small nuclear ribonucleoprotein associated polypeptide N accelerates cell proliferation in pancreatic adenocarcinoma. *Molecular medicine reports,* 12**,** 6060-6064.

MADURA, J. A., JARMAN, B. T., DOHERTY, M. G., YUM, M. N. & HOWARD, T. J. 1999. Adenosquamous carcinoma of the pancreas. *Archives of surgery,* 134**,** 599-603.

MAEHARA, Y., SAKAGUCHI, Y., MORIGUCHI, S., ORITA, H., KORENAGA, D., KOHNOE, S. & SUGIMACHI, K. 1992. Signet ring cell carcinoma of the stomach. *Cancer,* 69**,** 1645-50.

MAFTOUH, M., AVAN, A., SCIARRILLO, R., GRANCHI, C., LEON, L. G., RANI, R., FUNEL, N., SMID, K., HONEYWELL, R. & BOGGI, U. 2014. Synergistic interaction of novel lactate dehydrogenase inhibitors with gemcitabine against pancreatic cancer cells in hypoxia. *British journal of cancer,* 110**,** 172.

MAGDA, D., LEPP, C., GERASIMCHUK, N., LEE, I., SESSLER, J. L., LIN, A., BIAGLOW, J. E. & MILLER, R. A. 2001. Redox cycling by motexafin gadolinium enhances cellular

response to ionizing radiation by forming reactive oxygen species. *International Journal of Radiation Oncology• Biology• Physics,* 51**,** 1025-1036.

MAGDA, D. & MILLER, R. A. Motexafin gadolinium: a novel redox active drug for cancer therapy. Seminars in cancer biology, 2006. Elsevier, 466-476.

MAHADEVAN, D. & VON HOFF, D. D. 2007. Tumor-stroma interactions in pancreatic ductal adenocarcinoma. *Molecular cancer therapeutics,* 6**,** 1186-97.

MAISONNEUVE, P. & LOWENFELS, A. B. 2015. Risk factors for pancreatic cancer: a summary review of meta-analytical studies. *International journal of epidemiology,* 44**,** 186-98.

MAJUMDER, S. & CHARI, S. T. 2016. Chronic pancreatitis. *Lancet,* 387**,** 1957-66.

MAKINO, Y., YOSHIKAWA, N., OKAMOTO, K., HIROTA, K., YODOI, J., MAKINO, I. & TANAKA, H. 1999. Direct association with thioredoxin allows redox regulation of glucocorticoid receptor function. *The Journal of biological chemistry,* 274**,** 3182-8.

MALIEPAARD, M., WOLFS, A., GROOT, S., DE MOL, N. & JANSSEN, L. 1995. Indoloquinone EO9: DNA interstrand cross-linking upon reduction by DT-diaphorase or xanthine oxidase. *British journal of cancer,* 71**,** 836-839.

MALIK, N. K., MAY, K. S., CHANDRASEKHAR, R., WEE, W., FLAHERTY, L., IYER, R., GIBBS, J., KUVSHINOFF, B., WILDING, G., WARREN, G. & YANG, G. Y. 2012. Treatment of locally advanced unresectable pancreatic cancer: a 10-year experience. *Journal of Gastrointestinal Oncology,* 3**,** 326-334.

MALUMBRES, M. & BARBACID, M. 2003. RAS oncogenes: the first 30 years. *Nature reviews. Cancer,* 3**,** 459-65.

MANN, K. M., WARD, J. M., YEW, C. C., KOVOCHICH, A., DAWSON, D. W., BLACK, M. A., BRETT, B. T., SHEETZ, T. E., DUPUY, A. J., CHANG, D. K., BIANKIN, A. V., WADDELL, N., KASSAHN, K. S., GRIMMOND, S. M., RUST, A. G., ADAMS, D. J., JENKINS, N. A. & COPELAND, N. G. 2012. Sleeping Beauty mutagenesis reveals cooperating mutations and pathways in pancreatic adenocarcinoma. *Proceedings of the National Academy of Sciences of the United States of America,* 109**,** 5934-41.

MANTONI, T. S., LUNARDI, S., AL-ASSAR, O., MASAMUNE, A. & BRUNNER, T. B. 2011. Pancreatic stellate cells radioprotect pancreatic cancer cells through β1-integrin signaling. *Cancer research*.

MARZEC, J., MARZEC, L., MARTUS, P., ZIPS, D. & MÜLLER, A.-C. 2018. MATLAB®-based fitting method to evaluate survival fractions after multimodal treatment. *Clinical and translational radiation oncology,* 10**,** 36-41.

MATTHAEI, H., SCHULICK, R. D., HRUBAN, R. H. & MAITRA, A. 2011. Cystic precursors to invasive pancreatic cancer. *Nature reviews. Gastroenterology & hepatology,* 8**,** 141-50.

MCKEAGE, M. J., JAMESON, M. B., RAMANATHAN, R. K., RAJENDRAN, J., GU, Y., WILSON, W. R., MELINK, T. J. & TCHEKMEDYIAN, N. S. 2012. PR-104 a bioreductive pre-prodrug combined with gemcitabine or docetaxel in a phase Ib study of patients with advanced solid tumours. *BMC cancer,* 12**,** 496.

MCSHANE, L. M., ALTMAN, D. G., SAUERBREI, W., TAUBE, S. E., GION, M. & CLARK, G. M. 2006. REporting recommendations for tumor MARKer prognostic studies (REMARK). *Breast Cancer Res Treat,* 100**,** 229-35.

MEHTA, M. P., SHAPIRO, W. R., PHAN, S. C., GERVAIS, R., CARRIE, C., CHABOT, P., PATCHELL, R. A., GLANTZ, M. J., RECHT, L., LANGER, C., SUR, R. K., ROA, W. H., MAHE, M. A., FORTIN, A., NIEDER, C., MEYERS, C. A., SMITH, J. A., MILLER, R. A. & RENSCHLER, M. F. 2009. Motexafin Gadolinium Combined With Prompt Whole Brain Radiotherapy Prolongs Time to Neurologic Progression in Non–Small-Cell Lung Cancer Patients With Brain Metastases: Results of a Phase III Trial. *International Journal of Radiation Oncology*Biology*Physics,* 73**,** 1069-1076.

MEISTER, A. 1983. Selective modification of glutathione metabolism. *Science,* 220**,** 472-477.

MEISTER, A. 1994. Glutathione-ascorbic acid antioxidant system in animals. *The Journal of biological chemistry,* 269**,** 9397-400.

MICHAELS, H. B. & HUNT, J. W. 1978. A model for radiation damage in cells by direct effect and by indirect effect: a radiation chemistry approach. *Radiation research,* 74**,** 23-34.

MISTRY, I. N., THOMAS, M., CALDER, E. D., CONWAY, S. J. & HAMMOND, E. M. 2017. Clinical advances of hypoxia-activated prodrugs in combination with radiation therapy. *International Journal of Radiation Oncology• Biology• Physics,* 98**,** 1183-1196.

MITCHELL, J. B., RUSSO, A., BIAGLOW, J. E. & MCPHERSON, S. 1983. Cellular glutathione depletion by diethyl maleate or buthionine sulfoximine: no effect of glutathione depletion on the oxygen enhancement ratio. *Radiation Research,* 96**,** 422-8.

MOCHIZUKI, M., KWON, Y.-W., YODOI, J. & MASUTANI, H. 2009a. Thioredoxin Regulates Cell Cycle via the ERK1/2-Cyclin D1 Pathway. *Antioxidants & Redox Signaling,* 11**,** 2957-2971.

MOCHIZUKI, M., KWON, Y. W., YODOI, J. & MASUTANI, H. 2009b. Thioredoxin regulates cell cycle via the ERK1/2-cyclin D1 pathway. *Antioxidants & redox signaling* 11**,** 2957-71.

MOLBERG, K. H., HEFFESS, C., DELGADO, R. & ALBORES-SAAVEDRA, J. 1998. Undifferentiated carcinoma with osteoclast-like giant cells of the pancreas and periampullary region. *Cancer,* 82**,** 1279-87.

MOLLBRINK, A., JAWAD, R., VLAMIS-GARDIKAS, A., EDENVIK, P., ISAKSSON, B., DANIELSSON, O., STAL, P. & FERNANDES, A. P. 2014. Expression of thioredoxins and glutaredoxins in human hepatocellular carcinoma: correlation to cell proliferation, tumor size and metabolic syndrome. *Int J Immunopathol Pharmacol,* 27**,** 169-83.

MONTI, P., MARCHESI, F., RENI, M., MERCALLI, A., SORDI, V., ZERBI, A., BALZANO, G., DI CARLO, V., ALLAVENA, P. & PIEMONTI, L. 2004. A comprehensive in vitro characterization of pancreatic ductal carcinoma cell line biological behavior and its correlation with the structural and genetic profile. *Virchows Archiv,* 445**,** 236-247.

MOORE, P. S., BEGHELLI, S., ZAMBONI, G. & SCARPA, A. 2003. Genetic abnormalities in pancreatic cancer. *Molecular cancer,* 2**,** 7.

MORAK, M. J., VAN KOETSVELD, P. M., KANAAR, R., HOFLAND, L. J. & VAN EIJCK, C. H. 2011. Type I interferons as radiosensitisers for pancreatic cancer. *European Journal of Cancer and Clinical Oncology,* 47**,** 1938-45.

MUKHERJEE, S., HURT, C. N., BRIDGEWATER, J., FALK, S., CUMMINS, S., WASAN, H., CROSBY, T., JEPHCOTT, C., ROY, R., RADHAKRISHNA, G., MCDONALD, A., RAY, R., JOSEPH, G., STAFFURTH, J., ABRAMS, R. A., GRIFFITHS, G. & MAUGHAN, T. 2013. Gemcitabine-based or capecitabine-based chemoradiotherapy for locally advanced pancreatic cancer (SCALOP): a multicentre, randomised, phase 2 trial. *The Lancet Oncology,* 14**,** 317-326.

MURLEY, J. S., NANTAJIT, D., BAKER, K. L., KATAOKA, Y., LI, J. J. & GRDINA, D. J. 2008. Maintenance of manganese superoxide dismutase (SOD2)-mediated delayed radioprotection induced by repeated administration of the free thiol form of amifostine. *Radiation research,* 169**,** 495-505.

NAGOURNEY, R. A., FLAM, M., LINK, J., HAGER, S., BLITZER, J., LYONS, W., SOMMERS, B. L. & EVANS, S. 2008. Carboplatin plus gemcitabine repeating doublet therapy in recurrent breast cancer. *Clinical breast cancer,* 8**,** 432-435.

NAKAMURA, H., BAI, J., NISHINAKA, Y., UEDA, S., SASADA, T., OHSHIO, G., IMAMURA, M., TAKABAYASHI, A., YAMAOKA, Y. & YODOI, J. 2000. Expression of thioredoxin and glutaredoxin, redox-regulating proteins, in pancreatic cancer. *Cancer detection and prevention,* 24**,** 53-60.

NCCN. 2018. *NCCN Guidelines Version 1.2018* [Online]. Available: https://www.nccn.org/professionals/physician_gls/default.aspx#site.

NEOPTOLEMOS, J. P., PALMER, D. H., GHANEH, P., PSARELLI, E. E., VALLE, J. W., HALLORAN, C. M., FALUYI, O., O'REILLY, D. A., CUNNINGHAM, D., WADSLEY, J., DARBY, S., MEYER, T., GILLMORE, R., ANTHONEY, A., LIND, P., GLIMELIUS, B., FALK, S., IZBICKI, J. R., MIDDLETON, G. W., CUMMINS, S., ROSS, P. J., WASAN, H., MCDONALD, A., CROSBY, T., MA, Y. T., PATEL, K., SHERRIFF, D., SOOMAL, R., BORG, D., SOTHI, S., HAMMEL, P., HACKERT, T., JACKSON, R. & BÜCHLER, M. W. 2017. Comparison of adjuvant gemcitabine and capecitabine with gemcitabine monotherapy in patients with resected pancreatic cancer (ESPAC-4): a multicentre, open-label, randomised, phase 3 trial. *The Lancet,* 389**,** 1011-1024.

NISHIYAMA, A., MATSUI, M., IWATA, S., HIROTA, K., MASUTANI, H., NAKAMURA, H., TAKAGI, Y., SONO, H., GON, Y. & YODOI, J. 1999. Identification of thioredoxin-binding protein-2/vitamin D(3) up-regulated protein 1 as a negative regulator of thioredoxin function and expression. *The Journal of biological chemistry,* 274**,** 21645-50.

O'REILLY, E. M. 2010. Refinement of adjuvant therapy for pancreatic cancer. *JAMA,* 304**,** 1124-5.

OOSTVEEN, E. & SPECKAMP, W. 1987. Mitomycin analogs I. Indoloquinones as (potential) bisalkylating agents. *Tetrahedron,* 43**,** 255-262.

OVERGAARD, J., ERIKSEN, J. G., NORDSMARK, M., ALSNER, J. & HORSMAN, M. R. 2005. Plasma osteopontin, hypoxia, and response to the hypoxia sensitiser nimorazole

in radiotherapy of head and neck cancer: results from the DAHANCA 5 randomised double-blind placebo-controlled trial. *The lancet oncology,* 6**,** 757-764.

OVERGAARD, J., HANSEN, H. S., OVERGAARD, M., BASTHOLT, L., BERTHELSEN, A., SPECHT, L., LINDELØV, B. & JØRGENSEN, K. 1998. A randomized double-blind phase III study of nimorazole as a hypoxic radiosensitizer of primary radiotherapy in supraglottic larynx and pharynx carcinoma. Results of the Danish Head and Neck Cancer Study (DAHANCA) Protocol 5-85. *Radiotherapy and Oncology,* 46**,** 135-146.

OZBEN, T. 2007. Oxidative stress and apoptosis: Impact on cancer therapy. *Journal of Pharmaceutical Sciences,* 96**,** 2181-2196.

P. VASSILAKOPOULOS, T., LEVIDOU, G., MILIONIS, V., HARTMANN, S., LAKIOTAKI, E., SEPSA, A., THYMARA, I., NTAILIANI, P., SPANOU, K. & K. ANGELOPOULOU, M. 2017. Thioredoxin-1, chemokine (CXC motif) ligand-9 and interferon-γ expression in the neoplastic cells and macrophages of Hodgkin lymphoma: clinicopathologic correlations and potential prognostic implications. *Leukemia & lymphoma,* 58**,** 2227-2239.

PAAL, E., THOMPSON, L. D., FROMMELT, R. A., PRZYGODZKI, R. M. & HEFFESS, C. S. 2001. A clinicopathologic and immunohistochemical study of 35 anaplastic carcinomas of the pancreas with a review of the literature. *Annals of diagnostic pathology,* 5**,** 129-40.

PAN, X., ARUMUGAM, T., YAMAMOTO, T., LEVIN, P. A., RAMACHANDRAN, V., JI, B., LOPEZ-BERESTEIN, G., VIVAS-MEJIA, P. E., SOOD, A. K. & MCCONKEY, D. J. 2008. Nuclear factor-κB p65/relA silencing induces apoptosis and increases gemcitabine effectiveness in a subset of pancreatic cancer cells. *Clinical Cancer Research,* 14**,** 8143-8151.

PAPA, L., HAHN, M., MARSH, E. L., EVANS, B. S. & GERMAIN, D. 2014. SOD2 to SOD1 switch in breast cancer. *The Journal of biological chemistry,* 289**,** 5412-6.

PARKIN, D. M., BOYD, L. & WALKER, L. C. 2011. 16. The fraction of cancer attributable to lifestyle and environmental factors in the UK in 2010. *British journal of cancer,* 105 Suppl 2**,** S77-81.

PARSELS, L. A., MORGAN, M. A., TANSKA, D. M., PARSELS, J. D., PALMER, B. D., BOOTH, R. J., DENNY, W. A., CANMAN, C. E., KRAKER, A. J. & LAWRENCE, T. S. 2009. Gemcitabine sensitization by checkpoint kinase 1 inhibition correlates with inhibition of a Rad51 DNA damage response in pancreatic cancer cells. *Molecular cancer therapeutics,* 8**,** 45-54.

PAVLIDIS, N., HANAUSKE, A. R., GAMUCCI, T., SMYTH, J., LEHNERT, M., TE VELDE, A., LAN, J. & VERWEIJ, J. 1996. A randomized phase II study with two schedules of the novel indoloquinone EO9 in non-small-cell lung cancer: a study of the EORTC Early Clinical Studies Group (ECSG). *Annals of oncology,* 7**,** 529-31.

PAZ, M. M., ZHANG, X., LU, J. & HOLMGREN, A. 2012. A New Mechanism of Action for the Anticancer Drug Mitomycin C: Mechanism-Based Inhibition of Thioredoxin Reductase. *Chemical Research in Toxicology,* 25**,** 1502-1511.

PERMUTH-WEY, J. & EGAN, K. M. 2009. Family history is a significant risk factor for pancreatic cancer: results from a systematic review and meta-analysis. *Familial cancer,* 8**,** 109-17.

PFEIFFER, S. & TOLMACH, L. 1967. Inhibition of DNA synthesis in HeLa cells by hydroxyurea. *Cancer research,* 27**,** 124-129.

PHILLIPS, R. M. 1996. Bioreductive activation of a series of analogues of 5-aziridinyl-3-hydroxymethyl-1-methyl-2-[1H-indole-4, 7-dione] prop-β-en-α-ol (EO9) by human DT-diaphorase. *Biochemical pharmacology,* 52**,** 1711-1718.

PHILLIPS, R. M. 1998. Prospects for bioreductive drug development. *Expert opinion on investigational drugs,* 7**,** 905-928.

PHILLIPS, R. M., HENDRIKS, H. R. & PETERS, G. J. 2013. EO9 (Apaziquone): from the clinic to the laboratory and back again. *British journal of pharmacology,* 168**,** 11-8.

PHILLIPS, R. M., HULBERT, P., BIBBY, M., SLEIGH, N. & DOUBLE, J. 1992a. In vitro activity of the novel indoloquinone EO-9 and the influence of pH on cytotoxicity. *British journal of cancer,* 65**,** 359.

PHILLIPS, R. M., HULBERT, P. B., BIBBY, M. C., SLEIGH, N. R. & DOUBLE, J. A. 1992b. In vitro activity of the novel indoloquinone EO-9 and the influence of pH on cytotoxicity. *British journal of cancer,* 65**,** 359-64.

PIZZIMENTI, S., TOALDO, C., PETTAZZONI, P., DIANZANI, M. U. & BARRERA, G. 2010. The" two-faced" effects of reactive oxygen species and the lipid peroxidation product 4-hydroxynonenal in the hallmarks of cancer. *Cancers,* 2**,** 338-363.

PLUMB, J. A., GERRITSEN, M., MILROY, R., THOMSON, P. & WORKMAN, P. 1994a. Relative importance of DT-diaphorase and hypoxia in the bioactivation of E09 by human lung tumor cell lines. *International Journal of Radiation Oncology* Biology* Physics,* 29**,** 295-299.

PLUMB, J. A., GERRITSEN, M. & WORKMAN, P. 1994b. DT-diaphorase protects cells from the hypoxic cytotoxicity of indoloquinone EO9. *British Journal of Cancer,* 70**,** 1136-1143.

PLUNKETT, W., HUANG, P., SEARCY, C. E. & GANDHI, V. Gemcitabine: preclinical pharmacology and mechanisms of action. Seminars in oncology, 1996. 3-15.

POWIS, G. & MONTFORT, W. R. 2001. Properties and biological activities of thioredoxins. *Annual review of pharmacology and toxicology,* 41**,** 261-95.

PURDY, J. A. & EMAMI, B. 1995. *3D Radiation Treatment Planning and Conformal Therapy: Proceedings of an International Symposium, April 21-23, 1993*, Medical Physics Pub Corp.

PURVINIENĖ, R., KAZLAUSKAITĖ, N., ATKOČIUS, V., CHARACIEJUS, D. & LUKŠIENĖ, A. 2009. Relationship between growth fraction and clonogenic survival after ionizing irradiation in pancreatic MiaPaCa2 cells. *acta medica lituanica,* 16.

QIAO, Z., HE, M., HE, M., LI, W., WANG, X., WANG, Y., KUAI, Q., LI, C., REN, S. & YU, Q. 2016. Synergistic antitumor activity of gemcitabine combined with triptolide in pancreatic cancer cells. *Oncology letters,* 11**,** 3527-3533.

RAAYMAKERS, B., LAGENDIJK, J., OVERWEG, J., KOK, J., RAAIJMAKERS, A., KERKHOF, E., VAN DER PUT, R., MEIJSING, I., CRIJNS, S. & BENEDOSSO, F. 2009. Integrating a

1.5 T MRI scanner with a 6 MV accelerator: proof of concept. *Physics in Medicine & Biology,* 54**,** N229.

RADOJKOVIC, M., ILIC, D. & ILIC, I. 2017. Primary signet ring cell carcinoma of the pancreas with a good response to chemotherapy: case report and literature review. *Tumori,* 103**,** e50-e52.

RAFFEL, J., BHATTACHARYYA, A. K., GALLEGOS, A., CUI, H., EINSPAHR, J. G., ALBERTS, D. S. & POWIS, G. 2003. Increased expression of thioredoxin-1 in human colorectal cancer is associated with decreased patient survival. *Journal of Laboratory and Clinical Medicine,* 142**,** 46-51.

RAGO, R., MITCHEN, J., CHENG, A.-L., OBERLEY, T. & WILDING, G. 1991. Disruption of cellular energy balance by suramin in intact human prostatic carcinoma cells, a likely antiproliferative mechanism. *Cancer research,* 51**,** 6629-6635.

RAHIB, L., SMITH, B. D., AIZENBERG, R., ROSENZWEIG, A. B., FLESHMAN, J. M. & MATRISIAN, L. M. 2014. Projecting cancer incidence and deaths to 2030: the unexpected burden of thyroid, liver, and pancreas cancers in the United States. *Cancer Research,* 74**,** 2913-21.

RAMANATHAN, R. K., ABBRUZZESE, J., DRAGOVICH, T., KIRKPATRICK, L., GUILLEN, J. M., BAKER, A. F., PESTANO, L. A., GREEN, S. & VON HOFF, D. D. 2011. A randomized phase II study of PX-12, an inhibitor of thioredoxin in patients with advanced cancer of the pancreas following progression after a gemcitabine-containing combination. *Cancer Chemotherapy and Pharmacology,* 67**,** 503-9.

RAMANATHAN, R. K., DRAGOVICH, T., RICHARDS, D., STEPHENSON, J., PESTANO, L., HISCOX, A., LEOS, R., CHOW, S., MILLARD, J. & KIRKPATRICK, L. 2009. Results from phase Ib studies of PX-12, a thioredoxin inhibitor in patients with advanced solid malignancies. *Journal of Clinical Oncology,* 27**,** 2571-2571.

RAMANATHAN, R. K., KIRKPATRICK, D. L., BELANI, C. P., FRIEDLAND, D., GREEN, S. B., CHOW, H. S., CORDOVA, C. A., STRATTON, S. P., SHARLOW, E. R. & BAKER, A. 2007. A Phase I pharmacokinetic and pharmacodynamic study of PX-12, a novel inhibitor of thioredoxin-1, in patients with advanced solid tumors. *Clinical cancer research,* 13**,** 2109-2114.

RAMANATHAN, R. K., STEPHENSON, J. J., WEISS, G. J., PESTANO, L. A., LOWE, A., HISCOX, A., LEOS, R. A., MARTIN, J. C., KIRKPATRICK, L. & RICHARDS, D. A. 2012. A phase I trial of PX-12, a small-molecule inhibitor of thioredoxin-1, administered as a 72-hour infusion every 21 days in patients with advanced cancers refractory to standard therapy. *Invest New Drugs,* 30**,** 1591-6.

RANINGA, P. V., DI TRAPANI, G., VUCKOVIC, S. & TONISSEN, K. F. 2016. Cross-talk between two antioxidants, thioredoxin reductase and heme oxygenase-1, and therapeutic implications for multiple myeloma. *Redox Biology,* 8**,** 175-185.

RATHOS, M. J., JOSHI, K., KHANWALKAR, H., MANOHAR, S. M. & JOSHI, K. S. 2012. Molecular evidence for increased antitumor activity of gemcitabine in combination with a cyclin-dependent kinase inhibitor, P276-00 in pancreatic cancers. *Journal of translational medicine,* 10**,** 161.

RAUTALAHTI, M. T., VIRTAMO, J. R., TAYLOR, P. R., HEINONEN, O. P., ALBANES, D., HAUKKA, J. K., EDWARDS, B. K., KARKKAINEN, P. A., STOLZENBERG-SOLOMON, R.

Z. & HUTTUNEN, J. 1999. The effects of supplementation with alpha-tocopherol and beta-carotene on the incidence and mortality of carcinoma of the pancreas in a randomized, controlled trial. *Cancer,* 86**,** 37-42.

RECK, M., VON PAWEL, J., ZATLOUKAL, P., RAMLAU, R., GORBOUNOVA, V., HIRSH, V., LEIGHL, N., MEZGER, J., ARCHER, V. & MOORE, N. 2009. Phase III trial of cisplatin plus gemcitabine with either placebo or bevacizumab as first-line therapy for nonsquamous non–small-cell lung cancer: AVAiL. *Journal of Clinical Oncology,* 27**,** 1227-1234.

REIGAN, P., COLUCCI, M. A., SIEGEL, D., CHILLOUX, A., MOODY, C. J. & ROSS, D. 2007. Development of indolequinone mechanism-based inhibitors of NAD(P)H:quinone oxidoreductase 1 (NQO1): NQO1 inhibition and growth inhibitory activity in human pancreatic MIA PaCa-2 cancer cells. *Biochemistry,* 46**,** 5941-50.

RELA M, R. M. 2014. *Gray's Anatomy: Pancreas.* , Elsevier Limited.

REN, B., HUANG, W., ÅKESSON, B. & LADENSTEIN, R. 1997. The crystal structure of seleno-glutathione peroxidase from human plasma at 2.9 Å resolution1. *Journal of molecular biology,* 268**,** 869-885.

RIALL, T. S., CAMERON, J. L., LILLEMOE, K. D., WINTER, J. M., CAMPBELL, K. A., HRUBAN, R. H., CHANG, D. & YEO, C. J. 2006. Resected periampullary adenocarcinoma: 5-year survivors and their 6-to 10-year follow-up. *Surgery,* 140**,** 764-772.

RINEHART, K. L. & RINEHART, K. L. 1973. *Oxidation and reduction of organic compounds*, Prentice-Hall.

RISCHIN, D., PETERS, L. J., O'SULLIVAN, B., GIRALT, J., FISHER, R., YUEN, K., TROTTI, A., BERNIER, J., BOURHIS, J. & RINGASH, J. 2008. Tirapazamine, cisplatin, and radiation versus cisplatin and radiation for advanced squamous cell carcinoma of the head and neck (TROG 02.02, HeadSTART): a phase III trial of the Trans-Tasman Radiation Oncology Group. *Oncology*.

ROBERTSON, N., HAIGH, A., ADAMS, G. & STRATFORD, I. 1994. Factors affecting sensitivity to EO9 in rodent and human tumour cells in vitro: DT-diaphorase activity and hypoxia. *European Journal of Cancer,* 30**,** 1013-1019.

ROBERTSON, N., STRATFORD, I., HOULBROOK, S., CARMICHAEL, J. & ADAMS, G. 1992. The sensitivity of human tumour cells to quinone bioreductive drugs: what role for DT-diaphorase? *Biochemical pharmacology,* 44**,** 409-412.

ROCKWELL, S. & KENNEDY, K. A. 1979. Combination therapy with radiation and mitomycin C: Preliminary results with EMT6 tumor cells in vitro and in vivo. *International Journal of Radiation Oncology* Biology* Physics,* 5**,** 1673-1676.

ROCKWELL, S., KENNEDY, K. A. & SARTORELLI, A. C. 1982. Mitomycin-C as a prototype bioreductive alkylating agent: in vitro studies of metabolism and cytotoxicity. *International Journal of Radiation Oncology* Biology* Physics,* 8**,** 753-755.

RODMAN, S. N., SPENCE, J. M., RONNFELDT, T. J., ZHU, Y., SOLST, S. R., O'NEILL, R. A., ALLEN, B. G., GUAN, X., SPITZ, D. R. & FATH, M. A. 2016. Enhancement of Radiation Response in Breast Cancer Stem Cells by Inhibition of Thioredoxin- and Glutathione-Dependent Metabolism. *Radiation Research,* 186**,** 385-395.

ROED, H., AABO, K., VINDELØV, L., SPANG-THOMSEN, M., CHRISTENSEN, I. J. & HANSEN, H. H. 1989. In vitro and in vivo evaluation of the indoloquinone EO-9 (NSC 382 459) against human small cell carcinoma of the lung. *European Journal of Cancer and Clinical Oncology,* 25**,** 1197-1201.

ROMBOUTS, S. J., VOGEL, J. A., VAN SANTVOORT, H. C., VAN LIENDEN, K. P., VAN HILLEGERSBERG, R., BUSCH, O. R., BESSELINK, M. G. & MOLENAAR, I. Q. 2015. Systematic review of innovative ablative therapies for the treatment of locally advanced pancreatic cancer. *The British journal of surgery,* 102**,** 182-93.

ROZENBLUM, E., SCHUTTE, M., GOGGINS, M., HAHN, S. A., PANZER, S., ZAHURAK, M., GOODMAN, S. N., SOHN, T. A., HRUBAN, R. H., YEO, C. J. & KERN, S. E. 1997. Tumor-suppressive Pathways in Pancreatic Carcinoma. *Cancer Research,* 57**,** 1731.

SAH, R. P., NAGPAL, S. J. S., SHARMA, A., KAMBOJ, A. K., TAKAHASHI, N., MUKHOPADHYAY, D. & CHARI, S. T. 2017. Paraneoplastic Weight Loss and Rise in Blood Glucose Preceding Symptoms of Pancreatic Cancer (PC): Opportunity for Early Detection. *Gastroenterology,* 152**,** S491.

SAITOH, M., NISHITOH, H., FUJII, M., TAKEDA, K., TOBIUME, K., SAWADA, Y., KAWABATA, M., MIYAZONO, K. & ICHIJO, H. 1998. Mammalian thioredoxin is a direct inhibitor of apoptosis signal-regulating kinase (ASK) 1. *The EMBO journal,* 17**,** 2596-2606.

SAMUEL, A. H. & MAGEE, J. L. 1953. Theory of radiation chemistry. II. Track effects in radiolysis of water. *The Journal of Chemical Physics,* 21**,** 1080-1087.

SARMIENTO, J. M., NAGORNEY, D. M., SARR, M. G. & FARNELL, M. B. 2001. Periampullary cancers: are there differences? *Surgical Clinics of North America,* 81**,** 543-555.

SATO, F., SHIMADA, Y., SELARU, F. M., SHIBATA, D., MAEDA, M., WATANABE, G., MORI, Y., STASS, S. A., IMAMURA, M. & MELTZER, S. J. 2005. Prediction of survival in patients with esophageal carcinoma using artificial neural networks. *Cancer: Interdisciplinary International Journal of the American Cancer Society,* 103**,** 1596-1605.

SCHELLENS, J. H., PLANTING, A. S., VAN ACKER, B. A., LOOS, W. J., DE BOER-DENNERT, M., VAN DER BURG, M. E., KOIER, I., KREDIET, R. T., STOTER, G. & VERWEIJ, J. 1994. Phase I and pharmacologic study of the novel indoloquinone bioreductive alkylating cytotoxic drug E09. *JNCI: Journal of the National Cancer Institute,* 86**,** 906-12.

SCHENK, H., KLEIN, M., ERDBRÜGGER, W., DRÖGE, W. & SCHULZE-OSTHOFF, K. 1994. Distinct effects of thioredoxin and antioxidants on the activation of transcription factors NF-kappa B and AP-1. *Proceedings of the National Academy of Sciences of the United States of America,* 91**,** 1672-1676.

SCHEUFELE, F. & FRIESS, H. 2017. Palliative Surgery in Advanced Pancreatic Cancer. *In:* NEOPTOLEMOS, J. P., URRUTIA, R., ABBRUZZESE, J. & BÜCHLER, M. W. (eds.) *Pancreatic Cancer.* New York, NY: Springer New York.

SCHMELTZ, I., TOSK, J., JACOBS, G. & HOFFMANN, D. 1977. Redox potential and quinone content of cigarette smoke. *Analytical chemistry,* 49**,** 1924-1929.

SCHROEDER, P., POPP, R., WIEGAND, B., ALTSCHMIED, J. & HAENDELER, J. 2007. Nuclear Redox-Signaling Is Essential for Apoptosis Inhibition in Endothelial Cells. *Arterioscler Thromb Vasc Biol,* 27**,** 2325-2331.

SCHULTZ, M. A., DIAZ, A. M., SMITE, S., LAY, A. R., DECANT, B., MCKINNEY, R., MASCARINAS, W. E., XIA, Y., NEUMANN, C., BENTREM, D., DAWSON, D. W. & GRIPPO, P. J. 2017. Thioredoxin system-mediated regulation of mutant Kras associated pancreatic neoplasia and cancer. *Oncotarget,* 8**,** 92667-92681.

SCHUTTE, M., HRUBAN, R. H., HEDRICK, L., CHO, K. R., NADASDY, G. M., WEINSTEIN, C. L., BOVA, G. S., ISAACS, W. B., CAIRNS, P., NAWROZ, H., SIDRANSKY, D., CASERO, R. A., JR., MELTZER, P. S., HAHN, S. A. & KERN, S. E. 1996. DPC4 gene in various tumor types. *Cancer Research,* 56**,** 2527-30.

SE LEE, Y., SE LEE, Y., WON CHANG, H., SE LEE, Y., WON CHANG, H., EUN JEONG, J., LEE, S.-W. & YOON KIM, S. 2008. Proteomic analysis of two head and neck cancer cell lines presenting different radiation sensitivity. *Acta Oto-Laryngologica,* 128**,** 86-92.

SELENIUS, M., HEDMAN, M., BRODIN, D., GANDIN, V., RIGOBELLO, M. P., FLYGARE, J., MARZANO, C., BINDOLI, A., BRODIN, O., BJORNSTEDT, M. & FERNANDES, A. P. 2012. Effects of redox modulation by inhibition of thioredoxin reductase on radiosensitivity and gene expression. *Journal of cellular and molecular medicine,* 16**,** 1593-605.

SEN, C. K. & PACKER, L. 1996. Antioxidant and redox regulation of gene transcription. *The FASEB journal,* 10**,** 709-720.

SENER, S. F., FREMGEN, A., MENCK, H. R. & WINCHESTER, D. P. 1999. Pancreatic cancer: a report of treatment and survival trends for 100,313 patients diagnosed from 1985–1995, using the National Cancer Database11No competing interests declared. *Journal of the American College of Surgeons,* 189**,** 1-7.

SHI, C., YU, L., YANG, F., YAN, J. & ZENG, H. 2003. A novel organoselenium compound induces cell cycle arrest and apoptosis in prostate cancer cell lines. *Biochemical and Biophysical Research Communications,* 309**,** 578-583.

SHOUSHA, S. 1982. Signet-ring cell adenocarcinoma of rectum: a histological, histochemical and electron microscopic study. *Histopathology,* 6**,** 341-50.

SIEGEL, R., MA, J., ZOU, Z. & JEMAL, A. 2014. Cancer statistics, 2014. *CA: A Cancer Journal for Clinicians,* 64**,** 9-29.

SINGHI, A. D., ISHIDA, H., ALI, S. Z., GOGGINS, M., CANTO, M., WOLFGANG, C., MERIDEN, Z., ROBERTS, N., KLEIN, A. P. & HRUBAN, R. H. 2015. A histomorphologic comparison of familial and sporadic pancreatic cancers. *Pancreatology,* 15**,** 387-391.

SIPOS, B., FRANK, S., GRESS, T., HAHN, S. & KLOPPEL, G. 2009. Pancreatic intraepithelial neoplasia revisited and updated. *Pancreatology,* 9**,** 45-54.

SKEHAN, P., STORENG, R., SCUDIERO, D., MONKS, A., MCMAHON, J., VISTICA, D., WARREN, J. T., BOKESCH, H., KENNEY, S. & BOYD, M. R. 1990. New colorimetric cytotoxicity assay for anticancer-drug screening. *JNCI: Journal of the National Cancer Institute,* 82**,** 1107-1112.

SLATER, T., SAWYER, B. & STRÄULI, U. 1963. Studies on succinate-tetrazolium reductase systems: III. Points of coupling of four different tetrazolium salts III. Points of coupling of four different tetrazolium salts. *Biochimica et biophysica acta,* 77**,** 383-393.

SMART, D. K., ORTIZ, K. L., MATTSON, D., BRADBURY, C. M., BISHT, K. S., SIECK, L. K., BRECHBIEL, M. W. & GIUS, D. 2004. Thioredoxin reductase as a potential molecular target for anticancer agents that induce oxidative stress. *Cancer Research,* 64**,** 6716-24.

SMYTH, E. N., BAPAT, B., BALL, D. E., ANDRE, T. & KAYE, J. A. 2015. Metastatic Pancreatic Adenocarcinoma Treatment Patterns, Health Care Resource Use, and Outcomes in France and the United Kingdom Between 2009 and 2012: A Retrospective Study. *Clinical therapeutics*.

SOBHANI, M., TAHERI, A.-R., JAFARIAN, A.-H. & HASHEMY, S. I. 2016. The activity and tissue distribution of thioredoxin reductase in basal cell carcinoma. *Journal of cancer research and clinical oncology,* 142**,** 2303-2307.

SPERTI, C., PASQUALI, C., PICCOLI, A. & PEDRAZZOLI, S. 1996. Survival after resection for ductal adenocarcinoma of the pancreas. *British Journal of Surgery,* 83**,** 625-631.

SPIELBERGER, J. C., MOODY, A. D. & WATSON, W. H. 2008. Oxidation and nuclear localization of thioredoxin-1 in sparse cell cultures. *Journal of cellular biochemistry,* 104**,** 1879-1889.

STEEL, G. G., MCMILLAN, T. J. & PEACOCK, J. H. 1989. The 5Rs of radiobiology. *International journal of radiation biology,* 56**,** 1045-8.

STOLZENBERG-SOLOMON, R. Z., BLASER, M. J., LIMBURG, P. J., PEREZ-PEREZ, G., TAYLOR, P. R., VIRTAMO, J., ALBANES, D. & STUDY, A. 2001. Helicobacter pylori seropositivity as a risk factor for pancreatic cancer. *Journal of the National Cancer Institute,* 93**,** 937-41.

STORR, S. J., ZAITOUN, A. M., ARORA, A., DURRANT, L. G., LOBO, D. N., MADHUSUDAN, S. & MARTIN, S. G. 2012. Calpain system protein expression in carcinomas of the pancreas, bile duct and ampulla. *BMC Cancer,* 12**,** 511.

STORZ, P. 2005. Reactive oxygen species in tumor progression. *Frontiers in bioscience,* 10**,** 1881-96.

SUN, G., WANG, Y., HU, W. & LI, C. 2013. Effects of manganese superoxide dismutase (MnSOD) expression on regulation of esophageal cancer cell growth and apoptosis in vitro and in nude mice. *Tumour biology,* 34**,** 1409-19.

SUN, H., MA, H., HONG, G., SUN, H. & WANG, J. 2014. Survival improvement in patients with pancreatic cancer by decade: a period analysis of the SEER database, 1981-2010. *Scientific reports,* 4**,** 6747.

SUN, X., MAJUMDER, P., SHIOYA, H., WU, F., KUMAR, S., WEICHSELBAUM, R., KHARBANDA, S. & KUFE, D. 2000. Activation of the cytoplasmic c-Abl tyrosine kinase by reactive oxygen species. *The Journal of biological chemistry,* 275**,** 17237-40.

SUN, Y. & RIGAS, B. 2008. The thioredoxin system mediates redox-induced cell death in human colon cancer cells: implications for the mechanism of action of anticancer agents. *Cancer research,* 68**,** 8269-8277.

SUN, Y., ROWEHL, L. M., HUANG, L., MACKENZIE, G. G., VRANKOVA, K., KOMNINOU, D. & RIGAS, B. 2012. Phospho-ibuprofen (MDC-917) suppresses breast cancer growth: an effect controlled by the thioredoxin system. *Breast Cancer Research,* 14**,** R20.

SUZUKI, Y. J., CARINI, M. & BUTTERFIELD, D. A. 2010. Protein carbonylation. *Antioxidants & redox signaling,* 12**,** 323-325.

TALCOTT, J. A., ROSSI, C., SHIPLEY, W. U., CLARK, J. A., SLATER, J. D., NIEMIERKO, A. & ZIETMAN, A. L. 2010. Patient-reported long-term outcomes after conventional and high-dose combined proton and photon radiation for early prostate cancer. *Jama,* 303**,** 1046-1053.

TANNOCK, I. F. 2005. *The basic science of oncology*, McGraw-Hill.

TAVENDER, T. J., SHEPPARD, A. M. & BULLEID, N. J. 2008. Peroxiredoxin IV is an endoplasmic reticulum localised enzyme forming oligomeric complexes in human cells. *The Biochemical journal,* 411**,** 191-199.

TAYLOR, C. R., SHI, S.-R., CHAIWUN, B., YOUNG, L., IMAM, S. A. & COTE, R. J. 1994. Strategies for improving the immunohistochemical staining of various intranuclear prognostic markers in formalin-paraffin sections: androgen receptor, estrogen receptor, progesterone receptor, p53 protein, proliferating cell nuclear antigen, and Ki-67 antigen revealed by antigen retrieval techniques. *Human pathology,* 25**,** 263-270.

TEMPERO, M., BERLIN, J., DUCREUX, M., HALLER, D., HARPER, P., KHAYAT, D., SCHMOLL, H.-J., SOBRERO, A. & VAN CUTSEM, E. 2011. Pancreatic cancer treatment and research: an international expert panel discussion. *Annals of oncology,* 22**,** 1500-1506.

THOMAS, S. R. & KHUNTIA, D. 2011. Motexafin gadolinium: a promising radiation sensitizer in brain metastasis. *Expert opinion on drug discovery,* 6**,** 195-203.

THOMSON, R. 2012. *Naturally occurring quinones*, Burlington Elsevier Science.

TIMMERMAN, R. D., KAVANAGH, B. D., CHO, L. C., PAPIEZ, L. & XING, L. 2007. Stereotactic body radiation therapy in multiple organ sites. *Journal of Clinical Oncology,* 25**,** 947-952.

TRAMACERE, I., SCOTTI, L., JENAB, M., BAGNARDI, V., BELLOCCO, R., ROTA, M., CORRAO, G., BRAVI, F., BOFFETTA, P. & LA VECCHIA, C. 2010. Alcohol drinking and pancreatic cancer risk: a meta-analysis of the dose-risk relation. *International journal of cancer,* 126**,** 1474-86.

TRAVERSO, N., RICCIARELLI, R., NITTI, M., MARENGO, B., FURFARO, A. L., PRONZATO, M. A., MARINARI, U. M. & DOMENICOTTI, C. 2013. Role of glutathione in cancer progression and chemoresistance. *Oxidative medicine and cellular longevity,* 2013.

UCHIDA, K. 2003. 4-Hydroxy-2-nonenal: a product and mediator of oxidative stress. *Progress in lipid research,* 42**,** 318-343.

URIG, S. & BECKER, K. 2006. On the potential of thioredoxin reductase inhibitors for cancer therapy. *Seminars in Cancer Biology,* 16**,** 452-465.

VAN CUTSEM, E., LENZ, H.-J., FURUSE, J., TABERNERO, J., HEINEMANN, V., IOKA, T., BAZIN, I., UENO, M., CSŐSZI, T. & WASAN, H. 2016. Evofosfamide (TH-302) in

combination with gemcitabine in previously untreated patients with metastatic or locally advanced unresectable pancreatic ductal adenocarcinoma: Primary analysis of the randomized, double-blind phase III MAESTRO study. American Society of Clinical Oncology.

VAN DER GEEST, L. G. M., LEMMENS, V., DE HINGH, I., VAN LAARHOVEN, C., BOLLEN, T. L., NIO, C. Y., VAN EIJCK, C. H. J., BUSCH, O. R. C. & BESSELINK, M. G. 2017. Nationwide outcomes in patients undergoing surgical exploration without resection for pancreatic cancer. *The British journal of surgery,* 104**,** 1568-1577.

VAN PUTTEN, L. M. & KALLMAN, R. F. 1968. Oxygenation status of a transplantable tumor during fractionated radiation therapy. *Journal of the National Cancer Institute,* 40**,** 441-51.

VARGAS, R., NINO-MURCIA, M., TRUEBLOOD, W. & JEFFREY, R. B., JR. 2004. MDCT in Pancreatic adenocarcinoma: prediction of vascular invasion and resectability using a multiphasic technique with curved planar reformations. *AJR. American journal of roentgenology,* 182**,** 419-25.

VASEN, H. F., GRUIS, N. A., FRANTS, R. R., VAN DER VELDEN, P. A., HILLE, E. T. & BERGMAN, W. 2000. Risk of developing pancreatic cancer in families with familial atypical multiple mole melanoma associated with a specific 19 deletion of p16 (p16-Leiden). *International journal of cancer,* 87**,** 809-11.

VAUPEL, P., BRIEST, S. & HÖCKEL, M. 2002. Hypoxia in breast cancer: pathogenesis, characterization and biological/therapeutic implications. *Wiener Medizinische Wochenschrift,* 152**,** 334-342.

VAUPEL, P., SCHLENGER, K., KNOOP, C. & HÖCKEL, M. 1991. Oxygenation of human tumors: evaluation of tissue oxygen distribution in breast cancers by computerized O2 tension measurements. *Cancer research,* 51**,** 3316-3322.

VERWEIJ, J. & PINEDO, H. M. 1990. Mitomycin C: mechanism of action, usefulness and limitations. *Anticancer Drugs,* 1**,** 5-13.

VICHAI, V. & KIRTIKARA, K. 2006. Sulforhodamine B colorimetric assay for cytotoxicity screening. *Nature protocols,* 1**,** 1112.

VINCENT, A., HERMAN, J., SCHULICK, R., HRUBAN, R. H. & GOGGINS, M. 2011. Pancreatic cancer. *Lancet,* 378**,** 607-20.

VISSER, B. C., MA, Y., ZAK, Y., POULTSIDES, G. A., NORTON, J. A. & RHOADS, K. F. 2012. Failure to comply with NCCN guidelines for the management of pancreatic cancer compromises outcomes. *Hpb,* 14**,** 539-547.

VOGT, A., TAMURA, K., WATSON, S. & LAZO, J. S. 2000. Antitumor imidazolyl disulfide IV-2 causes irreversible g2/M cell cycle arrest without hyperphosphorylation of cyclin-dependent kinase Cdk1. *Journal of Pharmacology and Experimental Therapeutics,* 294**,** 1070-1075.

VUKMANOVIĆ, S. & ZAMOYSKA, R. 1991. Anti-CD3-induced cell death in T cell hybridomas: mitochondrial failure and DNA fragmentation are distinct events. *European journal of immunology,* 21**,** 419-424.

WADDELL, N., PAJIC, M., PATCH, A. M., CHANG, D. K., KASSAHN, K. S., BAILEY, P., JOHNS, A. L., MILLER, D., NONES, K., QUEK, K., QUINN, M. C., ROBERTSON, A. J., FADLULLAH, M. Z., BRUXNER, T. J., CHRIST, A. N., HARLIWONG, I., IDRISOGLU, S.,

MANNING, S., NOURSE, C., NOURBAKHSH, E., WANI, S., WILSON, P. J., MARKHAM, E., CLOONAN, N., ANDERSON, M. J., FINK, J. L., HOLMES, O., KAZAKOFF, S. H., LEONARD, C., NEWELL, F., POUDEL, B., SONG, S., TAYLOR, D., WADDELL, N., WOOD, S., XU, Q., WU, J., PINESE, M., COWLEY, M. J., LEE, H. C., JONES, M. D., NAGRIAL, A. M., HUMPHRIS, J., CHANTRILL, L. A., CHIN, V., STEINMANN, A. M., MAWSON, A., HUMPHREY, E. S., COLVIN, E. K., CHOU, A., SCARLETT, C. J., PINHO, A. V., GIRY-LATERRIERE, M., ROOMAN, I., SAMRA, J. S., KENCH, J. G., PETTITT, J. A., MERRETT, N. D., TOON, C., EPARI, K., NGUYEN, N. Q., BARBOUR, A., ZEPS, N., JAMIESON, N. B., GRAHAM, J. S., NICLOU, S. P., BJERKVIG, R., GRUTZMANN, R., AUST, D., HRUBAN, R. H., MAITRA, A., IACOBUZIO-DONAHUE, C. A., WOLFGANG, C. L., MORGAN, R. A., LAWLOR, R. T., CORBO, V., BASSI, C., FALCONI, M., ZAMBONI, G., TORTORA, G., TEMPERO, M. A., AUSTRALIAN PANCREATIC CANCER GENOME, I., GILL, A. J., ESHLEMAN, J. R., PILARSKY, C., SCARPA, A., MUSGROVE, E. A., PEARSON, J. V., BIANKIN, A. V. & GRIMMOND, S. M. 2015. Whole genomes redefine the mutational landscape of pancreatic cancer. *Nature,* 518**,** 495-501.

WADE, T. P., PRASAD, C. N., VIRGO, K. S. & JOHNSON, F. E. 1997. Experience with distal bile duct cancers in US Veterans Affairs hospitals: 1987–1991. *Journal of surgical oncology,* 64**,** 242-245.

WALTER, F. M., MILLS, K., MENDONCA, S. C., ABEL, G. A., BASU, B., CARROLL, N., BALLARD, S., LANCASTER, J., HAMILTON, W., RUBIN, G. P. & EMERY, J. D. 2016. Symptoms and patient factors associated with diagnostic intervals for pancreatic cancer (SYMPTOM pancreatic study): a prospective cohort study. *The lancet. Gastroenterology & hepatology,* 1**,** 298-306.

WANG, H., BOUZAKOURA, S., DE MEY, S., JIANG, H., LAW, K., DUFAIT, I., CORBET, C., VEROVSKI, V., GEVAERT, T., FERON, O., VAN DEN BERGE, D., STORME, G. & DE RIDDER, M. 2017. Auranofin radiosensitizes tumor cells through targeting thioredoxin reductase and resulting overproduction of reactive oxygen species. *Oncotarget,* 8**,** 35728-35742.

WANG, J., PAN, S. & BERK, B. C. 2007. Glutaredoxin Mediates Akt and eNOS Activation by Flow in a Glutathione Reductase-Dependent Manner. *Arteriosclerosis, Thrombosis, and Vascular Biology,* 27**,** 1283-1288.

WANG, L., FU, J. N., WANG, J. Y., JIN, C. J., REN, X. Y., TAN, Q., LI, J., YIN, H. W., XIONG, K., WANG, T. Y., LIU, X. M. & ZENG, H. H. 2011. Selenium-containing thioredoxin reductase inhibitor ethaselen sensitizes non-small cell lung cancer to radiotherapy. *Anticancer Drugs,* 22**,** 732-40.

WANG, P., CHEN, L., ZHANG, J., CHEN, H., FAN, J., WANG, K., LUO, J., CHEN, Z., MENG, Z. & LIU, L. 2014. Methylation-mediated silencing of the miR-124 genes facilitates pancreatic cancer progression and metastasis by targeting Rac1. *Oncogene,* 33**,** 514-24.

WANG, T., TAMAE, D., LEBON, T., SHIVELY, J. E., YEN, Y. & LI, J. J. 2005. The role of peroxiredoxin II in radiation-resistant MCF-7 breast cancer cells. *Cancer research,* 65**,** 10338-10346.

WARDMAN, P., DENNIS, M. F., EVERETT, S. A., PATEL, K. B., STRATFORD, M. R. & TRACY, M. Radicals from one-electron reduction of nitro compounds, aromatic N-oxides and quinones; the kinetic basis for hypoxia-selective, bioreductive drugs. Biochemical Society Symposia, 1995. PORTLAND PRESS-LONDON, 171-194.

WATSON, W. H., CHEN, Y. & JONES, D. P. 2003a. Redox state of glutathione and thioredoxin in differentiation and apoptosis. *Biofactors,* 17**,** 307-14.

WATSON, W. H., POHL, J., MONTFORT, W. R., STUCHLIK, O., REED, M. S., POWIS, G. & JONES, D. P. 2003b. Redox potential of human thioredoxin 1 and identification of a second dithiol/disulfide motif. *The Journal of biological chemistry,* 278**,** 33408-15.

WEI, M., JIAO, D., HAN, D., WU, J., WEI, F., ZHENG, G., GUO, Z., XI, W., YANG, F., XIE, P., ZHANG, L., YANG, A.-G., WANG, H., QIN, W. & WEN, W. 2017. Knockdown of RNF2 induces cell cycle arrest and apoptosis in prostate cancer cells through the upregulation of TXNIP. *Oncotarget,* 8**,** 5323-5338.

WEI, S. J., BOTERO, A., HIROTA, K., BRADBURY, C. M., MARKOVINA, S., LASZLO, A., SPITZ, D. R., GOSWAMI, P. C., YODOI, J. & GIUS, D. 2000. Thioredoxin nuclear translocation and interaction with redox factor-1 activates the activator protein-1 transcription factor in response to ionizing radiation. *Cancer research,* 60**,** 6688-6695.

WELLS, G., BRADSHAW, T. D., DIANA, P., SEATON, A., SHI, D.-F., WESTWELL, A. D. & STEVENS, M. F. 2000. Antitumour benzothiazoles. Part 10: the synthesis and antitumour activity of benzothiazole substituted quinol derivatives. *Bioorganic & medicinal chemistry letters,* 10**,** 513-515.

WEYDERT, C. J. & CULLEN, J. J. 2009. Measurement of superoxide dismutase, catalase and glutathione peroxidase in cultured cells and tissue. *Nature Protocols,* 5**,** 51.

WILENTZ, R. E., ALBORES-SAAVEDRA, J., ZAHURAK, M., TALAMINI, M. A., YEO, C. J., CAMERON, J. L. & HRUBAN, R. H. 1999. Pathologic examination accurately predicts prognosis in mucinous cystic neoplasms of the pancreas. *The American journal of surgical pathology,* 23**,** 1320-7.

WILENTZ, R. E., GERADTS, J., MAYNARD, R., OFFERHAUS, G. J., KANG, M., GOGGINS, M., YEO, C. J., KERN, S. E. & HRUBAN, R. H. 1998. Inactivation of the p16 (INK4A) tumor-suppressor gene in pancreatic duct lesions: loss of intranuclear expression. *Cancer Research,* 58**,** 4740-4.

WILENTZ, R. E., GOGGINS, M., REDSTON, M., MARCUS, V. A., ADSAY, N. V., SOHN, T. A., KADKOL, S. S., YEO, C. J., CHOTI, M., ZAHURAK, M., JOHNSON, K., TASCILAR, M., OFFERHAUS, G. J., HRUBAN, R. H. & KERN, S. E. 2000a. Genetic, immunohistochemical, and clinical features of medullary carcinoma of the pancreas: A newly described and characterized entity. *The American journal of pathology,* 156**,** 1641-51.

WILENTZ, R. E., IACOBUZIO-DONAHUE, C. A., ARGANI, P., MCCARTHY, D. M., PARSONS, J. L., YEO, C. J., KERN, S. E. & HRUBAN, R. H. 2000b. Loss of Expression of Dpc4 in Pancreatic Intraepithelial Neoplasia: Evidence That DPC4 Inactivation Occurs Late in Neoplastic Progression. *Cancer Research,* 60**,** 2002.

WILLIAMS, M. V., DENEKAMP, J. & FOWLER, J. F. 1985. A review of alpha/beta ratios for experimental tumors: implications for clinical studies of altered fractionation. *International Journal of Radiation Oncology* Biology* Physics,* 11**,** 87-96.

WILLIS, R. 1960. *Pathology of tumours,* London, Butterworth & Co.

WINSKI, S. L., FAIG, M., BIANCHET, M. A., SIEGEL, D., SWANN, E., FUNG, K., DUNCAN, M. W., MOODY, C. J., AMZEL, L. M. & ROSS, D. 2001. Characterization of a mechanism-based inhibitor of NAD(P)H:quinone oxidoreductase 1 by biochemical, X-ray crystallographic, and mass spectrometric approaches. *Biochemistry,* 40**,** 15135-42.

WITHERS, H. R. 1975a. Cell Cycle Redistribution as a Factor in Multifraction Irradiation. *Radiology,* 114**,** 199-202.

WITHERS, H. R. 1975b. The four R's of radiotherapy. *Advances in Radiation Biology,* 5**,** 241-271.

WITHERS, H. R., TAYLOR, J. M. G. & MACIEJEWSKI, B. 1988. The hazard of accelerated tumor clonogen repopulation during radiotherapy. *Acta Oncologica,* 27**,** 131-146.

WOOD, Z. A., SCHRODER, E., ROBIN HARRIS, J. & POOLE, L. B. 2003. Structure, mechanism and regulation of peroxiredoxins. *Trends in biochemical sciences,* 28**,** 32-40.

WOOLSTON, C. & MARTIN, S. 2011. Analysis of tumor and endothelial cell viability and survival using sulforhodamine B and clonogenic assays. *Mammalian Cell Viability.* Springer.

WOOLSTON, C. M., AL-ATTAR, A., STORR, S. J., ELLIS, I. O., MORGAN, D. A. & MARTIN, S. G. 2011a. Redox protein expression predicts radiotherapeutic response in early-stage invasive breast cancer patients. *Int J Radiat Oncol Biol Phys,* 79**,** 1532-40.

WOOLSTON, C. M., DEEN, S., AL-ATTAR, A., SHEHATA, M., CHAN, S. Y. & MARTIN, S. G. 2010. Redox protein expression predicts progression-free and overall survival in ovarian cancer patients treated with platinum-based chemotherapy. *Free Radic Biol Med,* 49**,** 1263-72.

WOOLSTON, C. M., MADHUSUDAN, S., SOOMRO, I. N., LOBO, D. N., REECE-SMITH, A. M., PARSONS, S. L. & MARTIN, S. G. 2013. Thioredoxin interacting protein and its association with clinical outcome in gastro-oesophageal adenocarcinoma. *Redox Biol,* 1**,** 285-91.

WOOLSTON, C. M., STORR, S. J., ELLIS, I. O., MORGAN, D. A. & MARTIN, S. G. 2011b. Expression of thioredoxin system and related peroxiredoxin proteins is associated with clinical outcome in radiotherapy treated early stage breast cancer. *Radiother Oncol,* 100**,** 308-13.

WOOLSTON, C. M., ZHANG, L., STORR, S. J., AL-ATTAR, A., SHEHATA, M., ELLIS, I. O., CHAN, S. Y. & MARTIN, S. G. 2012. The prognostic and predictive power of redox protein expression for anthracycline-based chemotherapy response in locally advanced breast cancer. *Mod Pathol,* 25**,** 1106-16.

WORKMAN, P. 1994. Enzyme-directed bioreductive drug development revisited: a commentary on recent progress and future prospects with emphasis on quinone anticancer agents and quinone metabolizing enzymes, particularly DT-

diaphorase. *Oncology Research Featuring Preclinical and Clinical Cancer Therapeutics,* 6**,** 461-75.

WORKMAN, P., BINGER, M. & KOOISTRA, K. L. 1992. Pharmacokinetics, distribution, and metabolism of the novel bioreductive alkylating indoloquinone EO9 in rodents. *International Journal of Radiation Oncology* Biology* Physics* 22**,** 713-6.

WORKMAN, P. & WALTON, M. I. 1990. Enzyme-directed bioreductive drug development. *Selective activation of drugs by redox processes.* Springer.

WU, Q. J., WU, L., ZHENG, L. Q., XU, X., JI, C. & GONG, T. T. 2016. Consumption of fruit and vegetables reduces risk of pancreatic cancer: evidence from epidemiological studies. *European journal of cancer prevention* 25**,** 196-205.

XIANG, L., XIE, G., LIU, C., ZHOU, J., CHEN, J., YU, S., LI, J., PANG, X., SHI, H. & LIANG, H. 2013. Knock-down of glutaminase 2 expression decreases glutathione, NADH, and sensitizes cervical cancer to ionizing radiation. *Biochimica et Biophysica Acta (BBA) - Molecular Cell Research,* 1833**,** 2996-3005.

XIE, Q., LAN, G., ZHOU, Y., HUANG, J., LIANG, Y., ZHENG, W., FU, X., FAN, C. & CHEN, T. 2014. Strategy to enhance the anticancer efficacy of X-ray radiotherapy in melanoma cells by platinum complexes, the role of ROS-mediated signaling pathways. *Cancer Letters,* 354**,** 58-67.

XU, Z. W., FRIESS, H., SOLIOZ, M., AEBI, S., KORC, M., KLEEFF, J. & BÜCHLER, M. W. 2001. Bcl-xl antisense oligonucleotides induce apoptosis and increase sensitivity of pancreatic cancer cells to gemcitabine. *International journal of cancer,* 94**,** 268-274.

YACHIDA, S., WHITE, C. M., NAITO, Y., ZHONG, Y., BROSNAN, J. A., MACGREGOR-DAS, A. M., MORGAN, R. A., SAUNDERS, T., LAHERU, D. A., HERMAN, J. M., HRUBAN, R. H., KLEIN, A. P., JONES, S., VELCULESCU, V., WOLFGANG, C. L. & IACOBUZIO-DONAHUE, C. A. 2012. Clinical significance of the genetic landscape of pancreatic cancer and implications for identification of potential long-term survivors. *Clinical cancer research,* 18**,** 6339-47.

YAMAGUCHI, F., TAKATA, M., KAMITORI, K., NONAKA, M., DONG, Y., SUI, L. & TOKUDA, M. 2008. Rare sugar D-allose induces specific up-regulation of TXNIP and subsequent G1 cell cycle arrest in hepatocellular carcinoma cells by stabilization of p27kip1. *International journal of oncology,* 32**,** 377-85.

YAMAO, K., YANAGISAWA, A., TAKAHASHI, K., KIMURA, W., DOI, R., FUKUSHIMA, N., OHIKE, N., SHIMIZU, M., HATORI, T., NOBUKAWA, B., HIFUMI, M., KOBAYASHI, Y., TOBITA, K., TANNO, S., SUGIYAMA, M., MIYASAKA, Y., NAKAGOHRI, T., YAMAGUCHI, T., HANADA, K., ABE, H., TADA, M., FUJITA, N. & TANAKA, M. 2011. Clinicopathological features and prognosis of mucinous cystic neoplasm with ovarian-type stroma: a multi-institutional study of the Japan pancreas society. *Pancreas,* 40**,** 67-71.

YAMAWAKI, H., PAN, S., LEE, R. T. & BERK, B. C. 2005. Fluid shear stress inhibits vascular inflammation by decreasing thioredoxin-interacting protein in endothelial cells. *The Journal of clinical investigation,* 115**,** 733-8.

YAN, C., SHIEH, B., REIGAN, P., ZHANG, Z., COLUCCI, M. A., CHILLOUX, A., NEWSOME, J. J., SIEGEL, D., CHAN, D., MOODY, C. J. & ROSS, D. 2009. Potent activity of

indolequinones against human pancreatic cancer: identification of thioredoxin reductase as a potential target. *Molecular pharmacology,* 76**,** 163-72.

YAN, C., SIEGEL, D., NEWSOME, J., CHILLOUX, A., MOODY, C. J. & ROSS, D. 2012. Antitumor indolequinones induced apoptosis in human pancreatic cancer cells via inhibition of thioredoxin reductase and activation of redox signaling. *Molecular pharmacology,* 81**,** 401-10.

YAN, H., ZHEN, X., CERVIÑO, L., JIANG, S. B. & JIA, X. 2013. Progressive cone beam CT dose control in image-guided radiation therapy. *Medical physics,* 40.

YAO, H. & RAHMAN, I. 2011. Current concepts on oxidative/carbonyl stress, inflammation and epigenetics in pathogenesis of chronic obstructive pulmonary disease. *Toxicology and applied pharmacology,* 254**,** 72-85.

YELLOW, W., BAMLET, W. R., OBERG, A. L., ANDERSON, K. E., OLSON, J. E., SINHA, R., PETERSEN, G. M., STOLZENBERG-SOLOMON, R. Z. & JANSEN, R. J. 2017. Association between Alcohol Consumption, Folate Intake, and Risk of Pancreatic Cancer: A Case-Control Study. *Nutrients,* 9.

YOU, B. R., SHIN, H. R., HAN, B. R., KIM, S. H. & PARK, W. H. 2015. Auranofin induces apoptosis and necrosis in HeLa cells via oxidative stress and glutathione depletion. *Molecular medicine reports,* 11**,** 1428-1434.

YOU, B. R., SHIN, H. R. & PARK, W. H. 2014. PX-12 inhibits the growth of A549 lung cancer cells via G2/M phase arrest and ROS-dependent apoptosis. *International journal of oncology,* 44**,** 301-8.

YUNIS, A. A., ARIMURA, G. K. & RUSSIN, D. J. 1977. Human pancreatic carcinoma (MIA PaCa-2) in continuous culture: sensitivity to asparaginase. *International journal of cancer,* 19**,** 128-135.

ZEITOUNI, D., PYLAYEVA-GUPTA, Y., DER, C. J. & BRYANT, K. L. 2016. KRAS mutant pancreatic cancer: no lone path to an effective treatment. *Cancers,* 8**,** 45.

ZEMAN, E. M., BROWN, J. M., LEMMON, M. J., HIRST, V. K. & LEE, W. W. 1986. SR-4233: a new bioreductive agent with high selective toxicity for hypoxic mammalian cells. *International Journal of Radiation Oncology• Biology• Physics,* 12**,** 1239-1242.

ZHANG, B., SU, Y., AI, G., WANG, Y., WANG, T. & WANG, F. 2005. Involvement of peroxiredoxin I in protecting cells from radiation-induced death. *Journal of radiation research,* 46**,** 305-12.

ZHANG, J., LI, X., HAN, X., LIU, R. & FANG, J. 2017a. Targeting the Thioredoxin System for Cancer Therapy. *Trends in Pharmacological Sciences,* 38**,** 794-808.

ZHANG, J., ZUO, C. J., JIA, N. Y., WANG, J. H., HU, S. P., YU, Z. F., ZHENG, Y., ZHANG, A. Y. & FENG, X. Y. 2015. Cross-modality PET/CT and contrast-enhanced CT imaging for pancreatic cancer. *World journal of gastroenterology* 21**,** 2988-96.

ZHANG, L. U. O. N. 2008. *Evaluation of thioredoxin system in breast cancer treatment. .*

ZHANG, Y. 2014. *REDOX PROTEIN REGULATION OF THERAPEUTIC RESPONSE IN BREAST CANCER* PhD, The University of Nottingham.

ZHANG, Y. & MARTIN, S. G. 2014. Redox proteins and radiotherapy. *Clinical Oncology,* 26**,** 289-300.

ZHANG, Y., STORR, S. J., JOHNSON, K., GREEN, A. R., RAKHA, E. A., ELLIS, I. O., MORGAN, D. A. & MARTIN, S. G. 2014. Involvement of metformin and AMPK in the radioresponse and prognosis of luminal versus basal-like breast cancer treated with radiotherapy. *Oncotarget,* 5**,** 12936-49.

ZHANG, Z., LANG, J., CAO, Z., LI, R., WANG, X. & WANG, W. 2017b. Radiation-induced SOD2 overexpression sensitizes colorectal cancer to radiation while protecting normal tissue. *Oncotarget,* 8**,** 7791-7800.

ZHAO, C., ZHANG, J., ZHANG, S., YU, D., CHEN, Y., LIU, Q., SHI, M., NI, C. & ZHU, M. 2013. Diagnostic and biological significance of microRNA-192 in pancreatic ductal adenocarcinoma. *Oncology reports,* 30**,** 276-84.

ZHAO, Y., SEEFELDT, T., CHEN, W., CARLSON, L., STOEBNER, A., HANSON, S., FOLL, R., MATTHEES, D. P., PALAKURTHI, S. & GUAN, X. 2009. Increase in thiol oxidative stress via glutathione reductase inhibition as a novel approach to enhance cancer sensitivity to X-ray irradiation. *Free Radical Biology and Medicine,* 47**,** 176-83.

ZIETMAN, A. L., BAE, K., SLATER, J. D., SHIPLEY, W. U., EFSTATHIOU, J. A., COEN, J. J., BUSH, D. A., LUNT, M., SPIEGEL, D. Y. & SKOWRONSKI, R. 2010. Randomized trial comparing conventional-dose with high-dose conformal radiation therapy in early-stage adenocarcinoma of the prostate: long-term results from proton radiation oncology group/american college of radiology 95-09. *Journal of clinical oncology,* 28**,** 1106.

ZIETMAN, A. L., DESILVIO, M. L., SLATER, J. D., ROSSI, C. J., MILLER, D. W., ADAMS, J. A. & SHIPLEY, W. U. 2005. Comparison of conventional-dose vs high-dose conformal radiation therapy in clinically localized adenocarcinoma of the prostate: a randomized controlled trial. *Jama,* 294**,** 1233-1239.

ZITKA, O., SKALICKOVA, S., GUMULEC, J., MASARIK, M., ADAM, V., HUBALEK, J., TRNKOVA, L., KRUSEOVA, J., ECKSCHLAGER, T. & KIZEK, R. 2012. Redox status expressed as GSH:GSSG ratio as a marker for oxidative stress in paediatric tumour patients. *Oncology Letters,* 4**,** 1247-1253.

ZOU, L., ZHONG, R., SHEN, N., CHEN, W., ZHU, B., KE, J., LU, X., ZHANG, T., LOU, J., WANG, Z., LIU, L., QI, L. & MIAO, X. 2014. Non-linear dose-response relationship between cigarette smoking and pancreatic cancer risk: evidence from a meta-analysis of 42 observational studies. *European journal of cancer,* 50**,** 193-203.

ZOU, P., CHEN, M., JI, J., CHEN, W., CHEN, X., YING, S., ZHANG, J., ZHANG, Z., LIU, Z. & YANG, S. 2015. Auranofin induces apoptosis by ROS-mediated ER stress and mitochondrial dysfunction and displayed synergistic lethality with piperlongumine in gastric cancer. *Oncotarget,* 6**,** 36505.

ZOU, P., XIA, Y., CHEN, W., CHEN, X., YING, S., FENG, Z., CHEN, T., YE, Q., WANG, Z., QIU, C., YANG, S. & LIANG, G. 2016. EF24 induces ROS-mediated apoptosis via targeting thioredoxin reductase 1 in gastric cancer cells. *Oncotarget,* 7**,** 18050-18064.

ZUO, L., ZHOU, T., PANNELL, B. K., ZIEGLER, A. C. & BEST, T. M. 2015. Biological and physiological role of reactive oxygen species – the good, the bad and the ugly. *Acta Physiologica,* 214**,** 329-348.

Appendix A: Supplementary information for Chapter 4

Figure A1: H-score histograms of TRX, TrxR and TxNIP in the PAD cohort. Histograms show the distribution of cytoplasmic/nuclear Trx, cytoplasmic/nuclear TrxR and TxNIP H-scored of PC tissue microarray from PAD cohort of 85 patients.

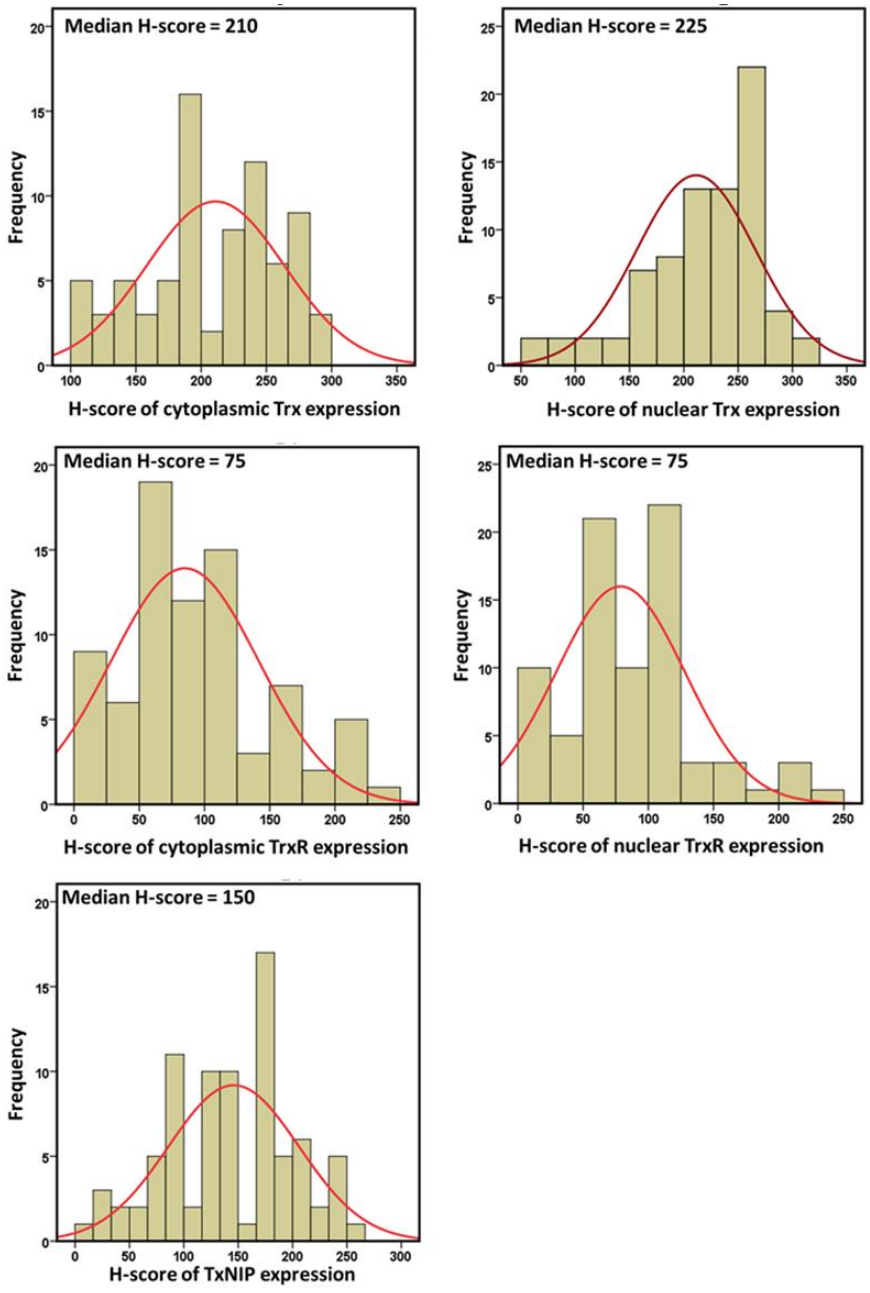
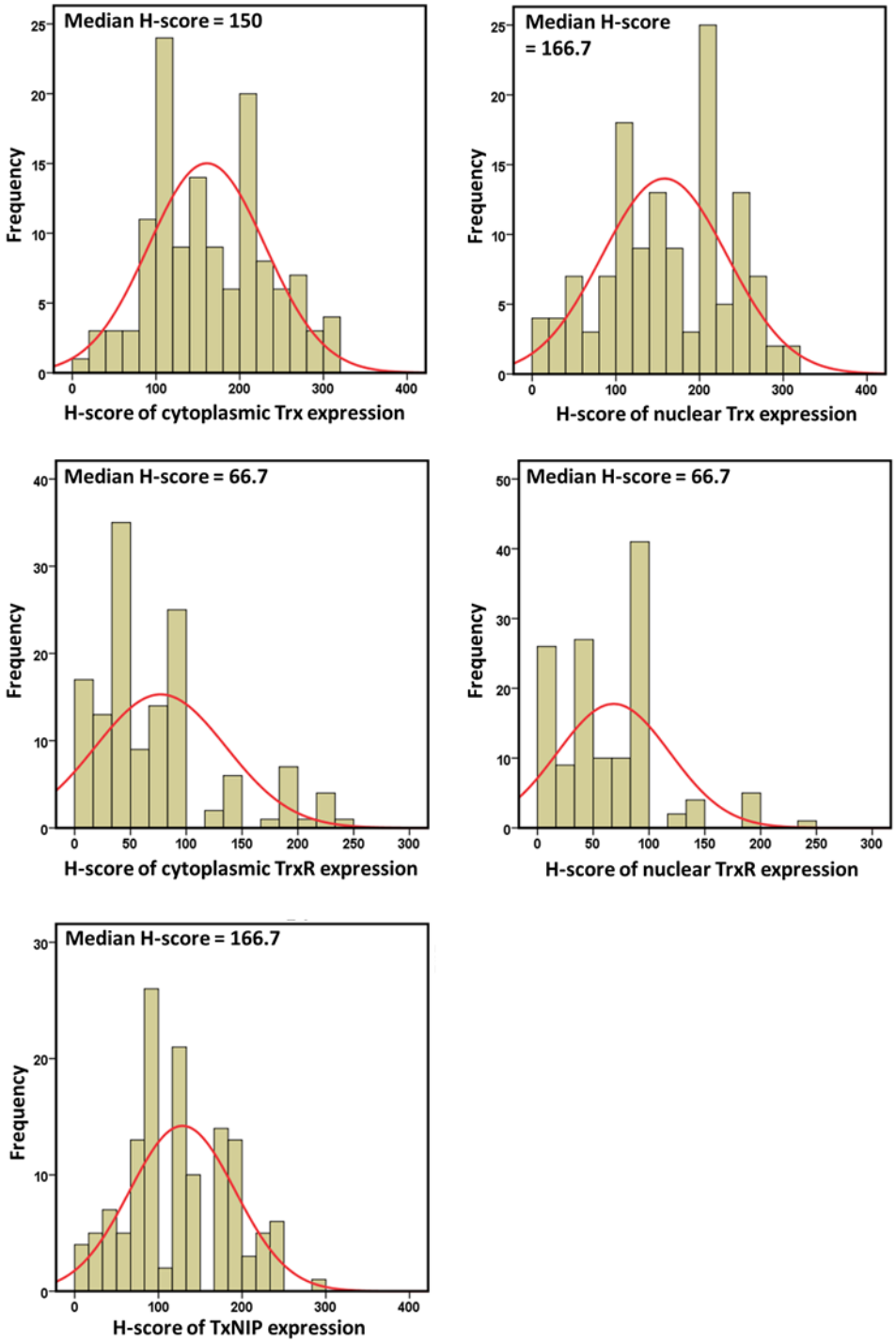


Figure A2: H-score histograms of TRX, TrxR and TxNIP in the bile duct and ampullary cancers cohort. Histograms show the distribution of cytoplasmic/nuclear Trx, cytoplasmic/nuclear TrxR and TxNIP H-scored of PC tissue microarray from bile duct and ampullary cancers cohort of 145 patients.



Appendix B: Copyright information

Copyright for Figure 1.1: Reproduced from Encyclopaedia Britannica, Inc., (https://www.britannica.com/science/human-digestive-system/Bile#ref212940, last update 12 November 2018), Human digestive system; copyright© 2003 by Encyclopaedia Britannica, Inc.

RE: Britannica Syndication Inquiry Form

WS Wallace, Sylvia <SWallace@eb.com>
Wed 12/6/2017, 1:03 AM
You

Reply

Flag for follow up.

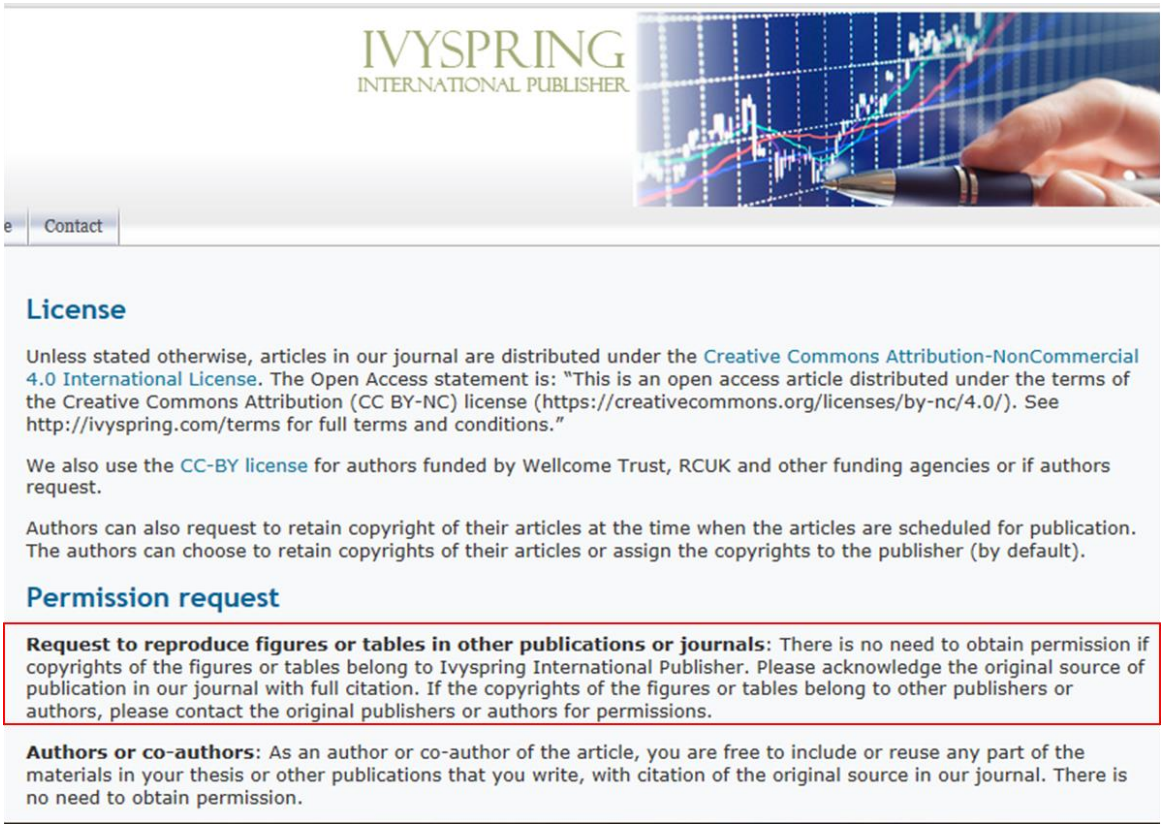
Dear Mr. Alhadyan,
Thank you for your permission request.

Encyclopaedia Britannica is happy to grant you permission to use our illustration "structures of the pancreas" only in your non-commercial thesis. We will waive the usual fee and just ask that you include the following credit in your paper: "By courtesy of Encyclopaedia Britannica, Inc., copyright 2003; used with permission."
Best regards,
Sylvia Wallace
Permissions
EB, Inc.

From: khadyan@hotmail.com [mailto:khadyan@hotmail.com]
Sent: Sunday, December 3, 2017 3:33 AM
To: Wallace, Sylvia <SWallace@eb.com>
Subject: Britannica Syndication Inquiry Form

This is Syndication Form Inquiry. Here is the information provided by the customer:

Copyright for Figure 1.3: Reproduced from (Guo et al., 2016), molecular biomarkers of pancreatic intraepithelial neoplasia and their implications in early diagnosis and therapeutic intervention of pancreatic cancer. *International journal of biological sciences*, 12(3), p.292; copyright© copyright is waived for reproduction by Ivyspring International Publisher.



IVYSPRING
INTERNATIONAL PUBLISHER

e Contact

License

Unless stated otherwise, articles in our journal are distributed under the Creative Commons Attribution-NonCommercial 4.0 International License. The Open Access statement is: "This is an open access article distributed under the terms of the Creative Commons Attribution (CC BY-NC) license (https://creativecommons.org/licenses/by-nc/4.0/). See http://ivyspring.com/terms for full terms and conditions."

We also use the CC-BY license for authors funded by Wellcome Trust, RCUK and other funding agencies or if authors request.

Authors can also request to retain copyright of their articles at the time when the articles are scheduled for publication. The authors can choose to retain copyrights of their articles or assign the copyrights to the publisher (by default).

Permission request

Request to reproduce figures or tables in other publications or journals: There is no need to obtain permission if copyrights of the figures or tables belong to Ivyspring International Publisher. Please acknowledge the original source of publication in our journal with full citation. If the copyrights of the figures or tables belong to other publishers or authors, please contact the original publishers or authors for permissions.

Authors or co-authors: As an author or co-author of the article, you are free to include or reuse any part of the materials in your thesis or other publications that you write, with citation of the original source in our journal. There is no need to obtain permission.

Copyright for Figure 1.4: Reproduced from (de Sousa Cavalcante and Monteiro, 2014), Gemcitabine: metabolism and molecular mechanisms of action, sensitivity and chemoresistance in pancreatic cancer. European journal of pharmacology, 741, 8-16; copyright© 2016 by Taylor & Francis with permission conveyed through Copyright Clearance Centre Inc.



Copyright Clearance Center RightsLink®

Home | Create Account | Help

Title: Gemcitabine: Metabolism and molecular mechanisms of action, sensitivity and chemoresistance in pancreatic cancer

Author: Lucas de Sousa Cavalcante,Gisele Monteiro

Publication: European Journal of Pharmacology

Publisher: Elsevier

Date: 15 October 2014

Copyright © 2014 Elsevier B.V. All rights reserved.

LOGIN

If you're a copyright.com user, you can login to RightsLink using your copyright.com credentials.

Already a RightsLink user or want to learn more?

Please note that, as the author of this Elsevier article, you retain the right to include it in a thesis or dissertation, provided it is not published commercially. Permission is not required, but please ensure that you reference the journal as the original source. For more information on this and on your other retained rights, please visit: https://www.elsevier.com/about/our-business/policies/copyright#Author-rights

BACK CLOSE WINDOW

Copyright © 2019 Copyright Clearance Center, Inc. All Rights Reserved. Privacy statement. Terms and Conditions.
Comments? We would like to hear from you. E-mail us at customercare@copyright.com

Copyright for Figures 1.10 and 2.1: Reproduced from (Zhang and Martin, 2014), redox proteins and radiotherapy. *Clinical Oncology*, 26, 289–300; copyright© 2014 by ELSEVIER with permission conveyed through Copyright Clearance Centre Inc.

This Agreement between The University of Nottingham -- khaled Alhadyan ("You") and Elsevier ("Elsevier") consists of your license details and the terms and conditions provided by Elsevier and Copyright Clearance Center.

License Number	4245970119409
License date	Dec 11, 2017
Licensed Content Publisher	Elsevier
Licensed Content Publication	Clinical Oncology
Licensed Content Title	Redox Proteins and Radiotherapy
Licensed Content Author	Y. Zhang,S.G. Martin
Licensed Content Date	May 1, 2014
Licensed Content Volume	26
Licensed Content Issue	5
Licensed Content Pages	12
Start Page	289
End Page	300
Type of Use	reuse in a thesis/dissertation
Intended publisher of new work	other
Portion	figures/tables/illustrations
Number of figures/tables/illustrations	4
Format	both print and electronic
Are you the author of this Elsevier article?	No
Will you be translating?	No
Original figure numbers	Figure 1,2,3 and 4
Title of your	Targeting thioredoxin reductase in pancreatic cancer

Copyright for Figure 1.11: Reproduced from (Ramanathan et al., 2007), a Phase I pharmacokinetic and pharmacodynamic study of PX-12, a novel inhibitor of thioredoxin-1, in patients with advanced solid tumours. *Clinical Cancer Research*, 13, 2109-2114; copyright© 2007 by American Association for Cancer Research with permission conveyed through Copyright Clearance Centre Inc.

AMERICAN ASSOCIATION FOR CANCER RESEARCH LICENSE TERMS AND CONDITIONS

Oct 22, 2018

This Agreement between The University of Nottingham -- khaled Alhadyan ("You") and American Association for Cancer Research ("American Association for Cancer Research") consists of your license details and the terms and conditions provided by American Association for Cancer Research and Copyright Clearance Center.

License Number	4310760218094
License date	Mar 16, 2018
Licensed Content Publisher	American Association for Cancer Research
Licensed Content Publication	Clinical Cancer Research
Licensed Content Title	A Phase I Pharmacokinetic and Pharmacodynamic Study of PX-12, a Novel Inhibitor of Thioredoxin-1, in Patients with Advanced Solid Tumors
Licensed Content Author	Ramesh K. Ramanathan,D. Lynn Kirkpatrick,Chandra P. Belani,David Friedland,Sylvan B. Green,H-H. Sherry Chow,Catherine A. Cordova,Steven P. Stratton,Elizabeth R. Sharlow,Amanda Baker,Tomislav Dragovich
Licensed Content Date	Apr 1, 2007
Licensed Content Volume	13
Licensed Content Issue	7
Type of Use	Thesis/Dissertation
Requestor type	academic/educational
Format	print and electronic
Portion	figures/tables/illustrations
Number of figures/tables/illustrations	1

Copyright for Figure 2.4: Reproduced from (Yan et al., 2009), potent activity of indolequinones against human PC: identification of TrxR as a potential target. *Molecular Pharmacology*, 76, 163-72**;** copyright© 2009 by Springer Nature with permission conveyed through Copyright Clearance Centre Inc.

Oct 22, 2018

This Agreement between The University of Nottingham -- khaled Alhadyan ("You") and Springer Nature ("Springer Nature") consists of your license details and the terms and conditions provided by Springer Nature and Copyright Clearance Center.

License Number	4267160502245
License date	Jan 13, 2018
Licensed Content Publisher	Springer Nature
Licensed Content Publication	British Journal of Cancer
Licensed Content Title	DT-diaphorase protects cells from the hypoxic cytotoxicity of indoloquinone EO9
Licensed Content Author	JA Plumb, M Gerritsen, P Workman
Licensed Content Date	Dec 1, 1994
Licensed Content Volume	70
Licensed Content Issue	6
Type of Use	Thesis/Dissertation
Requestor type	academic/university or research institute
Format	print and electronic
Portion	figures/tables/illustrations
Number of figures/tables/illustrations	1
High-res required	no
Will you be translating?	no
Circulation/distribution	<501

Copyright for Figure 3.1: Reproduced from (Erkan et al., 2016), The role of hypoxia in pancreatic cancer: a potential therapeutic target? *Expert review of gastroenterology & hepatology,* 10, 301-31; copyright© 2016 by Taylor & Francis with permission conveyed through Copyright Clearance Centre Inc.

